Adaptive control of interconnected and muliti-agent systems

Tao, T.

DOI
10.4233/uuid:4d1c2a64-6ea2-491c-820c-20811a8b49b7

Publication date
2022

Document Version
Final published version

Citation (APA)
Tao, T. (2022). *Adaptive control of interconnected and muliti-agent systems*. [Dissertation (TU Delft), Delft University of Technology]. https://doi.org/10.4233/uuid:4d1c2a64-6ea2-491c-820c-20811a8b49b7

Important note
To cite this publication, please use the final published version (if applicable).
Please check the document version above.

ADAPTIVE CONTROL OF INTERCONNECTED AND MULTI-AGENT SYSTEMS

Tian TAO

ADAPTIVE CONTROL OF INTERCONNECTED AND MULTI-AGENT SYSTEMS

Proefschrift

ter verkrijging van de graad van doctor
aan de Technische Universiteit Delft,
op gezag van de Rector Magnificus prof. dr. ir. T.H.J.J. van der Hagen,
voorzitter van het College voor Promoties,
in het openbaar te verdedigen
op woensdag 28 September 2022 om 12.30 uur

door

Tian TAO

Master of Engineering in Control Science and Engineering,
University of Electronic Science and Technology of China,
geboren te Tianmen, Hubei, China.

Dit proefschrift is goedgekeurd door de

promotoren: Prof. dr. ir. B. De Schutter
copromotor: Prof. dr. S. Baldi

Samenstelling promotiecommissie:

Rector Magnificus,	voorzitter
Prof. dr. S. Baldi,	Technische Universiteit Delft
Prof. dr. ir. B. De Schutter,	Technische Universiteit Delft
Onafhankelijke leden:	
Prof. dr. ir. M. Verhaegen,	Technische Universiteit Delft
Prof. dr. ir. H. Hellendoorn,	Technische Universiteit Delft
Prof. dr. ir. B. Jayawardhana,	Rijksuniversiteit Groningen
Prof. dr. D. V. imarogonas,	KTH Koninklijk Instituut voor Technische
Prof. dr. S. Roy,	International Institute of Information Technology Hyderabad

The work in the thesis was partly supported by China Scholarship Council under grant 201806070152.

Keywords: multi-agent systems, interconnected systems, distributed adaptive control, state-dependent uncertainty

Published by: Tian Tao

Email: taotian2017@gmail.com

Printed by: Gildeprint

ISBN: 978-94-6384-365-2

An electronic version of this dissertation is available at
http://repository.tudelft.nl/.

CONTENTS

Acknowledgements vii

Notations ix

1 Introduction 1
- 1.1 Motivation . . . 1
- 1.2 Main contributions . . . 2
- 1.3 Thesis outline . . . 4

2 Background and Preliminaries 7
- 2.1 Switched systems . . . 7
  - 2.1.1 Background of switched systems . . . 7
  - 2.1.2 The issue of robust adaptive control of switched systems . . . 9
- 2.2 Interconnected power systems . . . 10
  - 2.2.1 Background of interconnected power systems . . . 10
  - 2.2.2 The issue of adaptive switched control of power systems . . . 11
- 2.3 Multi-agent systems . . . 12
  - 2.3.1 Background of multi-agent systems . . . 12
  - 2.3.2 The issue of a priori existing interconnections . . . 14
- 2.4 Underactuated Euler-Lagrange systems . . . 15
  - 2.4.1 Background of underactuated Euler-Lagrange systems . . . 15
  - 2.4.2 The issue of structural knowledge . . . 15

3 Robust Adaptive Control of Uncertain Switched Linear Systems 17
- 3.1 Introduction . . . 17
- 3.2 Problem formulation . . . 18
- 3.3 Controller design . . . 20
  - 3.3.1 Adaptive control . . . 20
  - 3.3.2 Switching laws . . . 21
- 3.4 Stability analysis . . . 22
- 3.5 Simulation example . . . 28
  - 3.5.1 Design of the reference model . . . 29
  - 3.5.2 Comparisons . . . 29
  - 3.5.3 Additional comparisons . . . 32
- 3.6 Concluding remarks . . . 32

4 Robust Adaptive Control of Switched Interconnected Power Systems 37
- 4.1 Introduction . . . 37
- 4.2 Problem formulation . . . 38
  - 4.2.1 Single-area power system . . . 39

4.2.2 Multi-area power system . . . 39
4.2.3 Structure-preserving modelling . . . 41
4.3 Controller design . . . 43
4.4 Stability analysis . . . 45
4.5 Simulation example . . . 49
4.5.1 Design and considerations on control disaggregation . . . 49
4.5.2 Simulation results and discussion . . . 51
4.6 Concluding remarks . . . 55

5 Distributed Adaptive Synchronization in Euler-Lagrange Networks 57
5.1 Introduction . . . 57
5.2 Problem formulation . . . 58
5.3 Controller design . . . 59
5.3.1 Uncertainty analysis . . . 60
5.3.2 Adaptive synchronization laws . . . 61
5.4 Stability analysis . . . 62
5.5 Simulation example . . . 68
5.6 Concluding remarks . . . 72

6 Distributed Adaptive Synchronization in Underactuated Euler-Lagrange Networks 73
6.1 Introduction . . . 73
6.2 Problem formulation . . . 74
6.3 Controller design . . . 77
6.3.1 Distributed control law . . . 77
6.3.2 Synchronization error dynamics . . . 78
6.3.3 Uncertainty analysis . . . 80
6.3.4 Adaptive synchronization laws . . . 82
6.4 Stability analysis . . . 82
6.5 Simulation example . . . 91
6.5.1 System parameters (uncertain) and design parameters . . . 92
6.5.2 Simulation results . . . 94
6.6 Concluding remarks . . . 95

7 Conclusions and Recommendations 97
7.1 Conclusions . . . 97
7.2 Recommendations for future research . . . 98

Bibliography 101

Summary 115

Samenvatting 117

List of Publications 119

Curriculum Vitae 121

ACKNOWLEDGEMENTS

Well, the day comes even though I still cannot believe four years have passed by. At this moment, I would like to give my most sincere thanks to the people that accompanied me, helped me, encouraged me, and guided me. I am so lucky that I was able to spend four years with these nice people, creating so many unforgettable memories. Without all of you, I cannot imagine how would my life be like during these four years.

Firstly, I would like to acknowledge the China Scholarship Council (CSC) for the financial support, and the department of Delft Center for Systems and Control (DCSC) of Delft University of Technology for the research facilities and expenses.

I want to thank my supervisor Prof. Simone who provides me the chance to pursue a PhD at DCSC of TU Delft. Simone was patient and always responded quickly to my requests for feedback, he taught me a lot of preliminary knowledge, especially at the beginning of my PhD. I would give my sincere appreciation to him for his guidance and for being on my side during these four years. I would also like to thank Prof. Bart, who was always encouraging and often made me look at things from a global vision. In addition, as a department head, he was always very committed to providing us with a great work atmosphere. Despite his numerous duties, he always paid a lot of attention to my research progress. I would also like to thank Prof. Spandan, who helped me a lot with valuable support and inspired me a lot during my PhD research.

Furthermore, I would like to thank all the committee members, including Prof. Michel Verhaegen, Prof. Hans Hellendoorn, Prof. Bayu Jayawardhana, Prof. Dimos Dimarogonas for their attendance and valuable comments on my thesis.

During the year 2019 I faced some of the darkest hours during my PhD, I tended to be depressed and barely wanted to see or talk to anyone. I deeply thank Xiaogen who, despite being refused by me many times, still insisted on inviting me for her home-cooking and was a patient listener. I would like to thank my mentor Mascha who had many conversations with me and gave me a lot of comforts. I would like to thank Haoran for picking me up once I got lost and didn't know how to come back home. I would like to thank Ximan who helped me book the flight ticket when I trembled in great sorrow hearing my grandma passed away.

Unfortunately, my wrist got dislocated in 2021, it was quite inconvenient for everything. I would like to thank Xiuli, Xiang, and Yubao, who sent me to the hospital immediately and waited for several hours outside of the hospital on a cold winter night. I deeply thank Dengxiao for cooking for me every day for two months and I cannot imagine the efforts she had made. I would like to deeply thank Huimin for giving me the medicine when I was so sick that I could not get up from the bed. I would like to thank Wenxuan, who accompanied me to the emergency center several times in the middle of the night due to some urgent problems with my wrist. I would like to thank Dandan, who invited me for her home-cooking every weekend and tied the shoelace for me. I would like to thank Yongxia, who helped me to wash my hair and made dumplings for me. I would

like to thank Shuo, Xianfeng, Xiaoyu, Jingwei who helped me move to a new house when my hand was still in plaster.

Furthermore, I would like to thank all the lovely friends that I met in the Netherlands. Although I cannot list all of their names, I will remember all of the happy moments we spent together. Special thanks to Shanshan who helped me to conquer the fear of running, which totally changed my everyday life: my running distance started from 0.5 km and reached a half-marathon. Thanks to all the buddies for regular running, cycling around the Netherlands, having a trip to Italy, to the mid-sea, to Austria and Hungary.

I also would like to thank all the lovely colleagues in DCSC. I would like to thank Hai, Shuai, Laura, Ping, Yichao, Maolong, Dingshan, Yun, Shengling, Kanghui, Luyao, Yuchen who made me feel familiar in the department. I would like to thank my office mates Zhixin, Rogier, Jean for their accompany and friendly working atmosphere. Thanks to Amin for sharing his experience patiently with useful advice, and Frida for strongly encouraging me to talk with colleagues. Thanks to Emilio, Suad, Mattia for being warm to me especially when I felt rather isolated during Covid-19 pandemic, it was Suad who invited me to join the lunch group many times (the policies were relaxed then, so we didn't violate the rules). Also thanks to Shabnam, Shokri, Boveiri, Reza, Raja, Carlos, Ashkan, Manyu, Leila for pleasant moments in DCSC.

I would like to thank my English teacher Martine from the TPM department of TU Delft, who really paid a lot of attention to me and corrected a lot of my mistakes during the pronunciation class to improve my English. I would like to thank the secretaries of DCSC for organizing attractive activities for us with their professional abilities and considerate hearts.

I would like to thank my master's supervisor Prof. Jiangping Hu from the University of Electronic Science and Technology of China, who encouraged me to go abroad when I hesitated. He pushed me to step out of my comfort zone. Without his encouragement, I cannot imagine one day I would come to Delft.

Last but not the least, my greatest thanks to Anyuan for his love and understanding whenever I face up to challenges. Besides, greatest thanks to my family, especially my very cute nephew and niece for their emotional support.

Tian Tao
Delft, June 2022

NOTATIONS

$\mathbb{R}, \mathbb{R}^+$	sets of real numbers and positive real numbers
$\mathbb{N}^+$	set of positive natural numbers
I_n	identity matrix of dimension n
1_N	N-dimensional vector of ones
$\lambda_{\max}(\cdot)$	maximum eigenvalue of a matrix of $(\cdot)$
$\lambda_{\min}(\cdot)$	minimum eigenvalue of a matrix of $(\cdot)$
$\|\|(\cdot)\|\|$	Euclidean norm of a vector or matrix $(\cdot)$
diag$\{\ldots\}$	diagonal matrix with diagonal elements in the ordered set $\{\ldots\}$
$P > 0$	positive definite matrix
$\bar{\lambda}(\mathbf{P}_p)$	maximum of $\lambda_{\max}(\mathbf{P}_p)$ among all switching signal p
$\underline{\lambda}(\mathbf{P}_p)$	minimum of $\lambda_{\min}(\mathbf{P}_p)$ among all switching signal p
$\mathcal{N}_i$	neighbor set of agent i
$\mathcal{A} = [a_{ij}]$	adjacency matrix of a graph
$\mathcal{L} = [l_{ij}]$	Laplacian matrix of a graph
b_i	pinning gain for those agents i that can receive information from the leader
$\mathcal{L}_\infty$	set of bounded signals in the ∞-norm
Class $\mathcal{K}$	continuously strictly increasing function $\alpha : [0,\infty) \to [0,\infty)$
Class $\mathcal{KL}$	function $\beta(s,t) : [0,\infty) \to [0,\infty)$ is of class $\mathcal{K}$ function for each fixed $t \geq 0$, and decreases to zero as $t \to 0$ for each fixed $s \geq 0$
Class $\mathcal{K}_\infty$	unbounded function $\gamma : [0,\infty) \to [0,\infty)$ is of class $\mathcal{K}$ function, and $\gamma(0) = 0$
$\otimes$	Kronecker product

1

INTRODUCTION

In this chapter, we will present the motivation, main contributions, and outline of this thesis.

1.1. MOTIVATION

Interconnected and multi-agent systems (in the following, both will be abbreviated as MAS for compactness) have attracted tremendous attention from the control community (and from many other communities), due to their extensive application domains, including unmanned aerial vehicles, intelligent traffic systems, smart grids, sensor networks, and so on. MAS are constituted of multiple intelligent agents interconnected via a network, through which they can communicate/interact with the neighbors/the environment, in order to achieve a common behavior (also referred to as synchronized behavior) or some desired tasks.

Uncertainties are inevitable in practice, as they originate either from the network (e.g. *switching topologies*) or from the agent dynamics (e.g. *parametric uncertainty*). Furthermore, another important source of uncertainty originates from the interaction among agents: standard literature typically considers that the agents' interaction with neighbors/environment is only the result of coupling due to the control protocol. However, in practical scenarios, some form of interaction may exist before designing the control protocol (intrinsic interconnection). The picture becomes more complex when considering these *unmodelled intrinsic interconnection* terms to be *state-dependent*, which makes the control of uncertain MAS extremely challenging. The design of adaptive controllers that enable the interconnected and multi-agent systems to adapt to the time-varying environment while preserving stability is still an open problem.

As a motivating example, Fig. 1.1 shows a smart grid scenario where multiple nodes including power plants, electrical consumers, distribution companies, and transmission stations are connected via a power network. The nodes interact with each other by power flow through the tie lines, depending on the phase deviations from the equilibrium operating point. Such intrinsic interconnections exist even before designing a controller.

1

In order to stabilize the frequency/voltage, the interaction (i.e. power flow) among these nodes will dynamically change by switching the topology of the power network. Fig. 1.2 presents another motivating example with multiple cranes that must cooperate in lifting a heavy load. The interconnection between the cranes and the load via the wires will create a state-dependent interconnection depending on the load, and on the elastic and viscous force of the wires.

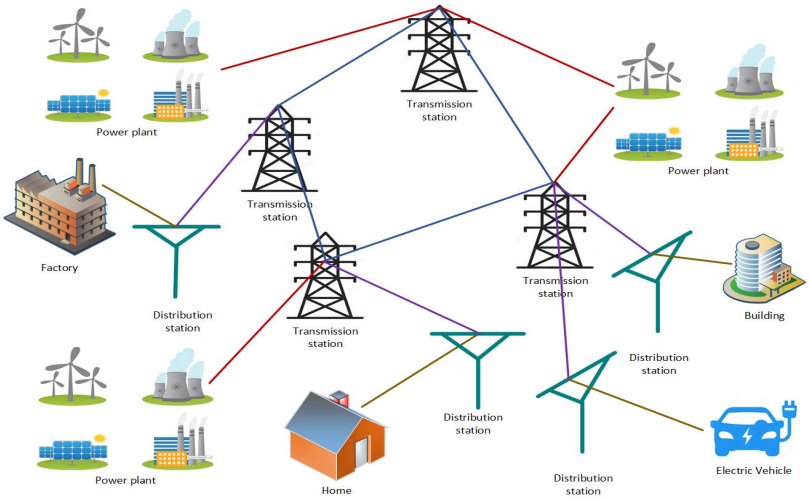

Figure 1.1: Smart grid

Figure 1.2: Heavy-lift vessel with multiple cranes (source: Heerema Marine Contractors)

1.2. MAIN CONTRIBUTIONS

This thesis proposes a set of adaptive control frameworks that enable the interconnected and multi-agent systems to adapt to changing circumstances including switching topolo-

gies, parametric uncertainties, and state-dependent uncertainties. The contributions of this thesis include:

- **Robust Adaptive Control of Switched Interconnected Linear Systems**
  We propose a robust adaptive control approach for switched uncertain linear systems by adopting a novel leakage-based method. The novelty is to allow the control gains to stay constant during the switched-off phase: this is not the case in state-of-the-art leakage methods, where the control gains of inactive subsystems must change even during the switched-off phase, causing a bad transient behavior whenever these inactive subsystems are switched on again. The auxiliary gain is designed so that the transient performance at each switching instant is improved significantly.

- **Robust Adaptive Control of Switched Interconnected Power Systems**
  We propose a switched adaptation framework for multi-area load frequency control (LFC) by considering a structure-preserving model. The main novelty is to consider the model to be affected by state-dependent uncertainty, which more appropriately captures dynamic uncertainties from aggregated area dynamics. In fact, state-dependent uncertainties cannot be bounded a priori by constants [63, 86, 100]. In this structure-preserving network formulation, we prove (via Lyapunov stability theory) that the proposed multi-area LFC approach can automatically enhance and lower the controller activity in a stable way, even in the presence of switching topologies.

- **Distributed Adaptive Synchronization in Euler-Lagrange Networks**
  We propose a distributed adaptive synchronization method for multiple Euler-Lagrange systems in the presence of state-dependent uncertainty, not necessarily in a linear-in-the-parameter (LIP) form. Different from standard literature where the interaction among agents is only the result of coupling caused by the control protocol, the novelty of our method is to consider that the interaction terms among agents may exist (and be uncertain) before the control design. The proposed adaptive controller is able to handle uncertainties both in linear and nonlinear forms.

- **Distributed Adaptive Synchronization in Underactuated Euler-Lagrange Networks**
  A distributed adaptive protocol for synchronization of underactuated Euler-Lagrange systems is designed in the presence of uncertain system terms. Besides, no structural constraints are imposed on the underactuated Euler-Lagrange dynamics, except the standard properties of Euler-Lagrange systems (positive definite mass matrix, bounded gravity terms, velocity-dependent bounds on the friction terms, etc). We do not impose the mass matrix to depend on the actuated states only, nor on the non-actuated states only. State-dependent uncertain interconnection terms among the underactuated systems are considered to exist before the control design.

1

1.3. THESIS OUTLINE

The thesis outline is illustrated in Fig. 1.3. The organization of this thesis is briefly illustrated as follows:

Chapter 2: The background on switched systems, interconnected power systems, multi-agent systems, and underactuated Euler-Lagrange systems is introduced. After introducing the art of the state, four research questions are brought forward. In addition, some basic concepts of control theory and graph theory are provided.

Chapter 3: By adopting an auxiliary adaptive gain in an uncertain switched linear system the control gains of each subsystem can stay unchanged during their switched-off intervals. The proposed strategy can consistently improve the transient of the closed-loop system under various families of slowly-switching signals (in the framework of dwell time and its extensions).

Chapter 4: Based on the switched linear systems of Chapter 3, we study switched nonlinear systems, which can be applied to multi-area LFC in power systems where both parametric uncertainty and state-dependent uncertainty exist. Besides, nonlinear interconnection terms presenting power flow between multi-areas also exhibit state-dependent uncertainty. The proposed adaptive controller is able to adapt to changing circumstances including parametric uncertainty, unmodelled dynamics, and dynamically changing topologies.

Chapter 5: Based on the centralized adaptive control approach for nonlinear systems of Chapter 4, we consider distributed adaptive control of multiple Euler-Lagrange agents. Without requiring a LIP structure of the systematic uncertainty on the dynamics, we achieve distributed adaptive synchronization of multiple Euler-Lagrange systems in the presence of state-dependent systematic uncertainty and interconnection intrinsically existing in the dynamics instead of the being the result of the control protocol.

Chapter 6: Based on the fully-actuated Euler-Lagrange systems in Chapter 5, we turn our attention to underactuated Euler-Lagrange systems. We relax structural restrictions imposed on the system terms (e.g. the mass matrix), and take into account the interconnection in the underactuated Euler-Lagrange dynamics instead of letting them be a result of control protocol. The error dynamics of both actuated states and nonactuated states are provided explicitly.

Chapter 7: The conclusion of this thesis and some future research recommendations are provided.

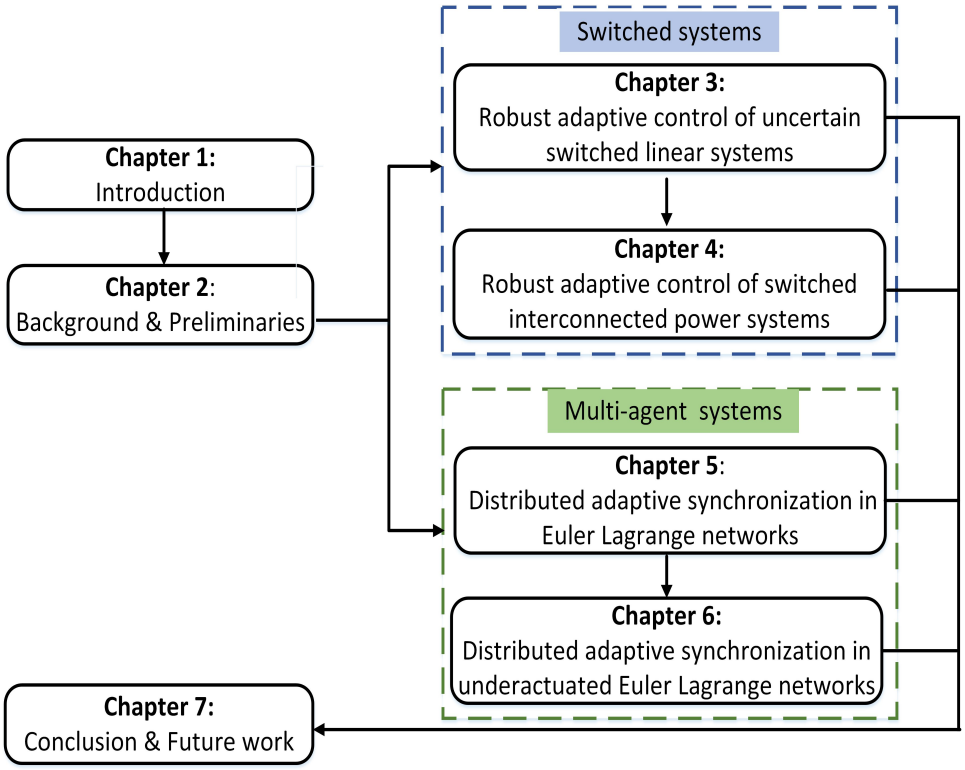

Figure 1.3: Thesis outline

2

BACKGROUND AND PRELIMINARIES

2.1. SWITCHED SYSTEMS

2.1.1. BACKGROUND OF SWITCHED SYSTEMS

With a wide range of applications in several fields, such as networked control systems [45, 67, 163], circuit and power systems [11, 62], multi-agent systems [93, 166], fault-tolerant control [147, 164], and many more, switched systems have drawn enormous interest over the last decades. Switched systems are a special type of hybrid dynamic systems, constituted of continuous-time subsystems, also called modes, and a switching law determining the activation of the subsystems (cf. Fig. 2.1). Switched systems not only find application in several technological areas but also bring several theoretical challenges, spanning from stability to control.

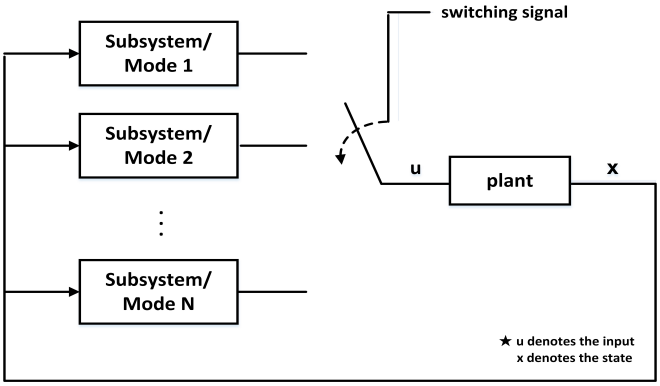

Figure 2.1: Example of a switched system

The switched system with time-dependent switching in Fig. 2.1 can be described as

$$\dot{x}(t) = f_{\sigma(t)}\big(x(t)\big) \tag{2.1}$$

where $x \in \mathbb{R}^n$ represents the state variable, $f_\sigma(\cdot)$ is the dynamics, and $\sigma : [0,\infty] \to \Omega = \{1,\dots,N\}$ denotes the switching signal. In other words, $\sigma(\cdot)$ is a piecewise constant signal taking values among the N subsystems, and with switching instants $t_1,\dots,t_N$.

Stability is the most basic desirable property for a switched system [17, 46, 66]. The state of the art has shown that stability under arbitrary switching cannot in general be achieved unless a common Lyapunov function to all subsystems exists [65, 127, 150, 169]; therefore, many researchers have concentrated on several classes of slowly-switching signals for which stability can be derived, as indicated next:

Definition 2.1. ***(Dwell Time)*** *[65]. Consider two consecutive switching time instants $t_{i+1} > t_i \geq 0$. We say that the switching signal $\sigma(\cdot)$ has* dwell time (DT) *ϑ_d if there exist $\vartheta_d > 0$ such that*

$$t_{i+1} - t_i \geq \vartheta_d, \forall i \in \mathbb{N}^+ \tag{2.2}$$

Definition 2.2. ***(Average Dwell Time)*** *[65]: For a switching signal $\sigma(\cdot)$, let $N_\sigma(t_1,t_2)$ denote the number of discontinuities in the time interval $[t_1,t_2)$ of $\sigma(\cdot)$. Then $\sigma(\cdot)$ has an average dwell time (ADT) ϑ_a if for a given scalar $N_0 > 0$*

$$N_\sigma(t_1,t_2) \leq N_0 + \frac{t_2 - t_1}{\vartheta_a}, \ \ \forall t_1,t_2 \text{ such that } t_2 \geq t_1 \geq 0$$

where N_0 is called the chatter bound.

Dwell time (DT) switching requires the time interval between consecutive switching to be no less than a sufficiently large constant. Average dwell time (ADT) switching was put forward in [47], as the extension of DT switching: in ADT switching the dwell time is defined in an average sense, i.e. fast switching is allowed, provided it is compensated by slow switching later on [142]. Some conservativeness of DT and ADT has been later relaxed by the concepts of mode-dependent dwell time (MDDT) [26] and mode-dependent average dwell time (MDADT) [167], where each mode has its own dwell time or average dwell time.

Definition 2.3. ***(Model-dependent Dwell Time)*** *[26]: Consider two consecutive switching time instants $t_{i+1}^{p_{\text{off}}} > t_i^{p_{\text{on}}} \geq 0$. Let $t_{i+1}^{p_{\text{off}}} - t_i^{p_{\text{on}}}$ denotes the running time of subsystem p during each switched-on period $[t_i^{p_{\text{on}}}, t_{i+1}^{p_{\text{off}}}]$. We say that the switching signal $\sigma(\cdot)$ has* model-dependent dwell time (MDDT) *ϑ_{pd} for any $p \in \Omega$ if there exist $\vartheta_{pd} > 0$ such that*

$$t_{i+1}^{p_{\text{off}}} - t_i^{p_{\text{on}}} \geq \vartheta_p, \ \forall i \in \mathbb{N}^+ \tag{2.3}$$

Definition 2.4. ***(Mode-dependent Average Dwell Time)*** *[167]. Consider two time instants $t_2 \geq t_1 \geq 0$. Let $N_p(t_1,t_2)$ be the number of times subsystem p is activated over the interval $[t_1,t_2)$, and let $T_p(t_1,t_2)$ denote the total running time of subsystem p over the interval $[t_1,t_2]$. We say that the switching signal $\sigma(\cdot)$ has* mode-dependent average dwell time (MDADT) *ϑ_{pa} for any $p \in \Omega$ if there exist $N_{0p} \geq 1$ and $\vartheta_{pa} > 0$ such that*

$$N_p(t_1,t_2) \leq N_{0p} + \frac{T_p(t_1,t_2)}{\vartheta_{pa}}, \ \ \forall t_1,t_2 \text{ such that } t_2 \geq t_1 \geq 0 \tag{2.4}$$

where N_{0p} is called the mode-dependent chatter bound.

Remark 2.1. *The MDADT class comprises various families of switching laws considered in literature [46], such as dwell time (DT) switching* ($N_{0p} = 1,\ \vartheta_{pa} = \vartheta_d,\ \forall p \in \Omega$)*, mode-dependent dwell time (MDDT) switching* ($N_{0p} = 1,\ \vartheta_{pa} = \vartheta_p,\ \forall p \in \Omega$)*, and average dwell-time (ADT) switching* ($N_{0p} = N_0,\ \vartheta_{pa} = \vartheta_a,\ \forall p \in \Omega$).

Consider multiple Lyapunov functions $V_p = x^T P_p x,\ p \in \Omega$ where P_p is a symmetric positive definite matrix. The following Lemma provides the DT switching law:

Lemma 2.1. *[65] Consider the family of switched system (2.1). Suppose that there exist* $V_p : \mathbb{R} \to \mathbb{R},\ p \in \Omega$*, two class* $\mathcal{K}_\infty$ *function* α_1 *and* α_2*, and two positive number* $\lambda > 0$ *and* $\mu > 1$ *for all* $p,\ q \in \Omega$ *with* $p \neq q$ *such that*

$$\alpha_1(|x|) \leq V_p(x) \leq \alpha_2(|x|), \forall x, p \in \Omega \tag{2.5}$$

and

$$\begin{aligned} \frac{\partial V_p}{\partial x} f(x) &\leq -2\lambda V_p(x) \\ V_p(x) &\leq \mu V_q(x) \end{aligned} \tag{2.6}$$

Then the switched system (2.1) is globally asymptotically stable for any switching signal $\sigma(\cdot)$ *with dwell time (DT)*

$$\vartheta_d > \frac{\ln \mu}{2\lambda} \tag{2.7}$$

2.1.2. THE ISSUE OF ROBUST ADAPTIVE CONTROL OF SWITCHED SYSTEMS

Robust adaptive control of switched systems refers to making the adaptive control robust in the presence of disturbances entering the switched system. In general, the stability of a switched system as (2.1) is intended as asymptotic stability [65]. However, in this thesis we will deal with robust adaptive control of switched systems with external disturbance or state-dependent uncertainty, which requires different notions of stability. The literature has shown that the presence of state-dependent uncertainties makes it challenging to attain adaptive asymptotic regulation or adaptive asymptotic tracking [24, 104, 129, 133, 172]. As a result, stability should be sought in the uniformly ultimately bounded sense, which is the approach we also follow.

Definition 2.5. ***(Uniform Ultimate Bounded (UUB))*** *[52]. An uncertain system with state variable* x *is uniformly ultimately bounded if there exists a convex and compact set* $\mathscr{C}$ *such that for every initial condition* $x(0) = x_0$*, there exists a finite time* $T(x_0)$ *such that* $x(t) \in \mathscr{C}$ *for all* $t \geq T(x_0)$.

Definition 2.6. *[55]* ***(Ultimate Bound)****. A signal* $\Phi(\cdot)$ *is said to have ultimate bound* b *if there exists a positive constant* b*, and for any* $a \geq 0$*, there exists* $T = T(a, b)$*, where* b *and* T *are independent of* t_0*, such that* $\|\Phi(t_0)\| \leq a \Rightarrow \|\Phi(t)\| \leq b, \forall t \geq t_0 + T$.

The notion of Uniform Ultimate Bounded (UUB) is the standard stability concept in robust adaptive control (cf. [100, Def. 3] or [52, Def. 3.4.12] for details). Some designs have been recently proposed aiming at robust adaptive control of switched systems [22, 109, 128, 154, 158, 168]. Such designs can be classified into two families:

- adopting a sliding mode approach, in which uncertainties can be compensated by sufficiently high robustification terms [22, 128, 168];

- extending the adaptive law modifications proposed for non-switched systems (projection/dead-zone/leakage) to the switched framework [109, 154, 158].

Unfortunately, the approaches in the first family require monotonically increasing the control gains, which might lead to unpractically high control inputs. For the second family, the leakage modification is quite interesting in view of the fact that it does not require any a priori knowledge of the uncertainty [52, Chap. 8], so it can potentially handle larger parametric uncertainty than projection-based robustification, as illustrated in [100, 156, 158]. However, in leakage-based robust adaptive control of switched systems, the control gains of the inactive subsystems will decrease during the switched-off phase due to the stabilizing effect of the leakage action. Consequently, a new learning transient will inevitably arise when the inactive subsystems are switched-on, as highlighted in the representative work [158]. This is up to now the biggest challenge in robust adaptive control of switched systems. Thus, such a research gap motivates the following research question:
Question 1: *How to design a robust adaptive controller for uncertain switched systems that does not require the control gains to vanish during their switched-off phase?*

2.2. INTERCONNECTED POWER SYSTEMS

2.2.1. BACKGROUND OF INTERCONNECTED POWER SYSTEMS

When considering multiple interconnected systems (also referred to as multi-agent systems), an additional source of uncertainty arises from the interconnection terms among the different systems. As an example, think about power systems where the interconnection terms represented by power flow across different areas might result in inter-area oscillations or other problems [24, 119, 133, 172]. The presence of these uncertain interconnection terms is often overlooked: in most distributed adaptive control approaches, the interconnection is only the result of the synchronization/consensus protocol, i.e. there is no interconnection before such protocol is designed [51, 64, 160].

In this section, we will illustrate the application of adaptive switched control on load frequency control (LFC) of power systems, where randomness from the power load demand and from renewable energy sources may cause frequency oscillations among interconnected areas. In recent years, with the widespread development of the smart grid technology, it was recognized as an essential feature for power system stability and security that local (i.e. intra-area) LFC should be complemented by multi-area LFC [165]: the idea of multi-area LFC is that multiple areas are connected via a power network and the frequency oscillations are balanced by adjusting the reference power of one or more governors in each area [36].

Fig. 2.2 presents a three-area power system where each area is interconnected by the tie line between distribution companies. In each area, one or more generators, in addition to producing power for the corresponding area, can be in charge of dampening frequency oscillations among areas. The load frequency is regulated via control commands delivered by such generators. It is clear that the system is intrinsically interconnected

via the physical network and the communication network. In addition, the system is uncertain since each generator in charge of LFC may not have an exact model for the aggregated dynamics of its own area and for the aggregated dynamics of the neighboring areas.

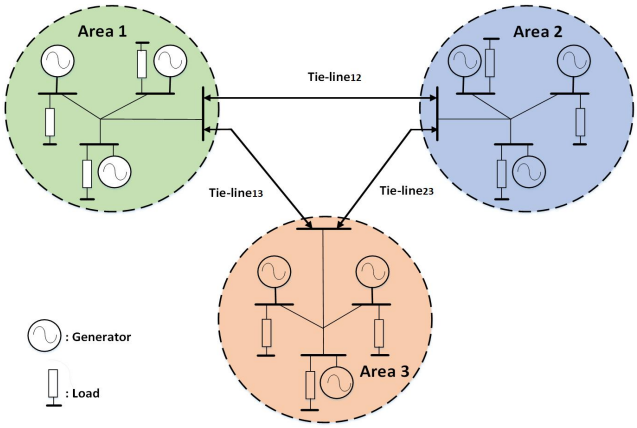

Figure 2.2: Multi-area LFC structure

2.2.2. THE ISSUE OF ADAPTIVE SWITCHED CONTROL OF POWER SYSTEMS

On the one hand, traditional multi-area LFC techniques are based on fixed-gain controllers [32, 77, 113], which are robust when uncertainties around the nominal power system parameters (time constants, speed droops, stiffness coefficients, etc.) are small [27, 122]. However, the aggregated dynamics of each area contain both parametric uncertainties and unmodelled dynamics, which are beyond the capacity of fixed-gain control [6, 10, 121]. Additionally, with the presence of renewable energy sources such as photovoltaic panels, wind farms, or microgrids, the level of uncertainty in power systems goes beyond the capabilities of fixed-gain control approaches [1, 33, 58], and stimulates new studies on multi-area LFC and related stability issues. Faced with such complex uncertainties in multi-area LFC, researchers have turned to adaptive control so as to enhance and lower the controller activity by assigning weights throughout the operation [44, 90]: adaptation ideas include having targets based on the covariances between area control errors [95], adapting participation factors [16, 97], or changing loads proportionally to frequency deviations [61].

On the other hand, since modern power systems operate flexibly in several modes (e.g. due to the changing power load demand), many different operating conditions are entailed for each mode. A unique controller may fail to handle such structural changes [1, 33, 58], whereas rapidly switching among different control configurations has been proposed as a sound solution. Recent works where this point has been highlighted are [68, 170] (showing the need for switching modes among different frequency regimes), [43, 159] (showing the need for switching interconnection among different areas), and [153] (showing the need for switching as the result of changing operating equilibria of

the power system). For example, [68, 95, 159] show how the frequency can be bounded by continuously switching interconnection among different control areas, or how the switching signal can be designed, orchestrating when the load-side controller should work in the mode of frequency restoration or in the mode of load restoration. Cyber attacks provide another reason for dynamically changing topologies, [5, 112, 149]: proposed countermeasures for mitigating attacks intentionally change the interconnections between areas, so as to prevent load manipulation from attackers [75, 92, 114].

From the perspective of control, the adaptive approaches based on switching linear dynamics cannot find a direct application in multi-area LFC because the power flow is intrinsically nonlinear (see [7, 53, 84, 141, 155] and references therein). Unfortunately, most literature on switching nonlinear dynamics either ignores the unmodelled dynamics [74, 148] or requires a priori bounded unmodelled dynamics [136], whereas aggregated area dynamics generate state-dependent uncertainty, such as bus dynamics [37]. Therefore, although adaptive switching control has been judged an effective framework to promote resilience, a multi-area LFC framework in which adaptation and switching are combined together with nonlinear interconnections in a provably stable way is still missing. This gives rise to the following research question:
Question 2: *How to design an adaptive controller for multi-area LFC that can adapt continuously to parametric uncertainty and state-dependent unmodelled dynamics, while discontinuously to structural changes?*

2.3. MULTI-AGENT SYSTEMS

2.3.1. BACKGROUND OF MULTI-AGENT SYSTEMS

Since the topic of multi-agent systems is studied by different communities, there is no unique definition for a multi-agent system: a quite general definition refers to a multi-agent system as a collection of systems cooperating with each other by exchanging communication/physical interaction via a network. In this sense, the aforementioned multi-area power system in Section 2.2 fits this definition as well. However, the multi-agent system literature generally puts more emphasis on the distributed nature of the controller in contrast to the centralized deployment of a single-agent system, i.e. the controller should use local information instead of information collected in a unique central unit (this implies that only a part of followers has the access to the leader's state information).

Therefore, after investigating adaptive control of uncertain switched systems (where the controller is centralized), this thesis will further explore distributed adaptive control of multi-agent systems with particular emphasis on Euler-Lagrange multi-agent systems. It is well known that Euler-Lagrange dynamics can describe the motion of various mechanical systems [13, 103], robotic manipulators [59, 79], aerospace systems [25], and so on. In addition, some electrical systems can also be described by Euler-Lagrange dynamics: for example, the Kuramoto model sometimes used to represent power system dynamics can be seen as special Euler-Lagrange dynamics.

Given the emphasis on distributed control, we use graphs to represent a network of nodes (or agents), cf. Fig. 2.3. A directed graph $\mathcal{G}$ can be described by the pair $(\mathcal{V},\mathcal{E})$, comprising the node set $\mathcal{V} \triangleq \{v_1,\dots,v_N\}$ and the edge set $\mathcal{E} \subseteq \mathcal{V}\times\mathcal{V}$. Typically,

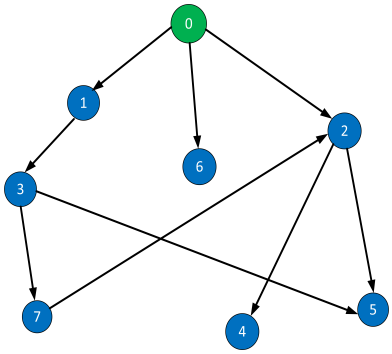

Figure 2.3: Example of leader-follower topology (agent 0 is the leader in green)

the node set does not include the leader node v_0, which is indexed by 0 due to its special role. An edge is a pair of nodes $(v_j, v_i) \in \mathscr{E}$, which represents that agent i has access to the information from agent j, i.e. agent j is a neighbor of agent i (not necessarily vice versa). The neighbor set of agent i is denoted by $\mathscr{N}_i$. For those agents i that can receive information from the leader, we have $b_i > 0$; otherwise, $b_i = 0$. Let $B = \text{diag}(b_1, \ldots, b_N) \in \mathbb{R}^{N\times N}$, called the pinning matrix. The edges in $\mathscr{E}$ are described by the adjacency matrix $\mathscr{A} = [a_{ij}] \in \mathbb{R}^{N\times N}$, where $a_{ij} > 0$ if $(v_j, v_i) \in \mathscr{E}$ and $a_{ij} = 0$ otherwise. The Laplacian matrix $\mathscr{L} = [\mathscr{L}_{ij}]$ is defined as $\mathscr{L}_{ij} = \sum_{j=1, j\neq i}^{N} a_{ij}$ if $i = j$, otherwise $\mathscr{L}_{ij} = -a_{ij}$.

Let $q_i, \dot{q}_i \in \mathbb{R}^n$ be the generalized coordinates and their derivatives of the followers, and $q_0, \dot{q}_0 \in \mathbb{R}^n$ be the state of the leader and its derivative. Define the synchronization error $e_i \in \mathbb{R}^n$ and its derivative $\dot{e}_i \in \mathbb{R}^n$ as

$$e_i = \sum_{j\in\mathscr{N}_i} a_{ij}(q_i - q_j) + b_i(q_i - q_0) \tag{2.8a}$$

$$\dot{e}_i = \sum_{j\in\mathscr{N}_i} a_{ij}(\dot{q}_i - \dot{q}_j) + b_i(\dot{q}_i - \dot{q}_0). \tag{2.8b}$$

Define $e = [e_1^T, \ldots, e_N^T]^T$, $q = [q_1^T, \ldots, q_N^T]^T$, $\underline{q}_0 = 1_N \otimes q_0$. Accordingly, the global synchronization error with the leader is $\delta = (q - \underline{q}_0) \in \mathbb{R}^{nN}$. Then we can obtain

$$e = -(\mathscr{L} + B) \otimes \delta. \tag{2.9}$$

Note that δ cannot be used for control design as it includes global leader state information (only available to some followers).

Definition 2.7. ***Asymptotic Synchronization*** *[82] A system is said to asymptotic synchronize if for all $q_i \in \mathbb{R}^n$ such that the synchronization error e_i satisfies $e_i(q_i, t) \leq \beta(e_i(q_i, 0), t)$, where β is a class $\mathscr{KL}$ function.*

The following is a standard condition for achieving synchronization among multi-agent systems in directed graphs [21, 31, 80] .

Assumption 2.1. *The directed augmented graph representing the connections between graph $\mathcal{G}$ and the leader node v_0 contains a directed spanning tree with the root being v_0 (existence of a directed path from the leader to any follower node in the graph).*

Lemma 2.2. *[12] Under Assumption 2.1, the local and global synchronization error are related by*

$$\|\delta\| \leq \frac{\|e\|}{\underline{\lambda}(\mathcal{L}+B)} \tag{2.10}$$

*with $\|\cdot\|$ the Euclidean norm, and $\underline{\lambda}(\mathcal{L}+B)$ the minimum singular value of $(\mathcal{L}+B)$, which is positive under **Assumption** 2.1. Under the disturbance and unmodelled dynamics in the dynamics, synchronization might not be achieved in asymptotic sense, e.g. practical synchronization.*

The problem becomes especially challenging in the presence of uncertainty in the Euler-Lagrange dynamics. Developments in this field use adaptive control tools and are often referred to as *adaptive synchronization* of uncertain multi-agent systems. Recent developments in adaptive synchronization consider sinusoidal leader signals or sinusoidal disturbances that guarantee persistence of excitation for proper estimation of uncertainties [72, 73] (see also [23, 101] for the importance of persistence of excitation in adaptive control and some recent efforts to relax this condition). Some adaptive distributed approaches have been proposed to achieve asymptotic synchronization of multi-agent systems in the presence of parametric uncertainties [3, 18, 78]. However, when it comes to state-dependent uncertainties, practical synchronization (UUB synchronization) is more appropriate to deal with this problem [162].

Definition 2.8. ***Practical Synchronization*** *[82] A system is said to practically synchronize if there exists an arbitrarily small positive scalar φ for all $q_i \in \mathbb{R}^n$ such that the synchronization error e_i satisfies $e_i(q_i,t) \leq \beta(e_i(q_i,0),t)+\varphi$, where β is a class $\mathcal{KL}$ function and φ is the bound of synchronization error.*

2.3.2. THE ISSUE OF A PRIORI EXISTING INTERCONNECTIONS

Despite the progress in adaptive synchronization of multiple Euler-Lagrange systems, existing results mainly rely on two important a priori assumptions:

- the uncertainty of the system dynamics having linear-in-the-parameters (LIP) structure [31, 64];
- absence of interaction among agents before protocol design.

The first assumption is rarely met in practical situations. In particular, except for viscous friction, most friction models do not satisfy the LIP structure [76]. Notably, the presence of friction is neglected in most adaptive synchronization works (cf. the Euler-Lagrange dynamics in all aforementioned literature in Section 2.3.1). Regarding the second assumption, most aforementioned literature (cf. also [12, 51, 171]) assumes that the interconnections between agents are nonexistent before control design. That is, the agents interact with each other only as the result of the synchronization protocol. Before the

control design, each agent is assumed to be unaffected by neighboring agents, which is unrealistic in many cases. When a priori interaction is considered, such as in [41, 129], the control strategy is decentralized (i.e. it assumes each agent can access the leader's information, and agents cannot communicate with each other). This assumption on the interaction among agents restricts the applicability for synchronization for many practical cases in which agents interact in some state-dependent way. For example, in power systems [119, 133], or in the recently proposed open multi-agent systems [35], interconnections exist before the control design, coming from the state difference between neighboring agents (e.g. power flow among neighboring areas). These a priori assumptions on the structure of uncertainties and the structure of interactions motivate us towards the following research question:

Question 3: *How to design an adaptive distributed controller for multiple Euler-Lagrange agents in the presence of state-dependent uncertainty and interaction terms while overcoming the restrictive assumptions of the state of the art (e.g. the uncertainty of the system dynamics having linear-in-the-parameters (LIP) structure, and absence of interaction among agents before protocol design)?*

2.4. UNDERACTUATED EULER-LAGRANGE SYSTEMS

2.4.1. BACKGROUND OF UNDERACTUATED EULER-LAGRANGE SYSTEMS

Often, either due to the limited actuators or to component failure, many mechanical systems are not fully-actuated. Thus, underactuated systems are proposed as a class of mechanical systems with fewer control inputs than their degrees of freedom. Practical examples include underactuated robots [40], underactuated cranes [71, 105, 126], or underactuated vehicles [2, 139]: sometimes these systems can be preferable to fully-actuated systems because of lower cost or more tolerance to faults.

2.4.2. THE ISSUE OF STRUCTURAL KNOWLEDGE

Classical approaches proposed to control underactuated systems include feedback linearization [85, 117, 123], sliding mode control [9, 50, 70, 151], passivity-based control [4, 49, 88], and optimal control [19].

However, the presence of system uncertainties can put most of these classical approaches at stake and requires dedicated designs. Adaptive-robust control, originally developed for fully-actuated systems [94, 118, 125], refers to a class of adaptive controllers only requiring the knowledge of an uncertainty bound around a nominal value of the mass matrix. All the other system terms (Coriolis, gravity, friction terms) can be unknown [73, 78]. While these methods constitute a general adaptive control framework for fully-actuated Euler-Lagrange systems, such generality is missing for underactuated Euler-Lagrange systems, where it is common to focus on special classes of dynamics [38] or on specific applications (cranes, vessels, etc. [34, 91]). A non-adaptive framework for underactuated Euler-Lagrange systems has been developed under structural assumptions on the mass matrix [4, 50, 57, 70, 85, 123]. Specifically, the mass matrix should depend on the actuated states only [50], or depend on the non-actuated states only [4, 57]. Unfortunately, this condition does not only require structural knowledge, but it also turns out to be falsified in several practical scenarios, such as biped robots [40],

cranes [71], vehicles [2], and surface vessels [91].

State-dependent and possibly uncertain interconnection terms have only been considered for some classes of fully-actuated dynamics in a decentralized control approach, i.e. when the agents do not communicate with each other [41, 129]. For underactuated dynamics, distributed control was considered in [2] with the exact knowledge of system terms and no uncertain interconnections, whereas the adaptive method in [69] and non-adaptive ones in [4, 49, 88] are for single agents, i.e. the issue of uncertain interconnections does not arise. This overview shows that distributed control of underactuated Euler-Lagrange systems with uncertain system terms and interconnection terms is still an open problem in the literature. A question automatically comes up:

Question 4: *How to achieve synchronization in multiple underactuated Euler-Lagrange systems with a lack of structural knowledge for system dynamics and interconnection terms?*

3

ROBUST ADAPTIVE CONTROL OF UNCERTAIN SWITCHED LINEAR SYSTEMS

The literature review in this chapter has shown that attaining good transient behavior in leakage-based robust adaptive control of uncertain switched systems is intrinsically challenging. In fact, because the gains of the inactive subsystems must exponentially vanish during inactive times as an effect of leakage action, new learning transients will repeatedly arise at each switching instant. In this chapter, a new leakage-based mechanism is designed for robust adaptive control of uncertain switched systems: in contrast to the available designs, the key innovation of the proposed one is that the adaptive gains of the inactive subsystems can be kept constant to their switched-off values, thus preventing vanishing gains. Bounded stability of the closed-loop switched system is guaranteed thanks to the introduction of an auxiliary gain playing the role of leakage. A benchmark example commonly adopted in adaptive switched literature shows that the proposed strategy can consistently improve the transient behavior under various families of switching signals.

3.1. INTRODUCTION

From the control point of view, adaptive control of switched systems is a quite recent research field aiming at controlling switched systems with parametric uncertainties [28, 29, 54, 109, 157]. In line with the issues highlighted in the famous Rohrs's counterexample [98] or in the books [52, 130], *adaptive control designs are generally not robust.* In contrast with (non-robust) adaptive control of switched systems, where the control gains of the inactive subsystems can be kept constant at their switched-off values [54, 109, 157], in leakage-based robust adaptive control of switched systems one requires the control

This chapter is based on [132]

gains of the inactive subsystems to *decrease exponentially during inactive intervals*. This is necessary in order to prove (bounded) stability, because such a exponential decrease is a stabilizing effect of the leakage action. Of course, *such a vanishing-gain mechanism would lead to a new learning transient whenever an inactive system is activated again.* This is up to now, the biggest challenge in robust adaptive control of switched systems.

The work in this chapter presented in this paper is motivated by the aforementioned ***Question 1:*** *How to design a robust adaptive controller for uncertain switched systems that does not require the control gains to vanish during their switched-off phase?*

A positive answer to this question is provided here. A new leakage-based framework is proposed, whose main contribution is to allow the control gains of the inactive subsystems to stay constant at their switched-off value, while guaranteeing the stability of the closed-loop switched system. This is achieved via a new auxiliary gain that provides a suitable leakage action during inactive time intervals. A benchmark example commonly adopted in adaptive and robust adaptive literature shows that the proposed strategy can consistently improve the transient of the closed-loop system under various families of slowly-switching signals (in the framework of dwell time and its extensions).

The rest of this chapter is organized as follows. The problem formulation and definition are presented in Section 3.2. The proposed robust adaptive mechanism is presented in Section 3.3, while its stability analysis is provided in Section 3.4. In Section 3.5, the effectiveness of the proposed controller is extensively studied using the benchmark example. Section 3.6 presents concluding remarks.

3.2. PROBLEM FORMULATION

In the following we recall the main concepts of model reference adaptive control, the most studied framework for adaptive control of switched systems [29, 54, 109, 157]. Consider the following switched linear system:

$$\dot{x}(t) = A_{\sigma(t)}x(t) + B_{\sigma(t)}u_{\sigma(t)}(t) + d(t),\ \sigma(t) \in \Omega \tag{3.1}$$

where $x \in \mathbb{R}^n$ is the state vector; $u_\sigma \in \mathbb{R}^m$ is the (switched) control input; $d \in \mathbb{R}^n$ is an external bounded disturbance with unknown bound, and $\sigma(\cdot)$ is the piecewise constant switching signal (to be defined later) taking values in $\Omega := \{1, 2, \dots, N\}$, with switching instants denoted by $t_l, t_{l+1}, \cdots$, and with intervals in between instants denoted by $[t_l, t_{l+1})$, $l = 1, 2, \cdots$, and with N the number of subsystems. The switched linear system (3.1) is uncertain when the entries of the matrices $A_p \in \mathbb{R}^{n\times n}$ and $B_p \in \mathbb{R}^{n\times m}$, $p \in \Omega$ are unknown.

A switched reference model representing the desired behavior for each subsystem is given as:

$$\dot{x}_m(t) = A_{m\sigma(t)}x_m(t) + B_{m\sigma(t)}r(t),\ \sigma(t) \in \Omega \tag{3.2}$$

where $x_m \in \mathbb{R}^n$ is the desired state vector, and $r \in \mathbb{R}^m$ is a bounded user-defined signal. The matrices $A_{mp} \in \mathbb{R}^{n\times n}$ and $B_{mp} \in \mathbb{R}^{n\times m}$ are known and $A_{mp}, p \in \Omega$, are Hurwitz matrices (so that the desired behavior of each subsystem is stable). It is known from literature [29, 54, 109, 157] that the state-feedback mode-dependent control law that makes (3.1) behave like (3.2) is

$$u^*_{\sigma(t)}(t) = K^{*T}_{\sigma(t)}x(t) + L^*_{\sigma(t)}r(t)$$

where $K_p^* \in \mathbb{R}^{n\times m}$ and $L_p^* \in \mathbb{R}^{m\times m}$, $p \in \Omega$, are nominal parameters satisfying the following matching conditions:

$$A_p + B_p K_p^{*T} = A_{mp}, \quad B_p L_p^* = B_{mp}. \tag{3.3}$$

As the matrices (A_p, B_p) are unknown, the gains K_p^* and L_p^* in (3.3) are unknown. Define K_p and L_p as the (time-dependent) estimates of the ideal parameters K_p^* and L_p^*, respectively. Thus, the following controller is introduced:

$$u_{\sigma(t)}(t) = K_{\sigma(t)}^T(t)x(t) + (L_{\sigma(t)}(t) + \Gamma_{\sigma(t)}(t))r(t), \tag{3.4}$$

where $K_p \in \mathbb{R}^{n\times m}$, $L_p \in \mathbb{R}^{m\times m}$ and $\Gamma_p = \text{diag}\{\gamma_{ip}\}$, $p \in \Omega$, $i = 1, \cdots, m$ are to be updated from appropriately designed adaptive laws. As compared to (3.3), the introduction of Γ_p in (3.4) is for robustness reasons, as it will become clear from Section 3.3.

Let $e(t) = x(t) - x_m(t)$ be the tracking error. After substituting (3.4) into (3.1) and subtracting (3.2), we obtain the dynamics of the tracking error as follows:

$$\dot{e}(t) = A_{m\sigma(t)}e(t) + B_{\sigma(t)}\big(\tilde{K}_{\sigma(t)}^T(t)x(t) + (\tilde{L}_{\sigma(t)}(t) + \Gamma_{\sigma(t)}(t))r(t)\big) + d(t) \tag{3.5}$$

where $\tilde{K}_\sigma = K_\sigma - K_\sigma^*$ and $\tilde{L}_\sigma = L_\sigma - L_\sigma^*$ are the parameter estimation errors.

When the switching sequence is known, we indicate the fact that the next mode to be switched on after p is q with $q \in \mathcal{N}(p)$. Then, we present the following definitions:

Definition 3.1. ***(Model-mode-dependent Dwell Time)*** *[158]: Consider two consecutive switching time instants $t_{i+1} > t_i \geq 0$ with $\sigma(t_i) = p$, $\sigma(t_{i+1}) = q$. We say that the switching signal $\sigma(\cdot)$ has* model-mode-dependent dwell time (MMDDT) *ϑ_{pq} for every pair of $p \in \Omega$, $q \in \mathcal{N}(p)$ if there exist $\vartheta_{pq} > 0$ such that*

$$t_{i+1} - t_i \geq \vartheta_{pq}, \forall i \in \mathbb{N}^+ \tag{3.6}$$

Definition 3.2. ***(Mode-mode-dependent Average Dwell Time)****. Let $N_{pq}(t_1, t_2)$ be the number of times subsystems p is activated over the interval $[t_1, t_2]$, $q \in \mathcal{N}(p)$, and let $T_{pq}(t_1, t_2)$ denote the total running time of subsystem p switching to q over the interval $[t_1, t_2]$. We say that $\sigma(\cdot)$ has* mode-mode-dependent average dwell time (MMDADT) *ϑ_{pqa} for every pair of $p \in \Omega$, $q \in \mathcal{N}(p)$ if there exist positive numbers $N_{0pq} \geq 1$ and ϑ_{pqa} such that*

$$N_{pq}(t_1, t_2) \leq N_{0pq} + \frac{T_{pq}(t_1, t_2)}{\vartheta_{pqa}}, \ \forall t_2 \geq t_1 \geq 0 \tag{3.7}$$

where N_{0pq} is called the mode-mode-dependent chatter bound.

Remark 3.1. *The MMDADT switching signal is an extension in an average sense of the MMDDT proposed in [158]. It is introduced for consistency, in order to be able to run fair comparisons with many switching families introduced in the literature.*

We now introduce some standard stability concepts. In robust adaptive control of uncertain switched systems, uniform boundedness of the tracking error and of the closed-loop signal is what one can aim at [22, 128, 154, 156, 158, 168]. This concept is formalized in the definitions of ***Uniform Ultimate Boundedness (UUB) and Ultimate Bound*** introduced in **Chapter 2**, **Definition** 2.5.

The following assumption is standard (see survey [131]), in order to handle adaptive control of multi-input linear subsystems in (3.1).

Assumption 3.1. *The matching conditions (3.3) hold for some unknown K_p^* and L_p^*, and there exists a family of known matrices $S_p \in \mathbb{R}^{m\times m}$, $p \in \Omega$, such that $M_p = L_p^* S_p = (L_p^* S_p)^T = S_p^T L_p^{*T} > 0,\ \forall p \in \Omega$.*

The problem formulation can be finally given as:

Problem 3.1. *Under **Assumption** 3.1, develop an adaptive law for the control parameters in (3.4) and a switching law based on MDADT (or MMDADT if the switching sequence is known) such that, without requiring knowledge of the nominal values of A_p and B_p, $\forall p \in \Omega$, uniform ultimate boundedness of all closed-loop signals is guaranteed, including the tracking error in (3.5).*

3.3. CONTROLLER DESIGN

In this section, novel adaptive laws for the gains in (3.4) are proposed to solve **Problem** 3.1. Correspondingly, stabilizing switching laws are given in the framework of MDADT switching (or MMDADT if the switching sequence is known).

3.3.1. ADAPTIVE CONTROL

For compactness, let us denote with p the index corresponding to the active subsystem at time t (e.g. in the interval $t \in [t_l, t_{l+1})$). If p is an active system, we use $\overline{p} \in \mathscr{I}(p) = \Omega\backslash\{p\}$ to indicate the set of inactive subsystems with respect to p. Let $P_p > 0$ be the solution to

$$A_{mp}^T P_p + P_p A_{mp} + (1+\kappa_p) P_p \le 0, \tag{3.8}$$

where κ_p is a user-defined scalar.

Then, consider the leakage-based adaptive laws

$$\dot{K}_p^T(t) = -S_p^T B_{mp}^T P_p e(t) x^T(t) - \delta_p K_p^T(t),\ \dot{K}_{\overline{p}}^T(t) = 0, \tag{3.9a}$$

$$\dot{L}_p(t) = -S_p^T B_{mp}^T P_p e(t) r^T(t) - \delta_p L_p(t),\ \dot{L}_{\overline{p}}(t) = 0, \tag{3.9b}$$

$$\dot{\gamma}_{ip}(t) = 0,$$

$$\dot{\gamma}_{i\overline{p}}(t) = -\left[\beta_{i\overline{p}} + \delta_{\overline{p}}\left(\left\{K_{\overline{p}}(t)K_{\overline{p}}^T(t)\right\}_{ii} + \left\{L_{\overline{p}}^T(t)L_{\overline{p}}(t)\right\}_{ii}\right)\right]\gamma_{i\overline{p}}(t) + \beta_{i\overline{p}}\epsilon_{i\overline{p}},\ \forall \overline{p} \in \mathscr{I}(p) \tag{3.9c}$$

$$\text{with } \delta_\sigma \ge \max_{\sigma\in\Omega}\left(\frac{(\lambda_{\max}(M_\sigma^{-1}) + \kappa_\sigma)}{2},\ 2\kappa_\sigma\lambda_{\max}(M_\sigma^{-1})\right) > 0, \tag{3.9d}$$

$$\text{and } \gamma_{ip}(t_0),\ \gamma_{i\overline{p}}(t_0) > \epsilon_{i\overline{p}} \tag{3.9e}$$

where the notations $\{K_{\overline{p}}K_{\overline{p}}^T\}_{ii}$ and $\{L_{\overline{p}}^T L_{\overline{p}}\}_{ii}$ are used to indicate diagonal elements along the corresponding matrices; $\beta_{i\overline{p}},\ \epsilon_{i\overline{p}} \in \mathbb{R}^+\ i = 1,\cdots,m$ are static design scalars and t_0 is the initial time. The condition (3.9d) stem from Assumption 3.1, which implies an upper bound knowledge on the perturbation in matrix B_σ is known. Such consideration is standard in literature and also valid in practical systems (cf. [106]).

Remark 3.2. *The inequality (3.8) is equivalent to the standard Lyapunov inequality*

$$\left(A_{mp}^T + (1+\kappa_p)/2I\right)P_p + P_p\left(A_{mp}^T + (1+\kappa_p)/2I\right) \leq 0 \tag{3.10}$$

which highlights how A_{mp} of the reference models should be chosen in such a way that their eigenvalues have sufficiently large real part (implying sufficiently high exponential decay). This is not restrictive, since it is a standard requirement for stability of switched systems, obtained by requiring that the possibly destabilizing effects of switching are compensated by the exponential decrease in between switching instants [46, 65, 66].

For comparison purposes, let us explicitly recall the robust adaptive law in [158]

$$\dot{K}_p^T(t) = -S_p^T B_{mp}^T P_p e(t) x^T(t) - \delta_p M_p K_p^T(t), \tag{3.11a}$$

$$\dot{L}_p(t) = -S_p^T B_{mp}^T P_p e(t) r^T(t) - \delta_p M_p L_p(t), \tag{3.11b}$$

$$\dot{K}_{\overline{p}}^T(t) = -\delta_{\overline{p}} M_{\overline{p}} K_{\overline{p}}^T(t),\ \forall \overline{p} \in \mathscr{I}(p) \tag{3.11c}$$

$$\dot{L}_{\overline{p}}(t) = -\delta_{\overline{p}} M_{\overline{p}} L_{\overline{p}}(t),\ \forall \overline{p} \in \mathscr{I}(p) \tag{3.11d}$$

where the leakage rates δ_p must satisfy: $\delta_p \geq \lambda_{\max}(M_p^{-1}) \geq 0$, and $\delta_{\overline{p}}$ must satisfy: $\delta_{\overline{p}} \geq \lambda_{\max}(M_{\overline{p}}^{-1}) \geq 0$.

It can be seen that the adaptive laws (3.11) are designed such that the gains for the inactive subsystems vanish exponentially during the inactive times, as an effect of leakage. This is required in order to prove UUB [158]. Unfortunately, this mechanism implies that the gains will drop to zero if a subsystem remains inactive for a sufficiently long time. This will lead to a new learning transient every time the subsystem is switched on again. This undesirable scenario is avoided by (3.9a) and (3.9b) where the adaptive gains are kept constant after the subsystem is switched-off. Such the slight difference in leakage action between (3.9) and (3.11) results significant difference in the transient performance (see the simulation section 3.5 for more details on this point).

3.3.2. SWITCHING LAWS

In this section, a stabilizing switching law is given in terms of MDADT switching (or MMDADT if the switching sequence is known).

We define $\varrho_{M\sigma} \triangleq \lambda_{\max}(P_\sigma)$, $\varrho_{m\sigma} \triangleq \lambda_{\min}(P_\sigma)$, $\overline{\varrho} \triangleq \max_{\sigma\in\Omega}(\varrho_{M\sigma})$ and $\underline{\varrho} \triangleq \min_{\sigma\in\Omega}(\varrho_{m\sigma})$. Following **Definition 2.4** of MDADT, the switching law is proposed via:

$$\vartheta_{pa} > \vartheta_{pa}^* = \frac{1}{\chi_p} \ln \mu_p,\ \forall p \in \Omega \tag{3.12}$$

and any $N_{0p} \geq 1$, where $\mu_p \triangleq \varrho_{Mp}/\varrho_{mp}$; χ_p is a user-defined scalar satisfying $0 < \chi_p < \kappa_p, \forall p \in \Omega$.

According to **Remark 2.1**, the switching law (3.12) includes DT, MDDT, and ADT as special cases. For the scenario when the next subsystem q to be switched after subsystem p is known, we propose a MMDADT switching law in line with **Definition** 3.2 via

$$\vartheta_{pqa} > \vartheta_{pqa}^* = \frac{1}{\chi_p} \ln \mu_{pq},\ \forall p \in \Omega,\ q = \mathscr{N}(p), \tag{3.13}$$

where $\mu_{pq} = \varrho_{Mq}/\varrho_{mp}$. The MMDADT law is proposed for subsequent comparisons with [158].

Remark 3.3. *It is important to notice that, when selecting the same κ_p as [158] (thus obtaining the same P_p and μ_p in in (3.8) and (3.12), respectively), one will obtain exactly the same ϑ_{pa} as [158] (since the design parameter ζ_p in [158] plays exactly the same role as χ_p here). Therefore, the proposed adaptation mechanism does not introduce any restriction in ϑ_{pa} as compared to the state of the art. This allows a fair comparison of the proposed method with the method in [158], i.e. the methods can be compared for the same switching signals.*

3

3.4. STABILITY ANALYSIS

The following lemma is useful for stability analysis:

Lemma 3.1. *[152] Let $\Phi \in \mathbb{R}^g, \varphi \in \mathbb{R}_s$ be vector-valued signals, and let $W \in \mathbb{R}^{g\times g}, G \in R^{g\times s}$ be constant matrices. Then, the following inequality holds:*

$$\pm 2\Phi^T WG\varphi \leq \Phi^T WW^T\Phi + \varphi^T G^T G\varphi$$

The stability properties of the proposed adaptation framework can now be stated:

Theorem 3.1. *Under **Assumption 3.1**, the closed-loop switched system formed by the switched system (3.1), the reference model (3.2), the controller (3.4), the adaptive laws (3.9), and the switching law (3.12), is Uniformly Ultimately Bounded (UUB) and an ultimate bound b on the tracking error e can be found as*

$$b \in \left[0, \sqrt{\frac{\overline{\varrho}}{\underline{\varrho}^2}\mathscr{B}\prod_{p=1}^{N}\mu_p^{N_{0p}}}\right], \tag{3.14}$$

$$\mathscr{B} \triangleq \max_{p\in\Omega}\left(\frac{\zeta_1}{\sqrt{\underline{\varrho}_m}(\kappa_p-\chi_p)} + \sqrt{\frac{\zeta_1^2}{\underline{\varrho}(\kappa_p-\chi_p)^2} + \frac{\zeta_2}{(\kappa_p-\chi_p)}}\right)^2,$$

where the scalars ζ_1, $\zeta_2 \in \mathbb{R}^+$ are defined during the proof.

Proof: Stability relies on the Lyapunov candidate defined by:

$$V(t) = e^T(t)P_{\sigma(t)}e(t) + \sum_{s=1}^{N}\mathrm{tr}\left[\tilde{K}_s(t)M_s^{-1}\tilde{K}_s^T(t)\right] + \sum_{s=1}^{N}\mathrm{tr}\left[\tilde{L}_s^T(t)M_s^{-1}\tilde{L}_s(t)\right] + \sum_{s=1}^{N}\mathrm{tr}\left[\underline{\Gamma}_s\Gamma_s(t)\right] \tag{3.15}$$

where $\underline{\Gamma}_\sigma = \mathrm{diag}\left\{1/\underline{\gamma}_{i\sigma}\right\}$. In fact, from (3.9c) and the initial conditions (3.9e), it can be verified that $\exists \underline{\gamma}_{i\sigma}, \overline{\gamma}_{i\sigma} \in \mathbb{R}^+$ such that

$$\underline{\gamma}_{i\sigma} \leq \gamma_{i\sigma}(t) \leq \overline{\gamma}_{i\sigma}, \ \forall t \geq t_0. \tag{3.16}$$

Analysis of (3.15) at the switching instants is required, since P_p is different for different subsystems generally (i.e. $V(\cdot)$ might be discontinuous at switching instants). Let

subsystem $\sigma(t_{l+1}^-)$ be active when $t \in [t_l, t_{l+1})$ and subsystem $\sigma(t_{l+1})$ be active when $t \in [t_{l+1}, t_{l+2})$. Without the loss of generality, the behavior of $V(\cdot)$ is studied at the switching instant $t_{l+1}, l \in \mathbb{N}^+$.

At the switching instant t_{l+1}, we have before switching

$$V(t_{l+1}^-) = e^T(t_{l+1}^-)P_{\sigma(t_{l+1}^-)}e(t_{l+1}^-) + \sum_{s=1}^{N} \mathrm{tr}\Big[\underline{\Gamma}_s(t_{l+1}^-)\Gamma_s(t_{l+1}^-)\Big] + \sum_{s=1}^{N} \mathrm{tr}\Big[\tilde{K}_s(t_{l+1}^-)M_s^{-1}\tilde{K}_s^T(t_{l+1}^-)\Big] + \sum_{s=1}^{N} \mathrm{tr}\Big[\tilde{L}_s^T(t_{l+1}^-)M_s^{-1}\tilde{L}_s(t_{l+1}^-)\Big]$$

and after switching

$$V(t_{l+1}) = e^T(t_{l+1})P_{\sigma(t_{l+1})}e(t_{l+1}) + \sum_{s=1}^{N} \mathrm{tr}\Big[\underline{\Gamma}_s(t_{l+1}^-)\Gamma_s(t_{l+1})\Big] + \sum_{s=1}^{N} \mathrm{tr}\Big[\tilde{K}_s(t_{l+1})M_s^{-1}\tilde{K}_s^T(t_{l+1})\Big] + \sum_{s=1}^{N} \mathrm{tr}\Big[\tilde{L}_s^T(t_{l+1})M_s^{-1}\tilde{L}_s(t_{l+1})\Big]$$

According to the continuity of the tracking error $e(\cdot)$ in (3.5) and the continuity of the parameter estimates updated via (3.9), we have $e(t_{l+1}^-) = e(t_{l+1})$, $\tilde{K}_s(t_{l+1}^-) = \tilde{K}_s(t_{l+1})$, $\tilde{L}_s(t_{l+1}^-) = \tilde{L}_s(t_{l+1})$, and $\Gamma_s(t_{l+1}^-) = \Gamma_s(t_{l+1})$ for any switching law. Due to $e^T(t)P_p e(t) \le \varrho_{Mp} e^T(t)e(t)$, and $e^T(t)P_p e(t) \ge \varrho_{mp} e^T(t)e(t)$ we have

$$\begin{aligned} &V(t_{l+1}) - V(t_{l+1}^-) = e^T(t_{l+1}^-)(P_{\sigma(t_{l+1})} - P_{\sigma(t_{l+1}^-)})e(t_{l+1}^-) \\ &\le \frac{\varrho_{Mp} - \varrho_{mp}}{\varrho_{mp}} e^T(t_{l+1}^-)P_{\sigma(t_{l+1}^-)}e(t_{l+1}^-) \le \frac{\varrho_{Mp} - \varrho_{mp}}{\varrho_{mp}} V(t_{l+1}^-) \end{aligned}$$

Then, we obtain the following inequality for $V(\cdot)$ at the switching instant t_{l+1}:

$$V(t_{l+1}) \le \mu_p V(t_{l+1}^-) \tag{3.17}$$

with $\mu_p = \varrho_{Mp}/\varrho_{mp} \ge 1$.

Next, the behavior of $V(t)$ is studied between two consecutive switching instants, i.e., when $t \in [t_l,\ t_{l+1})$. In the following, let $\sigma(t) = p$ denote an active subsystem and an inactive is denoted as $\overline{p} = \Omega\backslash\{p\}$ when $t \in [t_{l+1}, t_{l+2})$. Let us also use the notation $\mathscr{I}(p)$ to indicate all inactive subsystems when subsystem p is active. Then using (3.8), (3.5) and (3.9a)-(3.9c) we have

$$\begin{aligned} \dot{V} &\le -e^T(1+\kappa_p)P_p e + 2e^T P_p B_p(\tilde{K}_p x + (\tilde{L}_p + \Gamma_p)r) + 2e^T P_p d \\ &+ 2\sum_{s=1}^{N} \mathrm{tr}\Big[\tilde{K}_s M_s^{-1}\dot{K}_s^T\Big] + 2\sum_{s=1}^{N} \mathrm{tr}\Big[\tilde{L}_s^T M_s^{-1}\dot{L}_s\Big] + 2\sum_{s=1}^{N} \mathrm{tr}\Big[\underline{\Gamma}_s\dot{\Gamma}_s\Big] \\ &\le -\kappa_p e^T P_p e + 2e^T P_p B_p \Gamma_p r + d^T P_p d + \sum_{\overline{p}\in\mathscr{I}(p)} \mathrm{tr}\Big[\underline{\Gamma}_{\overline{p}}\dot{\Gamma}_{\overline{p}}\Big] \\ &\quad - 2\mathrm{tr}\Big[\tilde{K}_p\delta_p M_p^{-1}K_p^T\Big] - 2\mathrm{tr}\Big[\tilde{L}_p^T\delta_p M_p^{-1}L_p\Big]. \end{aligned} \tag{3.18}$$

The following simplification can be made using **Lemma** 3.1:

$$-2\text{tr}\left[\tilde{K}_p\delta_p M_p^{-1}K_p^T\right] < -\text{tr}\left[\tilde{K}_p M_p^{-1}(2\delta_p I - M_p^{-1})\tilde{K}_p^T\right] + \text{tr}[K_p^*\delta_p^2 K_p^{*T}], \tag{3.19a}$$

$$-2\text{tr}\left[\tilde{L}_p^T\delta_p M_p^{-1}L_p\right] < -\text{tr}\left[\tilde{L}_p^T M_p^{-1}(2\delta_p I - M_p^{-1})\tilde{L}_p\right] + \text{tr}\left[L_p^{*T}\delta_p^2 L_p^*\right]. \tag{3.19b}$$

Further, noting $\underline{\Gamma}_{\overline{p}}\dot{\Gamma}_{\overline{p}} = \text{diag}\left\{\dot{\gamma}_{i\overline{p}}/\underline{\gamma}_{i\overline{p}}\right\}$, $i = 1,\cdots,m$, the following can be deduced from (3.9c) and (3.16)

$$\begin{aligned}\frac{\dot{\gamma}_{i\overline{p}}}{\underline{\gamma}_{i\overline{p}}} &= \frac{-\left(\beta_{i\overline{p}} + \delta_{\overline{p}}\left(\{K_{\overline{p}}K_{\overline{p}}^T\}_{ii} + \{L_{\overline{p}}^T L_{\overline{p}}\}_{ii}\right)\right)\gamma_{i\overline{p}} + \beta_{i\overline{p}}\epsilon_{i\overline{p}}}{\underline{\gamma}_{i\overline{p}}} \\ &\leq -\delta_{\overline{p}}\left(\{K_{\overline{p}}K_{\overline{p}}^T\}_{ii} + \{L_{\overline{p}}^T L_{\overline{p}}\}_{ii}\right) + (\beta_{i\overline{p}}\epsilon_{i\overline{p}})/\underline{\gamma}_{i\overline{p}}.\end{aligned} \tag{3.20}$$

Moreover, using the relations $\tilde{K}_\sigma = K_\sigma - K_\sigma^*$, $\tilde{L}_\sigma = L_\sigma - L_\sigma^*$ and **Lemma** 3.1 we have

$$\text{tr}[\tilde{K}_\sigma^T\tilde{K}_\sigma] = \text{tr}[K_\sigma^T K_\sigma - 2K_\sigma^T K_\sigma^* + K_\sigma^{*T}K_\sigma^*] \leq 2\text{tr}[K_\sigma^T K_\sigma + K_\sigma^{*T}K_\sigma^*], \tag{3.21a}$$

$$\text{tr}[\tilde{L}_\sigma^T\tilde{L}_\sigma] = \text{tr}[L_\sigma^T L_\sigma - 2L_\sigma^T L_\sigma^* + L_\sigma^{*T}L_\sigma^*] \leq 2\text{tr}[L_\sigma^T L_\sigma + L_\sigma^{*T}L_\sigma^*]. \tag{3.21b}$$

Using (3.19)-(3.21), (3.18) is simplified as

$$\begin{aligned}&\dot{V} \leq -\kappa_p V + 2e^T P_p B_p \Gamma_p r + d^T P_p d \\ &-\text{tr}[\tilde{K}_p M_p^{-1}(2\delta_p I - (M_p^{-1} + \kappa_p I))\tilde{K}_p^T] + \text{tr}[K_p^{*T}\delta_p^2 K_p^*] - \text{tr}[\tilde{L}_p M_p^{-1}(2\delta_p I - (M_p^{-1} + \kappa_p I))\tilde{L}_p^T] \\ &+ \sum_{\overline{p}\in\mathscr{I}(p)}\text{tr}[\tilde{K}_{\overline{p}}^T\tilde{K}_{\overline{p}}(\kappa_{\overline{p}}\lambda_{\max}(M_{\overline{p}}^{-1}) - (1/2)\delta_{\overline{p}})] + (1/2)\text{tr}[K_{\overline{p}}^{*T}\delta_{\overline{p}}K_{\overline{p}}^*] + \sum_{s=1}^{N}\text{tr}[\kappa_s\underline{\Gamma}_s\Gamma_s] + \text{tr}[L_p^{*T}\delta_p^2 L_p^*] \\ &+ \sum_{\overline{p}\in\mathscr{I}(p)}\text{tr}[\tilde{L}_{\overline{p}}^T\tilde{L}_{\overline{p}}(\kappa_{\overline{p}}\lambda_{\max}(M_{\overline{p}}^{-1}) - (1/2)\delta_{\overline{p}})] + (1/2)\text{tr}[L_{\overline{p}}^{*T}\delta_{\overline{p}}L_{\overline{p}}^*] + \sum_{\overline{p}\in\mathscr{I}(p)}\sum_{i=1}^{m}(\beta_{i\overline{p}}\epsilon_{i\overline{p}})/\underline{\gamma}_{i\overline{p}} \\ &\leq -\kappa_p V + 2||e||||P_p B_p\Gamma_p r|| + \varrho_{Mp}||d||^2 + \text{tr}[K_p^{*T}\delta_p^2 K_p^*] + \text{tr}[L_p^{*T}\delta_p^2 L_p^*] \\ &+ \sum_{s=1}^{N}\text{tr}[\kappa_s\underline{\Gamma}_s\Gamma_s] + \sum_{\overline{p}\in\mathscr{I}(p)}\left((1/2)\text{tr}[K_{\overline{p}}^{*T}\delta_{\overline{p}}K_{\overline{p}}^*] + (1/2)\text{tr}[L_{\overline{p}}^{*T}\delta_{\overline{p}}L_{\overline{p}}^*] + \sum_{i=1}^{m}(\beta_{i\overline{p}}\epsilon_{i\overline{p}})/\underline{\gamma}_{i\overline{p}}\right).\end{aligned} \tag{3.22}$$

By definition $r \in \mathscr{L}_\infty$ and by design $\Gamma_s \in \mathscr{L}_\infty$ from (3.16). Therefore, $\exists\zeta_1 \in \mathbb{R}^+$ such that $||P_p B_p\Gamma_p r|| \leq \zeta_1\ \forall p \in \Omega$. Further we define a scalar ζ_2 as

$$\begin{aligned}\zeta_2 \triangleq\ &\overline{\varrho}||d||^2 + \max_{p\in\Omega}(\text{tr}[K_p^{*T}\delta_p^2 K_p^*] + \text{tr}[L_p^{*T}\delta_p^2 L_p^*]) + \sum_{s=1}^{N}\text{tr}[\kappa_s\underline{\Gamma}_s\Gamma_s] \\ &+ \sum_{\overline{p}\in\mathscr{I}(p)}\left((1/2)\text{tr}[K_{\overline{p}}^{*T}\delta_{\overline{p}}K_{\overline{p}}^*] + (1/2)\text{tr}[L_{\overline{p}}^{*T}\delta_{\overline{p}}L_{\overline{p}}^*] + \sum_{i=1}^{m}(\beta_{i\overline{p}}\epsilon_{i\overline{p}})/\underline{\gamma}_{i\overline{p}}\right).\end{aligned} \tag{3.23}$$

Again, the definition of the Lyapunov function (3.15) yields

$$V \geq \lambda_{\min}(P_p)||e||^2 \geq \underline{\varrho}_m||e||^2. \tag{3.24}$$

We had defined χ_p earlier such that $0 < \chi_p < \kappa_p$. Hence, using (3.23)-(3.24), (3.22) is simplified as

$$\dot{V} \leq -\chi_p V - (\kappa_p - \chi_p)V + 2\zeta_1\sqrt{V/\underline{\varrho}} + \zeta_2. \tag{3.25}$$

Thus, $\dot{V} \leq -\epsilon_p V$ is established when

$$V \geq \max_{p\in\Omega}\left(\frac{\zeta_1}{\sqrt{\underline{\varrho}}(\kappa_p-\chi_p)} + \sqrt{\frac{\zeta_1^2}{\underline{\varrho}(\kappa_p-\chi_p)^2} + \frac{\zeta_2}{(\kappa_p-\chi_p)}}\right)^2.$$

So we obtain that a positive scalar $\mathscr{B}$ as

$$\mathscr{B} = \max_{p\in\Omega}\left(\frac{\zeta_1}{\sqrt{\underline{\varrho}}(\kappa_p-\chi_p)} + \sqrt{\frac{\zeta_1^2}{\underline{\varrho}(\kappa_p-\chi_p)^2} + \frac{\zeta_2}{(\kappa_p-\chi_p)}}\right)^2. \tag{3.26}$$

In light of this, further analysis is needed to observe the behavior of $V(t)$ between the two consecutive switching instants, i.e. $t \in [t_l,\ t_{l+1})$, for two possible cases:

(i) when $V(t) \geq \mathscr{B}$, we have $\dot{V}(t) \leq -\chi_p V(t)$ from (3.25) implying exponential decrease of $V(t)$;

(ii) when $V(t) < \mathscr{B}$, no exponential decrease can be derived.

The behavior of $V(t)$ is discussed below individually for these two cases.

Case (i): There exists a time, call it T_1, when $V(t)$ enters into the bound $\mathscr{B}$ and $\overline{N}(t)$ denotes the number of all switching intervals for $t \in [t_0,\ t_0+T_1)$. Accordingly, for $t \in [t_0,\ t_0+T_1)$, using (3.17), (3.25) and from **Definition** 2.4 we have

$$\begin{aligned}
V(t) &\leq \exp\left(-\chi_{\sigma(\overline{N}(t)-1)}(t_{\overline{N}(t)} - t_{\overline{N}(t)-1})\right) V(t_{\overline{N}(t)-1})\\
&\leq \mu_{\sigma(\overline{N}(t)-1)} \exp\left(-\chi_{\sigma(\overline{N}(t)-1)}(t_{\overline{N}(t)} - t_{\overline{N}(t)-1})\right) V(t^-_{\overline{N}(t)-1})\\
&\leq \mu_{\sigma(\overline{N}(t)-1)} \exp\left(-\chi_{\sigma(\overline{N}(t)-1)}(t_{\overline{N}(t)} - t_{\overline{N}(t)-1})\right)\cdot\\
&\mu_{\sigma(\overline{N}(t)-2)} \exp\left(-\chi_{\sigma(\overline{N}(t)-2)}(t_{\overline{N}(t)-1} - t_{\overline{N}(t)-2})\right) V(t^-_{\overline{N}(t)-2})\\
&\qquad\qquad\vdots\\
&\leq \mu_{\sigma(\overline{N}(t)-1)} \exp\left(-\chi_{\sigma(\overline{N}(t)-1)}(t_{\overline{N}(t)} - t_{\overline{N}(t)-1})\right)\cdot\\
&\mu_{\sigma(\overline{N}(t)-2)} \exp\left(-\chi_{\sigma(\overline{N}(t)-2)}(t_{\overline{N}(t)-1} - t_{\overline{N}(t)-2})\right)\cdot\\
&\quad \cdots \mu_{\sigma(t_0)} \exp\left(-\chi_{\sigma t_0}(t_1 - t_0)\right) V(t_0)\\
&= \prod_{p=1}^{N} \mu_p^{N_p} \exp\big(\sum_{p=1}^{N} \chi_p T_p(t_0, t_0+T_1)\big) V(t_0)\\
&= c\exp\left(\sum_{p=1}^{m} (\frac{\ln\mu_p}{\vartheta_{pa}} - \chi_p) T_p(t_0, t_0+T_1)\right) V(t_0),
\end{aligned} \tag{3.27}$$

where $c \triangleq \exp(\sum_{p=1}^{m} N_{0p} \ln \mu_p)$ is a constant. Substituting the MDADT condition $\vartheta_{pa} > \ln \mu_p / \chi_p$ into (3.27) yields $V(t) < cV(t_0)$ for $t \in [t_0 \;\; t_0 + T_1)$. Moreover, as $V(t_0 + T_1) < \mathscr{B}$, one has $V(t_{\overline{N}+1}) < \mu_{\sigma(t^-_{\overline{N}+1})}\mathscr{B}$ from (3.17) at the next switching instant $t_{\overline{N}+1}$ after $t_0 + T_1$. This implies that $V(t)$ may be larger than $\mathscr{B}$ from the instant $t_{\overline{N}+1}$. This necessitates further analysis.

We assume $V(t) \geq \mathscr{B}$ for $t \in [t_{\overline{N}(t)+1},\ t_0 + T_2)$, where T_2 denotes the time before next switching. Let $\overline{N}(t)$ represent the number of all switching intervals for $t \in [t_{\overline{N}+1},\ t_0 + T_2)$. Then, substituting $V(t_0)$ with $V(t_{\overline{N}+1})$ in (3.27) and following the similar procedure for analysis as (3.27), we have $V(t) \leq cV(t_{\overline{N}(t)+1}) < c\mu_{\sigma(t^-_{\overline{N}(t)+1})}\mathscr{B}$ for $t \in [t_{\overline{N}(t)+1},\ t_0+T_2)$. Since $V(t_0 + T_2) < \mathscr{B}$, we have $V(t_{\overline{N}+\overline{N}+2}) < c\mu_{\sigma(t^-_{\overline{N}+\overline{N}+2})}\mathscr{B}$ at the next switching instant $t_{\overline{N}+\overline{N}+2}$ after $t_0 + T_2$. If we follow similar lines of proof recursively, we can come to the conclusion that $V(t) < c \max_{p\in\Omega}\{\varrho_{Mp}/\varrho_{mp}\}\mathscr{B} < c\mu\mathscr{B}$ where $\mu = \overline{\varrho}/\underline{\varrho}$ for $t \in [t_0 + T_1,\ \infty)$. This confirms that once $V(t)$ enters the interval $[0, \mathscr{B}]$, it cannot exceed the bound $c\mu\mathscr{B}$ any time later with the ADT switching law (3.12).

Case (ii): It can be easily verified that the same argument below (3.27) also holds for Case (ii).

Next, we study the dynamics of the tracking error: Based on the aforementioned analysis about UUB, it can be obtained that

$$V(t) \leq \max\left\{V(t_0), c\mu\mathscr{B}\right\}, \forall t \in t_0. \tag{3.28}$$

Then, it follows from that the tracking error is upper bounded in the following form:

$$\|e(t)\|^2 \leq \frac{1}{\underline{\varrho}} \max\left\{V(t_0), c\mu\mathscr{B}\right\}. \tag{3.29}$$

Substituting $c \triangleq \exp(\sum_{p=1}^{m} N_{0p} \ln \mu_p)$ and $\mu = \overline{\varrho}/\underline{\varrho}$ into (3.29), thus the tracking error is UUB with an ultimate bound b with

$$b \in \left[0, \sqrt{\frac{\overline{\varrho}}{\underline{\varrho}^2}\mathscr{B}\prod_{p=1}^{N}\mu_p^{N_{0p}}}\right] \tag{3.30}$$

Thus, observing the stability arguments of the Cases (i) and (ii), it can be concluded that the closed-loop system remains UUB. ■

Theorem 3.1 reveals that stability of the ideal model reference closed loop (i.e. the switched closed-loop system arising from (3.1), (3.2) and the ideal control law before (3.3)) can be proven via the first quadratic term of the Lyapunov function in (3.15): furthermore, because the ideal model reference closed loop is a linear switched system (in the absence of adaptation), on can easily prove asymptotic stability along the arguments of [46, 65, 66]. Other remarks to compare **Theorem** 3.1 with the state of the art follow:

Remark 3.4. *Because we keep the control gains constant during inactive times, one has to introduce a new mechanism to achieve stability. The proposed new mechanism is the*

auxiliary gain $\Gamma_{\sigma(t)}$ in (3.4), together with its adaptation law (3.9c). This gain plays the role of a leakage action for all inactive subsystems. Note that the second and the third term in the Lyapunov function (3.15) are summations over all (active and inactive) subsystems. In order to achieve exponential decrease of the Lyapunov function far enough from the origin (i.e. (3.22)), the items regarding active and inactive subsystems of $\dot{V}(t)$ should be offset by the corresponding items of $V(t)$, respectively. Since the derivative of the adaptive laws $K_{\overline{p}}, L_{\overline{p}}$ for inactive subsystems $\overline{p}$ equals to zero, only the relative items regarding the active subsystem remain in $\dot{V}(t)$. That's why $\Gamma_{\overline{p}}$ is put forward: to compensate the missing part of inactive systems in $\dot{V}(t)$ such that (3.22) can be attained. Therefore, the crucial difference between [158] and the proposed scheme is the use of auxiliary gains $\Gamma_{\sigma(t)}$ which avoids exponentially vanishing gains $K_{\overline{p}}, L_{\overline{p}}$ for the inactive subsystems $\overline{p}$. It is worth noticing that, with $\gamma_{i\sigma}$ being lower bounded by a positive value, the Lyapunov function V in (3.15) does not reach zero. However, the origin of the tracking error and the parametric estimation errors is not excluded; V may not reach the origin, but the tracking error e and parameters estimation error $\tilde{K}_\sigma, \tilde{L}_\sigma$ can still be zeros even if $\gamma_{i\sigma} \neq 0$. Eventually, the ultimate bound (3.30) on the tracking error e is still around the origin.

Remark 3.5. *It has to be noted that, for a certain subsystem p, Γ_p might be different at switched-off and switched-on times, due to the evolution of $\gamma_{\overline{p}}$ in (3.9c) during inactive time intervals. This might lead to some transient at switched-on instant. However, there are clear evidences for such transient to be smaller than the one in [158]. The first evidence is that any possible transient in (3.4) is contributed only by $\Gamma_{\sigma(t)}$ which enters as a feedforward term: feedforward terms have less effect on learning transients than feedback terms. In the proposed design, the feedback gains $K_{\sigma(t)}$ do not contribute any transient, whereas the transients in [158] arise from both feedback terms $K_{\sigma(t)}$ and feedforward terms $L_{\sigma(t)}$. The second evidence is that the effects of transients in $\Gamma_{\sigma(t)}$ can be reduced by properly tuning the design parameters: for example, selecting $\gamma_{i\overline{p}}(t_0)$ and $\beta_{i\overline{p}}$, $\epsilon_{i\overline{p}}$ in (3.9c) very close to each other, with relatively high $\beta_{i\overline{p}}$, will induce a fast decrease of $\gamma_{i\overline{p}}$ to its lower bound. Therefore, $\gamma_{i\overline{p}}$ will be almost the same at switched-on and switched-off times. This analysis is also confirmmed by the simulation example (see Section. 3.5)*

In other words, the intuition behind (3.4) and (3.9) is that it will reduce learning transients at switched on instants. Of course, improved transient behavior cannot be formally proven because any bound on the transient performance of adaptive closed-loop systems is in general very conservative [130]. Nevertheless, one can verify the improved transient performance in simulations, as done in Section 3.5.

For a proper comparison with [158], **Theorem** 3.1 is now modified to account for MMDADT in **Definition** 3.2.

Corollary 3.1. *Under **Assumption** 3.1, the closed-loop switched system formed by system (3.1), the reference model (3.2), the controller (3.4), the adaptive laws (3.9), and the switching law (3.13), is Uniformly Ultimately Bounded (UUB) and an ultimate bound b on the tracking error e can be found as*

$$b \in \left[0, \sqrt{\frac{1}{\underline{\varrho}} \max_{\substack{p,q\in\Omega \\ q\in\mathcal{N}(p)}} \{\mu_{pq}\} \mathscr{B} \prod_{p=1}^{N} \mu_{pq}^{N_{0pq}}}\right], \tag{3.31}$$

where the scalar $\mathscr{B}$ is the same positive constant as in ***Theorem 3.1****.*

Proof: The proof follows the same steps as **Theorem** 3.1 with the same Lyapunov function (3.15) being adopted. The main difference arises from the Lyapunov function's value at switching instant t_{l+1}, which can be expressed as:

$$V(t_{l+1}) \leq \frac{\varrho_{M\sigma(t_{l+1})}}{\varrho_{m\sigma(t_{l+1}^-)}} V(t_{l+1}^-) = \max_{\substack{p,q\in\Omega \\ q\in\mathscr{N}(p)}} \{\mu_{\sigma(t_{l+1})\sigma(t_{l+1}^-)}\} V(t_{l+1}^-). \tag{3.32}$$

Here, we define $\mu_{pq} = \mu_{\sigma(t_{l+1})\sigma(t_{l+1}^-)},\ p,q \in \Omega, q \in \mathscr{N}(p)$. The analysis of the Lyapunov function during the switching intervals is identical with (3.18)-(3.26). Since the switching sequence is known, the maximum increase of the Lyapunov function at the switching instants is $\max\limits_{\substack{p,q\in\Omega \\ q\in\mathscr{N}(p)}} \{\mu_{pq}\}$ instead of $\overline{\varrho}/\underline{\varrho}$ as in the MDADT case. The rest of the proof follows the lines from (3.22)-(3.30) after substituting $\mu_{\sigma(t_{l+1}^-)}$ with $\mu_{\sigma(t_{l+1})\sigma(t_{l+1}^-)}$ and $c \triangleq \exp(\sum\limits_{p=1}^{m} N_{0pq} \ln \mu_{pq})$. We conclude that the adaptive law (3.9) and the switching law with MMDADT (3.13) lead to UUB stability with bounds (3.31). ■

Table 3.1: Parameters for the six switching families under consideration (note that DT/ADT, MDDT/MDADT, and MMDDT/MMDADT have the same ϑ_d^*, ϑ_p^*, and ϑ_{pq}^*, as they only differ in terms of chattering bound).

Switching strategies	DT/ADT	MDDT/MDADT	MMDDT/MMDADT
Switching sequences	Unknown	Unknown	Known in advance
Parameters	$\vartheta^* = 23.7$	$\vartheta_1^* = 16.3, \vartheta_2^* = 11.8, \vartheta_3^* = 13.2$	$\vartheta_{13}^* = 16.3, \vartheta_{32}^* = 12.6$ $\vartheta_{21}^* = 11.8, \vartheta_{23}^* = 10$
	$\mu = 278.3$	$\mu_1 = 48.6, \mu_2 = 278.3, \mu_3 = 154.1$	$\mu_{13} = 48.6, \mu_{32} = 120.3$ $\mu_{21} = 272.4$
	$\kappa = 0.25$	$\kappa_1 = 0.25, \kappa_2 = 0.5, \kappa_3 = 0.4$	$\kappa_1 = 0.25, \kappa_2 = 0.5$ $\kappa_3 = 0.4$

3.5. SIMULATION EXAMPLE

A benchmark example commonly adopted in switched adaptive literature [14, 83, 108, 110, 146, 158] is considered to show how the proposed strategy compares to the state of the art, i.e. the approach in [158]. The example is a simplified model of a Highly Maneuverable Aircraft Technology (HiMAT) with the following three subsystems:

$$A_1 = \begin{bmatrix} -0.8435 & 0.97505 & -0.0048 \\ 8.7072 & -1.1643 & 0.0026 \\ 0 & 1 & 0 \end{bmatrix},\ B_1 = \begin{bmatrix} -0.1299 & -0.092 & -0.0107 & -0.0827 \\ -7.6833 & -4.7974 & 4.8178 & -5.7416 \\ 0 & 0 & 0 & 0 \end{bmatrix}.$$

$$A_2 = \begin{bmatrix} -1.8997 & 0.98312 & -0.00073 \\ 11.720 & -2.6316 & 0.00088 \\ 0 & 1 & 0 \end{bmatrix},\ B_2 = \begin{bmatrix} -0.2436 & -0.1708 & -0.00497 & -0.1997 \\ -46.206 & -31.604 & 22.396 & -31.179 \\ 0 & 0 & 0 & 0 \end{bmatrix}.$$

$$A_3 = \begin{bmatrix} -1.2206 & 0.99411 & -0.00084 \\ -64.071 & -1.8876 & 0.00046 \\ 0 & 1 & 0 \end{bmatrix}, B_3 = \begin{bmatrix} -0.0662 & -0.0315 & -0.0141 & -0.0749 \\ -27.333 & -13.163 & 11.058 & -26.878 \\ 0 & 0 & 0 & 0 \end{bmatrix}.$$

3.5.1. DESIGN OF THE REFERENCE MODEL

Three ideal controllers and reference models arise from the same design of [158], whose parameters are given below for completeness:

$$K_1^* = \begin{bmatrix} 0.6219 & 0.7469 & 1.4508 \\ 0.3969 & 0.4671 & 0.9013 \\ -0.3174 & -0.4621 & -0.9483 \\ 0.4534 & 0.5572 & 1.0902 \end{bmatrix}, L_1^* = I_{4\times 4}, A_{m1} = \begin{bmatrix} -0.9949 & 0.7939 & -0.3562 \\ -2.1076 & -14.5691 & -26.2966 \\ 0 & 1 & 0 \end{bmatrix}.$$

$$K_2^* = \begin{bmatrix} 0.1984 & 0.6793 & 1.5202 \\ 0.1368 & 0.4646 & 1.0392 \\ -0.0642 & -0.3289 & -0.7527 \\ 0.1431 & 0.4585 & 1.0212 \end{bmatrix}, L_2^* = I_{4\times 4}, A_{m2} = \begin{bmatrix} -1.9997 & 0.6484 & -0.7487 \\ -7.6710 & -70.3615 & -151.7803 \\ 0 & 1 & 0 \end{bmatrix}.$$

$$K_3^* = \begin{bmatrix} -0.6674 & 0.6397 & 1.4517 \\ -0.3220 & 0.3081 & 0.6995 \\ 0.3287 & -0.2599 & -0.6292 \\ -0.6423 & 0.6288 & 1.4175 \end{bmatrix}, L_3^* = I_{4\times 4}, A_{m3} = \begin{bmatrix} -1.1228 & 0.8986 & -0.2163 \\ -20.6916 & -43.2036 & -93.9421 \\ 0 & 1 & 0 \end{bmatrix}.$$

3.5.2. COMPARISONS

For a fair comparison purpose with [158], the leakage action in the adaptive laws in (3.9) is slightly modified as

$$\dot{K}_p^T(t) = -S_p^T B_{mp}^T P_p e(t) x^T(t) - \delta_p M_p K_p^T(t),\ \dot{K}_{\overline{p}}^T(t) = 0, \tag{3.33a}$$

$$\dot{L}_p(t) = -S_p^T B_{mp}^T P_p e(t) r^T(t) - \delta_p M_p L_p(t),\quad \dot{L}_{\overline{p}}(t) = 0, \tag{3.33b}$$

$$\dot{\gamma}_{ip}(t) = 0,$$

$$\dot{\gamma}_{i\overline{p}}(t) = -\left[\beta_{i\overline{p}} + \delta_{\overline{p}}\left(\left\{K_{\overline{p}}(t)K_{\overline{p}}^T(t)\right\}_{ii} + \left\{L_{\overline{p}}^T(t)L_{\overline{p}}(t)\right\}_{ii}\right)\right]\gamma_{i\overline{p}}(t) + \beta_{i\overline{p}}\epsilon_{i\overline{p}}, \tag{3.33c}$$

$$\text{with } \delta_p \geq \lambda_{\max}(M_p^{-1}) \geq 0, \tag{3.33d}$$

$$\delta_{\overline{p}} \geq (1/2)\lambda_{\max}(M_{\overline{p}}^{-1}) \geq 0, \tag{3.33e}$$

$$\text{and } \gamma_{ip}(t_0), \gamma_{i\overline{p}}(t_0) > \epsilon_{i\overline{p}}, \tag{3.33f}$$

which allows us a perfect comparison with [158] under the same choice of design parameters. Please note that the only difference between (3.11) and (3.9) is the special choice of the leakage gain, which requires some knowledge of L_p^*.

Let $\kappa_1 = 0.25, \kappa_2 = 0.5, \kappa_3 = 0.4$ as in [158]. By solving (3.8), we get the following positive definite matrices:

$$P_1 = \begin{bmatrix} 0.7337 & -0.0162 & -0.3781 \\ -0.0162 & 0.0549 & 0.0800 \\ -0.3781 & 0.0800 & 2.3960 \end{bmatrix}, P_2 = \begin{bmatrix} 0.5225 & -0.0028 & -0.0517 \\ -0.0028 & 0.0092 & 0.0132 \\ -0.0517 & 0.0132 & 1.9764 \end{bmatrix},$$

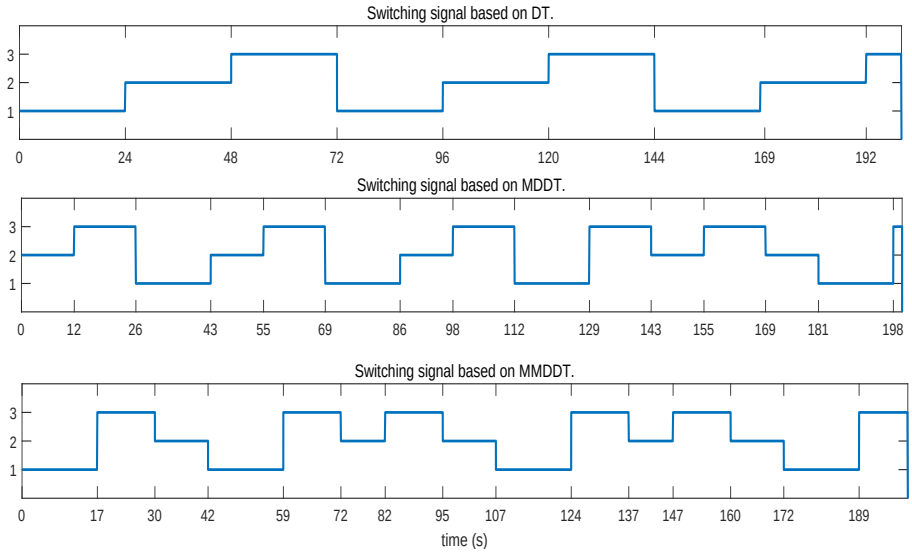

Figure 3.1: Switching signal based on DT, MDDT, MMDDT.

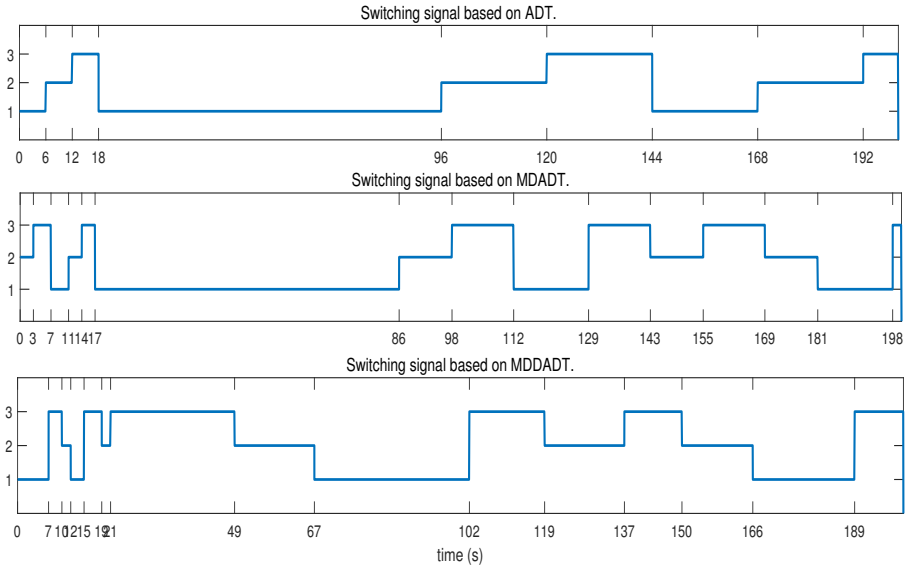

Figure 3.2: Switching signal based on ADT, MDADT, MMDADT.

$$P_3 = \begin{bmatrix} 0.7942 & -0.0063 & -0.3177 \\ -0.0063 & 0.0167 & 0.0241 \\ -0.3177 & 0.0241 & 2.4767 \end{bmatrix}.$$

As explained in **Remark** 2.1, this implies that the same parameters for DT, MDDT, MMDDT can be obtained as in [158]. Table 3.1 shows these parameters, whereas Fig. 3.1 shows three switching signals satisfying the DT, MDDT, and MMDDT requirements (such signals are the same as [158]). We also provide three additional switching families that satisfy the ADT, MDADT and MDDADT requirements: such signals have the same ϑ_d^*, ϑ_p^*, and ϑ_{pq}^* as DT, MDDT, MMDDT, and they only differ in terms of chattering bound. The chattering bound allows fast switching, compensated by slow switching later on: this can be seen from the three switching signals depicted in Fig. 3.2. Then,

Table 3.2: Total RMS and transient RMS errors for the six switching laws (the transient RMS error is calculated for one second after each switching).

	DT	ADT	MDDT	MDADT	MMDDT	MMDADT
Total RMS error						
Method in [158]	0.1295	0.1257	0.1172	0.1116	0.1369	0.1353
Proposed method	0.1153	0.1123	0.0895	0.0876	0.1195	0.1176
Improvement	11.0%	10.7%	23.6%	21.5%	12.7%	13.1%
Transient RMS error						
Method in [158]	0.1904	0.1893	0.1930	0.1938	0.2009	0.1520
Proposed method	0.1085	0.0785	0.1398	0.1382	0.1293	0.0820
Improvement	43.0%	58.6%	27.6%	28.7%	35.7%	46.1%

we consider for the proposed adaptation laws (3.9) the same design parameters as [158], i.e. the adaptive gains $S_1 = S_2 = S_3 = 10 I_{4\times 4}$, and the leakage rates $\delta_1 = \delta_2 = \delta_3 = 0.05$. What is left to design in (3.9) are the parameters for (3.9c) which are selected as follows: $\varepsilon_{i\overline{p}} = 0.1, \beta_{i\overline{p}} = 2$ for $i = 1,2,3,4$.

The initial conditions are $x(0) = [0 \quad 0 \quad 0]^T, x_m = [2 \quad 2 \quad 1]^T, K_p(0) = 0.8K_p^*, L_p(0) = 0.8L_p^*$, the disturbance is $d(t) = [0.2\sin(10t) \quad 0.15e^{-t} \quad 0.1\cos(\pi t)]^T$, and the reference input is $r(t) = [2\sin(t) \quad \cos(t) \quad 0.5\sin(0.5t) \quad 0]^T$.

The comparisons in terms of tracking errors are depicted in Fig. 3.3-3.5, for the three switching signals of Fig. 3.1 and in Fig. 3.6-3.8 for the three switching signals of Fig. 3.2 (the upper plots are the tracking errors for the approach in [158], the lower plots are the tracking errors for the proposed approach). From the lower plots of each figure, it is noticeable that the learning transients of the proposed methods are considerably reduced, in contrast with the method of [158]. This confirms that the bad effects of vanishing gains are alleviated. On the other hand, it has to be acknowledged that the learning transients are not completely removed because the adaptive gain Γ_σ evolves during inactive times. However, the intuition of **Remark 3.5** is confirmed, i.e. the feedforward term Γ_σ has less effect on the transient performance than the feedback gain K_σ in [158].

The performance improvements are quantified in Table 3.2 and visualized in Fig. 3.9,

which show that not only the total Root Mean Square (RMS) error is reduced, but especially the transient RMS error is significantly reduced. The transient RMS error is calculated for one second after each switching, as a way to measure the learning transients. The table shows that the improvement in terms of transient is much more pronounced than the improvement over the whole simulation: notice how the transient improvements range in 27%–58%, depending on the switching signal.

Table 3.3: Total RMS and transient RMS errors for the six switching laws with alternative leakage term (the transient RMS error is calculated for one second after each switching).

	DT	ADT	MDDT	MDADT	MMDDT	MMDADT
Total RMS error						
Method in [158]	0.0997	0.0990	0.0796	0.0776	0.1018	0.0998
Proposed method	0.0952	0.0961	0.0605	0.0620	0.0971	0.0960
Improvement	4.5%	2.9%	24.0%	20.0%	4.6%	3.8%
Transient RMS error						
Method in [158]	0.1738	0.1564	0.1364	0.1320	0.1437	0.0871
Proposed method	0.0794	0.0285	0.0787	0.0793	0.0907	0.0556
Improvement	54.3%	81.8%	42.3%	39.9%	36.9%	36.2%

3.5.3. ADDITIONAL COMPARISONS

To further elaborate on the consistency of the proposed result, we test a different leakage action, i.e. we test the proposed adaptive laws (3.9) against the state-of-the-art adaptive laws (3.11), where the terms $\delta_p M_p$ and $\delta_{\overline{p}} M_{\overline{p}}$ are replaced with δ_p and $\delta_{\overline{p}}$, respectively. This leakage action represents the case when M_p is unknown and thus cannot be used for control design. All the other parameters are left unchanged. The results are summarized in Table 3.3 and visualized in Fig. 3.10: again, consistent improvements can be noticed. The improvements in terms of total RMS error are sometimes smaller than before, while transient improvements range in 36%-82%, depending on the switching signal.

3.6. CONCLUDING REMARKS

This chapter has illustrated a new adaptive framework based on the leakage mechanism for robust control of uncertain switched linear systems. Owing to the introduction of an auxiliary gain, the proposed framework allows the adaptive gains of the inactive subsystems to keep the same values as they are switched-off: this is in clear contrast with the state of the art where the control gains of the inactive subsystems should vanish during inactive periods. This innovation significantly reduces the learning transient at switched on instants for various families of dwell-time based switching signals (and their extensions).

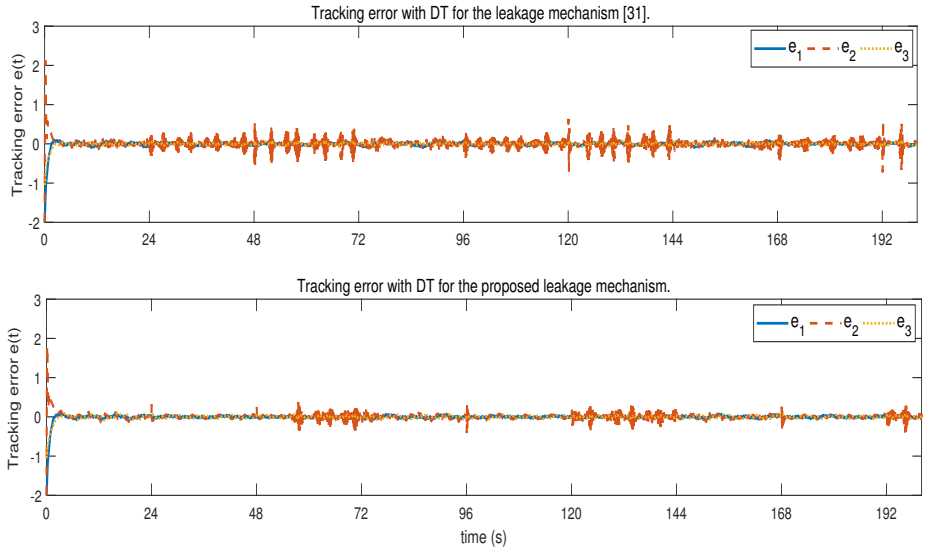

Figure 3.3: Tracking error for DT switching law.

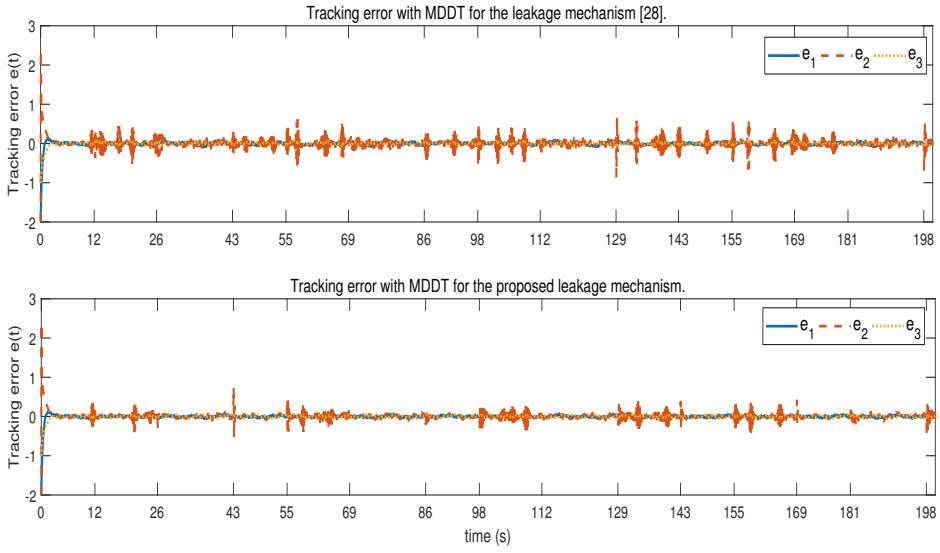

Figure 3.4: Tracking error for MDDT switching law.

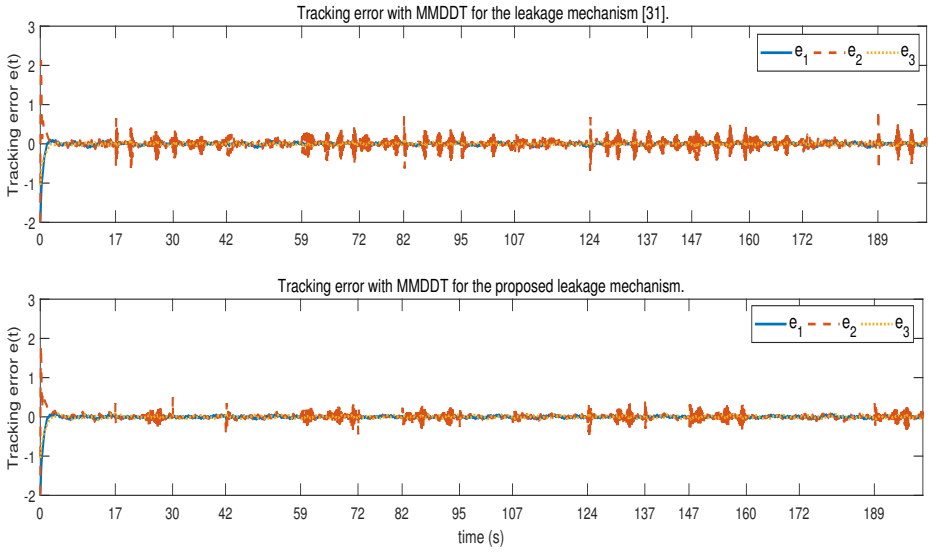

Figure 3.5: Tracking error for MMDDT switching law.

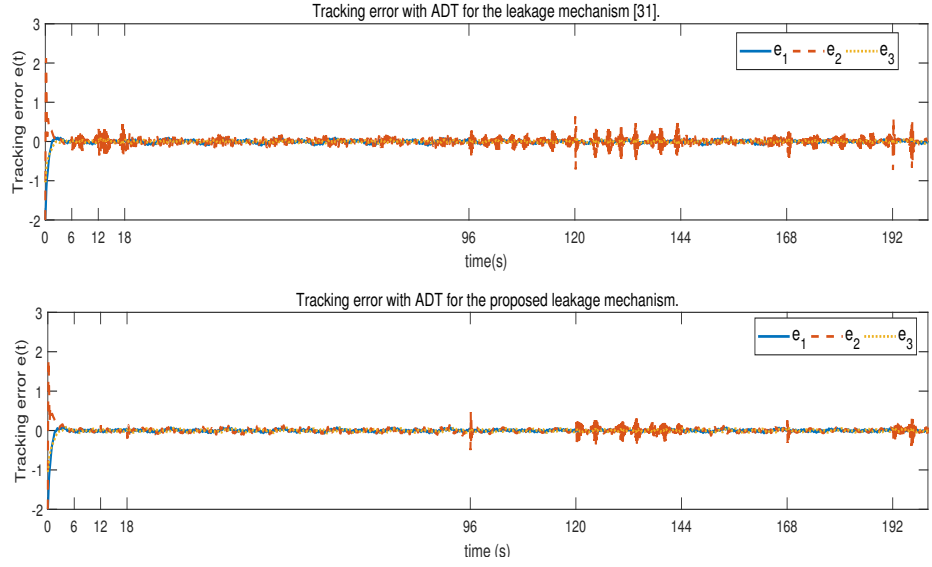

Figure 3.6: Tracking error for ADT switching law.

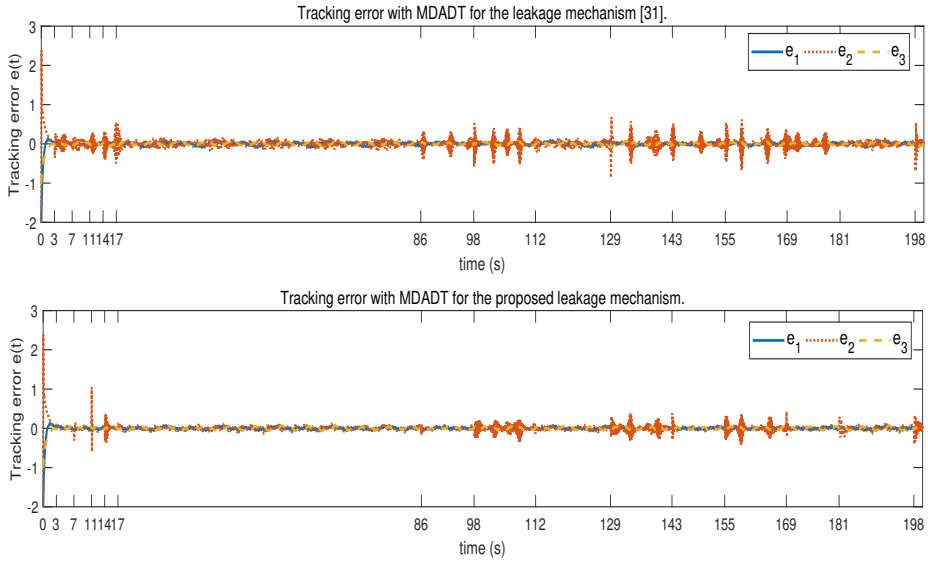

Figure 3.7: Tracking error for MDADT switching law.

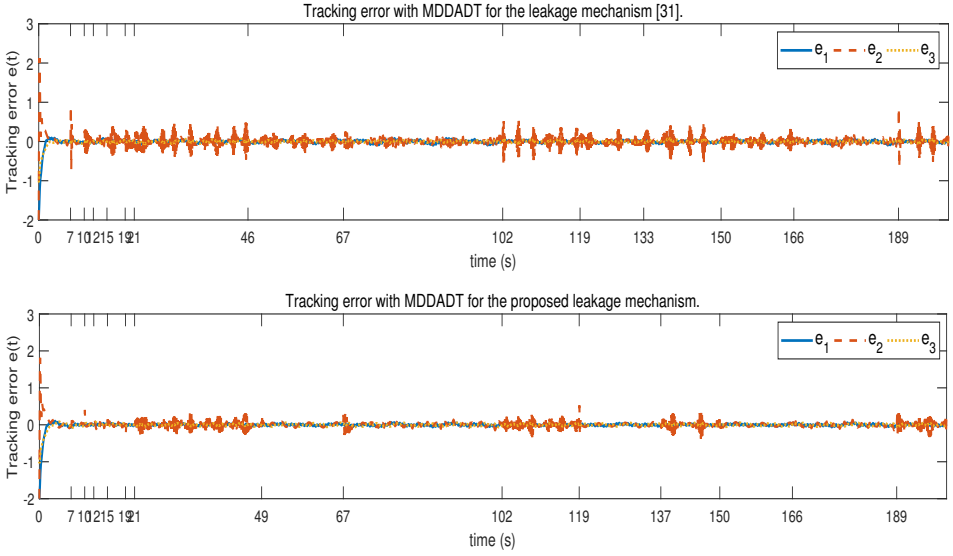

Figure 3.8: Tracking error for MMDADT switching law.

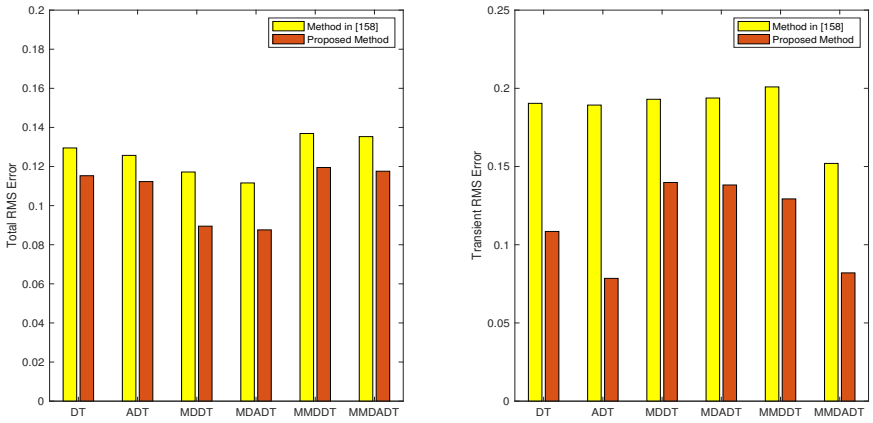

Figure 3.9: Visualization of the comparative results in Table 3.2.

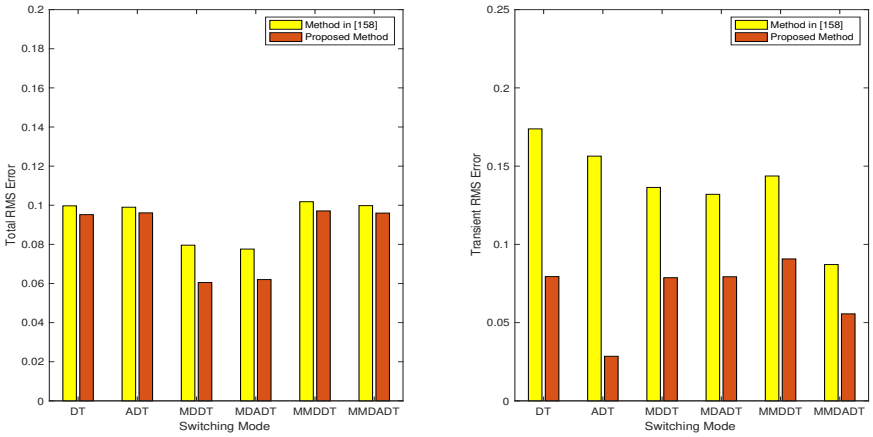

Figure 3.10: Visualization of the comparative results in Table 3.3.

4

ROBUST ADAPTIVE CONTROL OF SWITCHED INTERCONNECTED POWER SYSTEMS

Multi-area load frequency control (LFC) is a typical example showing the need for adaptive control for interconnected systems. Multi-area LFC selects and controls a few generators in each area of a power system in an effort to dampen inter-area frequency oscillations. To effectively dampen such oscillations, it is required to enhance and lower the control activity dynamically during operation, so as to adapt to changing circumstances. Changing circumstances should cover not only parametric uncertainties and unmodelled dynamics (e.g. aggregated area dynamics and bus dynamics), but also the increasing structural flexibility of modern power systems (e.g. protection mechanisms against faults and cyber-attacks, or topology reconfiguration mechanisms for demand response). As formal stability guarantees around such an attractive adaptive multi-area LFC concept are still lacking, we propose a new framework in which adaptation and switching are combined in a provably stable way to handle parametric uncertainty, unmodelled dynamics, and dynamical interconnections of the power system. Stability is studied in the Lyapunov theory sense using the standard structure-preserving modeling approach, and the resulting adaptive multi-area LFC design is validated using an IEEE 39-bus benchmark.

4.1. INTRODUCTION

In multi-area LFC, uncertainties naturally arise since the system parameters must be aggregated into equivalent time constants and coefficients, representing the dynamics at the area level [27, 48, 115, 145]. The aggregation of dynamics creates the need to handle both parametric uncertainties and unmodelled dynamics, which are challenging for

This chapter is based on [133]

fixed-gain control [6, 10, 121]. Especially, adaptive solutions should be sought, where the controller is not fixed-gain, but capable of adapting to changing circumstances. Due to their increased flexible structure, modern power systems operate in several modes, making it impossible for a unique controller to tackle all operating conditions [1, 33, 58]. Switched controllers should be proposed as a way to handle structural changes in the system, by rapidly switching among different control configurations.

The combination of adaptation and switching can result in a framework where the multi-area LFC control gains can change continuously to adapt to parametric uncertainty, and discontinuously to adapt to structural changes. Currently, no stable switched adaptation framework has been proposed to handle nonlinear interconnections in power systems that change dynamically, which gives rise to the aforementioned

Question 2: *how to design an adaptive controller for the multi-area LFC can adapt continuously to parametric uncertainty and state-dependent unmodelled dynamics, while discontinuously to structural changes?*

The framework is tested using a benchmark IEEE 39-bus power system, divided into three areas, where all ten generators implement local LFC, but only four out of ten implement the multi-area LFC (one generator for area 1, two for area 2, one for area 3): therefore, the system presents all the uncertainties resulting from aggregating single inertia/damping terms into equivalent inertia/damping terms. Effective performance is shown, even as compared to non-adaptive strategies.

The rest of this chapter is organized as follows: Section 4.2 introduces the system dynamics and problem formulation. The adaptive framework is presented in Section 4.3 with the corresponding stability analysis in 4.4. Simulations are provided in Section 4.5, with concluding remarks in Section 4.6.

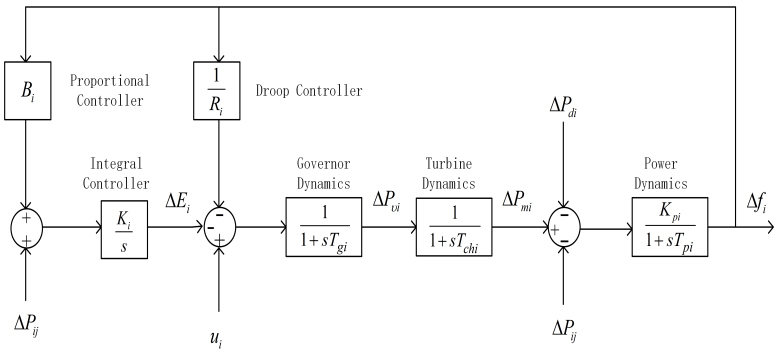

Figure 4.1: Single area power system for LFC purposes.

4.2. PROBLEM FORMULATION

Before introducing a multi-area power system and its dynamics, let us recall the standard dynamics for a single-area power system, indicated with subscript i (cf. Fig. 4.1).

Table 4.1: Nomenclature

ΔP_{vi}	Governor valve positions
ΔP_{mi}	Mechanical power output of the alternators
Δf_i	Frequency deviations
ΔE_i	Area control error signals
B_i	Proportional gains of local PI controllers
k_i	Integral gains of local PI controllers
T_{pi}	Power system time constants
k_{pi}	Power system steady-state gains
T_{gi}	Governor time constants
T_{chi}	Turbine time constants
R_i	Speed droops
T_i	Stiffness coefficients
ΔP_{di}	Load disturbances
u_i	Input signal

4.2.1. SINGLE-AREA POWER SYSTEM

The dynamics of a single-area power system can be described as [6, 10, 27, 48, 115, 121, 145]:

$$T_{chi}\Delta\dot{P}_{mi}(t) = \Delta P_{vi}(t) - \Delta P_{mi}(t) \tag{4.1a}$$

$$\Delta\dot{E}_i(t) = -k_i\Delta P_{ij}(t) + k_i B_i \Delta f_i(t) \tag{4.1b}$$

$$T_{gi}\Delta\dot{P}_{vi}(t) = -\frac{\Delta f_i(t)}{R_i} - \Delta P_{vi}(t) - \Delta E_i(t) + u_i(t) \tag{4.1c}$$

$$T_{pi}\Delta\dot{f}_i(t) = -k_{pi}\Delta P_{di}(t) - k_{pi}\Delta P_{ij}(t) + k_{pi}\Delta P_{mi}(t) - \Delta f_i(t) \tag{4.1d}$$

$$\Delta\dot{\theta}_i(t) = \Delta f_i(t) \tag{4.1e}$$

where constants and variables are explained in Table 4.1, and represent equivalent quantities, aggregated at the area level. For example, inertia, damping, and time constants are equivalent time constants for the area (cf. [6,10,27,48,115,121,145] and the discussion in **Remark** 4.3). Note that the proportional and integral gains in (4.1b) represent the gains of the local (intra-area) LFC. In (4.1), $\Delta P_{ij}(t)$ is a term coming from the interconnection with neighboring areas (indexed by subscript j), which will be clarified in the next subsection. The symbol Δ represents the deviation from the equilibrium operating point, resulting from the solution to the power flow (or optimal power flow) equations, giving the nominal operating point of the power system [39]. The purpose of the control is to keep the network close to such equilibrium, i.e., keep $\Delta f = [\Delta f_1, \Delta f_2, \ldots, \Delta f_n]^T$ close to 0, and $\Delta\theta = [\Delta\theta_1, \Delta\theta_2, \ldots, \Delta\theta_n]^T$ close to $\Delta\theta^d$, where $\Delta\theta^d$ collects the equilibrium phase angles resulting from the power flow equations.

4.2.2. MULTI-AREA POWER SYSTEM

To describe the dynamics of a multi-area power network in a compact way, let us introduce some notions of graph theory [15, 20].

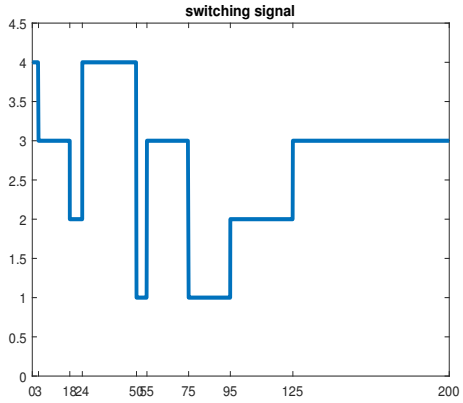

Figure 4.2: Example of switching topologies for a three-area power system. The switching topologies are indexed by a signal σ.

A power system is essentially a network of dynamical systems, which are linked to each other via a *communication graph* (or *physical graph*), that describes the allowed information flow (or the allowed physical interaction). We say that area i has an *undirected* connection to area j if the latter can receive information from (or interact with) the former and vice versa. The graph describing the connection between all areas is defined by the pair $\mathcal{G} = (\mathcal{V}, \mathcal{E})$, where $\mathcal{V} = \{1, \dots, N\}$ is the set of nodes (areas), and $\mathcal{E} \subseteq \mathcal{V} \times \mathcal{V}$ is the set of edges (pairs of connected areas). As standard in graph theory, we assume the graph to be connected, i.e., there is a path between every pair of vertices. For a node i, let us denote with $\mathcal{N}_i$ the set of node i is connected to.

For a set of vertices, there might be different possible interconnections or topologies. As an example, Fig. 4.2 shows a three-area power system where each node denotes one area, and where four possible connected topologies arise, indexed by $\sigma \in \Omega = \{1, 2, 3, 4\}$.

Dynamically changing topologies can be represented by a piecewise constant time-dependent signal σ, called the *switching signal* (cf. the example in Fig. 4.2). To represent the evolving topologies, the class of ADT switching signals is considered (cf. **Definition** 2.2).

Remark 4.1. *The class of ADT signals can represent situations in which fast switching occurs (over short intervals) as a consequence of sudden events (e.g. attacks or faults), compensated by a slower settlement phase (over long intervals) [132].*

Interaction among two interconnected areas i and j occurs via a power flow depending on the difference between phases [120, 137]. With switching topologies, the set of neighbors of area i will be time-dependent and denoted by $\mathcal{N}_{i\sigma(t)}$. For examples, in Fig. 4.2, when $\sigma = 1$ node 1 has $\mathcal{N}_{11} = \{2\}$; when $\sigma = 2$, node 1 has $\mathcal{N}_{12} = \{2, 3\}$ and so on. In the following, whenever convenient, we will not explicitly write the dependence of σ on

time. Then, the disturbance term ΔP_{ij} in (4.1d) can be defined as

$$\Delta P_{ij,\sigma}(t) = 2\pi T_i \sum_{j\in\mathcal{N}_{i\sigma}(t)}^{N} \sin(\Delta\theta_i(t) - \Delta\theta_j(t)) \tag{4.2}$$

$$\Delta P_{ij,\sigma}(t) = -\Delta P_{ji\sigma}(t) \tag{4.3}$$

If the j-th area is disconnected from the i-th area, then $\Delta P_{ij,\sigma}(t) = 0$.

4.2.3. STRUCTURE-PRESERVING MODELLING

The structure-preserving (or Kuramoto) model is commonly used to analyze multi-area power systems [30, 120]. With reference to the dynamics (4.1)-(4.3), a Kuramoto-like model can be derived by assuming that the generator and turbine time constants T_{gi} and T_{chi} are much smaller than the power time constant T_{pi} (in practice T_{gi} and T_{chi} are at least 10 times smaller than T_{pi} [27]). This leads to

$$\Delta P_{mi,\sigma}(t) = -\frac{\Delta f_i(t)}{R_i} + u_{i\sigma}(t) - \Delta E_{i\sigma}(t) \tag{4.4a}$$

$$\Delta \dot{E}_{i\sigma}(t) = -k_i \Delta P_{ij\sigma}(t) + k_i B_i \Delta f_i(t) \tag{4.4b}$$

$$\Delta \dot{f}_i(t) = -\frac{k_{pi}\Delta P_{di}(t)}{T_{pi}} - \frac{k_{pi}\Delta P_{ij,\sigma}(t)}{T_{pi}} + \frac{k_{pi}\Delta P_{mi,\sigma}(t)}{T_{pi}} - \frac{\Delta f_i(t)}{T_{pi}} \tag{4.4c}$$

$$\Delta P_{ij,\sigma}(t) = 2\pi T_i \sum_{j\in\mathcal{N}_{i\sigma}(t)}^{N} \sin(\Delta\theta_i(t) - \Delta\theta_j(t)) \tag{4.4d}$$

$$\Delta \dot{\theta}_i(t) = \Delta f_i(t) \tag{4.4e}$$

We then obtain the following switched LFC dynamics:

$$\begin{aligned}\Delta\ddot{\theta}_i(t) = (-\frac{1}{T_{pi}} - \frac{k_{pi}}{T_{pi}R_i})\Delta\dot{\theta}_i - \frac{k_{pi}}{T_{pi}} 2\pi T_i \sum_{j\in\mathcal{N}_{i\sigma}(t)}^{N} \sin(\Delta\theta_i - \Delta\theta_j) \\ - \frac{k_{pi}}{T_{pi}}\big(\Delta P_{di} + \Delta E_{i\sigma}(t)\big) + \frac{k_{pi}}{T_{pi}} u_{i\sigma}(t)\end{aligned} \tag{4.5}$$

For compactness, system (4.5) is represented as

$$\Delta\ddot{\theta}(t) = M_{\sigma(t)}(\Delta\theta(t), \Delta\dot{\theta}(t)) + L u_\sigma(t),\ \sigma(t) \in \Omega \tag{4.6}$$

with $\Delta\theta = [\Delta\theta_1, \Delta\theta_2, \ldots, \Delta\theta_n]^T$, $u_\sigma = [u_{1\sigma}, u_{2\sigma}, \ldots, u_{n\sigma}]^T$ and with $L \triangleq \text{diag}\{\frac{k_{pi}}{T_{pi}}\}$ representing the equivalent inertia of the power system. In (4.6), $M_\sigma(\Delta\theta(t), \Delta\dot{\theta}(t)) \triangleq H(\Delta\dot{\theta}) + G_\sigma(\Delta\theta) + d$ with

$$H(\Delta\dot{\theta}) = \text{diag}\Big\{-\frac{1}{T_{pi}} - \frac{k_{pi}}{T_{pi}R_i}\Big\}\Delta\dot{\theta}_i \tag{4.7a}$$

$$G_\sigma(\Delta\theta) = \text{col}\Big\{-\frac{k_{pi}}{T_{pi}} 2\pi T_i \sum_{j\in\mathcal{N}_{i\sigma}(t)}^{N} \sin(\Delta\theta_i - \Delta\theta_j)\Big\} \tag{4.7b}$$

$$d = \text{col}\Big\{-\frac{k_{pi}}{T_{pi}}\big(\Delta P_{di} + \Delta E_i\big)\Big\} \tag{4.7c}$$

for $i = 1,\dots,N$, where col{…} means the column vector and diag{…} is the diagonal matrix.

Based on the structure of (4.7), the following property holds:

Property 4.1. *There exist* $\overline{h}, \overline{g}_\sigma, \overline{d} \in \mathbb{R}$ *such that* $\|H(\Delta\dot{\theta})\| \le \overline{h}\|\Delta\dot{\theta}\|$, $\|G_\sigma(\Delta\theta)\| \le \overline{g}_\sigma$, *and* $\|d(t)\| \le \overline{d}_0 + \overline{d}_1\|\Delta\theta\|$.

Note that the bound on $\|H\|$ is proportional to $\|\Delta\dot{\theta}\|$ thanks to the linear structure in (4.7a), whereas the bound on $\|G\|$ is constant due to the sinusoidal a priori bounded terms in (4.7b). The term $\overline{d}_1$ in the disturbance arise from the phase-dependent ΔE_i, evaluated by integrating (4.4b).

It is worth mentioning that the exact values of most constants in power systems (cf. Table 4.1) are difficult to acquire. This implies that the dynamical terms H, G, d are uncertain and their upper bounds in **Property** 4.1 are unavailable. To describe uncertainty in L, let us decompose $L = \hat{L} + \Delta L$ into a known (nominal) $\hat{L}$ and an unknown ΔL. The following assumption on a priori knowledge is made:

Assumption 4.1. *Only nominal values* (k_{pi}, T_{pi}) *and upper bounds* $(\Delta k_{pi}, \Delta T_{pi})$ *around such nominal values are available. This is described by assuming the existence of a known scalar* $\bar{J}$ *such that for* $J \triangleq \left(L\hat{L}^{-1} - I\right)$ *the following holds*

$$\|J\| \le \bar{J} < 1 \tag{4.8}$$

Assumption 4.1 is standard in inverse dynamics-based control (cf. [118, 138, 140]), requiring that uncertainty around the nominal $\hat{L}$ is not arbitrarily large. Note that when there is no uncertainty, then $L = \hat{L}$ and (4.8) is satisfied with $\bar{J} = 0$; with more uncertainty, $\bar{J}$ tends to grow, and $\bar{J} \approx 1$ represents that $L \approx 2\hat{L}$ (i.e., uncertainty is around 100%). On the other hand, **Assumption** 4.1 allows arbitrarily large uncertainty in H, G, d.

Let us define $x \triangleq [\Delta\theta^T \ \ \Delta\dot{\theta}^T]^T$, considered available as feedback. Using **Property** 4.1, $M_\sigma(x)$ can be upper bounded as:

$$\|M_\sigma(x)\| \le \phi_{0\sigma} + \phi_{1\sigma}\|x\|, \tag{4.9}$$

where $\phi_{0\sigma} = \overline{g}_\sigma + \overline{d}, \phi_{1\sigma} = \overline{h} + \overline{d}_1$ (the subscript in $\phi_{1\sigma}$ is used for consistency in notation) are derived from (4.7), and are finite but *unknown scalars* according to **Assumption** 4.1.

The notion of Uniform Ultimate Boundedness (UUB) is the standard stability concept in robust adaptive control (cf. [100, Def. 3] or [52, Def. 3.4.12] for details). This leads to the LFC problem formulation:

Problem 4.1. *Under* ***Assumption*** *4.1, the aim is to design an adaptive multi-area LFC controller* u_σ *such that can track (in the sense of UUB) a desired constant frequency* $\Delta\dot{\theta}^d = \mathbf{0}$ *under uncertainty and ADT switching topologies.*

The following remarks clarify the distinguishing features and innovations of the proposed problem formulation.

Remark 4.2. *Compared to conventional multi-area LFC dynamics, where the linearized power flow* $(\Delta\theta_i - \Delta\theta_j)$ *is used, which is valid only for small phases [6, 10, 27, 48, 115, 121, 145], we consider the nonlinear power flow* $\sin(\Delta\theta_i - \Delta\theta_j)$. *This makes the dynamics more rich and the control design more challenging and open in literature.*

Table 4.2: Control variables and parameters

r_σ	tracking error variable
$K_{1\sigma}$	linear proportional gain
$K_{2\sigma}$	linear derivative gain
$\hat{L}$	nominal inertia
ε	anti-chattering constant
ω	ultimate bound parameter
ρ_σ	overall robust adaptive gain
$\hat{\phi}_{ip}$, $\hat{\phi}_{i\overline{p}}$	adaptive gains (active and inactive topologies)
γ_{ip}, $\gamma_{i\overline{p}}$	auxiliary gains (active and inactive topologies)
α_i	leakage rate of adaptive gains $\hat{\phi}_{ip}$, $\hat{\phi}_{i\overline{p}}$
β_i	leakage rate of auxiliary gain γ_{ip}, $\gamma_{i\overline{p}}$
ν_{ip}	nonlinear leakage of auxiliary gains γ_{ip}, $\gamma_{i\overline{p}}$
$\bar{J}$	maximum uncertainty in L

Remark 4.3. *The upper bound structure in (4.9) is state-dependent. In multi-area LFC, state-dependent uncertainties naturally arise since the system parameters must be aggregated into equivalent time constants and coefficients, representing the dynamics at the area level [27, 48, 115, 145]. Bus dynamics are also state-dependent uncertainties according to the structure-preserving model [37]. The aggregation of dynamics creates the need to handle both parametric uncertainties and state-dependent unmodelled dynamics [6, 10, 121].*

4.3. CONTROLLER DESIGN

Let $e(t) \triangleq \Delta\theta(t) - \Delta\theta^d(t)$ and $\xi(t) \triangleq [e^T(t)\ \dot{e}^T(t)]^T$. A summary of the control variables and parameters in this section can be found in Table II. Define a tracking error variable

$$r_\sigma \triangleq B^T P_\sigma \xi, \qquad \sigma \in \Omega \tag{4.10}$$

where $P_\sigma > 0$ is the solution to the Lyapunov equation

$$A_\sigma^T P_\sigma + P_\sigma A_\sigma = -Q_\sigma \tag{4.11}$$

for some $Q_\sigma > 0$ with $A_\sigma \triangleq \begin{bmatrix} 0 & I \\ -K_{1\sigma} & -K_{2\sigma} \end{bmatrix}$ and $B \triangleq \begin{bmatrix} 0 & I \end{bmatrix}^T$. Here, $K_{1\sigma}$ and $K_{2\sigma}$ are two user-defined positive definite gain matrices and their positive definiteness guarantees A_σ to be Hurwitz.

The switched multi-area LFC is designed as

$$u_\sigma = \hat{L}^{-1}(-K_{1\sigma} e - K_{2\sigma} \dot{e} - \Delta u_\sigma), \tag{4.12a}$$

$$\Delta u_\sigma = \omega \rho_\sigma \frac{r_\sigma}{\sqrt{\|r_\sigma\|^2 + \varepsilon}}, \tag{4.12b}$$

with $\varepsilon > 0$ a small scalar to avoid control chatter and $\omega > 1$ a user-defined scalar affecting the ultimate bound. The design of ρ_σ is discussed later. Substituting (4.12a) in (4.5)

yields

$$\begin{aligned}\ddot{e} = \Delta\ddot{\theta} &= M_\sigma + Lu_\sigma \\ &= M_\sigma + \big(L\hat{L}^{-1} - I\big)\big(-K_{1\sigma}e - K_{2\sigma}\dot{e} - \Delta u_\sigma\big) + (-K_{1\sigma}e - K_{2\sigma}\dot{e} - \Delta u_\sigma) \\ &= -K_{1\sigma}e - K_{2\sigma}\dot{e} - (I+J)\Delta u_\sigma + \Psi_\sigma, \end{aligned} \tag{4.13}$$

where $\Psi_\sigma \triangleq M_\sigma - J(K_{1\sigma}e + K_{2\sigma}\dot{e})$ is treated as the overall uncertainty. Hence, using **Assumption** 4.1, one can verify the existence of $\phi^*_{i\sigma} \in \mathbb{R}^+$ $i = 0,1$ such that for all $\sigma \in \Omega$

$$\|\Psi_\sigma\| \le \phi^*_{0\sigma} + \phi^*_{1\sigma}\|\xi\|, \tag{4.14}$$

where $\phi^*_{0\sigma} = \phi_{0\sigma} + \phi_{1\sigma}\|x^d\|$, $\phi^*_{1\sigma} = \phi_{1\sigma} + \|J\|(\|K_{1\sigma}\| + \|K_{2\sigma}\|)$ (based on the fact that $x = \Delta\theta^d + \xi$) are unknown finite scalars. After defining the structures of the upper bound of $\|\Psi_\sigma\|$ in (4.14), the gain ρ_σ in (4.12b) is proposed as

$$\rho_\sigma = \frac{1}{1-\bar{J}}\Big\{\big(\hat{\phi}_{0\sigma} + \gamma_{0\sigma}\big) + \big(\hat{\phi}_{1\sigma} + \gamma_{1\sigma}\big)\|\xi\|\Big\} \tag{4.15}$$

where $\hat{\phi}_{0\sigma}$, $\hat{\phi}_{1\sigma}$ are the estimates of the upper bounds $\phi^*_{0\sigma}$, $\phi^*_{1\sigma}$, and $\gamma_{0\sigma}$, $\gamma_{1\sigma}$ are auxiliary gains.

The main idea of switching structure (4.12) is that a different control action is activated depending on the active topology. Let p denote the index of the active topology for $t \in [t_l,\ t_{l+1})$, and let $\mathscr{I}(p) = \Omega\backslash\{p\}$ denote the set of inactive topologies. The gains in (4.15) are evaluated using the following laws:

$$\dot{\hat{\phi}}_{ip} = \|r_p\|\|\xi\|^i - \alpha_{ip}\hat{\phi}_{ip}, \quad \dot{\gamma}_{ip} = 0, \tag{4.16a}$$

$$\dot{\hat{\phi}}_{i\overline{p}} = 0, \ \ \dot{\gamma}_{i\overline{p}} = -\Big(\beta_{i\overline{p}} + \overline{\nu}_{i\overline{p}}\hat{\phi}^4_{i\overline{p}}\Big)\gamma_{i\overline{p}} + \beta_{i\overline{p}}\nu_{i\overline{p}}, \ \forall\overline{p} \in \mathscr{I}(p) \tag{4.16b}$$

$$\text{with } \hat{\phi}_{ip}(0) > 0, \ \gamma_{i\overline{p}}(0) > \nu_{i\overline{p}}, \tag{4.16c}$$

$$\alpha_{ip} > \zeta_p/2, \beta_{i\overline{p}} > \zeta_{\overline{p}}/2. \tag{4.16d}$$

where $\alpha_{ip}, \beta_{i\overline{p}}, \nu_{i\overline{p}}, \overline{\nu}_{i\overline{p}} \in \mathbb{R}^+$, $i = 0,1$ are static design scalars. Note that $\hat{\phi}_{i\sigma}$ is only updated for the active topology p, while the gain $\gamma_{i\sigma}$ is updated only for inactive topologies $\overline{p}$. The first term in $\dot{\hat{\phi}}_{ip}$ adjusts the gain according to the current error, whereas the second term in $\dot{\hat{\phi}}_{ip}$ and the first term in $\dot{\gamma}_{i\overline{p}}$ are stabilizing leakage factors (cf. the derivations in the proof of **Theorem** 4.1 (4.25), (4.29), (4.32)-(4.33)).

Using the framework of ADT, we can define the set of dynamically-changing topology variations that can be tolerated by controller (4.12), (4.15), (4.16) without losing stability. To this purpose, let us define $\bar{\zeta} \triangleq \max_{p\in\Omega}\lambda_{\max}(P_p)$ and $\underline{\zeta} \triangleq \min_{p\in\Omega}\lambda_{\min}(P_p)$. Following **Definition** 2.2 of ADT, the switching law condition to guarantee stability is proposed as

$$\vartheta > \ln\mu/\kappa, \tag{4.17}$$

where $\mu \triangleq \bar{\zeta}/\underline{\zeta}_m \ge 1$; κ is a scalar defined as $0 < \kappa < \zeta$ where $\zeta_p \triangleq \lambda_{\min}(Q_p)/\lambda_{\max}(P_p)$ and $\zeta \triangleq \min_{p\in\Omega}\{\zeta_p\}$.

Table 4.2 explains the meaning of control variables and parameters and **Algorithm** 1 summarizes the design steps to be followed to implement the proposed adaptive control framework. The following stability result is given in the context of Lyapunov theory [52], while the stability proof in Section 4.4 clarifies how the design (4.12), (4.15), (4.16) and (4.17) was obtained.

4.4. STABILITY ANALYSIS

Theorem 4.1. *Under **Property** 4.1 and **Assumption** 4.1, the closed-loop trajectories (including the tracking error) of power system (4.5) employing multi-area LFC (4.12) and (4.15) with adaptive law* (4.16) *and ADT switching law (4.17) are UUB.*

Proof. Stability is analyzed using the Lyapunov function V defined by

$$V(t) = \frac{1}{2}\xi^T(t)P_{\sigma(t)}\xi(t) + \frac{1}{2}\sum_{p=1}^{N}\sum_{i=0}^{1}\left\{\left(\hat{\phi}_{ip}(t) - \phi^*_{ip}\right)^2 + \gamma^2_{ip}(t)\right\}, \tag{4.18}$$

The following error dynamics is obtained from (4.13):

$$\dot{\xi} = A_\sigma \xi + B\left[\Psi_\sigma - (I+J)\Delta u_\sigma\right] \tag{4.19}$$

We first investigate the behavior of V at the switching instants. Let subsystem $\sigma(t^-_{l+1})$ be active when $t \in [t_l,\ t_{l+1})$ and subsystem $\sigma(t_{l+1})$ is active when $t \in [t_{l+1},\ t_{l+2})$. At the switching instant t_{l+1}, we have before switching

$$V(t^-_{l+1}) = \frac{1}{2}\xi^T(t^-_{l+1})P_{\sigma(t^-_{l+1})}\xi(t^-_{l+1}) + \frac{1}{2}\sum_{p=1}^{N}\sum_{i=0}^{1}\left[\left(\hat{\phi}_{ip}(t^-_{l+1}) - \phi^*_{ip}\right)^2 + \gamma^2_{ip}(t^-_{l+1})\right],$$

and after switching

$$V(t_{l+1}) = \frac{1}{2}\xi^T(t_{l+1})P_{\sigma(t_{l+1})}\xi(t_{l+1}) + \frac{1}{2}\sum_{p=1}^{N}\sum_{i=0}^{1}\left[\left(\hat{\phi}_{ip}(t_{l+1}) - \phi^*_{ip}\right)^2 + \gamma^2_{ip}(t_{l+1})\right].$$

In accordance with the continuity of the tracking error ξ in (4.19) and of the gains $\hat{\phi}_{i\sigma}$ and $\gamma_{i\sigma}$ in (4.16), we have $\xi(t^-_{l+1}) = \xi(t_{l+1})$, $(\hat{\phi}_{ip}(t^-_{l+1}) - \phi^*_{ip}) = (\hat{\phi}_{ip}(t_{l+1}) - \phi^*_{ip})$ and $\gamma_{ip}(t^-_{l+1}) = \gamma_{ip}(t_{l+1})$. Further, since $\xi^T(t)P_{\sigma(t)}\xi(t) \le \bar{\zeta}\xi^T(t)\xi(t)$ and $\xi^T(t)P_{\sigma(t)}\xi(t) \ge \underline{\zeta}\xi^T(t)\xi(t)$, one has

$$V(t_{l+1}) - V(t^-_{l+1}) \le \frac{\bar{\zeta} - \underline{\zeta}}{2\underline{\zeta}}\xi^T(t_{l+1})P_{\sigma(t^-_{l+1})}\xi(t_{l+1}) \le \frac{\bar{\zeta} - \underline{\zeta}}{\underline{\zeta}}V(t^-_{l+1}) \tag{4.20}$$

$$\Rightarrow V(t_{l+1}) \le \mu V(t^-_{l+1}), \tag{4.21}$$

The behavior of $V(t)$ between two consecutive switching instants, i.e., when $t \in [t_l,\ t_{l+1})$ is studied subsequently. Without the loss of generality, the closed-loop stability is analyzed by taking $p = \sigma(t^-_{l+1})$ as an active system.

Using (4.10), (4.19) and the Lyapunov equation $A_\sigma^T P_\sigma + P_\sigma A_\sigma = -Q_\sigma$, the time derivative of (4.18) yields

$$\dot{V}(t) \leq -\frac{1}{2}\xi^T(t)Q_{\sigma(t_{l+1}^-)}\xi(t) + \|\Psi_{\sigma(t_{l+1}^-)}\|\|r_{\sigma(t_{l+1}^-)}\| - (1-\bar{J})\rho_{\sigma(t_{l+1}^-)}\omega\frac{\|r_{\sigma(t_{l+1}^-)}\|^2}{\sqrt{\|r_{\sigma(t_{l+1}^-)}\|^2+\varepsilon}}$$
$$+\sum_{p=1}^{N}\sum_{i=0}^{1}\left\{(\hat{\phi}_{ip}(t)-\phi_{ip}^*)\dot{\hat{\phi}}_{ip}(t)+\gamma_{ip}(t)\dot{\gamma}_{ip}(t)\right\}. \tag{4.22}$$

For the ease of analysis, we define a region such that

$$\omega\frac{\|r_\sigma\|^2}{\sqrt{\|r_\sigma\|^2+\varepsilon}} \geq \|r_\sigma\| \Rightarrow \|r_\sigma\| \geq \sqrt{\frac{\varepsilon}{\omega^2-1}} \triangleq \varphi. \tag{4.23}$$

with $\omega > 1$ a user defined scalar. We analyse the behavior of the Lyapunov function for the two scenarios:

S1: $\|r_\sigma\| \geq \varphi$ and S2: $\|r_\sigma\| < \varphi$.

Scenario *S*1**:** It can be observed from the adaptive law (4.16) that the gains $\hat{\phi}_{i\overline{p}}$ and γ_{ip} remain constant during inactive and active intervals, respectively. Utilizing these observations and the upper bound structure (4.14) of uncertainty, (4.22) becomes

$$\dot{V}(t) \leq -\frac{1}{2}\xi^T(t)Q_{\sigma(t_{l+1}^-)}\xi(t) - \left[(\hat{\phi}_{0\sigma(t_{l+1}^-)}-\phi_{0\sigma(t_{l+1}^-)}^*)+(\hat{\phi}_{1\sigma(t_{l+1}^-)}-\phi_{1\sigma(t_{l+1}^-)}^*)\|\xi\|\right]\|r_{\sigma(t_{l+1}^-)}\|$$
$$+\sum_{i=0}^{1}(\hat{\phi}_{ip}(t)-\phi_{ip}^*)\dot{\hat{\phi}}_{ip}(t)+\sum_{\overline{p}\in\mathscr{I}(p)}\sum_{i=0}^{1}\gamma_{i\overline{p}}(t)\dot{\gamma}_{i\overline{p}}(t). \tag{4.24}$$

Using the adaptive law (4.16a) we have for $p = \sigma(t_{l+1}^-)$

$$\sum_{i=0}^{1}(\hat{\phi}_{ip}-\phi_{ip}^*)\dot{\hat{\phi}}_{ip} = \left[(\hat{\phi}_{0\sigma(t_{l+1}^-)}-\phi_{0\sigma(t_{l+1}^-)}^*)+(\hat{\phi}_{1\sigma(t_{l+1}^-)}-\phi_{1\sigma(t_{l+1}^-)}^*)\|\xi\|\right]\|r_\sigma(t_{l+1}^-)\|$$
$$+\sum_{i=0}^{1}(\alpha_{ip}\hat{\phi}_{ip}\phi_{ip}^* - \alpha_{ip}\hat{\phi}_{ip}^2). \tag{4.25}$$

Similarly, the adaptive law (4.16b) leads to

$$\gamma_{i\overline{p}}\dot{\gamma}_{i\overline{p}} = -\left(\beta_{i\overline{p}}+\overline{\nu}_{i\overline{p}}\hat{\phi}_{i\overline{p}}^4\right)\gamma_{i\overline{p}}^2 + \beta_{i\overline{p}}\nu_{i\overline{p}}\gamma_{i\overline{p}}. \tag{4.26}$$

Investigating the adaptive laws (4.16a)-(4.16b) and the initial gain conditions (4.16c), it can be verified that there exists a positive fixed scalar $\underline{\gamma}_{i\overline{p}}$ such that

$$\hat{\phi}_{ip}(t) \geq 0 \text{ and } \gamma_{i\overline{p}}(t) \geq \underline{\gamma}_{i\overline{p}} > 0 \quad \forall\, t \geq 0. \tag{4.27}$$

From (4.27) we have $\gamma_{i\overline{p}} \geq \underline{\gamma}_{i\overline{p}} \quad \forall\, t \geq 0$. Applying this relation to the second term of (4.26) yields

$$\gamma_{i\overline{p}}\dot{\gamma}_{i\overline{p}} \leq -\beta_{i\overline{p}}\gamma_{i\overline{p}}^2 - \underline{\gamma}_{i\overline{p}}^2\overline{\nu}_{i\overline{p}}\hat{\phi}_{i\overline{p}}^4 + \beta_{i\overline{p}}\nu_{i\overline{p}}\gamma_{i\overline{p}}. \tag{4.28}$$

The following simplification can be made:

$$-\underline{\gamma}_{i\overline{p}}^2\overline{\nu}_{i\overline{p}}\hat{\phi}_{i\overline{p}}^4+\frac{\zeta_p}{2}\hat{\phi}_{i\overline{p}}^2=-\underline{\gamma}_{i\overline{p}}^2\overline{\nu}_{i\overline{p}}\Big(\hat{\phi}_{i\overline{p}}^4-2\hat{\phi}_{ip}^2\cdot\frac{\zeta_p}{4\underline{\gamma}_{i\overline{p}}^2\overline{\nu}_{i\overline{p}}}\Big)$$

$$=-\underline{\gamma}_{i\overline{p}}^2\overline{\nu}_{i\overline{p}}\Big(\hat{\phi}_{i\overline{p}}^2-\frac{\zeta_p}{4\underline{\gamma}_{i\overline{p}}^2\overline{\nu}_{i\overline{p}}}\Big)^2+\frac{\zeta_p^2}{16\underline{\gamma}_{i\overline{p}}^2\overline{\nu}_{i\overline{p}}}. \tag{4.29}$$

Substituting (4.25), (4.28) and (4.29) into (4.24) yields

$$\dot{V}(t)\leq-\frac{1}{2}\lambda_{\min}(Q_{\sigma(t_{l+1}^-)})\|\xi(t)\|^2+\sum_{i=0}^{1}\Big(\alpha_{ip}\hat{\phi}_{ip}(t)\phi_{ip}^*-\alpha_{ip}\hat{\phi}_{ip}^2(t)\Big)$$

$$+\sum_{\overline{p}\in\mathscr{I}(p)}\sum_{i=0}^{1}\Big(\beta_{i\overline{p}}\nu_{i\overline{p}}\gamma_{i\overline{p}}-\beta_{i\overline{p}}\gamma_{i\overline{p}}^2-\frac{\zeta_p}{2}\hat{\phi}_{i\overline{p}}^2+\frac{\zeta_p^2}{16\underline{\gamma}_{i\overline{p}}^2\overline{\nu}_{i\overline{p}}}\Big). \tag{4.30}$$

Since $\hat{\phi}_{ip}\geq 0$ by (4.27), the Lyapunov function (4.18) satisfies

$$V\leq\frac{1}{2}\lambda_{\max}(P_\sigma)\|\xi\|^2+\frac{1}{2}\sum_{p=1}^{N}\sum_{i=0}^{1}(\hat{\phi}_{ip}^2+{\phi_{ip}^*}^2+\gamma_{ip}^2). \tag{4.31}$$

From the definitions of $\zeta,\zeta_p,\alpha_{ip},\beta_{i\overline{p}}$ and using (4.31), the condition (4.30) is further simplified to

$$\dot{V}(t)\leq-\zeta V(t)+\sum_{i=0}^{1}\Big(\alpha_{ip}\hat{\phi}_{ip}(t)\phi_{ip}^*-\bar{\alpha}_{ip}\hat{\phi}_{ip}^2(t)+\frac{\zeta_p}{2}\gamma_{ip}^2\Big)$$

$$+\sum_{p=1}^{N}\sum_{i=0}^{1}\frac{\zeta_p}{2}{\phi_{ip}^*}^2+\sum_{\overline{p}\in\mathscr{I}(p)}\sum_{i=0}^{1}\Big(\beta_{i\overline{p}}\nu_{i\overline{p}}\gamma_{i\overline{p}}(t)-\bar{\beta}_{i\overline{p}}\gamma_{i\overline{p}}^2(t)+\frac{\zeta_p^2}{16\underline{\gamma}_{i\overline{p}}^2\overline{\nu}_{i\overline{p}}}\Big) \tag{4.32}$$

where $\bar{\alpha}_{ip}\triangleq(\alpha_{ip}-\frac{\zeta_p}{2})>0$ and $\bar{\beta}_{i\overline{p}}\triangleq(\beta_{i\overline{p}}-\frac{\zeta_{\overline{p}}}{2})>0$. Again, the following simplification is made

$$\alpha_{ip}\hat{\phi}_{ip}\phi_{ip}^*-\bar{\alpha}_{ip}\hat{\phi}_{ip}^2=-\bar{\alpha}_{ip}\left(\hat{\phi}_{ip}-\frac{\alpha_{ip}\phi_{ip}^*}{2\bar{\alpha}_{ip}}\right)^2+\frac{\left(\alpha_{ip}\phi_{ip}^*\right)^2}{4\bar{\alpha}_{ip}}. \tag{4.33}$$

It can be noted from the adaptive laws (4.16) that $\gamma_{i\overline{p}}$ decreases for the inactive systems and remains unchanged for the active one. Coupled with the fact $\gamma_{ip}\geq\underline{\gamma}_{ip}\ \ \forall t\geq 0$, it is concluded that $\gamma_{ip}\in\mathscr{L}_\infty\ \forall p\in\Omega$. Then there exists $\bar{\gamma}_{ip}\in\mathbb{R}^+$ such that $\gamma_{ip}(t)\leq\bar{\gamma}_{ip}$. Using $0<\kappa<\zeta$, (4.33), $\dot{V}(t)$ in (4.32) simplifies to

$$\dot{V}(t)\leq-\kappa V(t)-(\zeta-\kappa)V(t)+\varsigma+\varsigma_2, \tag{4.34}$$

where $\varsigma\triangleq\sum_{p=1}^{N}\sum_{i=0}^{1}\frac{\zeta_p}{2}{\phi_{ip}^*}^2+\sum_{\overline{p}\in\mathscr{I}(p)}\sum_{i=0}^{1}\left[\beta_{ip}\nu_{i\overline{p}}\bar{\gamma}_{ip}+\zeta_p^2/(16\overline{\nu}_{i\overline{p}}\underline{\gamma}_{i\overline{p}}^2)\right]$ and $\varsigma_2\triangleq\sum_{i=0}^{1}\frac{\left(\alpha_{ip}\phi_{ip}^*\right)^2}{4\bar{\alpha}_{ip}}+\frac{\zeta_p}{2}\bar{\gamma}_{ip}^2$.

Scenario *S2***:** In this scenario we have $\|r_\sigma\| < \varphi$. Therefore,

$$\begin{aligned}\dot{V}(t) \leq & -(1/2)\xi^T(t)Q_{\sigma(t_{l+1}^-)}\xi(t) - (1-\bar{J})\rho_{\sigma(t_{l+1}^-)}\omega\frac{\|r_{\sigma(t_{l+1}^-)}\|^2}{\sqrt{\|r_{\sigma(t_{l+1}^-)}\|^2+\varepsilon}} \\ & + \left[\phi_{0\sigma}^* + \phi_{1\sigma}^*\|\xi\|\right]\|r_{\sigma(t_{l+1}^-)}\| + \sum_{i=0}^{1}\left(\hat{\phi}_{ip}(t)-\phi_{ip}^*\right)\dot{\hat{\phi}}_{ip}(t) + \sum_{\overline{p}\in\mathscr{I}(p)}\sum_{i=0}^{1}\gamma_{i\overline{p}}(t)\dot{\gamma}_{i\overline{p}}(t) \\ & \leq -\frac{1}{2}\xi^T(t)Q_{\sigma(t_{l+1}^-)}\xi(t) + \left[\phi_{0\sigma}^* + \phi_{1\sigma}^*\|\xi\|\right]\|r_{\sigma(t_{l+1}^-)}\| \\ & \sum_{i=0}^{1}\left(\hat{\phi}_{ip}(t)-\phi_{ip}^*\right)\dot{\hat{\phi}}_{ip}(t) + \sum_{\overline{p}\in\mathscr{I}(p)}\sum_{i=0}^{1}\gamma_{i\overline{p}}(t)\dot{\gamma}_{i\overline{p}}(t). \end{aligned} \tag{4.35}$$

Then, following similar lines as in Scenario *S*1, we have

$$\dot{V}(t) \leq -\kappa V(t) - (\zeta-\kappa)V(t) + \left[\hat{\phi}_{0\sigma} + \hat{\phi}_{1\sigma}\|\xi\|\right]\|r_{\sigma(t_{l+1}^-)}\| + \varsigma + \varsigma_2, \tag{4.36}$$

From (4.10) one has $\|r\| < \varphi \Rightarrow \|\xi\| \in \mathscr{L}_\infty$ and consequently, the adaptive law (4.16a) implies $\|r\|, \|\xi\| \in \mathscr{L}_\infty \Rightarrow \hat{\phi}_{ip}(t) \in \mathscr{L}_\infty$. Therefore, there exists $\varsigma_1 \in \mathbb{R}^+$ such that $Y^T\hat{\Phi}_p \leq \varsigma_1, \forall\sigma\in\Omega$ when $\|r_\sigma\| < \varphi$. Hence, replacing this relation in (4.36) yields

$$\dot{V}(t) \leq -\kappa V(t) - (\zeta-\kappa)V(t) + \varphi\varsigma_1 + \varsigma + \varsigma_2. \tag{4.37}$$

Further, combining (4.34) and (4.37) we define the scalar

$$\mathscr{B} \triangleq \frac{\varphi\varsigma_1 + \varsigma + \varsigma_2}{(\zeta-\kappa)}. \tag{4.38}$$

From the two scenarios *S*1 and *S*2, it can be concluded that $\dot{V}(t) \leq -\kappa V(t)$ when $V(t) \geq \mathscr{B}$. In light of this, further analysis is needed to observe the behavior of $V(t)$

(i) when $V(t) \geq \mathscr{B}$, we have $\dot{V}(t) \leq -\kappa V(t)$ from (4.34) implying exponential decrease of $V(t)$;

(ii) when $V(t) < \mathscr{B}$, $V(t)$ may increase.

Such behavior can be analyzed along the lines of [47, 100], and eventually leads to the bound

$$V(t) \leq \max\left\{cV(0), c\mu\mathscr{B}\right\}, \quad \forall\, t \geq 0. \tag{4.39}$$

Again, the definition of the Lyapunov function (4.18) yields

$$V(t) \geq (1/2)\lambda_{\min}(P_{\sigma(t)})\|\xi\|^2 \geq (\underline{\zeta}_m/2)\|\xi\|^2. \tag{4.40}$$

Using (4.39) and (4.40) we have

$$\|\xi\|^2 \leq (2/\underline{\zeta})\max\left\{cV(0), c\mu\mathscr{B}\right\}, \quad \forall\, t \geq 0. \tag{4.41}$$

Therefore, using the expression of $\mathscr{B}$ from (4.31), an ultimate bound b on the tracking error ξ can be found as

$$b = \sqrt{\frac{2\bar{\zeta}^{(N_0+1)}\left(\varphi\varsigma_1 + \varsigma + \varsigma_2\right)}{\underline{\zeta}^{(N_0+2)}(\zeta-\kappa)}} \tag{4.42}$$

□

4.5. SIMULATION EXAMPLE

The effectiveness of the proposed LFC design is tested using the IEEE 39 bus system [6]. To implement the multi-area LFC, the system is divided into three areas (cf. Fig. 4.3). Tie lines between buses 2 and 3, and buses 17 and 27 connect areas 1 and 2; tie lines between buses 5 and 8, and buses 7 and 8 connect areas 2 and 3, and a tie line between buses 1 and 2 connects areas 1 and 3. While all ten generators are equipped with a local LFC, only a few (four) generators implement the multi-area LFC to dampen oscillation among areas: the generator connected to bus 37 is responsible for multi-area LFC in area 1; the generators connected to buses 32 and 36 are responsible in equal percentage for multi-area LFC in area 2; the generator connected to bus 39 is responsible for multi-area LFC in area 3. This setting is consistent with [6].

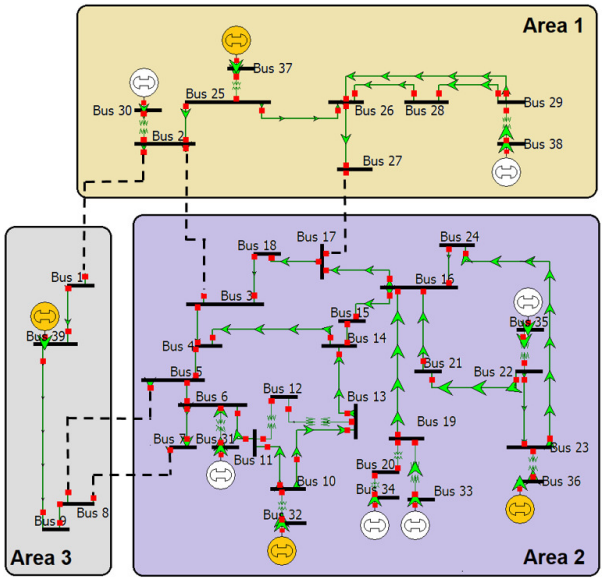

Figure 4.3: Benchmark IEEE 39-bus system divided into three areas. All ten generators implement local (intra-area) LFC, while four generators (indicated in yellow) additionally implement multi-area LFC.

4.5.1. DESIGN AND CONSIDERATIONS ON CONTROL DISAGGREGATION

Each generator responsible for multi-area LFC in one area "sees" the area as an aggregated dynamical system (where the aggregated dynamics also include the local LFC dynamics and the bus dynamics). The actual parameters of such aggregated dynamical system are mostly unknown and not available for control design and, in view of **Assumption** 4.1, the only available knowledge for control design is the inertia parameters of the generators (cf. Table 4.3). In our test case, only the inertia of generator 37, the average inertia of generators 32 and 36, and the inertia of generator 39 are used to obtain the nominal $\hat{L}$ in (4.12a), according to **Algorithm** 1. The solutions to the Lyapunov equations

Algorithm 1 Design and implementation steps of the proposed multi-area LFC

Design Step 1: with $\Delta\dot{\theta}^d = 0$, obtain the desired phase $\Delta\theta^d$ from power flow equations at the nominal operating point;
Design Step 2: define the tracking error variable as in (4.10) via the Lyapunov equation (4.11);
Design Step 3: compute the control law u_σ as in (4.12) and (4.15) with suitable $K_{1\sigma}$, $K_{2\sigma}$ and ω, ε;
Design Step 4: design the adaptive laws as in (4.16);
Design Step 5: design the switching law as in (4.17).

Implementation Step 1: for each area i, assign one or more generators for multi-area LFC; use the inertia of those generators (or their average) to obtain the nominal $\hat{L}$ in (4.12a);
Implementation Step 2: define $u_\sigma = [u_{1\sigma}, u_{2\sigma}, \ldots, u_{n\sigma}]^T$, where $u_{i\sigma}$ is the control assigned to area i;
Implementation Step 3: if only one generator is assigned for multi-area LFC in area i, assign $u_{i\sigma}$ to that generator; if more generators are assigned for multi-area LFC in area i, partition $u_{i\sigma}$ among those generators (e.g. in equal proportions).

are

$$\mathbf{P}_1 = \begin{bmatrix} 35.0728 & 0 & 0 & 0.2581 & 0 & 0 \\ 0 & 35.0728 & 0 & 0 & 0.2581 & 0 \\ 0 & 0 & 35.0728 & 0 & 0 & 0.2581 \\ 0.2581 & 0 & 0 & 2.0564 & 0 & 0 \\ 0 & 0.2581 & 0 & 0 & 2.0564 & 0 \\ 0 & 0 & 0.2581 & 0 & 0 & 2.0564 \end{bmatrix}$$

$$\mathbf{P}_2 = \begin{bmatrix} 32.2954 & 0 & 0 & 0.4753 & 0 & 0 \\ 0 & 32.2954 & 0 & 0 & 0.4753 & 0 \\ 0 & 0 & 32.2954 & 0 & 0 & 0.4753 \\ 0.4753 & 0 & 0 & 1.8929 & 0 & 0 \\ 0 & 0.4753 & 0 & 0 & 1.8929 & 0 \\ 0 & 0 & 0.4753 & 0 & 0 & 1.8929 \end{bmatrix}$$

$$\mathbf{P}_3 = \begin{bmatrix} 48.3565 & 0 & 0 & 0.5694 & 0 & 0 \\ 0 & 48.3565 & 0 & 0 & 0.5694 & 0 \\ 0 & 0 & 48.3565 & 0 & 0 & 0.5694 \\ 0.5694 & 0 & 0 & 2.8334 & 0 & 0 \\ 0 & 0.5694 & 0 & 0 & 2.8334 & 0 \\ 0 & 0 & 0.5694 & 0 & 0 & 2.8334 \end{bmatrix}$$

$$\mathbf{P}_4 = \begin{bmatrix} 48.5521 & 0 & 0 & 0.8575 & 0 & 0 \\ 0 & 97.1043 & 0 & 0 & 0.8575 & 0 \\ 0 & 0 & 97.1043 & 0 & 0 & 0.8575 \\ 0.8575 & 0 & 0 & 2.8483 & 0 & 0 \\ 0 & 0.8575 & 0 & 0 & 2.8483 & 0 \\ 0 & 0 & 0.8575 & 0 & 0 & 2.8483 \end{bmatrix}$$

We further select $K_{1\sigma} = 15\mathbf{I}$, $K_{2\sigma} = 0.8\mathbf{I}$, where we use the same values for every topology. The Lyapunov matrices yield $\zeta = 0.2059$, $\mu = 25.7588$, and, when $\kappa = 0.9\zeta$, the ADT satisfies $\ln\mu/\kappa = 17.5316$, according to (4.17). This implies that topology can switch up to every 17.5 seconds on average. The switching law σ previously presented in Fig. 4.2 is adopted in simulations.

Control design parameters are selected as: $\varepsilon = 0.1, \omega = 2$, $\bar{J} = 0.3$, $\alpha_{ip} = 0.2$, $\beta_{i\overline{p}} = 0.15$, $\bar{\nu}_{i\overline{p}} = 1$, $\nu_{i\overline{p}} = 0.7$ with $i = 0, 1$. The initial gains are $\hat{\phi}_{0p}(0) = 0.3$, $\gamma_{i\overline{p}}(0) = 25$.

Table 4.3: Inertia of generators in IEEE 39-bus system.

0.2653	Inertia of Generator 30
0.1607	Inertia of Generator 31
0.1899	Inertia of Generator 32
0.1517	Inertia of Generator 33
0.1379	Inertia of Generator 34
0.1846	Inertia of Generator 35
0.1401	Inertia of Generator 36
0.1289	Inertia of Generator 37
0.1830	Inertia of Generator 38
0.2228	Inertia of Generator 39

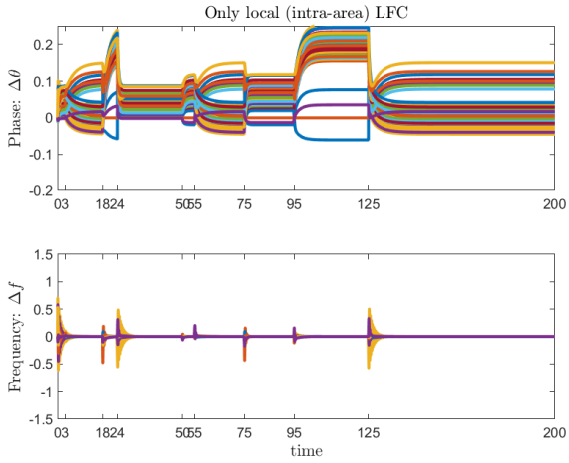

Figure 4.4: Phase and frequency deviations for all nodes with only local (intra-area) LFC (no multi-area LFC)

.

4.5.2. SIMULATION RESULTS AND DISCUSSION

To compare and assess the benefits of the proposed multi-area LFC approach, we implement the local LFC (without multi-area LFC), and a standard non-adaptive multi-area LFC, which is a proportional derivative controller with proportional gain equal to 3

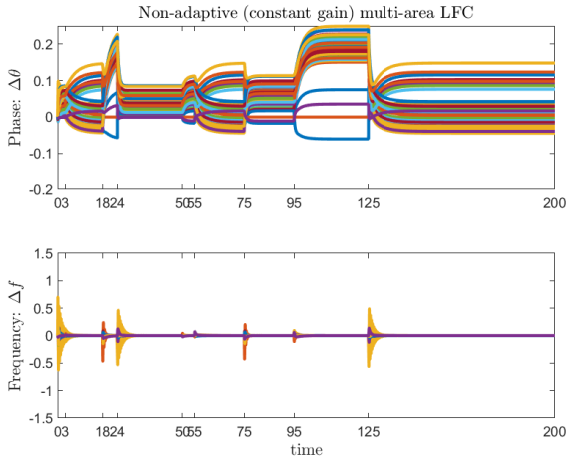

Figure 4.5: Phase and frequency deviations for all nodes with local (intra-area) LFC and non-adaptive (constant gain) multi-area LFC.

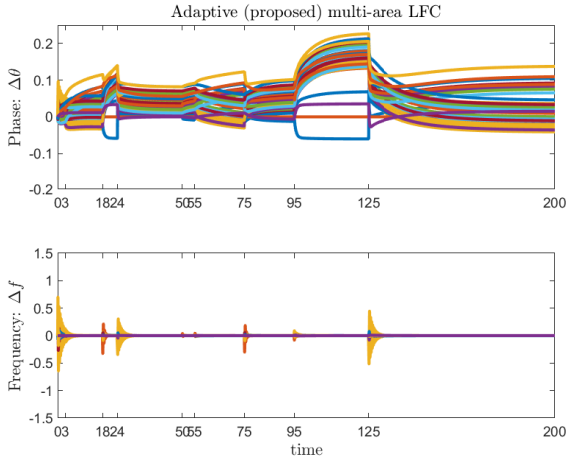

Figure 4.6: Phase and frequency deviations for all nodes with local (intra-area) LFC and adaptive (proposed) multi-area LFC.

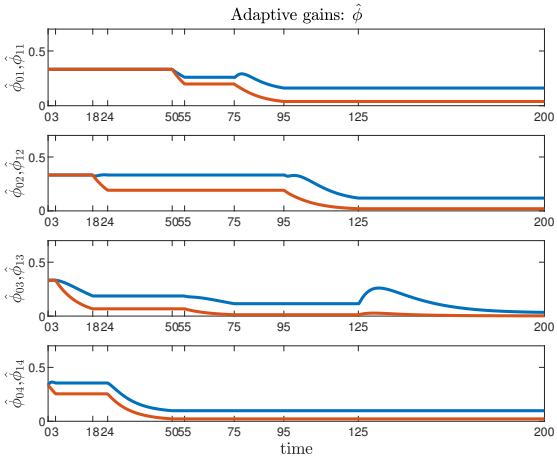

Figure 4.7: Adaptive gains $\hat{\phi}_{0p}$ (blue line) and $\hat{\phi}_{1p}$ (red line) for each topology.

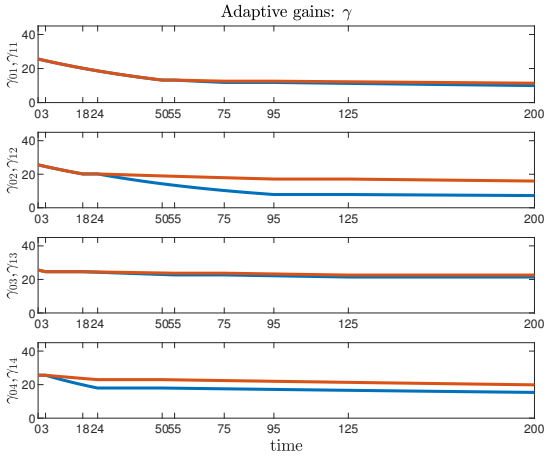

Figure 4.8: Adaptive gains $\hat{\gamma}_{0p}$ (blue line) and $\hat{\gamma}_{1p}$ (red line) for each topology.

Table 4.4: Error deviation norms for non-adaptive and adaptive multi-area LFC, with improvements reported as compared to the only-local LFC scenario (without multi-area LFC).

	Norm of Phase Deviation	Norm of Frequency Deviation
Only-Local LFC	226.06 (-)	85.35 (-)
Non-adaptive Multi-area LFC	219.35 (**-3.05%**)	70.86 (**-20.45%**)
Adaptive (proposed) Multi-area	192.01 (**-17.73%**)	53.27 (**-60.22%**)

and derivative gain equal to 30 (these gains have been tuned to provide the best performance).

The performance of the three approaches (only local LFC, non-adaptive multi-area LFC, and adaptive multi-area LFC) are reported in Table 4.4 in terms of the norm of phase deviations and norm of frequency deviations. Because synchronization of a power system to a constant frequency implies a rotation with a linearly increasing phase (the phase being the integral of the frequency), we use bus 9 as a rotating reference [81]. By this, we can evaluate the frequency deviation, and compare the phase deviation with the desired equilibrium phase resulting from the solution to the optimal power flow equilibrium. The percentage improvements in Table 4.4 show that the proposed adaptive multi-area LFC outperforms the non-adaptive multi-area LFC approach almost six times in terms of phase deviations (-3.05% vs -17.73%) and almost three times in terms of frequency deviations (-20.45% vs -60.22%). This implies reduced frequency oscillations and the smallest deviations from the optimal power flow phase.

The evolution of phase deviations and frequency deviations are reported in Fig. 4.4 for the local LFC approach, in Fig. 4.5 for non-adaptive multi-area LFC approach, and in Fig. 4.6 for the proposed adaptive multi-area LFC approach. In these figures, all phase deviations are bounded, transients occur due to topology changes at the switching instants in Fig. 4.2, and the size of the oscillations are also influenced by the generator parameters and the load.

Finally, Fig. 4.7 and Fig. 4.8 illustrate the adaptive gains for active and inactive topologies ($\hat{\phi}_{ip}$, $\hat{\phi}_{i\bar{p}}$, γ_{ip} and $\gamma_{i\bar{p}}$, $i = 0, 1$). The gains $\hat{\phi}_{i\bar{p}}$ remain constant when the corresponding topology is inactive, while the gains $\hat{\phi}_{ip}$ adapt when the corresponding topology is activated. On the other hand, the gains $\gamma_{i\bar{p}}$ adapt when the corresponding topology is inactive, while the gains γ_{ip} remain constant when the corresponding topology is activated.

Therefore, all gains automatically adapt or remain constant in order to obtain stability for any topology. This shows the adaptation capabilities of the proposed framework.

4.6. CONCLUDING REMARKS

This chapter has developed a switched adaptation framework for multi-area LFC based on nonlinear structure-preserving (Kuramoto) dynamics with state-dependent uncertainty. In this modeling framework, which provides a more rich description of uncertainties typically considered in multi-area LFC, stable self-reconfiguration was proven using Lyapunov theory in the presence of changing topologies among multi-area power systems.

5

DISTRIBUTED ADAPTIVE SYNCHRONIZATION IN EULER-LAGRANGE NETWORKS

This chapter discusses a new practical synchronization protocol for multiple Euler-Lagra-nge systems without structural linear-in-the-parameters (LIP) knowledge of the uncertainty and where the agents can be interconnected before the control design by unknown state-dependent interconnection terms. This setting is meant to overcome two standard a priori assumptions in the literature concerning uncertainty with LIP structure and the absence of interaction among agents before designing the synchronization protocol. To overcome these assumptions, we propose an adaptive distributed control mechanism having the purpose of estimating the coefficients of the resulting state-dependent uncertainty structure. Stability analysis and numerical validations are presented.

5.1. INTRODUCTION

Motivated by the advances in multi-agent systems, the problem of controlling a single Euler-Lagrange system to track desired trajectories [89, 102, 116] has been recently accompanied by the problem of controlling multiple Euler-Lagrange systems [129, 144] toward a common behavior. Euler-Lagrange dynamics can describe the motion of various mechanical systems [13, 103], robotic manipulators [59, 79], aerospace systems [25], and many more.

Crucial aspects worth considering in uncertain Euler-Lagrange systems include the a priori assumptions on the uncertainty: a typical assumption is the *linear-in-the-parameters (LIP) structure* [31, 64], which however is rarely met in practical situations. Another crucial aspect worth considering in multiple uncertain Euler-Lagrange systems

This chapter is based on the submitted paper [135]

includes the assumptions made on the *a priori structure of the interaction*, i.e. how the Euler-Lagrange systems interact before the control design. In most literature on multiple Euler-Lagrange systems [12, 51, 171], interconnections between agents are assumed nonexistent before the control design. Therefore, most approaches rely on two important a priori assumptions concerning uncertainty with LIP structure and the absence of interaction among agents before protocol design, which motivates the aforementioned ***Question 3:*** *How to design an adaptive distributed design for Euler-Lagrange agents in the presence of state-dependent uncertainty and interaction terms while overcoming the restrictive assumptions of the state of the art?*

To answer this question, firstly, we consider state-dependent uncertainty (not necessarily LIP). Then, differently from the standard literature, we consider that the interaction terms among agents exist before the control design, which are also state-dependent. In summarizing, the work presented in this chapter addresses and solves the leader-following synchronization for multiple uncertain Euler-Lagrange systems with state-dependent uncertainty and without a priori bounded interconnections. As a result of removing the a priori bounded structure [104], we must seek for practical synchronization (cf. **Definition** 2.8) instead of asymptotic synchronization (cf. **Definition** 2.7). To address the presence of state-dependent uncertainty and uncertain state-dependent interconnections, we propose an adaptive distributed control mechanism having the purpose of estimating the coefficients of the resulting uncertainty structure.

The rest of the chapter is organized as follows: the synchronization problem is formulated in Section 5.2. Adaptive synchronization laws are given in Section 5.3, with Lyapunov stability analysis in Section 5.4. Simulations are in Section 5.5, with concluding remarks in Section 5.6.

5.2. PROBLEM FORMULATION

Let each node $i = 1, \dots, N$ be represented by Euler-Lagrange dynamics (in the following, we may remove time dependency for brevity):

$$\begin{aligned} M_i(q_i(t))\ddot{q}_i(t) + C_i(q_i(t), \dot{q}_i(t))\dot{q}_i(t) + G_i(q_i(t)) \\ + F_i(\dot{q}_i(t)) + H_i(e_i(t), \dot{e}_i(t)) + d_i(t) = \tau_i(t) \end{aligned} \tag{5.1}$$

where $q_i, \dot{q}_i, \ddot{q}_i \in \mathbb{R}^n$ are the generalized coordinates and their derivatives, and $\tau_i \in \mathbb{R}^n$ is the control input. The system dynamics (5.1) comprise the mass/inertia matrix $M_i(q_i)$, the centripetal term $C_i(q_i, \dot{q}_i)$, the gravity term $G_i(q_i)$, the friction term $F_i(\dot{q}_i)$, and an external bounded disturbance $\|d_i\| \leq \bar{d}_i \ \forall t$ (with possibly unknown $\bar{d}_i$). In addition, (5.1) includes an interconnection term $H_i(e_i, \dot{e}_i)$ depending on the local synchronization error $e_i \in \mathbb{R}^n$ and its derivative $\dot{e}_i \in \mathbb{R}^n$:

$$e_i = \sum_{j \in \mathcal{N}_i} a_{ij}(q_i - q_j) + b_i(q_i - q_0) \tag{5.2a}$$

$$\dot{e}_i = \sum_{j \in \mathcal{N}_i} a_{ij}(\dot{q}_i - \dot{q}_j) + b_i(\dot{q}_i - \dot{q}_0) \tag{5.2b}$$

where $q_0, \dot{q}_0 \in \mathbb{R}^n$ represent the state of the leader and its derivative, and $\mathcal{N}_i$ denotes the neighboring set of agent i. As common in Euler-Lagrange literature, we consider $\|\dot{q}_0\| \leq \bar{q}_0$, $\|\ddot{q}_0\| \leq \check{q}_0$ [73, 78]. We take $\bar{q}_0, \check{q}_0$ as unknown constants.

Remark 5.1 (Interconnection before the control design)**.** *The dynamics in* (5.1) *depart from considering a priori disconnected dynamics, i.e. when the dynamics of each agent i are unaffected by neighboring states $q_j, \dot{q}_j$ before the control design [3, 12, 18, 51, 72, 78, 171]. On the other hand, the terms $H_i(e_i, \dot{e}_i)$ in* (5.1) *are active even before the control design. These interconnection terms, which cannot be designed and cannot be bounded a priori (cf.* ***Property*** *5.4), require a new design that is not available in the literature.*

The following properties for the dynamic terms in (5.1) are taken or further extended from standard and recent Euler-Lagrange literature [125, 161]:

Property 5.1. *There exist $\bar{c}_i$, $\bar{g}_i$, $\bar{f}_i \in \mathbb{R}^+$ such that $\|C_i(q_i, \dot{q}_i)\| \leq \bar{c}_i \|\dot{q}_i\|$, $\|G_i(q_i)\| \leq \bar{g}_i$, $\|F_i(\dot{q}_i)\| \leq \bar{f}_i \|\dot{q}_i\|$.*

Property 5.2. *The matrix $M_i(q_i)$ is symmetric and uniformly positive definite in q_i: there exist positive constants $\underline{m}$ and $\overline{m}$ such that $0 \leq \underline{m} I_n \leq M_i(q_i) \leq \overline{m} I_n, \forall q_i, \forall i$.*

Property 5.3. *The matrix $\dot{M}_i(q_i) - 2C_i(q_i, \dot{q}_i)$ is skew symmetric, i.e. for any non-zero vector s, we have $s^T(\dot{M}_i(q_i) - 2C_i(q_i, \dot{q}_i))s = 0$.*

Property 5.4. *There exist $\bar{h}_{1i}$, $\bar{h}_{2i}$, $\bar{h}_{3i}$, $\bar{h}_{4i}$, $\bar{h}_{5i} \in \mathbb{R}^+$ such that $\|H_i(e_i, \dot{e}_i)\| \leq \bar{h}_{1i} + \bar{h}_{2i}\|e_i\| + \bar{h}_{3i}\|\dot{e}_i\| + \bar{h}_{4i}\|e_i\|^2 + \bar{h}_{5i}\|\dot{e}_i\|^2$.*

All the constants in **Properties** 5.1, 5.2 and 5.4 are possibly unknown for the control design. In **Property** 5.4 we take the interconnection term $H_i(e_i, \dot{e}_i)$ with a quadratic upper bound. This is a natural choice in view of the fact that the other forces stemming from centripetal, gravity, or friction terms in **Property** 5.1, have linear or quadratic upper bounds.

As we will assume the presence of a directed spanning tree in the graph as in **Assumption** 2.1, we will make use of **Lemma** 2.2 for stability analysis.

Remark 5.2 (No structural knowledge)**.** *In* ***Properties*** *5.1-5.4, no assumption is made on the LIP structure of the dynamic terms, which marks another difference with standard Euler-Lagrange literature, since general friction terms are not in LIP form [76, 161]. The price to be paid as shown in [104, 161], is that practical synchronization (cf.* ***Definition*** *2.8) must be sought in place of asymptotic synchronization (cf.* ***Definition*** *2.7). That is, the synchronization error in this chapter will converge to a small uniformly ultimate bound around zero instead of asymptotically converge to zero.*

Problem 5.1. *Under* ***Assumption*** *2.1 and* ***Properties*** *5.1-5.4, the adaptive synchronization problem is to design a distributed adaptive law for the Euler-Lagrange network* (5.1) *that guarantees the local synchronization error e to be UUB, cf.* ***Definition*** *2.6 (this implies the global synchronization error δ being UUB, cf.* ***Lemma*** *2.2).*

5.3. CONTROLLER DESIGN

The controller design requires a preliminary step concerning uncertainty analysis, as explained hereafter.

5.3.1. UNCERTAINTY ANALYSIS

First, we rewrite (5.1) as

$$M_i \ddot{q}_i = Q_i(q_i, \dot{q}_i, e_i, \dot{e}_i) + \tau_i \tag{5.3}$$

where $Q_i(q_i, \dot{q}_i, e_i, \dot{e}_i) = -C_i(q_i, \dot{q}_i)\dot{q}_i - G_i(q_i) - F_i(\dot{q}_i) - H_i(e_i, \dot{e}_i) - d_i$. Using **Property 5.1**, we have

$$\begin{aligned} \|Q_i(q_i, \dot{q}_i, e_i, \dot{e}_i)\| \leq (\bar{g}_i + \bar{d}_i + \bar{h}_{1i}) + \bar{f}_i\|\dot{q}_i\| + \bar{c}_i\|\dot{q}_i\|^2 \\ + \bar{h}_{2i}\|e_i\| + \bar{h}_{3i}\|\dot{e}_i\| + \bar{h}_{4i}\|e_i\|^2 + \bar{h}_{5i}\|\dot{e}_i\|^2 \end{aligned} \tag{5.4}$$

We define a filtered tracking error

$$r_i = \dot{e}_i + P_i e_i \tag{5.5}$$

with $P_i \in \mathbb{R}^{n\times n}$ a designed positive definite diagonal matrix.

Let us define $\xi_i = [e_i^T, \dot{e}_i^T, q_i^T, \dot{q}_i^T]^T$. The control mechanism using local information is designed as

$$\tau_i = -K_i r_i - \bar{\tau}_i - \bar{K}_i P_i^{-1} e_i \tag{5.6a}$$

$$\bar{\tau}_i = \omega \rho_i \frac{r_i}{\sqrt{\|r_i\|^2 + \varepsilon}} \tag{5.6b}$$

$$\rho_i = \hat{\theta}_{0i} + \hat{\theta}_{1i}\|\xi_i\| + \hat{\theta}_{2i}\|\xi_i\|^2 + \gamma_i \tag{5.6c}$$

where $K_i \in \mathbb{R}^{n\times n}$ is a designed positive definite matrix, $\bar{K}_i \in \mathbb{R}^{n\times n}$ is a designed positive definite diagonal matrix, $\omega > 1, \varepsilon$ are user-defined scalars, and $\hat{\theta}_{0i}$, $\hat{\theta}_{1i}$, $\hat{\theta}_{2i}$ are adaptive parameters to be designed later.

The dynamics of $\dot{e}_i$ can be calculated as

$$\ddot{e}_i = \check{a}_i \ddot{q}_i - \sum_{j\in\mathcal{N}_i} a_{ij}\ddot{q}_j - b_i \ddot{q}_0 \tag{5.7}$$

where $\check{a}_i = b_i + \sum_{j\in\mathcal{N}_i} a_{ij} > 0$.

We multiply (5.7) with $\frac{1}{\check{a}_i} M_i$, and then add and subtract e_i, and use (5.3) to obtain

$$\begin{aligned} \frac{1}{\check{a}_i} M_i \ddot{e}_i &= M_i \ddot{q}_i - \sum_{j\in\mathcal{N}_i} \frac{a_{ij}}{\check{a}_i} (M_i M_j^{-1}) M_j \ddot{q}_j - \frac{1}{\check{a}_i} M_i b_i \ddot{q}_0 \\ &= -K_i r_i - \bar{K}_i P_i^{-1} e_i - \bar{\tau}_i + \sum_{j\in\mathcal{N}_i} A_{ij}\bar{\tau}_j + \Delta_{ij} \end{aligned} \tag{5.8}$$

where $A_{ij} = \frac{a_{ij}}{\check{a}_i}(M_i M_j^{-1})$, and Δ_{ij} is treated as an uncertainty term of agent i and agent j:

$$\Delta_{ij} \triangleq \Big[Q_i(q_i, \dot{q}_i, e_i, \dot{e}_i) - \frac{1}{\check{a}_i} M_i b_i \ddot{q}_0 - \sum_{j\in\mathcal{N}_i} A_{ij}\big[Q_j(q_j, \dot{q}_j, e_j, \dot{e}_j) - K_j r_j\big] \tag{5.9}$$

According to (5.5), we have

$$\frac{1}{\check{a}_i} M_i \ddot{e}_i = \frac{1}{\check{a}_i} M_i \dot{r}_i - \frac{1}{\check{a}_i} M_i P_i \dot{e}_i \tag{5.10}$$

Substituting (5.10) into (5.8), we get the dynamics of r_i:

$$\frac{1}{\check{a}_i} M_i \dot{r}_i = -K_i r_i - \bar{K}_i P_i^{-1} e_i - \bar{\tau}_i + \sum_{j \in \mathcal{N}_i} A_{ij} \bar{\tau}_j + \bar{\Delta}_{ij} - \frac{C_i r_i}{\check{a}_i} \tag{5.11}$$

where $\bar{\Delta}_{ij} = \Delta_{ij} + \frac{1}{\check{a}_i} M_i P_i \dot{e}_i + \frac{1}{\check{a}_i} C_i r_i$.

From the definition of ξ_i, it is implied that $\|e_i\| \le \|\xi_i\|$ and $\|\dot{e}_i\| \le \|\xi_i\|$, $\|q_i\| \le \|\xi_i\|$ and $\|\dot{q}_i\| \le \|\xi_i\|$. From (5.5), we can write $\|r_i\| \le (1 + \|P_i\|)\|\xi_i\|$. The following bound of the uncertainty $\|\bar{\Delta}_{ij}\|$ can be obtained:

$$\begin{aligned}
&\|\bar{\Delta}_{ij}\| \le (\bar{g}_i + \bar{d}_i + \bar{h}_{1i}) + \bar{f}_i \|\dot{q}_i\| + \bar{c}_i \|\dot{q}_i\|^2 + \bar{h}_{2i} \|e_i\| + \bar{h}_{3i} \|\dot{e}_i\| + \bar{h}_{4i} \|e_i\|^2 + \bar{h}_{5i} \|\dot{e}_i\|^2 \\
&+ \sum_{j \in \mathcal{N}_i} \bar{a}_{ij} \Big[(\bar{g}_j + \bar{d}_j + \bar{h}_{1j}) + \bar{f}_j \|\dot{q}_j\| + \bar{c}_j \|\dot{q}_j\|^2 + \bar{h}_{2j} \|e_j\| + \bar{h}_{3j} \|\dot{e}_j\| + \bar{h}_{4j} \|e_j\|^2 + \bar{h}_{5j} \|\dot{e}_j\|^2 \Big] \\
&+ \sum_{j \in \mathcal{N}_i} \bar{a}_{ij} \|K_j\| (1 + \|P_j\|) \|\xi_j\| + \frac{b_i}{\check{a}_i} \|M_i\| \|\ddot{q}_0\| + \frac{1}{\check{a}_i} \|P_i\| \|M_i\| \|\xi_i\| + \frac{\bar{c}_i}{\check{a}_i} (1 + \|P_i\|) \|\xi_i\| \\
&\le \theta_{0i}^* + \theta_{1i}^* \|\xi_i\| + \theta_{2i}^* \|\xi_i\|^2 + \sum_{j \in \mathcal{N}_i} \varphi_{1j}^* \|\xi_j\| + \sum_{j \in \mathcal{N}_i} \varphi_{2j}^* \|\xi_j\|^2
\end{aligned} \tag{5.12}$$

where $\bar{a}_{ij} = \|A_{ij}\|$, $\theta_{0i}^* = \big(\bar{g}_i + \bar{d}_i + \bar{h}_{1i}\big) + \sum_{j \in \mathcal{N}_i} \big[\bar{a}_{ij} (\bar{g}_j + \bar{d}_j + \bar{h}_{1j}\big] + \frac{b_i}{\check{a}_i} \overline{m} \check{q}_0$, $\theta_{1i}^* = \bar{h}_{2i} + \bar{h}_{3i} + \bar{f}_i + \frac{1}{\check{a}_i} \|P_i\| \|M_i\| + \frac{\bar{c}_i}{\check{a}_i} (1 + \|P_i\|)$, $\theta_{2i}^* = \bar{h}_{4i} + \bar{h}_{5i} + \bar{c}_i$, $\varphi_{1j}^* = \bar{a}_{ij} \big[\bar{h}_{2j} + \bar{h}_{3j} + \bar{f}_j + \|K_j\| (1 + \|P_j\|)\big]$, $\varphi_{2j}^* = \bar{a}_{ij} (\bar{h}_{4j} + \bar{h}_{5j} + \bar{c}_j)$.

Note that $\|A_{ij}\|$ can be bounded by a constant thanks to the uniform bounds for the mass matrix in **Property** 5.2. Also, $\theta_{0i}^*, \theta_{1i}^*, \theta_{2i}^*, \varphi_{1j}^*, \varphi_{2j}^*$ are all unknown constants according to **Properties** 5.1 and 5.4.

5.3.2. ADAPTIVE SYNCHRONIZATION LAWS

According to the structure of the upper bounds of $\bar{\Delta}_{ij}$ in (5.12), the adaptive laws for (5.6c) are designed as:

$$\dot{\hat{\theta}}_{0i} = \|r_i\| - \alpha_0 \hat{\theta}_{0i} \tag{5.13a}$$

$$\dot{\hat{\theta}}_{1i} = \|r_i\| \|\xi_i\| - \alpha_1 \hat{\theta}_{1i} \tag{5.13b}$$

$$\dot{\hat{\theta}}_{2i} = \|r_i\| \|\xi_i\|^2 - \alpha_2 \hat{\theta}_{2i} \tag{5.13c}$$

$$\dot{\gamma}_i = -(\epsilon_0 + \epsilon_1 \|\xi_i\|^7 - \epsilon_2 \|\xi_i\|^5) \gamma_i + \beta_i \tag{5.13d}$$

$$\text{where } \hat{\theta}_{0i}(0) > 0, \hat{\theta}_{1i}(0) > 0, \hat{\theta}_{2i}(0) > 0, \gamma_i(0) > 0 \tag{5.13e}$$

$$\epsilon_0, \epsilon_1, \epsilon_2, \alpha_i, \beta_i \in \mathbb{R}^+ \tag{5.13f}$$

with the inequalities

$$\epsilon_0 \ge 1 + \epsilon_2, \epsilon_1 \ge \epsilon_2 \tag{5.13g}$$

5.4. STABILITY ANALYSIS

Theorem 5.1. *Under **Assumption** 2.1 and **Properties** 5.1-5.4, the closed-loop trajectories of (5.1) employing control law (5.6) and adaptive law (5.13) are UUB with the following ultimate bound on the local synchronization error e:*

$$U = \sqrt{\frac{2\chi}{\min\limits_{i\in\Omega} \lambda_{\min}(\bar{K}_i P_i^{-1})(\zeta-\kappa)}} \tag{5.14}$$

where $\chi = \sum\limits_{i=1}^{N}\left(\frac{\alpha_0 {\theta_{0i}^*}^2}{2} + \frac{\alpha_1 {\theta_{1i}^*}^2}{2} + \frac{\alpha_2 {\theta_{2i}^*}^2}{2}\right) + \sum\limits_{i=1}^{N}\frac{2\zeta\bar{\gamma}_i}{\underline{\gamma}_i}$; *$\kappa$ is a scalar satisfying* $0<\kappa<\zeta$ *with* $\zeta = \dfrac{\min\left\{\underline{\lambda}(K_i), \underline{\lambda}(\bar{K}_i), \alpha_0/2, \alpha_1/2, \alpha_2/2\right\}}{\max\{\overline{m}/2\hat{a}, \overline{\lambda}(\bar{K}_i P_i^{-1})/2\}}$, *where* $\hat{a} = \min\limits_{i\in\Omega}\{\check{a}_i\}$.

Proof. Construct a Lyapunov function defined by:

$$\begin{aligned} V(t) =& \frac{1}{2}\sum_{i=1}^{N}\left(\frac{1}{\check{a}_i} {r_i}^T(t) M_i(t) r_i(t) + e_i^T(t)\bar{K}_i P_i^{-1} e_i(t)\right) \\ &+ \frac{1}{2}\sum_{i=1}^{N}\left\{(\hat{\theta}_{0i}(t)-\theta_{0i}^*)^2 + (\hat{\theta}_{1i}(t)-\theta_{1i}^*)^2 + (\hat{\theta}_{2i}(t)-\theta_{2i}^*)^2 + \frac{2\gamma_i(t)}{\underline{\gamma}_i}\right\}. \end{aligned} \tag{5.15}$$

Note that (5.13d) has a stable linear time-varying structure in the variable γ_i thanks to the inequalities (5.13g), since

a) for $\|\xi\| \geq 1$: According to $\epsilon_1 \geq \epsilon_2$, we have $\epsilon_1\|\xi\|^7 - \epsilon_2\|\xi\|^5 \geq \epsilon_1\left(\|\xi\|^7 - \|\xi\|^5\right) \geq 0$. Thus, according to $\epsilon_0 \geq 1+\epsilon_2$ and $\epsilon_2 > 0$, we obtain

$$\epsilon_0 + \epsilon_1\|\xi\|^7 - \epsilon_2\|\xi\|^5 \geq \epsilon_0 \geq 1+\epsilon_2 > 1$$

b) for $\|\xi\| < 1$: According to $\epsilon_0 \geq 1+\epsilon_2$, we have $\epsilon_0 - \epsilon_2\|\xi\|^5 \geq 1+\epsilon_2\left(1-\|\xi\|^5\right) > 1$. Thus, according to $\epsilon_1 > 0$, we obtain

$$\epsilon_0 - \epsilon_2\|\xi\|^5 + \epsilon_1\|\xi\|^7 > 1.$$

Then, $\epsilon_0 - \epsilon_2\|\xi\|^5 + \epsilon_1\|\xi\|^7 > 1$ always holds, i.e. the system in (5.13d) can be seen as a stable linear time-varying system.

Based on the linear time-varying structure of (5.13d), the positive input β_i and positive initial condition (5.13e), Based on the adaptive laws (5.13a)-(5.13d) and initial conditions (5.13e), it can be verified that $\hat{\theta}_{li}(t) \geq 0$, $l = 0,1,2, \gamma_i(t) \geq \underline{\gamma}_i > 0\ \forall t \geq t_0$ for a positive scalar $\underline{\gamma}_i$. The above condition will be used in the subsequent stability analysis.

The proof is organized as follows: first, we calculate the time derivative of the Lyapunov function. Then, based on the structure of (5.6b), we study the behavior of the Lyapunov function under the three possible scenarios:

1) $\omega\frac{\|r_i\|^2}{\sqrt{\|r_i\|^2+\epsilon}} \geq \|r_i\|$ for all i;

2) $\omega\frac{\|r_i\|^2}{\sqrt{\|r_i\|^2+\epsilon}} < \|r_i\|$ for all i;

3) $\omega\frac{\|r_i\|^2}{\sqrt{\|r_i\|^2+\epsilon}} \geq \|r_i\|$ for $i = 1,...,k$, and $\omega\frac{\|r_i\|^2}{\sqrt{\|r_i\|^2+\epsilon}} < \|r_i\|$ for $i = k+1,...,N$.

Notice that a similar analysis along three scenarios is known in the literature [64]. Finally, combining the results of these three scenarios, we obtain the ultimate bound on the local synchronization error e. In subsequent analysis, we omit variable dependency for compactness. Using (5.5) and (5.11), the time derivative of (5.15) satisfies

$$\begin{aligned}
\dot{V} \leq & -\sum_{i=1}^{N} r_i^T K_i r_i + \sum_{i=1}^{N} r_i^T \bar{\Delta}_{ij} - \sum_{i=1}^{N} r_i^T \bar{\tau}_i + \sum_{i=1}^{N} r_i^T \sum_{j\in\mathcal{N}_i} A_{ij}\bar{\tau}_j \\
& + \frac{1}{2}\sum_{i=1}^{N}\frac{1}{\check{a}_i} r_i{}^T\big(\dot{M}_i - 2C_i\big)r_i + \sum_{i=1}^{N}\left\{\frac{\dot{\gamma}_i}{\underline{\gamma}_i} + \sum_{l=0}^{2}(\hat{\theta}_{li}-\theta_{li}^*)\dot{\hat{\theta}}_{li}\right\} - \sum_{i=1}^{N} e_i^T \bar{K}_i e_i \\
\leq & -\sum_{i=1}^{N} r_i^T K_i r_i + \sum_{i=1}^{N}\|r_i^T\|\|\bar{\Delta}_{ij}\| - \sum_{i=1}^{N} e_i^T \bar{K}_i e_i + \sum_{i=1}^{N}\left\{\frac{\dot{\gamma}_i}{\underline{\gamma}_i} + \sum_{l=0}^{2}(\hat{\theta}_{li}-\theta_{li}^*)\dot{\hat{\theta}}_{li}\right\} \\
& + \sum_{i=1}^{N}\left\{\sum_{j\in\mathcal{N}_j}\bar{a}_{ij}\rho_j\omega\frac{\|r_i\|\|r_j\|}{\sqrt{\|r_j\|^2+\varepsilon}} - \rho_i\omega\frac{\|r_i\|^2}{\sqrt{\|r_i\|^2+\varepsilon}}\right\}
\end{aligned} \tag{5.16}$$

Combined with (5.11) and (5.12), we obtain the uncertainty structure as

$$\begin{aligned}
\sum_{i=1}^{N}\|r_i\|\|\bar{\Delta}_{ij}\| \leq & \sum_{i=1}^{N}\|r_i\|\Big\{\theta_{0i}^* + \theta_{1i}^*\|\xi_i\| + \theta_{2i}^*\|\xi_i\|^2\Big\} \\
& + \sum_{i=1}^{N}\|r_i\|\Big\{\sum_{j\in\mathcal{N}_i}\varphi_{1j}^*\|\xi_j\| + \sum_{j\in\mathcal{N}_i}\varphi_{2j}^*\|\xi_j\|^2\Big\}.
\end{aligned} \tag{5.17}$$

According to (5.5), we have $\|r_i\| \leq (1+\|P_i\|)\|\xi_i\|$. Thus, the following two bounds hold:

$$\sum_{i=1}^{N}\|r_i\|\sum_{j\in\mathcal{N}_i}\varphi_{1j}^*\|\xi_j\| \leq \sum_{i=1}^{N}\sum_{j\in\mathcal{N}_i}\varphi_{1j}^*(1+\|P_i\|)\|\xi_i\|\|\xi_j\| \tag{5.18}$$

$$\sum_{i=1}^{N}\|r_i\|\sum_{j\in\mathcal{N}_i}\varphi_{2j}^*\|\xi_j\|^2 \leq \sum_{i=1}^{N}\sum_{j\in\mathcal{N}_i}\varphi_{2j}^*(1+\|P_i\|)\|\xi_i\|\|\xi_j\|^2 \tag{5.19}$$

The bounded-input-bounded-output property of the stable linear time-varying system (6.27d) with positive constant input β_i guarantees that $\gamma_i \in \mathscr{L}_\infty$, i.e. there exists $\bar{\gamma}_i \in \mathbb{R}^+$ such that $\gamma_i \leq \bar{\gamma}_i$. From $\frac{\|r_j\|}{\sqrt{\|r_j\|^2+\varepsilon}} \leq 1$, we get

$$\begin{aligned}
\sum_{i=1}^{N}\sum_{j\in\mathcal{N}_i}\bar{a}_{ij}\rho_j\omega\frac{\|r_i\|\|r_j\|}{\sqrt{\|r_j\|^2+\varepsilon}} \leq & \ \omega\sum_{i=1}^{N}\sum_{j\in\mathcal{N}_i}\bar{a}_{ij}\rho_j\|r_i\| \\
\leq \omega\sum_{i=1}^{N}\sum_{j\in\mathcal{N}_i}\Big\{\sum_{k=0}^{2}\bar{a}_{ij}\hat{\theta}_{kj}\|r_i\|\|\xi_j\|^k + \bar{a}_{ij}\gamma_j\|r_i\|\Big\}.
\end{aligned} \tag{5.20}$$

5

Meanwhile, the fact that the following dynamics $\dot{\hat{\theta}}_{0j} = -\alpha_0\hat{\theta}_{0j}, \dot{\hat{\theta}}_{1j} = -\alpha_1\hat{\theta}_{1j}, \dot{\hat{\theta}}_{2j} = -\alpha_2\hat{\theta}_{2j}$, in the adaptive laws (5.13a)-(5.13c) are first-order stable dynamics gives, the standard input/output stability properties [52, Sect. 3.3] gives

$$\hat{\theta}_{0j} \le \bar{\theta}_{0j} + \check{\theta}_{0j}\|r_j\| \tag{5.21a}$$
$$\hat{\theta}_{1j} \le \bar{\theta}_{1j} + \check{\theta}_{1j}\|r_j\|\|\xi_j\| \tag{5.21b}$$
$$\hat{\theta}_{2j} \le \bar{\theta}_{2j} + \check{\theta}_{2j}\|r_j\|\|\xi_j\|^2 \tag{5.21c}$$

with $\bar{\theta}_{0j}, \check{\theta}_{0j}, \bar{\theta}_{1j}, \check{\theta}_{1j}, \bar{\theta}_{2j}, \check{\theta}_{2j} \in \mathbb{R}^+$. This in turn leads to

$$\begin{aligned}\omega\sum_{i=1}^{N}\sum_{j\in\mathcal{N}_i}\bar{a}_{ij}\hat{\theta}_{2j}\|r_i\|\|\xi_j\|^2 \le& \omega\sum_{i=1}^{N}\sum_{j\in\mathcal{N}_i}\bar{a}_{ij}\bar{\theta}_{2j}(1+\|P_i\|)\|\xi_i\|\|\xi_j\| \\ &+\omega\sum_{i=1}^{N}\sum_{j\in\mathcal{N}_i}\bar{a}_{ij}\check{\theta}_{2j}(1+\|P_i\|)(1+\|P_j\|)\|\xi_i\|\|\xi_j\|^5.\end{aligned} \tag{5.22}$$

Similarly, we obtain the overall terms from the neighboring agents $j \in \mathcal{N}_i$:

$$\begin{aligned}&\sum_{i=1}^{N}\sum_{j\in\mathcal{N}_i}\left\{\bar{a}_{ij}\rho_j\omega\frac{\|r_i\|\|r_j\|}{\sqrt{\|r_j\|^2+\varepsilon}} + \|r_i\|\left(\varphi_{1j}^*\|\xi_j\| + \varphi_{2j}^*\|\xi_j\|^2\right)\right\} \\ \le&\sum_{i=1}^{N}\sum_{j\in\mathcal{N}_i}\Big\{\omega\bar{a}_{ij}(1+\|P_i\|)(\bar{\theta}_{0j}+\bar{\gamma}_j)\|\xi_i\| \\ &+(1+\|P_i\|)\left[\omega\bar{a}_{ij}(\check{\theta}_{0j}(1+\|P_j\|)+\bar{\theta}_{1j})+\varphi_{1j}^*\right]\|\xi_i\|\|\xi_j\| \\ &+(1+\|P_j\|)\left(\omega\bar{a}_{ij}\bar{\theta}_{2j}+\varphi_{2j}^*\right)\|\xi_i\|\|\xi_j\|^2 \\ &+\omega\bar{a}_{ij}(1+\|P_i\|)(1+\|P_j\|)\|\xi_i\|\|\xi_j\|^3(\check{\theta}_{1j}+\check{\theta}_{2j}\|\xi_j\|^2)\Big\}.\end{aligned} \tag{5.23}$$

Using (5.13a)-(5.13c), we have

$$(\hat{\theta}_{li}-\theta_{li}^*)\dot{\hat{\theta}}_{li} = (\hat{\theta}_{li}-\theta_{li}^*)\|\xi_i\|^l\|r_i\| + \left(\alpha_l\hat{\theta}_{li}\theta_{li}^* - \alpha_l\hat{\theta}_{li}^2\right) \tag{5.24}$$

for $l = 0, 1, 2$ and $i = 1, \cdots, N$. The last term of (5.24) can be rewritten as

$$\left(\alpha_l\hat{\theta}_{li}\theta_{li}^* - \alpha_l\hat{\theta}_{li}^2\right) = -\frac{\alpha_l(\hat{\theta}_{li}-\theta_{li}^*)^2}{2} + \frac{\alpha_l{\theta_{li}^*}^2}{2}. \tag{5.25}$$

Similarly, with $\gamma_i(t) \ge \underline{\gamma}_i > 0$, (5.13d) leads to

$$\begin{aligned}\frac{\dot{\gamma}_i(t)}{\gamma_i} =& \frac{1}{\gamma_i}\left[-(\epsilon_0+\epsilon_1\|\xi_i\|^7-\epsilon_2\|\xi_i\|^5)\gamma_i+\beta_i\right] \\ \le&\left[-\left(\epsilon_0+\epsilon_1|\xi_i\|^7-\epsilon_2\|\xi_i\|^5\right)+(\beta_i/\underline{\gamma}_i)\right]\end{aligned} \tag{5.26}$$

According to (5.17)-(5.26), from (5.16) we have

$$\begin{aligned}\dot{V} \leq & -\underline{\lambda}(K_i)\sum_{i=1}^{N}\|r_i\|^2 - \underline{\lambda}(\bar{K}_i)\sum_{i=1}^{N}\|e_i\|^2 + \sum_{i=1}^{N}\sum_{j\in\mathcal{N}_i}\Big\{\omega\bar{a}_{ij}(1+\|P_i\|)(\bar{\theta}_{0j}+\bar{\gamma}_j)\|\xi_i\| \\ & + (1+\|P_i\|)\Big[\omega\bar{a}_{ij}(\check{\theta}_{0j}(1+\|P_j\|)+\bar{\theta}_{1j})+\varphi^*_{1j}\Big]\|\xi_i\|\|\xi_j\| - \sum_{i=1}^{N}\rho_i\omega\frac{\|r_i\|^2}{\sqrt{\|r_i\|^2+\varepsilon}} \\ & + (1+\|P_j\|)\big(\omega\bar{a}_{ij}\bar{\theta}_{2j}+\varphi^*_{2j}\big)\|\xi_i\|\|\xi_j\|^2 - \sum_{i=1}^{N}\Big[\big(\epsilon_0+\epsilon_1|\xi_i\|^7-\epsilon_2\|\xi_i\|^5\big)+(\beta_i/\underline{\gamma}_i)\Big] \\ & + \omega\bar{a}_{ij}(1+\|P_i\|)(1+\|P_j\|)\|\xi_i\|\|\xi_j\|^3(\check{\theta}_{1j}+\check{\theta}_{2j}\|\xi_j\|^2)\Big\} + \sum_{i=1}^{N}\sum_{l=0}^{2}\theta^*_{li}\|\xi_i\|^l\|r_i\| \\ & + \sum_{i=1}^{N}\sum_{l=0}^{2}\Big\{(\hat{\theta}_{li}-\theta^*_{li})\|\xi_i\|^l\|r_i\| - \Big[\frac{\alpha_l(\hat{\theta}_{li}-\theta^*_{li})^2}{2} - \frac{\alpha_l{\theta^*_{li}}^2}{2}\Big]\Big\} \end{aligned} \tag{5.27}$$

where $\underline{\lambda}(K_i) = \min_{i\in\Omega}\lambda_{\min}(K_i)$, $\underline{\lambda}(\bar{K}_i) = \min_{i\in\Omega}\lambda_{\min}(\bar{K}_i)$.

We study the behavior of the Lyapunov function for the three aforementioned scenarios:

Scenario 1: We have $\omega\frac{\|r_i\|^2}{\sqrt{\|r_i\|^2+\varepsilon}} \geq \|r_i\|$ for all $i = 1,\ldots,N$. Then, according to (5.6c), we obtain

$$-\sum_{i=1}^{N}\rho_i\omega\frac{\|r_i\|^2}{\sqrt{\|r_i\|^2+\varepsilon}} \leq -\sum_{i=1}^{N}\rho_i\|r_i\| \leq -\sum_{i=1}^{N}\sum_{l=0}^{2}\Big[\hat{\theta}_{li}\|\xi_i\|^l+\gamma_i\Big]\|r_i\|. \tag{5.28}$$

Substituting (5.28) into (5.27), yields

$$\begin{aligned}\dot{V} \leq & -\underline{\lambda}(K_i)\sum_{i=1}^{N}\|r_i\|^2 - \underline{\lambda}(\bar{K}_i)\sum_{i=1}^{N}\|e_i\|^2 \\ & - \sum_{i=1}^{N}\sum_{l=0}^{2}\left\{\frac{\alpha_l(\hat{\theta}_{li}-\theta^*_{li})^2}{2} - \frac{\alpha_l{\theta^*_{li}}^2}{2}\right\} + Z_1(\|\xi\|)\end{aligned} \tag{5.29}$$

where $\Omega = \{1,\ldots,N\}$ and $\xi = [\xi_1^T,\ldots,\xi_N^T]^T$ with

$$\begin{aligned}Z_1(\|\xi\|) \triangleq & -\epsilon_1\sum_{i=1}^{N}\|\xi_i\|^7 + \epsilon_2\sum_{i=1}^{N}\|\xi_i\|^5 + \sum_{i=1}^{N}\Big(-\epsilon_0+\frac{\beta_i}{\underline{\gamma}_i}\Big) \\ & + \sum_{i=1}^{N}\sum_{j\in\mathcal{N}_i}\Big\{\omega\bar{a}_{ij}(1+\|P_i\|)(\bar{\theta}_{0j}+\bar{\gamma}_j)\|\xi_i\| \\ & + (1+\|P_i\|)\Big[\omega\bar{a}_{ij}(\check{\theta}_{0j}(1+\|P_j\|)+\bar{\theta}_{1j})+\varphi^*_{1j}\Big]\|\xi_i\|\|\xi_j\| \\ & + (1+\|P_j\|)\big(\omega\bar{a}_{ij}\bar{\theta}_{2j}+\varphi^*_{2j}\big)\|\xi_i\|\|\xi_j\|^2 \\ & + \omega\bar{a}_{ij}(1+\|P_i\|)(1+\|P_j\|)\|\xi_i\|\|\xi_j\|^3(\check{\theta}_{1j}+\check{\theta}_{2j}\|\xi_j\|^2)\Big\}.\end{aligned}$$

Using Descartes' rules of sign change and Bolzano's Theorem [107], the polynomial Z_1 has exactly one positive real root $\eta_1 \in \mathbb{R}^+$. The coefficient of the highest degree of Z_1 is negative: $-\epsilon_1$. Therefore, $Z_1(\|\xi\|) \leq 0$ when $\|\xi\| \geq \eta_1$.

Since $\hat{\theta}_{0i}(t) \geq 0, \hat{\theta}_{1i}(t) \geq 0, \hat{\theta}_{2i}(t) \geq 0$, the Lyapunov function (5.15) satisfies

$$V \leq \frac{\overline{m}}{2\hat{a}} \sum_{i=1}^{N} \|r_i\|^2 + \frac{\overline{\lambda}(\bar{K}_i P_i^{-1})}{2} \sum_{i=1}^{N} ||e_i||^2 + \frac{1}{2} \sum_{i=1}^{N} \left\{ \sum_{l=0}^{2} (\hat{\theta}_{li} - \theta_{li}^*)^2 + \frac{2\gamma_i}{\underline{\gamma}_i} \right\} \tag{5.30}$$

where $\overline{\lambda}(\bar{K}_i P_i^{-1}) = \max_{i \in \Omega} \overline{\lambda}(\bar{K}_i P_i^{-1})$.

Substituting (5.30) into (5.29) yields

$$\dot{V} \leq -\zeta V + \sum_{i=1}^{N} \left\{ \sum_{l=0}^{2} \frac{\alpha_l \theta_{li}^{*\,2}}{2} + \frac{2\zeta\bar{\gamma}_i}{\underline{\gamma}_i} \right\} + Z_1(\|\xi\|). \tag{5.31}$$

Defining a scalar $0 < \kappa < \zeta$, (5.31) is further simplified to

$$\dot{V} \leq -\kappa V - (\zeta - \kappa) V + \chi \tag{5.32}$$

where $Z_1(\|\xi\|)$ is defined as in (5.14).

Scenario 2: In this case, we have $0 \leq \frac{\omega \|r_i\|^2}{\sqrt{\|r_i\|^2 + \epsilon}} \leq \|r_i\|$ for all $i = 1, \ldots, N$. Then,

$$-\sum_{i=1}^{N} \rho_i \omega \frac{\|r_i\|^2}{\sqrt{\|r_i\|^2 + \varepsilon}} \leq 0 \tag{5.33}$$

Substituting (5.33) into (5.27), the time derivative of V satisfies

$$\begin{aligned}
\dot{V} \leq & -\underline{\lambda}(K_i) \sum_{i=1}^{N} \|r_i\|^2 - \underline{\lambda}(\bar{K}_i) \sum_{i=1}^{N} \|e_i\|^2 \\
& + \sum_{i=1}^{N} \sum_{j \in \mathcal{N}_i} \Big\{ \omega \bar{a}_{ij} (1 + \|P_i\|)(\bar{\theta}_{0j} + \bar{\gamma}_j) \|\xi_i\| \\
& + (1 + \|P_i\|) \Big[\omega \bar{a}_{ij} (\check{\theta}_{0j} (1 + \|P_j\|) + \bar{\theta}_{1j}) + \varphi_{1j}^* \Big] \|\xi_i\| \|\xi_j\| \\
& + (1 + \|P_j\|) \big(\omega \bar{a}_{ij} \bar{\theta}_{2j} + \varphi_{2j}^* \big) \|\xi_i\| \|\xi_j\|^2 \\
& + \omega \bar{a}_{ij} (1 + \|P_i\|)(1 + \|P_j\|) \|\xi_i\| \|\xi_j\|^3 (\check{\theta}_{1j} + \check{\theta}_{2j} \|\xi_i\|^2) \Big\} \\
& + \sum_{i=1}^{N} \sum_{l=0}^{2} \theta_{li}^* \|\xi_i\|^l \|r_i\| + \sum_{i=1}^{N} \sum_{l=0}^{2} (\hat{\theta}_{li} - \theta_{li}^*) \|\xi_i\|^l \|r_i\| \\
& - \sum_{i=1}^{N} \sum_{l=0}^{2} \left\{ \frac{\alpha_l (\hat{\theta}_{li} - \theta_{li}^*)^2}{2} - \frac{\alpha_l \theta_{li}^{*\,2}}{2} \right\} - \sum_{i=1}^{N} \Big[\big(\epsilon_0 + \epsilon_1 |\xi_i\|^7 - \epsilon_2 \|\xi_i\|^5 \big) + (\beta_i / \underline{\gamma}_i) \Big].
\end{aligned} \tag{5.34}$$

Then, following a similar reasoning as in Scenario 1, we have

$$\dot{V} \leq -\underline{\lambda}(K_i)\sum_{i=1}^{N}\|r_i\|^2 - \underline{\lambda}(\bar{K}_i)\sum_{i=1}^{N}\|e_i\|^2 + \sum_{i=1}^{N}\sum_{l=0}^{2}\left\{\hat{\theta}_{li}\|\xi_i\|^l\|r_i\| - \left[\frac{\alpha_l(\hat{\theta}_{li}-\theta_{li}^*)^2}{2} - \frac{\alpha_l\theta_{li}^{*\,2}}{2}\right]\right\}. \tag{5.35}$$

According to (5.21), with $\|r_i\| \leq (1+\|P_i\|)\|\xi_i\|$, if follows that

$$\sum_{i=1}^{N}\sum_{l=0}^{2}\hat{\theta}_{li}\|\xi_i\|^l\|r_i\| \leq \sum_{i=1}^{N}\left(\bar{\theta}_{li}+\check{\theta}_{li}\|r_i\|\|\xi_i\|^l\right)\|\xi_i\|^l\|r_i\| \leq \sum_{i=1}^{N}\bar{\theta}_{li}(1+\|P_i\|)\|\xi_i\|^{l+1} + \check{\theta}_{li}(1+\|P_i\|)^2\|\xi_i\|^{2(l+1)}. \tag{5.36}$$

Substituting (5.36) into (5.35), yields

$$\dot{V} \leq -\underline{\lambda}(K_i)\sum_{i=1}^{N}\|r_i\|^2 - \underline{\lambda}(\bar{K}_i)\sum_{i=1}^{N}\|e_i\|^2 - \sum_{i=1}^{N}\sum_{l=0}^{2}\left\{\frac{\alpha_l(\hat{\theta}_{li}-\theta_{li}^*)^2}{2} - \frac{\alpha_l\theta_{li}^{*\,2}}{2}\right\} + Z_2(\|\xi\|) \tag{5.37}$$

where $Z_2(\|\xi\|) = Z_1(\|\xi\|) + \sum_{i=1}^{N}\bar{\theta}_{0i}(1+\|P_i\|)\|\xi_i\| + \sum_{i=1}^{N}\bar{\theta}_{li}(1+\|P_i\|)\|\xi_i\|^{l+1} + \check{\theta}_{li}(1+\|P_i\|)^2 \cdot \|\xi_i\|^{2(l+1)}$. Similarly, there exists a unique positive real root $\eta_2 \in \mathbb{R}^+$ so that $Z_2(\|\xi\|) \leq 0$ when $\|\xi\| \geq \eta_2$. The coefficient of Z_2 with the highest degree is still $-\epsilon_1$. Finally, we get

$$\dot{V} \leq -\kappa V - (\zeta-\kappa)V + \chi. \tag{5.38}$$

Scenario 3: $\omega\frac{\|r_i\|^2}{\sqrt{\|r_i\|^2+\varepsilon}} \geq \|r_i\|$ for $i = 1,...,k$, and $\omega\frac{\|r_i\|^2}{\sqrt{\|r_i\|^2+\varepsilon}} < \|r_i\|$ for $i = k+1,...,N$. Then, following the steps as in Scenario1 and Scenario 2, we derive

$$\begin{aligned}\dot{V} &\leq -\underline{\lambda}(K_i)\sum_{i=1}^{N}\|r_i\|^2 - \underline{\lambda}(\bar{K}_i)\sum_{i=1}^{N}\|e_i\|^2(\bar{K}_i)\sum_{i=1}^{N}\|e_i\|^2 + Z_1(\|\xi\|) \\ &+ \sum_{i=k+1}^{N}\sum_{l=0}^{2}\hat{\theta}_{li}\|\xi_i\|^l\|r_i\| - \sum_{i=1}^{N}\sum_{l=0}^{2}\left\{\frac{\alpha_l(\hat{\theta}_{li}-\theta_{li}^*)^2}{2} - \frac{\alpha_l\theta_{li}^{*\,2}}{2}\right\}. \\ &\leq -\underline{\lambda}(K_i)\sum_{i=1}^{N}\|r_i\|^2 - \underline{\lambda}(\bar{K}_i)\sum_{i=1}^{N}\|e_i\|^2(\bar{K}_i)\sum_{i=1}^{N}\|e_i\|^2 + Z_3(\|\xi\|) \\ &- \sum_{i=1}^{N}\sum_{l=0}^{2}\left\{\frac{\alpha_l(\hat{\theta}_{li}-\theta_{li}^*)^2}{2} - \frac{\alpha_l\theta_{li}^{*\,2}}{2}\right\}\end{aligned} \tag{5.39}$$

where $Z_3(\|\xi\|) = Z_1(\|\xi\|) + \sum_{i=k+1}^{N}\sum_{i=1}^{N}\bar{\theta}_{li}(1+\|P_i\|)\|\xi_i\|^{l+1} + \check{\theta}_{li}(1+\|P_i\|)^2\|\xi_i\|^{2(l+1)}$. There will exist a unique root η_3 such that $Z_3(\|\xi\|) \leq 0$ when $\|\xi\| \geq \eta_3$. Similarly, the following is

obtained:

$$\dot{V} \leq -\kappa V - (\zeta - \kappa)V + \chi. \tag{5.40}$$

Combining (5.32), (5.38) and (5.40) from Scenarios 1, 2 and 3 respectively, it can be concluded that $\dot{V} \leq -\kappa V$ when $V \geq Y$ and $\|\xi\| \geq \max\{\eta_1, \eta_2, \eta_3\}$ where

$$Y = \frac{\chi}{(\zeta - \kappa)} \tag{5.41}$$

and thus, the closed-loop system remains UUB with the bound

$$V(t) \leq \max\{V(0), Y\}, \ \forall t \geq 0 \tag{5.42}$$

The definition of the Lyapunov function (5.15) satisfies

$$V(t) \geq \frac{\underline{\lambda}(\bar{K}_i P_i^{-1})}{2} \|e\|^2 \tag{5.43}$$

5

where $e = [e_i^T, \ldots, e_N^T]^T$.

Using (5.42) and (5.43), it can be obtained that $\|e\|^2 \leq \dfrac{2}{\underline{\lambda}(\bar{K}_i P_i^{-1})} \max\{V(0), Y\}, \ \forall t \geq 0$, giving the uniform ultimate bound U (cf. **Definition** 2.6) in (5.14). □

Remark 5.3 (Ultimate bound and gain tuning)**.** *Owing to the user-defined diagonal matrices $\bar{K}_i$ and P_i, one can notice that the ultimate bound U in (5.14) can be reduced by tuning $\bar{K}_i$ and P_i (i.e. with higher values of $\bar{K}_i P_i^{-1}$). However, the fact that $\bar{m}$, θ_{li}^* are completely unknown prevents reduction of the bound to a arbitrary small level: this is consistent with robust adaptive control literature with leakage terms α_i as in (5.13a)-(5.13c) [52]. In addition, it can be noticed from (5.29), (5.35), and (5.39) that higher values of K_i, ϵ_1, ϵ_0 and lower values of ϵ_2 lead to faster convergence of the Lyapunov function, which may in turn cause a larger control effort. Therefore, tuning choices have to be made according to application requirements.*

5.5. SIMULATION EXAMPLE

We will consider six Euler-Lagrange systems (cf. Fig 5.1), representing two-link robot arms with equations of motion as [60]:

$$\begin{bmatrix} M_i^{11} & M_i^{12} \\ M_i^{12} & M_i^{22} \end{bmatrix} \begin{bmatrix} \ddot{q}_{i1} \\ \ddot{q}_{i2} \end{bmatrix} + \begin{bmatrix} c_i \dot{q}_{i2} & c_i(\dot{q}_{i1} + \dot{q}_{i2}) \\ -c_i \dot{q}_{i1} & 0 \end{bmatrix} \begin{bmatrix} \dot{q}_{i1} \\ \dot{q}_{i2} \end{bmatrix} + d_i$$
$$+ \begin{bmatrix} m_{i4} g \cos(q_{i1}) + g_i \\ g_i \end{bmatrix} + \begin{bmatrix} F_{i1}(\dot{q}_i) \\ F_{i2}(\dot{q}_i) \end{bmatrix} + H_i(e_i, \dot{e}_i) = \begin{bmatrix} \tau_{i1} \\ \tau_{i2} \end{bmatrix} \tag{5.44}$$

where $c_i = -m_{i3} \sin(q_{i2})$ and

$$M_i^{11} = m_{i1} + m_{i2} + 2m_{i3} \cos(q_{i2}),$$
$$M_i^{12} = m_{i2} + m_{i3} \cos(q_{i2}),$$
$$M_i^{22} = m_{i2}, \ g_i = m_{i5} g \cos(q_{i1} + q_{i2}).$$

The friction term is taken in non-LIP form as [76]: $F_{i1}(\dot{q}_{i1}) = f_{i1}\big(\tanh(f_{i2}\dot{q}_{i1}) - \tanh(f_{i3}\dot{q}_{i1})\big) + f_{i4}\tanh(f_{i5}\dot{q}_{i1}) + f_{i6}\dot{q}_{i1}$, $F_{i2}(\dot{q}_i) = f_{i1}\big(\tanh(f_{i2}\dot{q}_{i2}) - \tanh(f_{i3}\dot{q}_{i2})\big) + f_{i4}\tanh(f_{i5}\dot{q}_{i2}) + f_{i6}\dot{q}_{i2}$. The parameters are compactly represented as $\Theta_i = [m_{i1}\ m_{i2}\ m_{i3}\ m_{i4}\ m_{i5}\ f_{i1}\ f_{i2}\ f_{i3}\ f_{i4}\ f_{i5}\ f_{i6}]^T$ with

$$\begin{aligned}
\Theta_1 &= \text{col}(0.6, 1.1, 0.1, 0.6, 0.3, 0.5, 0.8, 0.9, 1.2, 0.5, 0.4),\\
\Theta_2 &= \text{col}(0.8, 1.2, 0.1, 0.9, 0.5, 0.5, 0.8, 0.9, 1.2, 0.5, 0.4),\\
\Theta_3 &= \text{col}(0.9, 1.3, 0.2, 1.3, 0.6, 0.5, 0.8, 0.9, 1.2, 0.5, 0.4),\\
\Theta_4 &= \text{col}(1.1, 1.4, 0.3, 1.7, 0.7, 0.5, 0.8, 0.9, 1.2, 0.5, 0.4),\\
\Theta_5 &= \text{col}(1.1, 1.4, 0.3, 1.7, 0.7, 0.5, 0.8, 0.9, 1.2, 0.5, 0.4),\\
\Theta_6 &= \text{col}(1.1, 1.4, 0.3, 1.7, 0.7, 0.5, 0.8, 0.9, 1.2, 0.5, 0.4)
\end{aligned}$$

(all these values, inspired by [72], are used for simulation but are unknown for control design). We select $d_i(t) = 0.1\sin(0.001\,l\,t)[1\ 1]^T$, $l = 1, \ldots, 6$.

Inspired by the viscoelasticity model in [8, 56], the interconnections among some agents in the form of springs-dampers

$$H_i = \sum_{j=0}^{N} s_{ij}(q_i - q_j) + \sum_{j=0}^{N} \delta_{ij}(\dot{q}_i - \dot{q}_j) \tag{5.45}$$

where s_{ij} is the stiffness parameter, δ_{ij} is the damping factor (which are $s_{10} = s_{01} = 0.48, s_{12} = s_{21} = 1.21, s_{25} = s_{52} = 0.085, s_{36} = s_{63} = 0.37, s_{46} = s_{64} = 0.29$ and $\delta_{01} = \delta_{10} = 40, \delta_{12} = \delta_{21} = 20, \delta_{25} = \delta_{52} = 25, \delta_{36} = \delta_{63} = 19, \delta_{46} = \delta_{64} = 9$ (all these values, inspired by [8, 56], are used for simulation and are unknown for control design).

To test the robustness, we consider two different interconnected structures as shown in Fig 5.1. Let us remark that each local controller is only aware of which agents are its neighbors: it knows neither the dynamics of the neighbors, nor whether there are spring-damper interconnections.

The controller is as in (5.6) with $K_i = 7.5I_2$, $\bar{K}_i = I_2$, $\omega = 2, \varepsilon = 0.1$, $P_i = 33I_2$. The parameters in the adaptive law (5.13) are $\epsilon_0 = 1, \epsilon_1 = 3\cdot 10^{-4}, \epsilon_2 = 7.5\cdot 10^{-5}, \alpha_{0i} = \alpha_{1i} = \alpha_{2i} = 3000, \beta_i = 10$.

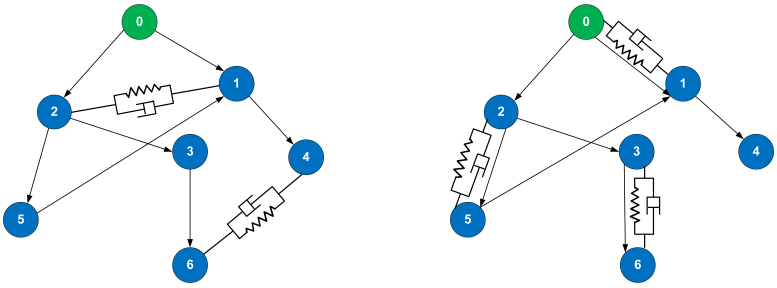

(a) Interconnection 1 (b) Interconnection 2

Figure 5.1: Networks used for simulations.

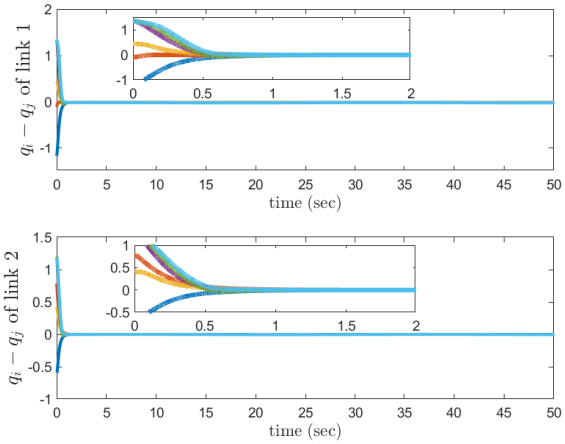

(a) Local position errors

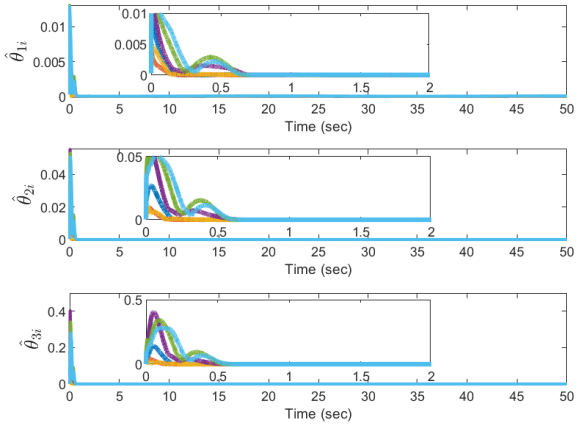

(b) Adaptive parameters $\hat{\theta}_{li}, l = 0, 1, 2$

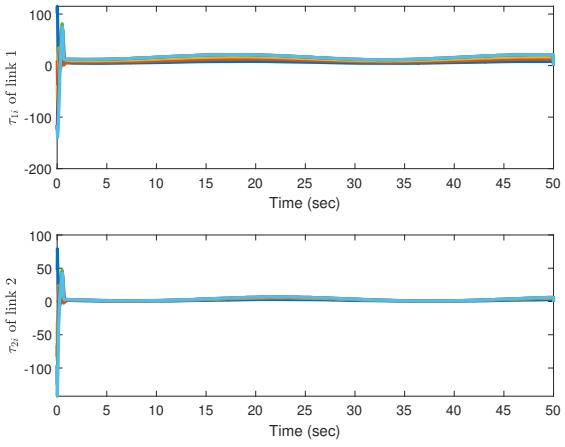

(c) Control inputs τ_i

Figure 5.2: Adaptive synchronization behavior for interconnection 1.

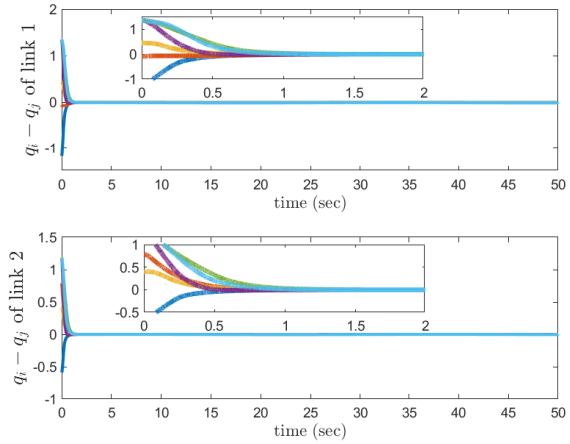

(a) Local position errors

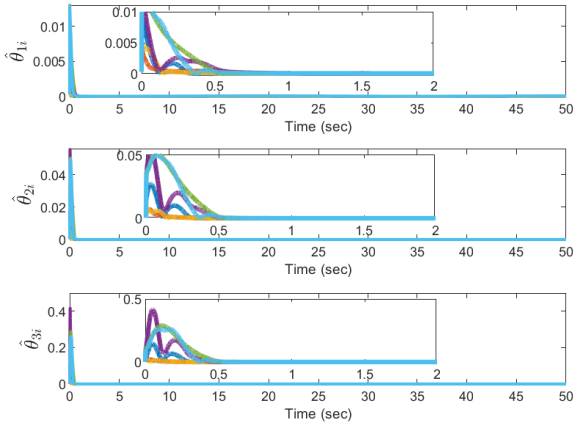

(b) Adaptive parameters $\hat{\theta}_{li}, l = 0, 1, 2$

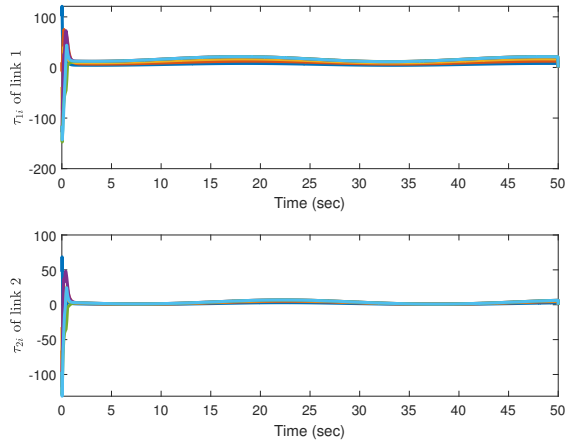

(c) Control inputs τ_i

Figure 5.3: Adaptive synchronization behavior for interconnection 2.

Figs. 5.2(a) and 5.3(a) show that the synchronization error converges close to zero for both interconnection structures and, consequently, the adaptive gains in Figs. 5.2(b) and 5.3(b) also converge close to zero. The inputs are in Figs. 5.2(c) and 5.3(c), where it can be noticed that input oscillations are in a bounded range caused by the sinusoidal disturbance d.

5.6. CONCLUDING REMARKS

A new adaptive synchronization protocol for Euler-Lagrange networks has been presented addressing problems usually neglected in related literature. The main feature of the protocol is to cope with reduced structural knowledge, i.e. not requiring a linear-in-the-parameter structure of the uncertainty and allowing the agents to be interconnected before the control design by unknown state-dependent terms with no a priori bound.

6

DISTRIBUTED ADAPTIVE SYNCHRONIZATION IN UNDERACTUATED EULER-LAGRANGE NETWORKS

This chapter discusses a framework for adaptive synchronization of uncertain underactuated Euler-Lagrange agents. The designed distributed controller can handle both state-dependent uncertain system dynamics terms and state-dependent uncertain interconnection terms among neighboring agents. No structural knowledge of such terms is required other than the standard properties of Euler-Lagrange systems (positive definite mass matrix, bounded gravity terms, velocity-dependent bounds on the friction terms, etc.). The study of stability relies on a suitable analysis of the non-actuated and actuated synchronization errors, which results in stable error dynamics perturbed by parametrized state-dependent uncertainty. This uncertainty is tackled via appropriate adaptation laws. The stability analysis is in the uniformly ultimate boundedness sense, which is in line with the available literature addressing state-dependent system uncertainty and/or state-depend-ent interconnections. An example with a network of boom cranes is used to validate the proposed approach.

6.1. INTRODUCTION

Adaptive-robust control, originally developed for fully-actuated systems [94, 118, 125], refers to a class of adaptive controllers only requiring the knowledge of an uncertainty bound around a nominal value of the mass matrix. All the other system terms (Coriolis, gravity, friction terms) can be unknown [73, 78]. While these methods constitute a

This chapter is based on the submitted paper [134]

general adaptive control framework for fully-actuated systems, such generality is missing for underactuated systems [34, 38, 91]) or requires structural knowledge on the mass matrix [4, 50, 57]. When considering multiple interconnected systems (also referred to as multi-agent systems), an additional source of uncertainty arises from the interconnection terms among the different systems. The presence of these uncertain interconnection terms is often overlooked: in most distributed control approaches, the interconnection is only the result of the synchronization/consensus protocol, i.e. there is no interconnection before such protocol is designed [51, 64, 160]. Therefore, we put forward the aforementioned

Question 4: *How to achieve synchronization in underactuated multi-agent systems with a lack of structural knowledge for system dynamics and interconnection terms?*

On the one hand, the approach presented in this chapter can be considered a suitable "underactuated" extension of the adaptive-robust control framework (indeed, we also require the knowledge of an uncertainty bound around a nominal value of the mass matrix with all other system terms being unknown); on the other hand, we present some distinguishing contributions that make this extension possible: a) derivation of dynamics for the actuated and non-actuated state errors that are suitable for adaptive control (cf. the stable dynamics perturbed by parametrized state-dependent uncertainty in Section 6.3.2, which are analyzed in Section 6.3.3; b) a new stability analysis, which is able to handle distributed information (each agent can only communicate with a few neighbors) and different state space regions (cf. the proof of **Theorem** 6.1); c) adaptive laws as proposed in Section 6.3.4, which are not designed using the standard leakage approach, but based on an appropriate state-dependent leakage action.

The rest of this chapter is organized as follows. The problem of synchronizing multiple underactuated uncertain Euler-Lagrange systems is formulated in Section 6.2. Preliminary steps about distributed control law and synchronization error dynamics are given in Section 6.3. In addition, in this chapter uncertainties are analyzed, resulting in the design of adaptive synchronization laws. Stability analysis is provided in in Section 6.4. Section 6.5 provides the simulation results for a network of boom cranes. Concluding remarks are in Section 6.6.

6.2. PROBLEM FORMULATION

Consider the following network of underactuated Euler-Lagrange (Euler-Lagrange) agents ($i = 1, \dots, N$):

$$\begin{aligned} M_i(q_i)\ddot{q}_i + C_i(q_i, \dot{q}_i)\dot{q}_i + G_i(q_i) + F_i(\dot{q}_i) \\ + H_i(e_i, \dot{e}_i) + d_i = [0_{(n-m)}^T \ \tau_i^T]^T \end{aligned} \tag{6.1}$$

where $q_i, \dot{q}_i \in \mathbb{R}^n$ are the generalized coordinates and their derivatives, $d_i \in \mathbb{R}^n$ is an external bounded disturbance with $\|d_i\| \leq \bar{d}_i$ ($\bar{d}_i$ is an unknown constant), $\tau_i \in \mathbb{R}^m$ with $n - m \leq m < n$ is the control input. For convenience of analysis, consider that the generalized coordinates are arranged according to non-actuated and actuated dynamics as $q_i = [q_{ui}^T \ q_{ai}^T]^T$ with $q_{ui} \in \mathbb{R}^{n-m}$ and $q_{ai} \in \mathbb{R}^m$. The system dynamics in (6.1) comprises the symmetric positive definite mass matrix $M_i(q_i) \in \mathbb{R}^{n\times n}$, the Coriolis matrix $C_i(q_i, \dot{q}_i) \in \mathbb{R}^{n\times n}$, the gravity term $G_i(q_i) \in \mathbb{R}^n$, the friction term $F_i(\dot{q}_i) \in \mathbb{R}^n$, and the in-

terconnection term $H_i(e_i, \dot{e}_i) \in \mathbb{R}^n$, depending on the local synchronization error and its derivative.

Accordingly, the local synchronization error e_i can be decomposed as $e_i = [e_{\mathrm{u}i}^T \; e_{\mathrm{a}i}^T]^T$, resulting in

$$e_{\mathrm{u}i}(t) = \sum_{j \in \mathcal{N}_i} a_{ij}\big[q_{\mathrm{u}i}(t) - q_{\mathrm{u}j}(t)\big] + b_i\big[q_{\mathrm{u}i}(t) - q_{\mathrm{u}0}\big] \tag{6.2a}$$

$$e_{\mathrm{a}i}(t) = \sum_{j \in \mathcal{N}_i} a_{ij}\big[q_{\mathrm{a}i}(t) - q_{\mathrm{a}j}(t)\big] + b_i(q_{\mathrm{a}i}(t) - q_{\mathrm{a}0}) \tag{6.2b}$$

and analogously for $\dot{e}_i = [\dot{e}_{\mathrm{u}i}^T \; \dot{e}_{\mathrm{a}i}^T]^T$

$$\dot{e}_{\mathrm{u}i}(t) = \sum_{j \in \mathcal{N}_i} a_{ij}\big[\dot{q}_{\mathrm{u}i}(t) - \dot{q}_{\mathrm{u}j}(t))\big] + b_i \dot{q}_{\mathrm{u}i}(t) \tag{6.3a}$$

$$\dot{e}_{\mathrm{a}i}(t) = \sum_{j \in \mathcal{N}_i} a_{ij}\big[\dot{q}_{\mathrm{a}i}(t) - \dot{q}_{\mathrm{a}j}(t)\big] + b_i \dot{q}_{\mathrm{a}i}(t). \tag{6.3b}$$

In principle, one could consider time-varying leader trajectories (cf. [73, 78, 104, 129] for fully-actuated Euler-Lagrange systems and [38] for a specific class of underactuated Euler-Lagrange systems); however, this poses the challenging problem of how to define a feasible trajectory for a general underactuated system. Because this problem goes beyond the scope of this work, as is standard in literature (cf. [9, 49, 57, 69, 70, 85, 88, 151]), in (6.2a)-(6.2b) $q_0 = [q_{\mathrm{u}0}^T, \; q_{\mathrm{a}0}^T]^T \in \mathbb{R}^n$ is a fixed-point equilibrium of the leader (accordingly, no leader velocity appears in (6.3a)-(6.3b)).

In line with standard Euler-Lagrange literature [60, 125], the following system properties are assumed:

Property 6.1. *There exist $\bar{c}_i$, $\bar{g}_i$, $\bar{f}_i$, $\bar{h}_{1i}$, $\bar{h}_{2i}$, $\bar{h}_{3i}$, $\bar{h}_{4i}$, $\bar{h}_{5i} \in \mathbb{R}^+$ (possibly unknown) such that $\|C_i(q_i, \dot{q}_i)\| \le \bar{c}_i\|\dot{q}_i\|$, $\|G_i(q_i)\| \le \bar{g}_i$, $\|F_i(\dot{q}_i)\| \le \bar{f}_i\|\dot{q}_i\|$, $\|H_i(e_i, \dot{e}_i)\| \le \bar{h}_{1i} + \bar{h}_{2i}\|e_i\| + \bar{h}_{3i}\|\dot{e}_i\| + \bar{h}_{4i}\|e_i\|^2 + \bar{h}_{5i}\|\dot{e}_i\|^2$.*

Property 6.2. *The matrix $M_i(q_i)$ is symmetric, positive definite and there exist positive constants $\underline{m}$ and $\overline{m}$ such that $0 \le \underline{m} I_n \le M_i(q_i) \le \overline{m} I_n$, $\forall q_i, \forall i$.*

Remark 6.1. *The interconnection term H_i represents the uncertain interaction between agents, existent before the design of the synchronization protocol. Literature on multi-agent systems typically neglects this term [51, 64, 160], whereas we consider it and its presence requires a novel synchronization protocol.*

The upper bounds of C_i, G_i, F_i, H_i, d_i in **Property** 6.1 are taken to be unknown, i.e. they are not used in the design of adaptive law. The upper bound structure of H_i is taken to be quadratic in accordance with the quadratic effect of the term $C_i\dot{q}_i$ in (6.1).

For brevity, let us omit the dependence of the system dynamics terms on the state variables. This leads to organize the dynamic terms as

$$M_i \triangleq \begin{bmatrix} M_{\mathrm{uu}i} & M_{\mathrm{au}i} \\ M_{\mathrm{ua}i} & M_{\mathrm{aa}i} \end{bmatrix}, \tag{6.4a}$$

$$E_i \triangleq C_i\dot{q}_i + G_i + F_i + H_i + d_i = [E_{\mathrm{u}i}^T \; E_{\mathrm{a}i}^T]^T \tag{6.4b}$$

where $M_{\mathrm{uu}i} \in \mathbb{R}^{(n-m)\times(n-m)}$, $M_{\mathrm{au}i} \in \mathbb{R}^{(n-m)\times m}$, $M_{\mathrm{aa}i} \in \mathbb{R}^{m\times m}$, $E_{\mathrm{u}i} \in \mathbb{R}^{n-m}$, $E_{\mathrm{a}i} \in \mathbb{R}^{m}$. Therefore, the dynamics (6.1) for each agent can be represented as

$$\ddot{q}_{\mathrm{u}i} = -M_{\mathrm{uu}i}^{-1} M_{\mathrm{au}i} \ddot{q}_{\mathrm{a}i} - R_{\mathrm{u}i} \tag{6.5a}$$

$$\ddot{q}_{\mathrm{a}i} = M_{\mathrm{s}i}^{-1} \tau_i + R_{\mathrm{a}i} \tag{6.5b}$$

with

$$\begin{aligned} R_{\mathrm{u}i} &\triangleq M_{\mathrm{uu}i}^{-1} E_{\mathrm{u}i}, \\ R_{\mathrm{a}i} &\triangleq M_{\mathrm{s}i}^{-1} (M_{\mathrm{ua}i} M_{\mathrm{uu}i}^{-1} E_{\mathrm{u}i} - E_{\mathrm{a}i}), \\ M_{\mathrm{s}i} &\triangleq M_{\mathrm{aa}i} - M_{\mathrm{ua}i} M_{\mathrm{uu}i}^{-1} M_{\mathrm{au}i}. \end{aligned}$$

Since M_i in (6.4a) is positive definite, $M_{\mathrm{s}i}$ and $M_{\mathrm{uu}i}$ are both positive definite (thus invertible). The following assumption, going under the name of Strong Inertial Coupling, has been proposed in the literature to ensure controllability of underactuated Euler-Lagrange dynamics.

Assumption 6.1. *(Strong Inertial Coupling [117,123]) The following rank condition holds:*

$$rank(M_{\mathrm{au}i}(q_i)) = n - m < m, \ \forall q_i \in \mathbb{R}^n. \tag{6.6}$$

Remark 6.2. *The Strong Inertial Coupling condition has a structural motivation in the framework of backstepping. It allows using backstepping to design a virtual control for the non-actuated states. Note that this condition appears in most works about underactuated Euler-Lagrange systems [87, 99, 124].*

Due to the block structure in (6.4a), the uncertainty in the mass matrix M_i is addressed in a different way from the other dynamic terms. It is assumed that $M_{\mathrm{s}i} \in \mathbb{R}^{m\times m}$ can be decomposed as $M_{\mathrm{s}i} = \hat{M}_{\mathrm{s}i} + \Delta M_{\mathrm{s}i}$ where $\hat{M}_{\mathrm{s}i}$ is the nominal term (used for control design) and $\Delta M_{\mathrm{s}i}$ is the unknown part satisfying the following bound conditions:

Assumption 6.2. *Define the matrix $T_i = M_{\mathrm{s}i}^{-1} \hat{M}_{\mathrm{s}i} - I_m$. Then there exists a known scalar $\bar{T} \in \mathbb{R}^+$ such that*

$$\|T_i\| \leq \bar{T} < 1. \tag{6.7}$$

Assumption 6.2 implies that an upper bound on the uncertainty of $M_{\mathrm{s}i}$ is known. It is often adopted in the literature to describe uncertainty in mass matrix [94, 118, 125].

Use graphs $\mathcal{G}$ to represent a network of nodes (or agents) under **Assumption** 2.1, which can be described by the pair $(\mathcal{V}, \mathcal{E})$, comprising the node set $\mathcal{V} \triangleq \{v_1, \ldots, v_N\}$ and the edge set $\mathcal{E} \subseteq \mathcal{V} \times \mathcal{V}$. Typically, the node set does not include the leader node v_0, which is indexed by 0 due to its special role. An edge is a pair of nodes $(v_j, v_i) \in \mathcal{E}$, which represents that agent i has access to the information from agent j, i.e. agent j is a neighbor of agent i (not necessarily vice versa). Let $B = \mathrm{diag}(b_1, \ldots, b_N) \in \mathbb{R}^{N\times N}$. The edges in $\mathcal{E}$ are described by the adjacency matrix $\mathcal{A} = [a_{ij}] \in \mathbb{R}^{N\times N}$, where $a_{ij} > 0$ if $(v_j, v_i) \in \mathcal{E}$

and $a_{ij} = 0$ otherwise. The Laplacian matrix $\mathscr{L}$ is defined as $\mathscr{L}_{ij} = \sum_{j=1, j\neq i}^{N} a_{ij}$ if $i = j$, otherwise $\mathscr{L}_{ij} = -a_{ij}$. From (6.2), we obtain

$$e_{\mathrm{u}} = -(\mathscr{L} + B) \otimes (q_{\mathrm{u}} - \underline{q}_{\mathrm{u0}}) = -(\mathscr{L} + B) \otimes \delta_{\mathrm{u}}$$
$$e_{\mathrm{a}} = -(\mathscr{L} + B) \otimes (q_{\mathrm{a}} - \underline{q}_{\mathrm{a0}}) = -(\mathscr{L} + B) \otimes \delta_{a}$$

where $e_{\mathrm{u}} = [e_{\mathrm{u1}}^T, \ldots, e_{\mathrm{uN}}^T]^T$, $e_{\mathrm{a}} = [e_{\mathrm{a1}}^T, \ldots, e_{\mathrm{aN}}^T]^T$, $q_{\mathrm{u}} = [q_{\mathrm{u1}}^T, \ldots, q_{\mathrm{uN}}^T]^T$, $q_{\mathrm{a}} = [q_{\mathrm{a1}}^T, \ldots, q_{\mathrm{aN}}^T]^T$, $\underline{q}_{\mathrm{a0}} = 1_N \otimes q_{\mathrm{a0}}$, $\underline{q}_{\mathrm{u0}} = 1_N \otimes q_{\mathrm{u0}}$. The errors $\delta_{\mathrm{a}} = (q_{\mathrm{a}} - \underline{q}_{\mathrm{a0}}) \in \mathbb{R}^{nN}$, $\delta_{\mathrm{u}} = (q_{\mathrm{u}} - \underline{q}_{\mathrm{u0}}) \in \mathbb{R}^{nN}$ represent the global synchronization error with the leader in actuated and non-actuated states, respectively. In a distributed control setting δ_{a}, δ_{u} cannot be used for control design because they involve information from the leader that is not available to all followers.

Due to the directed spanning tree property in **Assumption** 2.1, the following lemma is known from the literature [160].

Lemma 6.1. *The local and global synchronization errors are related by*

$$\|\delta_{\mathrm{u}}\| \leq \frac{\|e_{\mathrm{u}}\|}{\lambda_{\min}(\mathscr{L} + B)} \tag{6.9a}$$
$$\|\delta_{\mathrm{a}}\| \leq \frac{\|e_{\mathrm{a}}\|}{\lambda_{\min}(\mathscr{L} + B)} \tag{6.9b}$$

with $\lambda_{\min}(\mathscr{L} + B)$ the minimum singular value of $\mathscr{L} + B$.

Due to the presence of state-dependent uncertainties, it has been shown in the literature that adaptive asymptotic synchronization (cf. **Definition** 2.7) is hard to achieve even for a fully-actuated system. Therefore, practical synchronization (cf. **Definition** 2.8) is sought in the uniformly ultimately bounded sense, which is in line with the existing literature considering a priori interconnection [24, 129, 133, 172].

Problem 6.1. *Let $\delta_i = [\delta_{\mathrm{ui}}^T \ \delta_{\mathrm{ai}}^T]^T$. Under **Assumptions** 2.1, 6.1-6.2 and **Properties** 6.1-6.2, design a distributed (i.e. using state information of the neighboring agents) adaptive mechanism for the network of underactuated systems (6.1) that guarantees that the global synchronization errors state $\delta = [\delta_1^T, \ldots, \delta_N^T]^T$ is uniformly ultimately bounded (UUB) (cf. **Definition** 2.5).*

6.3. CONTROLLER DESIGN

In the following, we give the distributed control law (Section 6.3.1) and the dynamics of the synchronization error (Section 6.3.2). These preliminary steps will be useful to derive the proposed adaptation mechanisms in Section 6.3.3- 6.3.4.

6.3.1. DISTRIBUTED CONTROL LAW

Define a tracking error variable :

$$r_i = \Theta_{\mathrm{a}i}\dot{e}_{\mathrm{a}i} + \Xi_{\mathrm{a}i}e_{\mathrm{a}i} + \Theta_{\mathrm{u}i}\dot{e}_{\mathrm{u}i} + \Xi_{\mathrm{u}i}e_{\mathrm{u}i} \tag{6.10}$$

where $\Theta_{ai}, \Xi_{ai} \in \mathbb{R}^{m\times m}$ are user-defined positive definite matrices, and $\Theta_{ui}, \Xi_{ui} \in \mathbb{R}^{m\times(n-m)}$ are user-defined full rank matrices.

The distributed controller is designed as

$$\tau_i = \frac{\hat{M}_{si}}{\check{a}_i}\big(-r_i - \bar{\tau}_i\big), \quad \bar{\tau}_i = \rho_i \text{sat}(S_i, \varphi) \tag{6.11}$$

where $\text{sat}(S_i,\varphi) = \begin{cases} \frac{S_i}{\|S_i\|}, & \|S_i\| \geq \varphi \\ \frac{S_i}{\varphi}, & \|S_i\| < \varphi \end{cases}$ is a standard saturation function with $S_i = B_1^T P_{ai}\cdot \omega_{ai}$; φ is a user-defined scalar; $B_1 = [0\ I_m]^T$; $P_{ai} > 0$ is the solution to the Lyapunov equation $A_{ai}^T P_{ai} + P_{ai} A_{ai} = -Q_{ai}$ where $A_{ai} = \begin{bmatrix} 0 & I_m \\ -\Xi_{ai} & -\Theta_{ai} \end{bmatrix}$ is Hurwitz by design, and Q_{ai} is a user-designed positive definite matrix; ρ_i will be defined later in Section 6.3.4 to deal with the uncertainty in the system dynamics.

6.3.2. SYNCHRONIZATION ERROR DYNAMICS

Using (6.3b) and (6.5b), we obtain the synchronization error dynamics in the actuated dynamics as

$$\ddot{e}_{ai} = \check{a}_i\big(M_{si}^{-1}\tau_i + R_{ai}\big) - \sum_{j\in\mathcal{N}_i} a_{ij}\big(M_{sj}^{-1}\tau_j + R_{aj}\big) \tag{6.12}$$

where $\check{a}_i = b_i + \sum_{j\in\mathcal{N}_i} a_{ij}$.

After substituting (6.11) into (6.12), we obtain

$$\begin{aligned} \ddot{e}_{ai} =& \big(M_{si}^{-1}\hat{M}_{si} - I_m\big)\big(-r_i - \bar{\tau}_i\big) - \big(r_i + \bar{\tau}_i\big) + \check{a}_i R_{ai} \\ & - \sum_{j\in\mathcal{N}_i} \bar{a}_{ij}\Big[\big(M_{sj}^{-1}\hat{M}_{sj} - I_m\big)\big(-r_j - \bar{\tau}_j\big) - \big(r_j + \bar{\tau}_j\big)\Big] - a_{ij}R_{aj} \\ =& -r_i - (I_m + T_i)\bar{\tau}_i + \sum_{j\in\mathcal{N}_i} \bar{a}_{ij}(I_m + T_j)\bar{\tau}_j + \phi_{ij} \end{aligned} \tag{6.13}$$

where $\bar{a}_{ij} = \frac{a_{ij}}{\check{a}_j}$ and $\phi_{ij} = -T_i r_i + \sum_{j\in\mathcal{N}_i} \bar{a}_{ij} T_j r_j + \check{a}_i R_{ai} - a_{ij} R_{aj}$.

According to (6.10), (6.13) can be rewritten as

$$\ddot{e}_{ai} = -\Theta_{ai}\dot{e}_{ai} - \Xi_{ai} e_{ai} - (I_m + T_i)\bar{\tau}_i + \sum_{j\in\mathcal{N}_i} \bar{a}_{ij}(I_m + T_j)\bar{\tau}_j + \psi_{ij} \tag{6.14}$$

with $\psi_{ij} = \phi_{ij} - \big(\Theta_{ui}\dot{e}_{ui} + \Xi_{ui} e_{ui}\big)$. Let us arrange the actuated state error as $\omega_{ai} = [e_{ai}^T\ \dot{e}_{ai}^T]^T$. Using (6.14), we have

$$\dot{\omega}_{ai} = A_{ai}\omega_{ai} + B_1\Big[-(I_m + T_i)\bar{\tau}_i + \psi_{ij} + \sum_{j\in\mathcal{N}_i} \bar{a}_{ij}(I_m + T_j)\bar{\tau}_j\Big]. \tag{6.15}$$

Similarly, using (6.3a) and (6.5a), the synchronization error in the non-actuated dynamics turns out to be

$$\begin{aligned}\ddot{e}_{\mathrm{u}i} =& -\check{a}_i\big(M_{\mathrm{uu}i}^{-1}M_{\mathrm{au}i}\ddot{q}_{\mathrm{a}i}+R_{\mathrm{u}i}\big)+\sum_{j\in\mathcal{N}_i}a_{ij}\big(M_{\mathrm{uu}j}^{-1}M_{\mathrm{au}j}\ddot{q}_{\mathrm{a}j}+R_{\mathrm{u}j}\big)\\ =& -\check{a}_i\Big[M_{\mathrm{uu}i}^{-1}M_{\mathrm{au}i}\big(M_{\mathrm{s}i}^{-1}\tau_i+R_{\mathrm{a}i}\big)+R_{\mathrm{u}i}\Big]+\sum_{j\in\mathcal{N}_i}a_{ij}\Big[M_{\mathrm{uu}j}^{-1}M_{\mathrm{au}j}\big(M_{\mathrm{s}j}^{-1}\tau_i+R_{\mathrm{a}j}\big)+R_{\mathrm{u}j}\Big].\end{aligned}\tag{6.16}$$

Similar to (6.13), substituting (6.11) into (6.16), gives

$$\begin{aligned}\ddot{e}_{\mathrm{u}i} =& -M_{\mathrm{uu}i}^{-1}M_{\mathrm{au}i}M_{\mathrm{s}i}^{-1}\hat{M}_{\mathrm{s}i}\big(-r_i-\bar{\tau}_i\big)-\check{a}_i\big(M_{\mathrm{uu}i}^{-1}M_{\mathrm{au}i}R_{\mathrm{a}i}+R_{\mathrm{u}i}\big)\\ &+\sum_{j\in\mathcal{N}_i}\bar{a}_{ij}M_{\mathrm{uu}j}^{-1}M_{\mathrm{au}j}M_{\mathrm{s}j}^{-1}\hat{M}_{\mathrm{s}j}\big(-K_jr_j-\bar{\tau}_j\big)+\sum_{j\in\mathcal{N}_i}a_{ij}\big(M_{\mathrm{uu}j}^{-1}M_{\mathrm{au}j}R_{\mathrm{a}j}+R_{\mathrm{u}j}\big)\\ =& -M_{\mathrm{uu}i}^{-1}M_{\mathrm{au}i}\Big[\big(M_{\mathrm{s}i}^{-1}\hat{M}_{\mathrm{s}i}-I_m\big)\big(-r_i-\bar{\tau}_i\big)-\big(r_i+\bar{\tau}_i\big)\Big]\\ &+\sum_{j\in\mathcal{N}_i}\bar{a}_{ij}M_{\mathrm{uu}j}^{-1}M_{\mathrm{au}j}\Big[\big(M_{\mathrm{s}j}^{-1}\hat{M}_{\mathrm{s}j}-I_m\big)\big(-r_j-\bar{\tau}_j\big)\\ &-\big(r_j+\bar{\tau}_j\big)\Big]+\check{a}_i\big(M_{\mathrm{uu}i}^{-1}M_{\mathrm{au}i}R_{\mathrm{a}i}+R_{\mathrm{u}i}\big)+\sum_{j\in\mathcal{N}_i}a_{ij}\big(M_{\mathrm{uu}j}^{-1}M_{\mathrm{au}j}R_{\mathrm{a}j}+R_{\mathrm{u}j}\big)\\ =& M_{\mathrm{uu}i}^{-1}M_{\mathrm{au}i}\big(I_m+T_i\big)\bar{\tau}_i+\phi'_{ij}-\sum_{j\in\mathcal{N}_i}\bar{a}_{ij}M_{\mathrm{uu}j}^{-1}M_{\mathrm{au}j}\big(I_m+T_j\big)\bar{\tau}_j\end{aligned}\tag{6.17}$$

where

$$\begin{aligned}\phi'_{ij} =& M_{\mathrm{uu}i}^{-1}M_{\mathrm{au}i}\big(I_m+T_i\big)r_i-\sum_{j\in\mathcal{N}_i}\bar{a}_{ij}M_{\mathrm{uu}j}^{-1}M_{\mathrm{au}j}\big(I_m+T_j\big)r_j\\ &-\check{a}_i\big(M_{\mathrm{uu}i}^{-1}M_{\mathrm{au}i}R_{\mathrm{a}i}+R_{\mathrm{u}i}\big)+\sum_{j\in\mathcal{N}_i}a_{ij}\big(M_{\mathrm{uu}j}^{-1}M_{\mathrm{au}j}R_{\mathrm{a}j}+R_{\mathrm{u}j}\big).\end{aligned}$$

Let us design a full-rank matrix $\Gamma_i\in\mathbb{R}^{(n-m)\times m}$ such that $\Lambda_{1i}=\Gamma_i\Theta_{\mathrm{u}i}>0$, $\Lambda_{2i}=\Gamma_i\Xi_{\mathrm{u}i}>0$. Adding and subtracting $\Gamma_i r_i$ to (6.17), the following is obtained:

$$\begin{aligned}\ddot{e}_{\mathrm{u}i} =& M_{\mathrm{uu}i}^{-1}M_{\mathrm{au}i}\big(I_m+T_i\big)\bar{\tau}_i-\sum_{j\in\mathcal{N}_i}\bar{a}_{ij}M_{\mathrm{uu}j}^{-1}M_{\mathrm{au}j}\big(I_m+T_j\big)\bar{\tau}_j\\ &+\phi'_{ij}-\Gamma_i\big(\Theta_{\mathrm{a}i}\dot{e}_{\mathrm{a}i}+\Xi_{\mathrm{a}i}e_{\mathrm{a}i}+\Theta_{\mathrm{u}i}\dot{e}_{\mathrm{u}i}+\Xi_{\mathrm{u}i}e_{\mathrm{u}i}\big)+\Gamma_i r_i\\ =& -\Gamma_i\Theta_{\mathrm{u}i}\dot{e}_{\mathrm{u}i}-\Gamma_i\Xi_{\mathrm{u}i}e_{\mathrm{u}i}+M_{\mathrm{uu}i}^{-1}M_{\mathrm{au}i}\big(I_m+T_i\big)\bar{\tau}_i\\ &-\sum_{j\in\mathcal{N}_i}\bar{a}_{ij}M_{\mathrm{uu}j}^{-1}M_{\mathrm{au}j}\big(I_m+T_j\big)\bar{\tau}_j+\psi'_{ij}\end{aligned}\tag{6.18}$$

where $\psi'_{ij}=\phi'_{ij}-\big(\Theta_{\mathrm{a}i}\dot{e}_{\mathrm{a}i}+\Xi_{\mathrm{a}i}e_{\mathrm{a}i}\big)+\Gamma_i r_i$. Arrange the non- actuated state error as $\omega_{\mathrm{u}i}=[e_{\mathrm{u}i}^T\ \dot{e}_{\mathrm{u}i}^T]^T$. Using (6.18), we have

$$\dot{\omega}_{\mathrm{u}i}=A_{\mathrm{u}i}\omega_{\mathrm{u}i}+B_2\Big[M_{\mathrm{uu}i}^{-1}M_{\mathrm{au}i}\big(I_m+T_i\big)\bar{\tau}_i-\sum_{j\in\mathcal{N}_i}\bar{a}_{ij}M_{\mathrm{uu}j}^{-1}M_{\mathrm{au}j}\big(I_m+T_j\big)\bar{\tau}_j+\psi'_{ij}\Big]\tag{6.19}$$

where we have defined $A_{\mathrm{u}i} = \begin{bmatrix} 0 & I_{(n-m)} \\ -\Lambda_{1i} & -\Lambda_{2i} \end{bmatrix}$, which is Hurwitz by design, and $B_2 = [0\ I_{(n-m)}]^T$.

Remark 6.3. *The analysis of the error dynamics has led to* (6.15) *and* (6.19)*, which are stable dynamics (due to the Hurwitz state matrices $A_{\mathrm{a}i}$ and $A_{\mathrm{u}i}$) perturbed by state-dependent terms.*

In the rest of the analysis, the idea is to find an upper bound for these perturbation terms, which in turns leads to define an appropriate ρ_i for stabilizing the error dynamics. In the following, we provide the uncertainty analysis (Section 6.3.3), leading to the adaptive synchronization laws (Section 6.3.4).

6.3.3. UNCERTAINTY ANALYSIS

Define $\xi_i = [e_i^T\ \dot{e}_i^T\ q_i^T\ \dot{q}_i^T]^T$, $\xi = [\xi_1^T, \ldots, \xi_N^T]^T$. Therefore, $\|e_{\mathrm{a}i}\| \leq \|\xi_i\|$, $\|e_{\mathrm{u}i}\| \leq \|\xi_i\|$, $\|\dot{e}_{\mathrm{a}i}\| \leq \|\xi_i\|$, $\|\dot{e}_{\mathrm{u}i}\| \leq \|\xi_i\|$. According to (6.10), we have

$$\|r_i\| \leq \vartheta_i \|\xi_i\| \tag{6.20}$$

with $\vartheta_i = \|\Theta_{\mathrm{a}i}\| + \|\Xi_{\mathrm{a}i}\| + \|\Theta_{\mathrm{u}i}\| + \|\Xi_{\mathrm{u}i}\|$.

Using **Assumption** 6.2 and (6.14), the following bound for ψ_{ij} in (6.15) can be obtained:

$$\begin{aligned}
\|\psi_{ij}\| &\leq \|T_i r_i\| + \sum_{j\in\mathcal{N}_i} \bar{a}_{ij}\|T_j r_j\| + \check{a}_i\|R_{\mathrm{a}i}\| + a_{ij}\|R_{\mathrm{a}j}\| + \|\Theta_{\mathrm{u}i}\dot{e}_{\mathrm{u}i}\| + \|\Xi_{\mathrm{u}i}e_{\mathrm{u}i}\| \\
&\leq \bar{T}\vartheta_i\|\xi_i\| + \bar{T}\sum_{j\in\mathcal{N}_i} \bar{a}_{ij}\vartheta_j\|\xi_j\| + \check{a}_i\|M_{\mathrm{s}i}^{-1}\|\big(\|E_{\mathrm{a}i}\| + \|M_{\mathrm{ua}i}M_{\mathrm{uu}i}^{-1}\|\|E_{\mathrm{u}i}\|\big) \\
&\quad + \sum_{j\in\mathcal{N}_i} \bar{a}_{ij}\|M_{\mathrm{s}j}^{-1}\|\big(\|E_{\mathrm{a}j}\| + \|M_{\mathrm{ua}j}M_{\mathrm{uu}j}^{-1}\|\|E_{\mathrm{u}j}\|\big) + \|\Theta_{\mathrm{u}i}\dot{e}_{\mathrm{u}i}\| + \|\Xi_{\mathrm{u}i}e_{\mathrm{u}i}\|.
\end{aligned} \tag{6.21}$$

According to the definition of ξ_i, $\|q_i\| \leq \|\xi_i\|$ can be obtained. Using **Property** 6.1, we have

$$\begin{aligned}
\|E_i(q_i, \dot{q}_i, e_i, \dot{e}_i)\| &\leq \big(\bar{g}_i + d_i + \bar{h}_{1i}\big) + \bar{f}_i\|\dot{q}_i\| + \bar{c}_i\|\dot{q}_i\|^2 \\
&\quad + \bar{h}_{2i}\|e_i\| + \bar{h}_{3i}\|\dot{e}_i\| + \bar{h}_{4i}\|e_i\|^2 + h_{5i}\|\dot{e}_i\|^2 \\
&\leq (\bar{g}_i + \bar{d}_i + \bar{h}_{1i}) + (\bar{f}_i + \bar{h}_{2i} + \bar{h}_{3i})\|\xi_i\| \\
&\quad + \big(\bar{c}_i + \bar{h}_{4i} + \bar{h}_{5i}\big)\|\xi_i\|^2.
\end{aligned} \tag{6.22}$$

From (6.4b) we have $\|E_{\mathrm{a}i}\| \leq \|E_i\|$, $\|E_{\mathrm{u}i}\| \leq \|E_i\|$. Then, (6.21) yields

$$\begin{aligned}
\|P_{\mathrm{a}i}B_1\|\|\psi_{ij}\| \leq &\|P_{\mathrm{a}i}B_1\|\Big[\bar{T}\vartheta_i\|\xi_i\| + \bar{T}\sum_{j\in\mathcal{N}_i} \bar{a}_{ij}\vartheta_j\|\xi_j\| + \check{a}_i\|M_{\mathrm{s}i}^{-1}\|\big(1 + \|M_{\mathrm{ua}i}M_{\mathrm{uu}i}^{-1}\|\big)\|E_i\| \\
&+ \sum_{j\in\mathcal{N}_i} \bar{a}_{ij}\|M_{\mathrm{s}j}^{-1}\|\big(1 + \|M_{\mathrm{ua}j}M_{\mathrm{uu}j}^{-1}\|\big)\|E_j\| + \big(\|\Theta_{\mathrm{u}i}\| + \|\Xi_{\mathrm{u}i}\|\big)\|\xi_i\|\Big] \\
\leq\ &\theta_{0i} + \theta_{1i}\|\xi_i\| + \theta_{2i}\|\xi_i\|^2 + \sum_{j\in\mathcal{N}_i}\big(\varphi_{1j}\|\xi_j\| + \varphi_{2j}\|\xi_j\|^2\big)
\end{aligned} \tag{6.23}$$

where

$$\theta_{0i} = \|P_{ai}B_1\|\Big[\mu_i\big(\bar{g}_i + \bar{d}_i + \bar{h}_{1i}\big) + \sum_{j\in\mathcal{N}_i}\bar{\mu}_{ij}\big(\bar{g}_j + \bar{d}_j + \bar{h}_{1j}\big)\Big]$$
$$\theta_{1i} = \|P_{ai}B_1\|\Big[\mu_i\big(\bar{f}_i + \bar{h}_{2i} + \bar{h}_{3i}\big) + \bar{T}\vartheta_i + \big(\|\Theta_{ui}\| + \|\Xi_{ui}\|\big)\Big]$$
$$\theta_{2i} = \|P_{ai}B_1\|\mu_i\big(\bar{c}_i + \bar{h}_{4i} + \bar{h}_{5i}\big),\ \varphi_{1j} = \|P_{ai}B_1\|\Big[\bar{\mu}_{ij}\big(\bar{f}_j + \bar{h}_{2j} + \bar{h}_{3j}\big) + \bar{T}\bar{a}_{ij}\vartheta_j\Big]$$
$$\varphi_{2j} = \|P_{ai}B_1\|\bar{\mu}_{ij}\big(\bar{c}_j + \bar{h}_{4j} + \bar{h}_{5j}\big),\ \mu_i = \check{a}_i\|M_{si}^{-1}\|\big(1 + \|M_{uai}M_{uui}^{-1}\|\big)$$
$$\bar{\mu}_{ij} = \sum_{j\in\mathcal{N}_i}\bar{a}_{ij}\|M_{sj}^{-1}\|\big(1 + \|M_{uaj}M_{uuj}^{-1}\|\big).$$

Similar to (6.21), the following upper bound on ψ'_{ij} is obtained from (6.19):

$$\begin{aligned}
\|\psi'_{ij}\| &\le \|\phi'_{ij}\| + \|\Theta_{ai}\dot{e}_{ai}\| + \|\Xi_{ai}e_{ai}\| + \|\Gamma_i r_i\| \\
&\le \|M_{uui}^{-1}M_{aui}\|\|I_m + T_i\|\|r_i\| + \check{a}_i\|M_{uui}^{-1}M_{aui}R_{ai} + R_{ui}\| \\
&\quad + \sum_{j\in\mathcal{N}_i}\bar{a}_{ij}\|M_{uuj}^{-1}M_{auj}\|\|I_m + T_j\|\|r_j\| + \sum_{j\in\mathcal{N}_i}a_{ij}\|M_{uuj}^{-1}M_{auj}R_{aj} + R_{uj}\| \\
&\le \Big[\big(1+\bar{T}\big)\|M_{uui}^{-1}M_{aui}\| + 1\Big]\vartheta_i\|\xi_i\| + \check{a}_i\|M_{uui}^{-1}\|\|E_{ui}\| \\
&\quad + \check{a}_i\|M_{uui}^{-1}M_{aui}\|\|M_{si}^{-1}\|\big(\|E_{ai}\| + \|M_{uai}M_{uui}^{-1}\|\|E_{ui}\|\big) \\
&\quad + \big(1+\bar{T}\big)\sum_{j\in\mathcal{N}_i}\bar{a}_{ij}\vartheta_j\|M_{uuj}^{-1}M_{auj}\|\|\xi_j\| + \sum_{j\in\mathcal{N}_i}\bar{a}_{ij}\|M_{uuj}^{-1}M_{auj}\|\|M_{sj}^{-1}\|\big(\|E_{aj}\| \\
&\quad + \|M_{uaj}M_{uuj}^{-1}\|\|E_{uj}\|\big) + \sum_{j\in\mathcal{N}_i}\bar{a}_{ij}\|M_{uuj}^{-1}\|\|E_{uj}\| + \|\Theta_{ai}\dot{e}_{ai}\| + \|\Xi_{ai}e_{ai}\|. \qquad (6.24)
\end{aligned}$$

Define $P_{ui} > 0$ as the solution to the Lyapunov equation $A_{ui}^T P_{ui} + P_{ui}A_{ui} = -Q_{ui}$ with Q_{ui} being a user-designed positive definite matrix. Then, we finally obtain

$$\begin{aligned}
&\|P_{ui}B_2\|\|\psi'_{ij}\| \le \|P_{ui}B_2\|\Big\{\Big[\big(1+\bar{T}\big)\|M_{uui}^{-1}M_{aui}\| + 1\Big]\vartheta_i\|\xi_i\| \\
&+ \check{a}_i\|M_{uui}^{-1}\|\Big[\|M_{aui}\|\|M_{si}^{-1}\|\big(1 + \|M_{uai}M_{uui}^{-1}\|\big) + 1\Big]\|E_i\| + \big(1+\bar{T}\big)\sum_{j\in\mathcal{N}_i}\bar{a}_{ij}\vartheta_j\|M_{uuj}^{-1}M_{auj}\|\|\xi_j\| \\
&+ \sum_{j\in\mathcal{N}_i}\bar{a}_{ij}\|M_{uuj}^{-1}\|\Big[\|M_{auj}\|\|M_{sj}^{-1}\|\big(1 + \|M_{uaj}M_{uuj}^{-1}\|\big) + 1\Big]\|E_j\| + \big(\|\Theta_{ai}\| + \|\Xi_{ai}\|\big)\|\xi_i\|\Big\} \\
&\le \theta'_{0i} + \theta'_{1i}\|\xi_i\| + \theta'_{2i}\|\xi_i\|^2 + \sum_{j\in\mathcal{N}_i}\big(\varphi'_{1j}\|\xi_j\| + \varphi'_{2j}\|\xi_j\|^2\big) \qquad (6.25)
\end{aligned}$$

where

$$\theta'_{0i} = \|P_{\mathrm{u}i}B_2\|\Big[\mu'_i(\bar{g}_i+\bar{d}_i+\bar{h}_{1i})+\sum_{j\in\mathcal{N}_i}\bar{\mu}'_{ij}(\bar{g}_j+\bar{d}_j+\bar{h}_{1j})\Big]$$
$$\theta'_{1i} = \|P_{\mathrm{u}i}B_2\|\Big[\mu'_i(\bar{f}_i+\bar{h}_{2i}+\bar{h}_{3i})+\big(\|\Theta_{\mathrm{u}i}\|+\|\Xi_{\mathrm{u}i}\|\big)\Big]+\Big[\big(1+\bar{T}\big)\|M^{-1}_{\mathrm{uu}i}M_{\mathrm{au}i}\|+1\Big]\vartheta_i$$
$$\theta'_{2i} = \|P_{\mathrm{u}i}B_2\|\mu'_i(\bar{c}_i+\bar{h}_{4i}+\bar{h}_{5i}),\ \varphi'_{2j} = \|P_{\mathrm{u}i}B_2\|\bar{\mu}'_{ij}(\bar{c}_j+\bar{h}_{4j}+\bar{h}_{5j})$$
$$\varphi'_{1j} = \|P_{\mathrm{u}i}B_2\|\Big[\bar{\mu}'_{ij}(\bar{f}_j+\bar{h}_{2j}+\bar{h}_{3j})+\big(1+\bar{T}\big)\bar{a}_{ij}\vartheta_j\|M^{-1}_{\mathrm{uu}j}M_{\mathrm{au}j}\|\Big]$$
$$\mu'_i = \check{a}_i\|M^{-1}_{\mathrm{uu}i}\|\Big[\|M_{\mathrm{au}i}\|\|M^{-1}_{\mathrm{s}i}\|\big(1+\|M_{\mathrm{ua}i}M^{-1}_{\mathrm{uu}i}\|\big)+1\Big]$$
$$\bar{\mu}'_{ij} = \bar{a}_{ij}\|M^{-1}_{\mathrm{uu}j}\|\|\Big[\|M_{\mathrm{au}j}\|\|M^{-1}_{\mathrm{s}j}\|\big(1+\|M_{\mathrm{ua}j}M^{-1}_{\mathrm{uu}j}\|\big)+1\Big].$$

The upper bounds in (6.23) and (6.25) put us in the position to design an appropriate ρ_i in (6.11), as will be explained later in Section 6.3.4.

6.3.4. ADAPTIVE SYNCHRONIZATION LAWS

According to the structure of the upper bounds of ψ_{ij} in (6.23) and ψ'_{ij} in (6.25), ρ_i is designed as

$$\rho_i = \frac{1}{\big(1-\bar{T}\big)}\Big(\hat{\theta}_{0i}+\hat{\theta}_{1i}\|\xi_i\|+\hat{\theta}_{2i}\|\xi_i\|^2+\gamma_i\Big) \tag{6.26}$$

with the adaptive laws for $l=0,1,2$

$$\dot{\hat{\theta}}_{li} = \chi_{li}\big(\|\omega_{\mathrm{a}i}\|+\|\omega_{\mathrm{u}i}\|+\|S_i\|\big)\|\xi_i\|^l-\alpha_{li}\big(\|\omega_{\mathrm{a}i}\|+\|\omega_{\mathrm{u}i}\|\big)\|\xi_i\|^l\hat{\theta}_{li} \tag{6.27a}$$
$$\dot{\gamma}_i = -\Big[\epsilon_0+\epsilon_1(\|\xi_i\|^7-\|\xi_i\|^5)+\epsilon_2\|\xi_i\|\Big]\gamma_i+\epsilon_0\big(\|S_i\|+\|\xi_i\|\big)+\beta_i \tag{6.27b}$$
$$\text{where } \hat{\theta}_{0i}(0)>0, \hat{\theta}_{1i}(0)>0, \hat{\theta}_{2i}(0)>0, \gamma_i(0)>\nu \tag{6.27c}$$
$$\epsilon_0,\ \epsilon_1,\ \epsilon_2,\ \chi_{li},\ \alpha_{li},\ \beta_i,\ \nu\in\mathbb{R}^+ \tag{6.27d}$$
$$\text{with } \epsilon_2\geq\epsilon_1. \tag{6.27e}$$

Remark 6.4. *The proposed adaptive laws use a leakage term dependent on the synchronization error. This turns out to be useful in the Lyapunov analysis of the derivative of* $(\hat{\theta}_{li}-\bar{\theta}_{li})^2$. *Specifically, the common factor* $\big(\|\omega_{\mathrm{a}i}\|+\|\omega_{\mathrm{u}i}\|\big)\|\xi_i\|^l$ *can be extracted to construct negative square terms of* $\hat{\theta}_{li}$ *as shown in* (6.39)-(6.40) *in Section 6.4. Compared to the standard leakage term (cf. [24, 129], [52, Chapter 8]), a more concise UUB condition for* $\omega_{\mathrm{a}i}$ *and* $\omega_{\mathrm{u}i}$ *is obtained in* (6.47), (6.52) *and* (6.54).

6.4. STABILITY ANALYSIS

Theorem 6.1. *Under* ***Properties*** *6.1-6.2 and* ***Assumptions*** *2.1,* ***Assumptions*** *6.1-6.2, the closed-loop trajectories of* (6.1) *employing the distributed control law* (6.11) *with adaptive law* (6.27) *are uniformly ultimately bounded.*

Proof. Construct a Lyapunov function:

$$V(t) = \frac{1}{2}\sum_{i=1}^{N}\Big\{\omega_{\mathrm{a}i}^TP_{\mathrm{a}i}\omega_{\mathrm{a}i}+\omega_{\mathrm{u}i}^TP_{\mathrm{u}i}\omega_{\mathrm{u}i}\Big\}+\frac{1}{2}\sum_{i=1}^{N}\Big\{\sum_{l=0}^{2}\frac{1}{\chi_{li}}(\hat{\theta}_{li}-\bar{\theta}_{li})^2+\frac{\gamma_i^2}{\epsilon_0}\Big\} \tag{6.28}$$

where $\bar{\theta}_{li} = \max\{\theta_{li}, \theta'_{li}\},\ l = 0,1,2.$
The proof is organized as follows:

a) the bound of uncertainty for the overall network is calculated;

b) based on such uncertainty bound, we calculate the time derivative of the Lyapunov function;

c) based on different regions of saturation function $\text{sat}(S_i, \varphi)$, we study the behaviour of the Lyapunov function for three possible scenarios.

Combining all the results, we will finally obtain a uniform ultimate bound on the actuated error $\omega_{\text{a}i}$ and on the non-actuated error $\omega_{\text{u}i}$.

a) The bound of overall uncertainty term

According to (6.15), we obtain

$$\begin{aligned}\omega_{\text{a}i}^T P_{\text{a}i}\dot{\omega}_{\text{a}i} =& \omega_{\text{a}i}^T P_{\text{a}i}\Big\{A_{\text{a}i}\omega_{\text{a}i} + B_1\big[-(I_m+T_i)\bar{\tau}_i + \sum_{j\in\mathcal{N}_i}\bar{a}_{ij}(I_m+T_j)\bar{\tau}_j + \psi_{ij}\big]\Big\}\\ \leq& -\frac{1}{2}\omega_{\text{a}i}^T Q_{\text{a}i}\omega_{\text{a}i} + \|\omega_{\text{a}i}^T\|\|P_{\text{a}i}B_1\|\|\psi_{ij}\| - \omega_{\text{a}i}^T P_{\text{a}i}B_1(I_m+T_i)\rho_i\text{sat}(S_i,\varphi)\\ &+ \sum_{j\in\mathcal{N}_i}\bar{a}_{ij}\omega_{\text{a}i}^T P_{\text{a}i}B_1(I_m+T_j)\rho_j\text{sat}(S_j,\varphi).\end{aligned} \tag{6.29}$$

Analogously, according to (6.19), we obtain

$$\begin{aligned}\omega_{\text{u}i}^T P_{\text{u}i}\dot{\omega}_{\text{u}i} =& \omega_{\text{u}i}^T P_{\text{u}i}\Big\{A_{\text{u}i}\omega_{\text{u}i} + B_2\big[M_{\text{uu}i}^{-1}M_{\text{au}i}\big(I_m+T_i\big)\bar{\tau}_i\\ &- \sum_{j\in\mathcal{N}_i}\bar{a}_{ij}M_{\text{uu}j}^{-1}M_{\text{au}j}\big(I_m+T_j\big)\bar{\tau}_j + \psi'_{ij}\big]\Big\}\\ \leq& -\frac{1}{2}\omega_{\text{u}i}^T Q_{\text{u}i}\omega_{\text{u}i} + \sum_{j\in\mathcal{N}_i}\bar{a}_{ij}\omega_{\text{u}i}^T P_{\text{u}i}B_2M_{\text{uu}j}^{-1}M_{\text{au}j}(I_m+T_j)\rho_j\text{sat}(S_j,\varphi)\\ &+ \omega_{\text{u}i}^T P_{\text{u}i}B_2M_{\text{uu}i}^{-1}M_{\text{au}i}(I_m+T_i)\rho_i\text{sat}(S_i,\varphi) + +\|\omega_{\text{u}i}^T\|\|P_{\text{u}i}B_2\|\|\psi'_{ij}\|.\end{aligned} \tag{6.30}$$

Adding (6.29) and (6.30), combined with (6.23)-(6.25), we obtain

$$\begin{aligned}&\omega_{\text{a}i}^T P_{\text{a}i}\dot{\omega}_{\text{a}i} + \omega_{\text{u}i}^T P_{\text{u}i}\dot{\omega}_{\text{u}i}\\ \leq& -\lambda_{\min,i}\Big[\|\omega_{\text{a}i}\|^2 + \|\omega_{\text{u}i}\|^2\Big] + \sum_{l=0}^{2}\bar{\theta}_{li}\|\xi_i\|^l\big(\|\omega_{\text{a}i}\| + \|\omega_{\text{u}i}\|\big)\\ &+ \sum_{j\in\mathcal{N}_i}\Big[\bar{\varphi}_{1j}\|\xi_j\| + \bar{\varphi}_{2j}\|\xi_j\|^2\Big]\big(\|\omega_{\text{a}i}\| + \|\omega_{\text{u}i}\|\big)\\ &- \omega_{\text{a}i}^T P_{\text{a}i}B_1(I_m+T_i)\rho_i\text{sat}(S_i,\varphi) + \omega_{\text{u}i}^T P_{\text{u}i}B_2M_{\text{uu}i}^{-1}M_{\text{au}i}(I_m+T_i)\rho_i\text{sat}(S_i,\varphi)\\ &+ \sum_{j\in\mathcal{N}_i}\bar{a}_{ij}\omega_{\text{u}i}^T P_{\text{u}i}B_2M_{\text{uu}j}^{-1}M_{\text{au}j}(I_m+T_j)\rho_j\text{sat}(S_j,\varphi)\\ &+ \sum_{j\in\mathcal{N}_i}\bar{a}_{ij}\omega_{\text{a}i}^T P_{\text{a}i}B_1(I_m+T_j)\rho_j\text{sat}(S_j,\varphi)\end{aligned} \tag{6.31}$$

where $\lambda_{\min,i} = \min\Big\{\lambda_{\min}(Q_{\text{a}i})/2, \lambda_{\min}(Q_{\text{u}i})/2\Big\}$, $\bar{\varphi}_{1j} = \max\{\varphi_{1j},\ \varphi'_{1j}\}$, $\bar{\varphi}_{2j} = \max\{\varphi_{2j},\ \varphi'_{2j}\}$, $j \in \mathcal{N}_i$.

Next, we will analyze the last three terms in (6.31) by using the inequality $\|\text{sat}(S_i,\varphi)\| \leq 1$. From the input-output property of the adaptive law in (6.27), it can be verified that

$$\hat{\theta}_{li} \leq \mathring{\theta}_{li} + \check{\theta}_{li}\big(\|\omega_{\text{a}i}\| + \|\omega_{\text{u}i}\| + \|S_i\|\big)\|\xi_i\|^l \tag{6.32a}$$
$$\gamma \leq \mathring{\gamma}_i + \check{\gamma}_i\big(\|S_i\| + \|\xi_i\|\big) \tag{6.32b}$$

with $\mathring{\theta}_{li}$, $\check{\theta}_{li}$, $\mathring{\gamma}_i$, $\check{\gamma}_i \in \mathbb{R}^+$, $l = 0,1,2$.

Using (6.32), together with $\|\omega_{\text{a}i}\| \leq \|\xi_i\|$ and $\|\omega_{\text{u}i}\| \leq \|\xi_i\|$, the following can be obtained:

$$\begin{aligned}
&\omega_{\text{u}i}^T P_{\text{u}i} B_2 M_{\text{uu}i}^{-1} M_{\text{au}i}(I_m + T_i)\rho_i \text{sat}(S_i,\varphi) \\
\leq& \bar{\bar{T}}_{1i}\Big[\sum_{l=0}^{2}\hat{\theta}_{li}\|\xi_i\|^l + \gamma_i\Big]\|\omega_{\text{u}i}^T\| \\
\leq& \bar{\bar{T}}_{1i}\Big\{\sum_{l=0}^{2}\mathring{\theta}_{li}\|\xi_i\|^{l+1} + \Big[\mathring{\gamma}_i + \check{\gamma}_i\big(\|S_i\| + \|\xi_i\|\big)\Big]\|\xi_i\| + \check{\theta}_{li}\big(\|\omega_{\text{a}i}\| + \|\omega_{\text{u}i}\| + \|S_i\|\big)\|\xi_i\|^{2l+1}\Big\} \\
\leq& \bar{\bar{T}}_{1i}\Big\{\sum_{l=0}^{2}\mathring{\theta}_{li}\|\xi_i\|^{l+1} + \check{\theta}_{li}\big(2 + \|B_1^T P_{\text{a}i}\|\big)\|\xi_i\|^{2l+2} + \mathring{\gamma}_i\|\xi_i\| + \check{\gamma}_i\big(1 + \|B_1^T P_{\text{a}i}\|\big)\|\xi_i\|^2\Big\}
\end{aligned} \tag{6.33}$$

where $\bar{\bar{T}}_{1i} = \dfrac{\big(1+\bar{T}\big)\|P_{\text{u}i}B_2\|\|M_{\text{uu}i}^{-1}M_{\text{au}i}\|}{\big(1-\bar{T}\big)}$.

In an analogous way, the following can be obtained:

$$\begin{aligned}
&\sum_{j\in\mathcal{N}_i}\bar{a}_{ij}\omega_{\text{u}i}^T P_{\text{u}i}B_2 M_{\text{uu}j}^{-1}M_{\text{au}j}(I_m + T_j)\rho_j\text{sat}(S_j,\varphi) \\
\leq& \sum_{j\in\mathcal{N}_i}\bar{\bar{T}}_{2j}\Big[\sum_{l=0}^{2}\hat{\theta}_{lj}\|\xi_j\|^l + \gamma_j\Big]\|\omega_{\text{u}i}^T\| \\
\leq& \sum_{j\in\mathcal{N}_i}\bar{\bar{T}}_{2j}\Big\{\sum_{l=0}^{2}\mathring{\theta}_{lj}\|\xi_i\|\|\xi_j\|^l + \check{\theta}_{lj}\big(\|\omega_{\text{a}j}\| + \|\omega_{\text{u}j}\| + \|S_j\|\big)\|\xi_i\|\|\xi_j\|^{2l} \\
&+\mathring{\gamma}_j\|\xi_i\| + \check{\gamma}_j\big(1 + \|B_1^T P_{\text{a}i}\|\big)\|\xi_i\|^2\Big\} \\
\leq& \sum_{j\in\mathcal{N}_i}\bar{\bar{T}}_{2j}\Big\{\sum_{l=0}^{2}\mathring{\theta}_{lj}\|\xi_i\|\|\xi_j\|^l + \check{\gamma}_j\big(1 + \|B_1^T P_{\text{a}i}\|\big)\|\xi_i\|^2 + \mathring{\gamma}_j\|\xi_i\| \\
&+\check{\theta}_{lj}\big(2 + \|B_1^T P_{\text{a}j}\|\big)\|\xi_i\|\|\xi_j\|^{2l+1}\Big\}
\end{aligned} \tag{6.34}$$

where $\bar{\bar{T}}_{2j} = \dfrac{\bar{a}_{ij}\big(1+\bar{T}\big)\|P_{\text{u}i}B_2\|\|M_{\text{uu}j}^{-1}M_{\text{au}j}\|}{\big(1-\bar{T}\big)}$.

In addition,

$$\begin{aligned}
&\sum_{j\in\mathcal{N}_i} \bar{a}_{ij}\omega_{\mathrm{a}i}^T P_{\mathrm{a}i} B_1 (I_m + T_j)\rho_j \mathrm{sat}(S_j,\varphi) \\
&\leq \sum_{j\in\mathcal{N}_i} \bar{\bar{T}}_{3j}\Big[\sum_{l=0}^{2}\hat{\theta}_{lj}\|\xi_j\|^l + \gamma_j\Big]\|\omega_{\mathrm{a}i}^T\| \\
&\leq \sum_{j\in\mathcal{N}_i} \bar{\bar{T}}_{3j}\Big\{\sum_{l=0}^{2}\mathring{\theta}_{lj}\|\xi_i\|\|\xi_j\|^l + \check{\gamma}_j\big(1+\|B_1^T P_{\mathrm{a}i}\|\big)\|\xi_i\|^2 + \mathring{\gamma}_j\|\xi_i\| \\
&\quad + \check{\theta}_{lj}\big(2+\|B_1^T P_{\mathrm{a}j}\|\big)\|\xi_i\|\|\xi_j\|^{2l+1}
\end{aligned} \tag{6.35}$$

where $\bar{\bar{T}}_{3j} = \frac{\left(1+\bar{T}\right)\|P_{\mathrm{a}i}B_1\|}{\left(1-\bar{T}\right)}$.

Using (6.33)-(6.35), the following aggregate term Ψ_{ij} can be defined from (6.31)

$$\begin{aligned}
&\sum_{i=1}^{N}\sum_{j\in\mathcal{N}_i}\Psi_{ij} \\
&= \sum_{j\in\mathcal{N}_i}\Big[\bar{\varphi}_{1j}\|\xi_j\| + \bar{\varphi}_{2j}\|\xi_j\|^2\Big]\big(\|\omega_{\mathrm{a}i}\| + \|\omega_{\mathrm{u}i}\|\big) + \omega_{\mathrm{u}i}^T P_{\mathrm{u}i} B_2 M_{\mathrm{uu}i}^{-1} M_{\mathrm{au}i}(I_m + T_i)\rho_i \mathrm{sat}(S_i,\varphi) \\
&+ \sum_{j\in\mathcal{N}_i}\bar{a}_{ij}\omega_{\mathrm{u}i}^T P_{\mathrm{u}i} B_2 M_{\mathrm{uu}j}^{-1} M_{\mathrm{au}j}(I_m + T_j)\rho_j \mathrm{sat}(S_j,\varphi) \\
&+ \sum_{j\in\mathcal{N}_i}\bar{a}_{ij}\omega_{\mathrm{a}i}^T P_{\mathrm{a}i} B_1 (I_m + T_j)\rho_j \mathrm{sat}(S_j,\varphi) \\
&\leq \sum_{i=1}^{N}\sum_{j\in\mathcal{N}_i}\check{\theta}_{2j}\big(\bar{\bar{T}}_{2j} + \bar{\bar{T}}_{3j}\big)\big(2+\|B_1^T P_{\mathrm{a}j}\|\big)\|\xi_i\|\|\xi_j\|^5 + \sum_{i=1}^{N}\bar{\bar{T}}_{1i}\check{\theta}_{2i}\big(2+\|B_1^T P_{\mathrm{a}i}\|\big)\|\xi_i\|^6 \\
&+ \sum_{i=1}^{N}\sum_{j\in\mathcal{N}_i}\check{\theta}_{1j}\big(\bar{\bar{T}}_{2j} + \bar{\bar{T}}_{3j}\big)\big(2+\|B_1^T P_{\mathrm{a}j}\|\big)\|\xi_i\|\|\xi_j\|^3 + \sum_{i=1}^{N}\bar{\bar{T}}_{1i}\check{\theta}_{1i}\big(2+\|B_1^T P_{\mathrm{a}i}\|\big)\|\xi_i\|^4 \\
&+ \bar{\bar{T}}_{1i}\mathring{\theta}_{2i}\|\xi_i\|^3 + \sum_{i=1}^{N}\sum_{j\in\mathcal{N}_i}\Big[2\bar{\varphi}_{2j} + \big(\bar{\bar{T}}_{2j} + \bar{\bar{T}}_{3j}\big)\mathring{\theta}_{2j}\Big]\|\xi_i\|\|\xi_j\|^2 \\
&+ \sum_{i=1}^{N}\sum_{j\in\mathcal{N}_i}\Big\{2\bar{\varphi}_{1j} + \big(\bar{\bar{T}}_{2j} + \bar{\bar{T}}_{3j}\big)\Big[\check{\theta}_{0j}\big(2+\|B_1^T P_{\mathrm{a}j}\|\big) + \mathring{\theta}_{1j}\Big]\Big\}\|\xi_i\|\|\xi_j\| \\
&+ \Big\{\bar{\bar{T}}_{1i}\Big[\check{\theta}_{0i}\big(2+\|B_1^T P_{\mathrm{a}i}\|\big) + \mathring{\theta}_{1i} + \check{\gamma}_i\big(1+\|B_1^T P_{\mathrm{a}i}\|\Big] + \check{\gamma}_j\big(\bar{\bar{T}}_{2j} + \bar{\bar{T}}_{3j}\big)\big(1+\|B_1^T P_{\mathrm{a}i}\|\big)\Big\}\|\xi_i\|^2 \\
&+ \Big[\bar{\bar{T}}_{1i}\big(\mathring{\theta}_{0i} + \mathring{\gamma}_i\big) + \big(\bar{\bar{T}}_{2j} + \bar{\bar{T}}_{3j}\big)\big(\mathring{\gamma}_j + \mathring{\theta}_{0j}\big)\Big]\|\xi_i\|.
\end{aligned} \tag{6.36}$$

b) Time derivative of the Lyapunov function based on the uncertainty bound

Up to now, we have calculated the time derivative of the first line in (6.28). We will proceed with the time derivative of the other terms. Using the adaptive laws (6.27a)-

(6.27c), we have

$$\begin{aligned}
&\sum_{l=0}^{2}\frac{1}{\chi_{li}}(\hat{\theta}_{li}-\bar{\theta}_{li})\dot{\hat{\theta}}_{li}\\
&=\sum_{l=0}^{2}\frac{1}{\chi_{li}}(\hat{\theta}_{li}-\bar{\theta}_{li})\Big[\chi_{li}\big(\|\omega_{ai}\|+\|\omega_{ui}\|+\|S_i\|\big)\|\xi_i\|^l-\alpha_{li}\big(\|\omega_{ai}\|+\|\omega_{ui}\|\big)\|\xi_i\|^l\hat{\theta}_{li}\Big]\\
&=\sum_{l=0}^{2}\hat{\theta}_{li}\big(\|\omega_{ai}\|+\|\omega_{ui}\|+\|S_i\|\big)\|\xi_i\|^l-\sum_{l=0}^{2}\bar{\theta}_{li}\big(\|\omega_{ai}\|+\|\omega_{ui}+\|S_i\|\|\big)\|\xi_i\|^l\\
&\quad-\sum_{l=0}^{2}\bar{\alpha}_{li}\hat{\theta}_{li}^2\big(\|\omega_{ai}\|+\|\omega_{ui}\|\big)\|\xi_i\|^l+\sum_{l=0}^{2}\bar{\alpha}_{li}\hat{\theta}_{li}\bar{\theta}_{li}\big(\|\omega_{ai}\|+\|\omega_{ui}\|\big)\|\xi_i\|^l
\end{aligned}\tag{6.37}$$

where $\bar{\alpha}_{li}=\alpha_{li}/\chi_{li}$.

In addition,

$$\begin{aligned}
\frac{\gamma_i\dot{\gamma}_i}{\epsilon_0}&=\frac{\gamma_i}{\epsilon_0}\Big\{-\Big[\epsilon_0+\epsilon_1(\|\xi_i\|^7-\|\xi_i\|^5)+\epsilon_2\|\xi_i\|\Big]\gamma_i+\epsilon_0\big(\|S_i\|+\|\xi_i\|\big)+\beta_i\Big\}\\
&=-\gamma_i^2\Big[1+\bar{\epsilon}_1(\|\xi_i\|^7-\|\xi_i\|^5)+\bar{\epsilon}_2\|\xi_i\|\Big]+\gamma_i\big(\|S_i\|+\|\xi_i\|\big)+\gamma_i\bar{\beta}_i
\end{aligned}\tag{6.38}$$

where $\bar{\epsilon}_1=\frac{\epsilon_1}{\epsilon_0},\bar{\epsilon}_2=\frac{\epsilon_2}{\epsilon_0},\bar{\beta}_i=\frac{\beta_i}{\epsilon_0}$.

Using (6.31), (6.36) and (6.37)-(6.38), the time derivative of V satisfies

$$\begin{aligned}
\dot{V}\le&-\sum_{i=1}^{N}\lambda_{\min,i}\Big[\|\omega_{ai}\|^2+\|\omega_{ui}\|^2\Big]+\sum_{l=0}^{2}\bar{\theta}_{li}\|\xi_i\|^l\big(\|\omega_{ai}\|+\|\omega_{ui}\|\big)+\gamma_i\bar{\beta}_i\\
&-\omega_{ai}^TP_{ai}B_1(I_m+T_i)\rho_i\mathrm{sat}(S_i,\varphi)+\sum_{i=1}^{N}\sum_{j\in\mathcal{N}_i}\Psi_{ij}+\sum_{i=1}^{N}\gamma_i\big(\|S_i\|+\|\xi_i\|\big)\\
&+\sum_{i=1}^{N}\sum_{l=0}^{2}\hat{\theta}_{li}\big(\|\omega_{ai}\|+\|\omega_{ui}\|+\|S_i\|\big)\|\xi_i\|^l-\sum_{i=1}^{N}\sum_{l=0}^{2}\bar{\theta}_{li}\big(\|\omega_{ai}\|+\|\omega_{ui}+\|S_i\|\|\big)\|\xi_i\|^l\\
&-\sum_{i=1}^{N}\sum_{l=0}^{2}\bar{\alpha}_{li}\hat{\theta}_{li}^2\big(\|\omega_{ai}\|+\|\omega_{ui}\|\big)\|\xi_i\|^l+\sum_{i=1}^{N}\sum_{l=0}^{2}\bar{\alpha}_{li}\hat{\theta}_{li}\bar{\theta}_{li}\big(\|\omega_{ai}\|+\|\omega_{ui}\|\big)\|\xi_i\|^l\\
&-\sum_{i=1}^{N}\gamma_i^2\Big[1+\bar{\epsilon}_1(\|\xi_i\|^7-\|\xi_i\|^5)+\bar{\epsilon}_2\|\xi_i\|\Big]\\
\le&-\sum_{i=1}^{N}\lambda_{\min,i}\Big[\|\omega_{ai}\|^2+\|\omega_{ui}\|^2\Big]-\gamma_i^2\bar{\epsilon}_1(\|\xi_i\|^7-\|\xi_i\|^5)+\sum_{i=1}^{N}\sum_{j\in\mathcal{N}_i}\Psi_{ij}+\sum_{i=1}^{N}\gamma_i\|\xi_i\|\\
&-\omega_{ai}^TP_{ai}B_1(I_m+T_i)\rho_i\mathrm{sat}(S_i,\varphi)+\sum_{i=1}^{N}\Big[\sum_{l=0}^{2}\hat{\theta}_{li}\|\xi_i\|^l+\gamma_i\Big]\|S_i\|\\
&+\sum_{i=1}^{N}\sum_{l=0}^{2}\Big[\hat{\theta}_{li}-\bar{\alpha}_{li}\hat{\theta}_{li}^2+\bar{\alpha}_{li}\hat{\theta}_{li}\bar{\theta}_{li}\Big]\big(\|\omega_{ai}\|+\|\omega_{ui}\|\big)\|\xi_i\|^l-\sum_{i=1}^{N}\sum_{l=0}^{2}\bar{\theta}_{li}\|S_i\|\|\xi_i\|^l\\
&+\sum_{i=1}^{N}\Big[\gamma_i\bar{\beta}_i-\gamma_i^2\big(1+\bar{\epsilon}_2\|\xi_i\|\big)\Big].
\end{aligned}\tag{6.39}$$

The following inequality holds:

$$\begin{aligned}
&\sum_{l=0}^{2}\Big[\hat{\theta}_{li}-\bar{\alpha}_{li}\hat{\theta}_{li}^{2}+\bar{\alpha}_{li}\hat{\theta}_{li}\bar{\theta}_{li}\Big]\\
&\leq\sum_{l=0}^{2}-\frac{\bar{\alpha}_{li}}{3}\hat{\theta}_{li}^{2}-\Big[\frac{\bar{\alpha}_{li}}{3}(\hat{\theta}_{li}+\frac{3}{2\bar{\alpha}_{li}})^{2}-\frac{3}{4\bar{\alpha}_{l}^{2}}\Big]-\Big[\frac{\bar{\alpha}_{li}}{3}(\hat{\theta}_{li}-\frac{3}{2\bar{\alpha}_{li}}\bar{\theta}_{li})^{2}-\frac{3\bar{\theta}_{li}^{2}}{4\bar{\alpha}_{l}^{2}}\Big]\\
&\leq\sum_{l=0}^{2}\Big[-\frac{\bar{\alpha}_{li}}{3}\hat{\theta}_{li}^{2}+\frac{3}{4\bar{\alpha}_{li}}+\frac{3\bar{\theta}_{li}^{2}}{4\bar{\alpha}_{li}}\Big].
\end{aligned}\tag{6.40}$$

In addition,

$$\begin{aligned}
&\sum_{i=1}^{N}-\gamma_{i}^{2}\big(1+\bar{\epsilon}_{2}\|\xi_{i}\|\big)+\gamma_{i}\bar{\beta}_{i}+\gamma_{i}\|\xi_{i}\|\\
&\leq\sum_{i=1}^{N}-\frac{\bar{\epsilon}_{2}}{2}\|\xi_{i}\|\gamma_{i}^{2}-\Big\{\Big[\gamma_{i}-\frac{1}{2}\bar{\beta}_{i}\Big]^{2}-\frac{1}{4}\bar{\beta}_{i}^{2}\Big\}-\frac{\bar{\epsilon}_{2}}{2}\|\xi_{i}\|\Big\{\Big[\gamma_{i}-\frac{1}{\bar{\epsilon}_{2}}\Big]^{2}-\frac{1}{2\bar{\epsilon}_{2}^{2}}\Big\}\\
&\leq\sum_{i=1}^{N}\Big[-\frac{\bar{\epsilon}_{2}}{2}\|\xi_{i}\|\gamma_{i}^{2}+\frac{1}{4}\bar{\beta}_{i}^{2}+\frac{1}{4\bar{\epsilon}_{2}}\|\xi_{i}\|\Big].
\end{aligned}\tag{6.41}$$

According to the adaptive law in (6.27b), there exist $\underline{\gamma}_{i}\in\mathbb{R}^{+},\ i\in\{1,\ldots,N\}$ such that $\gamma_{i}>\underline{\gamma}_{i}$. Substituting (6.40)-(6.41) into (6.39), yields

$$\begin{aligned}
\dot{V}\leq&-\sum_{i=1}^{N}\lambda_{\min,i}\Big[\|\omega_{\mathrm{a}i}\|^{2}+\|\omega_{\mathrm{u}i}\|^{2}\Big]-\sum_{i=1}^{N}\underline{\gamma}_{i}^{2}\bar{\epsilon}_{1}(\|\xi_{i}\|^{7}-\|\xi_{i}\|^{5})\\
&+\sum_{i=1}^{N}\sum_{l=0}^{2}\Big[-\frac{\bar{\alpha}_{li}}{3}\hat{\theta}_{li}^{2}+\frac{3}{4\bar{\alpha}_{li}}+\frac{3\bar{\theta}_{li}^{2}}{4\bar{\alpha}_{li}}\Big]\big(\|\omega_{\mathrm{a}i}\|+\|\omega_{\mathrm{u}i}\|\big)\|\xi_{i}\|^{l}\\
&+\sum_{i=1}^{N}\Big[-\frac{\bar{\epsilon}_{2}}{2}\|\xi_{i}\|\gamma_{i}^{2}+\frac{1}{4}\bar{\beta}_{i}^{2}+\frac{1}{4\bar{\epsilon}_{2}}\|\xi_{i}\|\Big]+\sum_{i=1}^{N}\sum_{j\in\mathcal{N}_{i}}\Psi_{ij}\\
&-\omega_{\mathrm{a}i}^{T}P_{\mathrm{a}i}B_{1}(I_{m}+T_{i})\rho_{i}\mathrm{sat}(S_{i},\varphi)+\sum_{i=1}^{N}\Big[\sum_{l=0}^{2}\hat{\theta}_{li}\|\xi_{i}\|^{l}+\gamma_{i}\Big]\|S_{i}\|.
\end{aligned}\tag{6.42}$$

c) The behavior of Lyapunov function based on saturation regions

Based on the regions of the saturation function $\mathrm{sat}(S_{i},\varphi)$, we study the behaviour of the Lyapunov function according to three scenarios similar to [64] as follows:

- **Scenario 1:** $\|S_{i}\|\geq\varphi,\ i=1,\ldots,N.$

  In this scenario, we have $\mathrm{sat}(S_{i},\varphi)=\frac{S_{i}}{\|S_{i}\|}$. According to (6.26), we obtain the following as $S_{i}^{T}=\omega_{\mathrm{a}i}^{T}P_{\mathrm{a}i}B_{1}$:

$$-S_{i}^{T}(I_{m}+T_{i})\rho_{i}\mathrm{sat}(S_{i},\varphi)\leq-\sum_{i=1}^{N}(1-\bar{T})\frac{S_{i}^{T}S_{i}}{\|S_{i}\|}\rho_{i}\leq-\sum_{i=1}^{N}\Big[\sum_{l=0}^{2}\hat{\theta}_{li}\|\xi_{i}\|^{l}+\gamma_{i}\Big]\|S_{i}\|.\tag{6.43}$$

Using (6.43), the time derivative (6.42) is simplified to

$$\begin{aligned}\dot{V} \le & -\sum_{i=1}^{N}\lambda_{\min,i}\left[\|\omega_{ai}\|^2+\|\omega_{ui}\|^2\right]-\sum_{i=1}^{N}\underline{\gamma}_i^2\bar{\epsilon}_1(\|\xi_i\|^7-\|\xi_i\|^5)\\ & +\sum_{i=1}^{N}\sum_{l=0}^{2}\Big[-\frac{\bar{\alpha}_{li}}{3}\hat{\theta}_{li}^2+\frac{3}{4\bar{\alpha}_{li}}+\frac{3\bar{\theta}_{li}^2}{4\bar{\alpha}_{li}}\Big]\big(\|\omega_{ai}\|+\|\omega_{ui}\|\big)\|\xi_i\|^l\\ & +\sum_{i=1}^{N}\Big[-\frac{\bar{\epsilon}_2}{2}\|\xi_i\|\gamma_i^2+\frac{1}{4}\bar{\beta}_i^2+\frac{1}{4\bar{\epsilon}_2}\|\xi_i\|\Big]+\sum_{i=1}^{N}\sum_{j\in\mathcal{N}_i}\Psi_{ij}. \end{aligned}\tag{6.44}$$

The definition of Lyapunov function (6.28) leads to

$$V\le\sum_{i=1}^{N}\overline{\lambda}_i\big(\|\omega_{ai}\|^2+\|\omega_{ui}\|^2\big)+\sum_{i=1}^{N}\Big[\sum_{l=0}^{2}\frac{1}{\chi_{li}}\Big(\hat{\theta}_{li}^2+\bar{\theta}_{li}^2\Big)+\frac{\gamma_i^2}{\epsilon_0}\Big]\tag{6.45}$$

where $\overline{\lambda}_i=\max\Big\{\lambda_{\max}(P_{ai})/2,\lambda_{\max}(P_{ui})/2\Big\}$.

Define $\zeta=\frac{\min_i\{\lambda_{\min,i}\}}{\max_i\{\overline{\lambda}_i\}}$. Substituting (6.45) into (6.44) yields

$$\begin{aligned}\dot{V}\le & -\zeta V+\sum_{i=1}^{N}\Big[\sum_{l=0}^{2}\frac{\zeta}{\chi_{li}}\Big(\hat{\theta}_{li}^2+\bar{\theta}_{li}^2\Big)+\frac{\zeta\gamma_i^2}{\epsilon_0}\Big]+\sum_{i=1}^{N}\sum_{l=0}^{2}\Big\{-\frac{\bar{\alpha}_{li}}{3}\hat{\theta}_{li}^2\big(\|\omega_{ai}\|^{l+1}+\|\omega_{ui}\|^{l+1}\big)\\ & +\Big(\frac{3}{4\bar{\alpha}_{li}}+\frac{3\bar{\theta}_{li}^2}{4\bar{\alpha}_{li}}\Big)\big(\|\omega_{ai}\|+\|\omega_{ui}\|\big)\|\xi_i\|^l\Big\}+\sum_{i=1}^{N}\Big[-\frac{\bar{\epsilon}_2}{2}\|\xi_i\|\gamma_i^2+\frac{1}{4}\bar{\beta}_i^2+\frac{1}{4\bar{\epsilon}_2}\|\xi_i\|\Big]\\ & -\sum_{i=1}^{N}\underline{\gamma}_i^2\bar{\epsilon}_1(\|\xi_i\|^7-\|\xi_i\|^5)+\sum_{i=1}^{N}\sum_{j\in\mathcal{N}_i}\Psi_{ij}\\ \le & -\zeta V-\sum_{i=1}^{N}\sum_{l=0}^{2}\hat{\theta}_{li}^2\Big[\frac{\bar{\alpha}_{li}}{3}\big(\|\omega_{ai}\|^{l+1}+\|\omega_{ui}\|^{l+1}\big)-\frac{\zeta}{\chi_{li}}\Big]\\ & -\sum_{i=1}^{N}\gamma_i^2\Big[\frac{\bar{\epsilon}_2}{2}\|\xi_i\|-\frac{\zeta}{\epsilon_0}\Big]+Z_1(\|\xi\|). \end{aligned}\tag{6.46}$$

According to (6.36), we have

$$\begin{aligned}Z_1(\|\xi\|)= & \sum_{i=1}^{N}\sum_{j\in\mathcal{N}_i}\Psi_{ij}-\sum_{i=1}^{N}\underline{\gamma}_i^2\bar{\epsilon}_1(\|\xi_i\|^7-\|\xi_i\|^5)\\ & +\sum_{i=1}^{N}\sum_{l=0}^{2}\Big(\frac{3}{4\bar{\alpha}_{li}}+\frac{3\bar{\theta}_{li}^2}{4\bar{\alpha}_{li}}\Big)\big(\|\omega_{ai}\|+\|\omega_{ui}\|\big)\|\xi_i\|^l+\sum_{i=1}^{N}\Big[\frac{1}{4}\bar{\beta}_i^2+\frac{1}{4\bar{\epsilon}_2}\|\xi_i\|+\sum_{l=0}^{2}\frac{\zeta}{\chi_{li}}\bar{\theta}_{li}^2\Big]\\ \triangleq & \sum_{i=1}^{N}-\bar{\epsilon}_1\underline{\gamma}_i^2\|\xi_i\|^7+\sum_{i=1}^{N}c_{12}\|\xi_i\|^6+\sum_{i=1}^{N}\sum_{j\in\mathcal{N}_i}c_{11}\|\xi_i\|\|\xi_j\|^5++\sum_{i=1}^{N}\bar{\epsilon}_1\underline{\gamma}_i^2\|\xi_i\|^5\sum_{i=1}^{N}c_6\\ & +\sum_{i=1}^{N}c_{22}\|\xi_i\|^4+\sum_{i=1}^{N}\sum_{j\in\mathcal{N}_i}c_{21}\|\xi_i\|\|\xi_j\|^3+\sum_{i=1}^{N}\sum_{j\in\mathcal{N}_i}c_{31}\|\xi_i\|\|\xi_j\|^2+\sum_{i=1}^{N}c_{32}\|\xi_i\|^3\\ & +\sum_{i=1}^{N}\sum_{j\in\mathcal{N}_i}c_{41}\|\xi_i\|\|\xi_j\|+\sum_{i=1}^{N}c_{42}\|\xi_i\|^2+\sum_{i=1}^{N}c_5\|\xi_i\| \end{aligned}$$

6

with

$$
\begin{aligned}
c_{11} =& \check{\theta}_{2j}\big(\bar{\bar{T}}_{2j}+\bar{\bar{T}}_{3j}\big)\big(2+\|B_1^T P_{\mathrm{a}j}\|\big),\ c_{12}=\bar{\bar{T}}_{1i}\check{\theta}_{2i}\big(2+\|B_1^T P_{\mathrm{a}i}\|\big),\ c_6=\frac{1}{4}\bar{\beta}_i^2+\zeta\bar{\theta}_{li}^2\\
c_{21} =& \check{\theta}_{1j}\big(\bar{\bar{T}}_{2j}+\bar{\bar{T}}_{3j}\big)\big(2+\|B_1^T P_{\mathrm{a}j}\|\big),\ c_{22}=\bar{\bar{T}}_{1i}\check{\theta}_{1i}\big(2+\|B_1^T P_{\mathrm{a}i}\|\big)\\
c_{31} =& 2\bar{\varphi}_{2j}+\big(\bar{\bar{T}}_{2j}+\bar{\bar{T}}_{3j}\big)\bar{\theta}_{2j},\ c_{32}=2\Big(\frac{3}{4\alpha_{2i}}+\frac{3\bar{\theta}_{2i}^2}{4\alpha_{2i}}\Big)+\bar{\bar{T}}_{1i}\mathring{\theta}_{2i}\\
c_{41} =& 2\bar{\varphi}_{1j}+\big(\bar{\bar{T}}_{2j}+\bar{\bar{T}}_{3j}\big)\Big[\check{\theta}_{0j}\big(2+\|B_1^T P_{\mathrm{a}j}\|\big)+\mathring{\theta}_{1j}\Big]\\
c_{42} =& 2\Big(\frac{3}{4\alpha_{1i}}+\frac{3\bar{\theta}_{1i}^2}{4\alpha_{1i}}\Big)+\bar{\bar{T}}_{1i}\Big[\check{\theta}_{0i}\big(2+\|B_1^T P_{\mathrm{a}i}\|\big)+\mathring{\theta}_{1i}+\check{\gamma}_i\big(1+\|B_1^T P_{\mathrm{a}i}\|\big)\Big]\\
&+\check{\gamma}_j\big(\bar{\bar{T}}_{2j}+\bar{\bar{T}}_{3j}\big)\big(1+\|B_1^T P_{\mathrm{a}i}\|\big)\\
c_5 =& \bar{\bar{T}}_{1i}\big(\mathring{\theta}_{0i}+\mathring{\gamma}_i\big)+\big(\bar{\bar{T}}_{2j}+\bar{\bar{T}}_{3j}\big)\big(\mathring{\gamma}_j+\mathring{\theta}_{0j}\big)+2\Big(\frac{3}{4\alpha_{0i}}+\frac{3\bar{\theta}_{0i}^2}{4\alpha_{0i}}\Big)+\frac{1}{4\bar{\varphi}_2}.
\end{aligned}
$$

Using Descartes' rules of sign change and Bolzano's Theorem [107], the polynomial Z_1 has exactly one positive real root $\iota\in\mathbb{R}^+$. The coefficient of the highest degree of Z_1 is negative as $-\underline{\gamma}_i^2\bar{\epsilon}_1$. Therefore, $Z_1(\|\xi\|)\le 0$ when $\|\xi\|\ge\eta_1$, where $\xi=[\xi_1^T,\ldots,\xi_N^T]^T$. Define $\iota_1=\frac{3\zeta}{2\chi_{0i}\bar{\alpha}_{0i}}$, $\iota_2=\sqrt{\frac{3\zeta}{2\chi_{1i}\bar{\alpha}_{1i}}}$, $\iota_3=\Big(\frac{3\zeta}{2\chi_{2i}\bar{\alpha}_{2i}}\Big)^{1/3}$, $\iota_4=\frac{2\zeta}{\bar{\epsilon}_2}$. According to (6.46), $\dot{V}\le-\zeta V$ when

$$
\begin{aligned}
&\min\{\|\omega_{\mathrm{a}i}\|,\|\omega_{\mathrm{u}i}\|,\|\xi_i\|\}\ge\max\{\eta_1,\iota_1,\iota_2,\iota_3,\iota_4\}\\
&\Rightarrow\min\{\|\omega_{\mathrm{a}i}\|,\|\omega_{\mathrm{u}i}\|\}\ge\max\{\eta_1,\iota_1,\iota_2,\iota_3,\iota_4\}
\end{aligned}
\tag{6.47}
$$

- **Scenario 2:** $\|S_i\|<\varphi$, $i=1,\ldots,N$.

In this scenario, we have $\mathrm{sat}(S_i,\varphi)=\frac{S_i}{\varphi}$. According to (6.26), we have

$$
-\sum_{i=1}^{N}S_i^T(I_m+T_i)\rho_i\mathrm{sat}(S_i,\varphi)\le 0. \tag{6.48}
$$

Substituting (6.48) into (6.42) gives

$$
\begin{aligned}
\dot{V}\le&-\zeta V-\sum_{i=1}^{N}\sum_{l=0}^{2}\hat{\theta}_{li}^2\Big[\frac{\bar{\alpha}_{li}}{3}\big(\|\omega_{\mathrm{a}i}\|^{l+1}+\|\omega_{\mathrm{u}i}\|^{l+1}\big)-\frac{\zeta}{\chi_{li}}\Big]+Z_1(\|\xi\|)\\
&-\sum_{i=1}^{N}\gamma_i^2\Big[\frac{\bar{\epsilon}_2}{2}\|\xi_i\|-\frac{\zeta}{\epsilon_0}\Big]+\sum_{i=1}^{N}\Big[\sum_{l=0}^{2}\hat{\theta}_{li}\|\xi_i\|^l+\gamma_i\Big]\|S_i\|.
\end{aligned}
\tag{6.49}
$$

According to (6.32), together with $\|S_i\| < \varphi$, we obtain

$$\begin{aligned}
&\sum_{i=1}^{N}\Big[\sum_{l=0}^{2}\hat{\theta}_{li}\|\xi_i\|^l+\gamma_i\Big]\|S_i\| \\
\leq&\sum_{i=1}^{N}\Big[\sum_{l=0}^{2}\mathring{\theta}_{li}\|\xi_i\|^l+\mathring{\gamma}_i\|S_i\|+\check{\gamma}_i\big(1+\|B_1^TP_{\mathrm{a}i}\|\big)\|S_i\|^2 \\
&+\check{\theta}_{li}\big(\|\omega_{\mathrm{a}i}\|+\|\omega_{\mathrm{u}i}\|+\|S_i\|\big)\|\xi_i\|^{2l}\Big]\|S_i\| \\
\leq&\sum_{i=1}^{N}\big(\mathring{\theta}_{0i}+\varphi\check{\theta}_{0i}+\varphi\mathring{\gamma}_i\big)+\check{\gamma}_i\big(1+\|B_1^TP_{\mathrm{a}i}\|\big)\varphi+\big(2\check{\theta}_{0i}+\mathring{\theta}_{1i}\big)\|\xi_i\| \\
&+\sum_{i=1}^{N}\Big[\varphi\check{\theta}_{1i}+\mathring{\theta}_{1i}\Big]\|\xi_i\|^2+2\check{\theta}_{1i}\|\xi_i\|^3+\varphi\check{\theta}_{2i}\|\xi_i\|^4+\sum_{i=1}^{N}2\check{\theta}_{2i}\|\xi_i\|^5. \qquad (6.50)
\end{aligned}$$

Substituting (6.50) into (6.49) gives

$$\dot{V}\leq-\zeta V-\sum_{i=1}^{N}\sum_{l=0}^{2}\hat{\theta}_{li}^2\Big[\frac{\bar{\alpha}_{li}}{3}\big(\|\omega_{\mathrm{a}i}\|^{l+1}+\|\omega_{\mathrm{u}i}\|^{l+1}\big)-\frac{\zeta}{\chi_{li}}\Big]-\sum_{i=1}^{N}\gamma_i^2\Big[\frac{\bar{\epsilon}_2}{2}\|\xi_i\|-\frac{\zeta}{\epsilon_0}\Big]+Z_2(\|\xi\|) \qquad (6.51)$$

with $Z_2(\|\xi\|)=Z_1(\|\xi\|)+\sum_{i=1}^{N}\big(\mathring{\theta}_{0i}+\varphi\check{\theta}_{0i}+\varphi\mathring{\gamma}_i\big)+\check{\gamma}_i\big(1+\|B_1^TP_{\mathrm{a}i}\|\big)\varphi+\big(2\check{\theta}_{0i}+\mathring{\theta}_{1i}\big)\|\xi_i\|+\sum_{i=1}^{N}\Big[\varphi\check{\theta}_{1i}+\mathring{\theta}_{1i}\Big]\|\xi_i\|^2+2\check{\theta}_{1i}\|\xi_i\|^3+\varphi\check{\theta}_{2i}\|\xi_i\|^4+\sum_{i=1}^{N}2\check{\theta}_{2i}\|\xi_i\|^5$.

Analogously to Scenario 1, $\dot{V}\leq-\zeta V$ when

$$\begin{aligned}
&\min\{\|\omega_{\mathrm{a}i}\|,\|\omega_{\mathrm{u}i}\|,\|\xi_i\|\}\geq\max\{\eta_2,\iota_1,\iota_2,\iota_3,\iota_4\} \\
&\Rightarrow\min\{\|\omega_{\mathrm{a}i}\|,\|\omega_{\mathrm{u}i}\|\}\geq\max\{\eta_2,\iota_1,\iota_2,\iota_3,\iota_4\} \qquad (6.52)
\end{aligned}$$

where η_2 is the positive real root of Z_2 such that $Z_2(\|\xi\|)\leq 0$ when $\|\xi\|\geq\eta_2$.

- **Scenario 3:** $\|S_i\|$ satisfies neither Scenario 1 nor Scenario 2. Without loss of generality, consider $\|S_i\|\geq\varphi$ for $i=1,\ldots,k$, and $\|S_i\|<\varphi$ for $i=k+1,\ldots,N$ where $1\leq k\leq N-1$. For $i=1,\ldots,k$, we have $\mathrm{sat}(S_i,\varphi)=\frac{S_i}{\|S_i\|}$; For $i=k+1,\ldots,N$, $\mathrm{sat}(S_i,\varphi)=\frac{S_i}{\varphi}$. Similarly to Scenario 1 and Scenario 2, we get

$$\begin{aligned}
\dot{V}\leq&-\zeta V-\sum_{i=1}^{N}\sum_{l=0}^{2}\hat{\theta}_{li}^2\Big[\frac{\bar{\alpha}_{li}}{3}\big(\|\omega_{\mathrm{a}i}\|^{l+1}+\|\omega_{\mathrm{u}i}\|^{l+1}\big)-\frac{\zeta}{\chi_{li}}\Big]+Z_1(\|\xi\|) \\
&-\sum_{i=1}^{N}\gamma_i^2\Big[\frac{\bar{\epsilon}_2}{2}\|\xi_i\|-\frac{\zeta}{\epsilon_0}\Big]+\sum_{i=k+1}^{N}\Big[\sum_{l=0}^{2}\hat{\theta}_{li}\|\xi_i\|^l+\gamma_i\Big]\|S_i\| \\
\leq&-\zeta V-\sum_{i=1}^{N}\sum_{l=0}^{2}\hat{\theta}_{li}^2\Big[\frac{\bar{\alpha}_{li}}{3}\big(\|\omega_{\mathrm{a}i}\|^{l+1}+\|\omega_{\mathrm{u}i}\|^{l+1}\big)-\frac{\zeta}{\chi_{li}}\Big]-\sum_{i=1}^{N}\gamma_i^2\Big[\frac{\bar{\epsilon}_2}{2}\|\xi_i\|-\frac{\zeta}{\epsilon_0}\Big]+Z_3(\|\xi\|) \qquad (6.53)
\end{aligned}$$

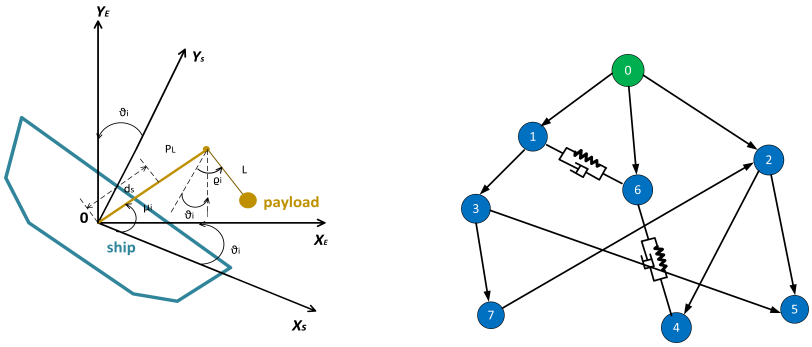

(a) Schematic boom crane on ship

(b) Network

Figure 6.1: System used for simulations.

with $Z_3(\|\xi\|) = Z_1(\|\xi\|) + \sum_{i=k+1}^{N} \left(\mathring{\theta}_{0i} + \varphi\check{\theta}_{0i} + \varphi\mathring{\gamma}_i\right) + \check{\gamma}_i\left(1 + \|B_1^T P_{ai}\|\right)\varphi + \left(2\check{\theta}_{0i} + \mathring{\theta}_{1i}\right)\|\xi_i\| +$
$\sum_{i=k+1}^{N} \left[\varphi\check{\theta}_{1i} + \mathring{\theta}_{1i}\right]\|\xi_i\|^2 + 2\check{\theta}_{1i}\|\xi_i\|^3 + \varphi\check{\theta}_{2i}\|\xi_i\|^4 + \sum_{i=k+1}^{N} 2\check{\theta}_{2i}\|\xi_i\|^5.$
Analogously to Scenario 1, $\dot{V} \le -\zeta V$ when

$$\begin{aligned} &\min\{\|\omega_{ai}\|, \|\omega_{ui}\|, \|\xi_i\|\} \ge \max\{\eta_3, \iota_1, \iota_2, \iota_3, \iota_4\} \\ &\Rightarrow \min\{\|\omega_{ai}\|, \|\omega_{ui}\|\} \ge \max\{\eta_3, \iota_1, \iota_2, \iota_3, \iota_4\} \end{aligned} \tag{6.54}$$

where η_3 is the positive real root of Z_3 such that $Z_3(\|\xi\|) \le 0$ when $\|\xi\| \ge \eta_3$.

Finally, combining (6.47) in Scenario 1 with (6.52) in Scenario 2 and (6.54) in Scenario 3, we obtain $\omega_{ui}, \omega_{ai} \in \mathcal{L}_\infty$ when $\|\xi\| \ge \max\{\eta_1, \eta_2, \eta_3, \iota_1, \iota_2, \iota_3, \iota_4\}$, which leads to $e_u, e_a \in \mathcal{L}_\infty$. Both the local actuated synchronization error and local non-actuated synchronization error are thus proved to reach UUB. According to (6.9) in **Lemma** 6.1, the global synchronization errors δ_u, δ_a are also uniformly ultimately bounded. □

Remark 6.5. *The proof of **Theorem** 6.1 provides estimates for the uniform ultimate bounds, which can be tuned as follows. Larger β_i and ϵ_1 leads to more negative $-\underline{\gamma}_i^2\bar{\epsilon}_1$, which is the fifth degree coefficient of the polynomials $Z_1(\|\xi\|)$, $Z_2(\|\xi\|)$, $Z_3(\|\xi\|)$ in (6.46), (6.51), and (6.53). Making this coefficient more negative makes the roots η_1, η_2, η_3 closer to zero, which in turn contributes to reducing the ultimate bound on the error. Larger χ_{li} and smaller ζ, which can be obtained from larger P_{ui}, P_{ai}, result in ι_1, ι_2, ι_3 being closer to zero. A larger ϵ_2 leads to a smaller ι_4. This also contributes to reducing the ultimate bound on the error. Let us mention that a smaller error might require a larger input: this is a standard trade-off [111, 143], which might be seen from the fact that larger χ_{li} and β_i leads to larger ρ_i.*

6.5. SIMULATION EXAMPLE

A network of underactuated systems is considered, where each system has boom crane dynamics mounted on a ship: the network can be thought as an abstraction of a cooper-

ative lifting scenario. Here, ϱ_i is the payload swing with respect to Y_s, ϑ_i is the ship roll angle caused by sea waves, μ_i is the luffing angle of the boom, and L denotes the length of the rope. The length, mass, and moment of inertia of the boom are P_L, m, and J. The distance between the barycenter of the boom and the origin is denoted by d_s. The states of the crane system are $q_{1i} = \varrho_i - \vartheta_i$, $q_{2i} = \mu_i - \vartheta_i$, and $q_{3i} = L$ (q_{1i} is the non-actuated state, q_{2i}, q_{3i} are the actuated states), leading to the dynamics as (6.1) with $n = 3, m = 2$, and

$$M_i = \begin{bmatrix} m_{\mathrm{p}i} q_{3i}^2 & -m_{\mathrm{p}i} P_L q_{3i} S_{21,i} & 0 \\ -m_{\mathrm{p}i} P_L q_{3i} S_{21,i} & J_i + m_{\mathrm{p}i} P_L^2 & -m_{\mathrm{p}i} P_L C_{21,i} \\ 0 & -m_{\mathrm{p}i} P_L C_{21,i} & m_{\mathrm{p}i} \end{bmatrix}$$

$$C_i = \begin{bmatrix} m_{\mathrm{p}i} q_{3i} \dot{q}_{3i} & -m_{\mathrm{p}i} P_L q_{3i} C_{21,i} \dot{q}_{2i} & m_{\mathrm{p}i} q_{3i} \dot{q}_{1i} \\ U_{3i} & 0 & -m_{\mathrm{p}i} P_L S_{21,i} \dot{q}_{1i} \\ -m_{\mathrm{p}i} q_{3i} \dot{q}_{1i} & m_{\mathrm{p}i} P_L S_{21,i} \dot{q}_{2i} & 0 \end{bmatrix}$$

$$U_{3i} = -m_P P_L (S_{21,i} \dot{q}_{3i} - C_{21,i} q_{3i} \dot{q}_{1i}), \ \tau_i = [\tau_{1i} \ \ \tau_{2i}]$$

$$G_i = \begin{bmatrix} m_{\mathrm{p}i} g_a q_{2i} \sin(q_{1i}) \\ (m_{\mathrm{p}i} P_L + m_i d_{si}) g_a \cos(q_{2i}) \\ -m_{\mathrm{p}i} g_a \cos(q_{1i}) \end{bmatrix}, \ q_i = \begin{bmatrix} q_{1i} \\ q_{2i} \\ q_{3i} \end{bmatrix}$$

$$H_i = \sum_{j=0}^{N} s_{ij}(q_i - q_j) + \sum_{j=0}^{N} \delta_{ij}(\dot{q}_i - \dot{q}_j)$$

with $S_{21,i} \triangleq \sin(q_{2i} - q_{1i})$, $C_{21,i} \triangleq \cos(q_{2i} - q_{1i})$ and $F_i = [F_{i1} \ F_{i2} \ F_{i3}]^T$ where $F_{i1}(\dot{q}_{1i}) \triangleq f_{i1} \tanh(f_{i2} \dot{q}_{i1}) - \tanh(f_{i3} \dot{q}_{i1})) + f_{i4} \tanh(f_{i5} \dot{q}_{i1}) + f_{i6} \dot{q}_{i1}$, $F_{i2}(\dot{q}_{2i}) \triangleq f_{i1} \tanh(f_{i2} \dot{q}_{i2}) - \tanh(f_{i3} \dot{q}_{i2})) + f_{i4} \tanh(f_{i5} \dot{q}_{i2}) + f_{i6} \dot{q}_{i2}$, $F_{i3}(\dot{q}_{3i}) \triangleq f_{i1} \tanh(f_{i2} \dot{q}_{i3}) - \tanh(f_{i3} \dot{q}_{i3})) + f_{i4} \tanh(f_{i5} \dot{q}_{i3}) + f_{i6} \dot{q}_{i3}$. The friction term F_i is taken in non-linear-in-the-parameters form according to [76], whereas the interconnection term H_i follows a standard spring-damper model where s_{ij} is the stiffness parameter, and δ_{ij} is the damping factor (this can represent some interconnection among the cranes via the crane wires due to the load). The goal is to bring the payload to a desired position defined by $q_{01} = 0$, $q_{02} = \arccos(a_L / P_L)$, $q_{03} = \sqrt{P_L^2 - a_L^2} - b_L$.

6.5.1. SYSTEM PARAMETERS (UNCERTAIN) AND DESIGN PARAMETERS

The following system parameters are only used for simulation purposes, but they are unknown for the control design. The vector of (unknown) parameters in friction term is compactly represented as $\Theta_i = [f_{i1} \ f_{i2} \ f_{i3} \ f_{i4} \ f_{i5} \ f_{i6}]^T$, where

$\Theta_1 = [0.5 \ 0.8 \ 0.9 \ 1.2 \ 0.5 \ 0.4]^T$, $\Theta_2 = [0.5 \ 0.7 \ 0.9 \ 1.0 \ 0.5 \ 0.4]^T$, $\Theta_3 = [0.3 \ 0.7 \ 0.7 \ 1.0 \ 0.7 \ 0.3]^T$, $\Theta_4 = [0.5 \ 0.9 \ 0.7 \ 1.2 \ 0.4 \ 0.5]^T$, $\Theta_5 = [0.5 \ 0.8 \ 0.6 \ 1.3 \ 0.5 \ 0.6]^T$, $\Theta_6 = [0.6 \ 1.0 \ 0.9 \ 1.5 \ 0.2 \ 0.5]^T$ $\Theta_7 = [0.4 \ 1.0 \ 0.8 \ 1.2 \ 0.4 \ 0.8]^T$.

According to interconnection network in Fig. 6.1 (b), the spring-damper parameters are chosen as $s_{16} = s_{61} = 0.37$, $s_{46} = s_{64} = 0.29$ and $\delta_{16} = \delta_{61} = 25$, $\delta_{46} = \delta_{64} = 9$. The disturbance is $d_i(t) = 0.1 \sin(0.001 i t)[1 \ 1 \ 1]^T$.

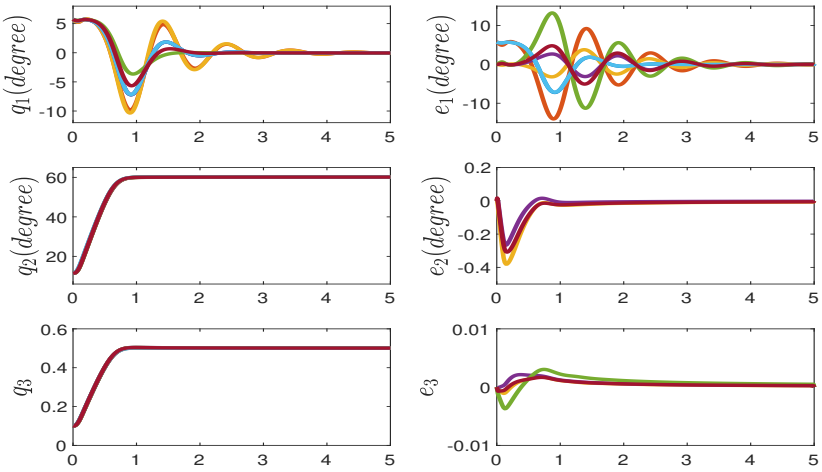

Figure 6.2: States and corresponding synchronization errors for the example of Section 6.5

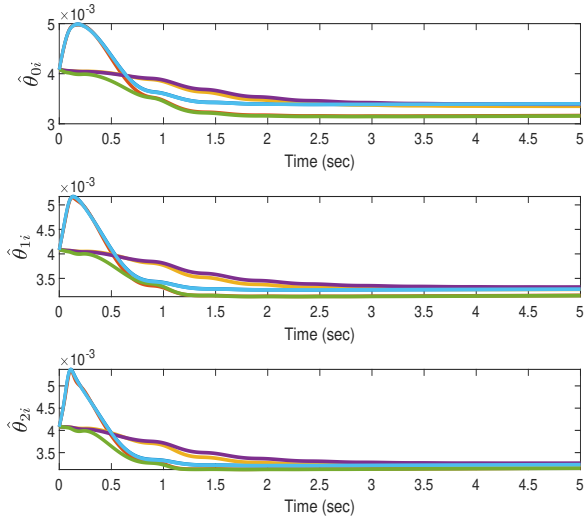

Figure 6.3: Adaptive parameters θ_{li}, $l = 0,1,2.$ for the example of Section 6.5

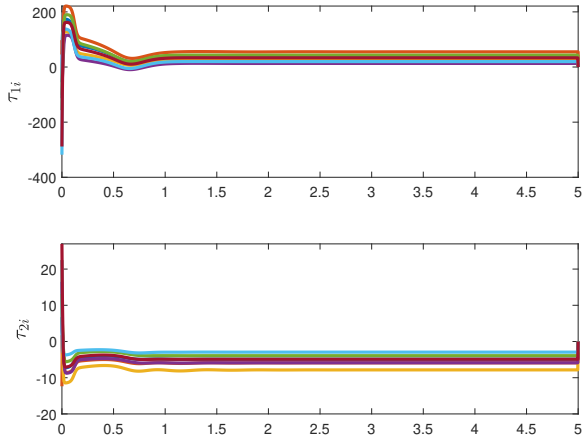

Figure 6.4: Control inputs τ_{1i} and τ_{2i} for the example of Section 6.5

Physical parameters are chosen as:

$$[m_1\ m_2\ m_3\ m_4\ m_5\ m_6\ m_7] = [20\ 18\ 15\ 22\ 17\ 19\ 16]$$
$$[m_{\mathrm{p}1}\ m_{\mathrm{p}2}\ m_{\mathrm{p}3}\ m_{\mathrm{p}4}\ m_{\mathrm{p}5}\ m_{\mathrm{p}6}\ m_{\mathrm{p}7}] = [0.5\ 0.6\ 0.8\ 0.6\ 0.4\ 0.3\ 0.5]$$
$$[J_1\ J_2\ J_3\ J_4\ J_5\ J_6\ J_7] = [6.5\ 7.8\ 5.3\ 6.2\ 7.2\ 6.8\ 6.6]$$
$$[d_{\mathrm{s}1}\ d_{\mathrm{s}2}\ d_{\mathrm{s}3}\ d_{\mathrm{s}4}\ d_{\mathrm{s}5}\ d_{\mathrm{s}6}\ d_{\mathrm{s}7}] = [0.4\ 0.6\ 0.3\ 0.1\ 0.5\ 0.2\ 0.4].$$

The parameters $a_L = 0.4m$, $b_L = 0.2m$, $P_L = 0.8m$ give the desired position $q_{01} = 0$, $q_{02} = 1.05$, $q_{03} = 0.5$.

The nominal parameters (used for control design of $\hat{M}_{\mathrm{s}}$) are selected as $[\hat{m}_{\mathrm{p}1}\ \hat{m}_{\mathrm{p}2}\ \hat{m}_{\mathrm{p}3}\ \hat{m}_{\mathrm{p}4}\ \hat{m}_{\mathrm{p}5}\ \hat{m}_{\mathrm{p}6}\ \hat{m}_{\mathrm{p}7}] = [0.45\ 0.55\ 0.75\ 0.55\ 0.35\ 0.25\ 0.45]$, $[\hat{J}_1\ \hat{J}_2\ \hat{J}_3\ \hat{J}_4\ \hat{J}_5\ \hat{J}_6\ \hat{J}_7] = [6\ 7\ 5\ 6\ 7\ 6\ 8]$, then it is can be verified that **Assumption** 6.2 holds with $\bar{T} = 0.5$. The initial states are $[q_{1i}(0)\ q_{2i}(0)\ q_{3i}(0)] = [0\ 0.1\ 0.2]$.

The control design parameters are $\Theta_{\mathrm{a}i} = 335I_2$, $\Xi_{\mathrm{a}i} = 0.003I_2$, $\Theta_{\mathrm{u}i} = 0.03[1\ 1]^T$, $\Xi_{\mathrm{u}i} = 0.01[1\ 1]^T$, $\Gamma_i = 0.01[1\ 1]^T$, $Q_{\mathrm{a}i} = 0.015I_2$, $Q_{\mathrm{u}i} = 560I_2$, $\alpha_{li} = 3.15$, $\chi_{li} = 0.01, \epsilon_0 = 0.001, \epsilon_1 = 0.003$, $\epsilon_2 = 0.015$, $\beta_i = 3150$.

6.5.2. SIMULATION RESULTS

The non-actuated and actuated states, and the corresponding synchronization errors are reported in Fig. 6.2. It can be seen that the errors converge to a neighborhood of zero. In Fig. 6.3, the adaptive parameters $\hat{\theta}_{li}$, $l = 0,1,2$ are shown, whereas the control inputs are given in Fig. 6.4. Note that the control inputs converge to different values due to the heterogeneity of the system in mass, inertia, friction, etc.

6.6. CONCLUDING REMARKS

This work has proposed for the first time an adaptive distributed protocol for synchronization of uncertain underactuated Euler-Lagrange systems. The protocol can tackle not only unknown system terms but also uncertain state-dependent interconnection among multiple Euler-Lagrange systems.

7

CONCLUSIONS AND RECOMMENDATIONS

In this thesis, we have introduced new adaptive approaches for designing controllers for interconnected and multi-agent systems that can adapt to changing circumstances without requiring structural knowledge of the dynamics. The main contribution of the thesis is that the proposed controllers are able to handle both parametric uncertainties and state-dependent uncertainties. This chapter will present the main results of this thesis and some ideas for future research.

7.1. CONCLUSIONS

The main results of this thesis are discussed here:

Chapter 3 has answered ***Question 1***. A new leakage-based framework was proposed for switched linear systems, with the advantage of keeping the control gains of inactive subsystems constant at their switched-off values while guaranteeing the stability of the closed-loop switched system. A new auxiliary gain was introduced to play the role of leakage action during inactive time intervals. It was shown that the proposed strategy can consistently improve the transient of the closed-loop system under various families of slowly-switching signals (in the framework of dwell time and its extensions).

Chapter 4 has answered ***Question 2***. We have proposed an adaptive framework for multi-area load frequency control (LFC) based on nonlinear structure-preserving (Kuramoto) dynamics under switching topologies. Instead of modeling the interconnections among different areas as linear terms, nonlinear interconnections were considered. It was shown that the system is able to self-reconfiguration in the presence of parametric uncertainty and state-dependent uncertainty in multi-area power systems.

Chapter 5 has answered ***Question 3***. We have addressed and solved the leader-following synchronization problem for multiple uncertain Euler-Lagrange systems with state-dep-endent uncertainty and without a priori bounded interconnections. As a result of removing the a priori bounded structure, we sought practical synchronization instead

of asymptotic synchronization. To address the presence of state-dependent uncertainty and uncertain state-dependent interconnections, we proposed an adaptive distributed control mechanism to estimate the coefficients of the resulting uncertainty structure.

Chapter 6 has answered ***Question 4***. We have proposed a new distributed approach for interconnected underactuated systems with limited knowledge of the system dynamics and the interconnection terms. We neither impose the mass matrix to depend on the actuated states only, nor on the non-actuated states only. State-dependent uncertain interconnection terms among the underactuated systems have been considered to exist before the control design, instead of only being a result of coupling caused by the control protocol.

7.2. RECOMMENDATIONS FOR FUTURE RESEARCH

The methodologies proposed in this thesis can be possibly extended along several directions, listed as follows:

- **Uncertain switched systems with time-varying delays and switching delays**

  Since delay often occurs in switched systems, time-varying delays and switching delays (also called asynchronous delays) can be introduced and studied in the framework of robust adaptive control. The challenge is to show if in such a setting we can still let the control gains of inactive subsystems keep constant values during the switched-off phase.

- **Adaptive or switched adaptive wide-area damping control**

  With the expansion of smart grids, regional power systems at remote distances are more and more interconnected by longer transmission lines. Future work is to extend the proposed methodology of multi-area load frequency control to wide-area damping control. The challenge is to devise a modeling approach beyond the structure-preserving model [42, 96].

- **Distributed adaptive control of Euler-Lagrange systems under switching topologies**

  Since the multiple Euler-Lagrange systems we studied can be interconnected, considering dynamically changing topologies is natural. The challenge is that the system dynamics in (5.1) (or (6.1) for underactuated systems) will change to switched dynamics. Accordingly, the adaptive laws in (5.6), and (5.13) (or (6.11), (6.26), and (6.27) for underactuated systems) must be changed to adapt to the switching structure of the topologies. A similar concern also applies to underactuated Euler-Lagrange systems.

- **Switching topologies in both the communication network and the physical network**

  In this thesis, we did not distinguish between communication interactions and physical interactions. In practice, these different kinds of interactions among agents can be described by different networks: a communication network and a physical network. Therefore, an interesting topic for future work is to introduce explicitly

these two different networks in multi-agent systems. The challenge is that two different types of error will also arise (the communication synchronization error and the physical synchronization error), which would require a different stability analysis and control design approach. It would be also interesting to assess how the switching topologies of these two kinds of networks affect the system performance.

- **Output-feedback adaptive control of Euler-Lagrange systems**

  All of our methods assume that the states are directly accessible for feedback, which can be quite restrictive. In most practical situations, the full state of a system is not measurable directly, and only the measured output can be used for feedback (partial state feedback). The challenge is to design observer-based approaches that can deal with state-dependent uncertainty.

- **Underactuated Euler-Lagrange systems subject to nonholonomic constraints**

  When considering nonholonomic constraints in a system, one can determine a differential relationship between state and inputs, but one cannot determine a closed-form geometric relationship. This means that the history of states is needed to determine the current state. Wheeled vehicles are good examples of Euler-Lagrange systems subject to nonholonomic constraints. Since in wheeled vehicles there is no unique relationship between the direction and the position, one would have to know the rolling history. How to tackle such nonholonomic constraints in Euler-Lagrange dynamics is an open challenge.

- **Optimal adaptive synchronization of multi-agent systems subject to constraints**

  Adaptive control usually aims to adapt to the changing environment while guaranteeing stability to achieve a common task. However, in many real-world multi-agent systems, only guaranteeing stability is not sufficient because we may desire other various control objectives in the presence of constraints such as cost, distance constraints, capacity constraints, or other equality/inequality constraints. How to satisfy these constraints optimally in multi-agent systems while ensuring stability and synchronization is an important open issue.

- **Application of interconnected systems in multi-robot manipulation**

  Interconnected systems can be used to describe several multi-robot cooperative manipulation tasks, where a group of mobile robots is interconnected via either a communication network or a physical network to achieve a task cooperatively (e.g. cooperative loading lifting, cooperative load transfer, and so on). Multi-robot manipulation has been proposed and applied extensively in transportation, assembling, and 3D printing, just to name a few. It would be of practical interest to study how the frameworks proposed in this thesis can find application in these fields, in order to deliver improved resource utilization, reduced cost time, and high adaptivity.

- **Safety-critical adaptive systems**

For many safety-critical systems like aircraft, autonomous vehicles, and fuel cell systems, the control goal requires not only a prescribed performance but also escaping from some dangerous sets. This is e.g. because when the configuration exceeds the safety region, high uncertainty will occur in the dynamics, which is beyond the controllability of the system. This thesis has partly addressed this problem in terms of handling uncertainties with a highly unstructured nature. However, proposing an adaptive control approach enabling the operation of safety-critical systems would definitely require further efforts in terms of embedding safety constraints and dangerous sets into the control design, and in terms of adapting to unexpected regimes while ensuring safety.

- **Fault tolerance in Euler-Lagrange systems**

  It is very common for a mechanical system to shift from a fully-actuated setting to an under-actuated setting due to unpredictable faults (e.g. actuator failures), leading to a different dynamic structure. Although this thesis has studied fully-actuated systems and under-actuated systems, it could be of practical interest to consider a mixed scenario where some agents are fully actuated and other agents are under-actuated (e.g. due to actuator failures). A challenging point is to define a suitable synchronization manifold that can be attained by all agents despite the faults. To compensate for the failures occurring on some agents, the controller needs to be devised with different philosophy compared to pure fully-actuated agents. The challenge is how to enable systems to adapt to the changing circumstances in case of failures.

- **System identification tackling uncertainty in dynamics**

  In this thesis, we mainly consider dynamics with either unknown parameters or unknown structures. However, it is well known that having some parametric or structural information may help in providing a better control performance. System identification is a typical approach that is able to determine the mathematical model of a system by estimating parameters or structures from input and output data. It could be of interest to embed a system identification module in the proposed framework (e.g. to identify the unknown interconnection terms), so as to study if such additional information can be used to improve performance.

BIBLIOGRAPHY

[1] A. Abazari, H. Monsef, and B. Wu, "Coordination strategies of distributed energy resources including FESS, DEG, FC and WTG in load frequency control (LFC) scheme of hybrid isolated micro-grid," *International Journal of Electrical Power & Energy Systems*, vol. 109, pp. 535 – 547, 2019.

[2] A. Abdessameud, I. G. Polushin, and A. Tayebi, "Motion coordination of thrust-propelled underactuated vehicles with intermittent and delayed communications," *Systems & Control Letters*, vol. 79, pp. 15–22, 2015.

[3] A. Abdessameud, A. Tayebi, and I. G. Polushin, "Leader-follower synchronization of Euler-Lagrange systems with time-varying leader trajectory and constrained discrete-time communication," *IEEE Transactions on Automatic Control*, vol. 62, no. 5, pp. 2539–2545, 2016.

[4] J. A. Acosta, R. Ortega, A. Astolfi, and A. D. Mahindrakar, "Interconnection and damping assignment passivity-based control of mechanical systems with underactuation degree one," *IEEE Transactions on Automatic Control*, vol. 50, no. 12, pp. 1936–1955, 2005.

[5] S. Alhalali, C. Nielsen, and R. El-Shatshat, "Mitigation of cyber-physical attacks in multi-area automatic generation control," *International Journal of Electrical Power & Energy Systems*, vol. 112, pp. 362–369, 2019.

[6] A. Ameli, A. Hooshyar, E. F. El-Saadany, and A. M. Youssef, "Attack detection and identification for automatic generation control systems," *IEEE Transactions on Power Systems*, vol. 33, no. 5, pp. 4760–4774, 2018.

[7] L. An and G. Yang, "Decentralized adaptive fuzzy secure control for nonlinear uncertain interconnected systems against intermittent DoS attacks," *IEEE Transactions on Cybernetics*, vol. 49, no. 3, pp. 827–838, 2019.

[8] S. Arimoto and M. Sekimoto, "Human-like movements of robotic arms with redundant DOFs: virtual spring-damper hypothesis to tackle the Bernstein problem," in *Proceedings 2006 IEEE International Conference on Robotics and Automation (ICRA 2006)*, 2006, pp. 1860–1866.

[9] H. Ashrafiuon and R. S. Erwin, "Sliding mode control of underactuated multibody systems and its application to shape change control," *International Journal of Control*, vol. 81, no. 12, pp. 1849–1858, 2008.

[10] P. Babahajiani, Q. Shafiee, and H. Bevrani, "Intelligent demand response contribution in frequency control of multi-area power systems," *IEEE Transactions on Smart Grid*, vol. 9, no. 2, pp. 1282–1291, 2018.

[11] S. Baldi, A. Papachristodoulou, and E. B. Kosmatopoulos, "Adaptive pulse width modulation design for power converters based on affine switched systems," *Nonlinear Analysis: Hybrid Systems*, vol. 30, pp. 306 – 322, 2018.

[12] C. P. Bechlioulis and G. A. Rovithakis, "Decentralized robust synchronization of unknown high order nonlinear multi-agent systems with prescribed transient and steady state performance," *IEEE Transactions on Automatic Control*, vol. 62, no. 1, pp. 123–134, 2016.

[13] A. M. Bloch, D. E. Chang, N. E. Leonard, and J. E. Marsden, "Controlled Lagrangians and the stabilization of mechanical systems. ii. potential shaping," *IEEE Transactions on Automatic Control*, vol. 46, no. 10, pp. 1556–1571, 2001.

[14] P. Bo, Y. Lingyu, and Y. Xiaoke, "Lpv-mrac method for aircraft with structural damage," in *2016 35th Chinese Control Conference (CCC)*, July 2016, pp. 3262–3267.

[15] J. A. Bondy, U. S. R. Murty *et al.*, *Graph Theory with Applications*. Macmillan London, 1976, vol. 290.

[16] C. Boonchuay, "Improving regulation service based on adaptive load frequency control in lmp energy market," *IEEE Transactions on Power Systems*, vol. 29, no. 2, pp. 988–989, 2014.

[17] M. S. Branicky, "Multiple Lyapunov functions and other analysis tools for switched and hybrid systems," *IEEE Transactions on Automatic Control*, vol. 43, no. 4, pp. 475–482, 1998.

[18] H. Cai and J. Huang, "The leader-following consensus for multiple uncertain Euler-Lagrange systems with an adaptive distributed observer," *IEEE Transactions on Automatic Control*, vol. 61, no. 10, pp. 3152–3157, 2015.

[19] D. N. Cardoso, S. Esteban, and G. V. Raffo, "A robust optimal control approach in the weighted Sobolev space for underactuated mechanical systems," *Automatica*, vol. 125, p. 109474, 2021.

[20] G. Chartrand, *Introductory Graph Theory*. Courier Corporation, 1977.

[21] C. Chen, K. Xie, F. L. Lewis, S. Xie, and A. Davoudi, "Fully distributed resilience for adaptive exponential synchronization of heterogeneous multi-agent systems against actuator faults," *IEEE Transactions on Automatic Control*, vol. 64, no. 8, pp. 3347–3354, 2018.

[22] M.-L. Chiang and L.-C. Fu, "Adaptive stabilization of a class of uncertain switched nonlinear systems with backstepping control," *Automatica*, vol. 50, no. 8, pp. 2128 – 2135, 2014.

[23] N. Cho, H. Shin, Y. Kim, and A. Tsourdos, "Composite model reference adaptive control with parameter convergence under finite excitation," *IEEE Transactions on Automatic Control*, vol. 63, no. 3, pp. 811–818, 2018.

[24] D. Chowdhury and H. K. Khalil, "Practical synchronization in networks of nonlinear heterogeneous agents with application to power systems," *IEEE Transactions on Automatic Control*, vol. 66, no. 1, pp. 184–198, 2020.

[25] S.-J. Chung, S. Bandyopadhyay, I. Chang, and F. Y. Hadaegh, "Phase synchronization control of complex networks of Lagrangian systems on adaptive digraphs," *Automatica*, vol. 49, no. 5, pp. 1148–1161, 2013.

[26] M. Dehghan and C.-J. Ong, "Computations of mode-dependent dwell times for discrete-time switching system," *Automatica*, vol. 49, no. 6, pp. 1804–1808, 2013.

[27] R. Dey, S. Ghosh, G. Ray, and A. Rakshit, "$\mathscr{H}\infty$ load frequency control of interconnected power systems with communication delays," *International Journal of Electrical Power & Energy Systems*, vol. 42, no. 1, pp. 672 – 684, 2012.

[28] M. di Bernardo, U. Montanaro, R. Ortega, and S. Santini, "Extended hybrid model reference adaptive control of piecewise affine systems," *Nonlinear Analysis: Hybrid Systems*, vol. 21, pp. 11 – 21, 2016.

[29] M. di Bernardo, U. Montanaro, and S. Santini, "Hybrid model reference adaptive control of piecewise affine systems," *IEEE Transactions on Automatic Control*, vol. 58, no. 2, pp. 304–316, 2013.

[30] F. Dorfler and F. Bullo, "Synchronization and transient stability in power networks and nonuniform Kuramoto oscillators," *SIAM Journal on Control and Optimization*, vol. 50, no. 3, pp. 1616–1642, 2012.

[31] S. El-Ferik, A. Qureshi, and F. L. Lewis, "Neuro-adaptive cooperative tracking control of unknown higher-order affine nonlinear systems," *Automatica*, vol. 50, no. 3, pp. 798–808, 2014.

[32] A. M. Ersdal, L. Imsland, and K. Uhlen, "Model predictive load-frequency control," *IEEE Transactions on Power Systems*, vol. 31, no. 1, pp. 777–785, 2016.

[33] L. Fan, Z. Miao, and D. Osborn, "Wind farms with hvdc delivery in load frequency control," *IEEE Transactions on Power Systems*, vol. 24, no. 4, pp. 1894–1895, 2009.

[34] Y. Fang, B. Ma, P. Wang, and X. Zhang, "A motion planning-based adaptive control method for an underactuated crane system," *IEEE Transactions on Control Systems Technology*, vol. 20, no. 1, pp. 241–248, 2011.

[35] M. Franceschelli and P. Frasca, "Stability of open multi-agent systems and applications to dynamic consensus," *IEEE Transactions on Automatic Control*, pp. 1–1, 2020.

[36] S. Ghosh, K. A. Folly, and A. Patel, "Synchronized versus non-synchronized feedback for speed-based wide-area PSS: Effect of time-delay," *IEEE Transactions on Smart Grid*, vol. 9, no. 5, pp. 3976–3985, 2018.

[37] J. Giraldo, E. Mojica-Nava, and N. Quijano, "Synchronisation of heterogeneous kuramoto oscillators with sampled information and a constant leader," *International Journal of Control*, vol. 92, no. 11, pp. 2591–2607, 2019.

[38] M. Gnucci and R. Marino, "Adaptive tracking control for underactuated mechanical systems with relative degree two," *Automatica*, vol. 129, p. 109633, 2021.

[39] J. J. Grainger and W. D. Stevenson, *Power System Analysis*. McGraw-Hill, 1994.

[40] J. W. Grizzle, G. Abba, and F. Plestan, "Asymptotically stable walking for biped robots: Analysis via systems with impulse effects," *IEEE Transactions on Automatic Control*, vol. 46, no. 1, pp. 51–64, 2001.

[41] B. C. Gruenwald, E. Arabi, T. Yucelen, A. Chakravarthy, and D. McNeely, "Decentralised adaptive architectures for control of large-scale active–passive modular systems with stability and performance guarantees," *International Journal of Control*, vol. 93, no. 3, pp. 490–504, 2020.

[42] J. Guo, I. Zenelis, X. Wang, and B.-T. Ooi, "Wams-based model-free wide-area damping control by voltage source converters," *IEEE Transactions on Power Systems*, vol. 36, no. 2, pp. 1317–1327, 2021.

[43] Y. Han, H. Li, P. Shen, E. A. A. Coelho, and J. M. Guerrero, "Review of active and reactive power sharing strategies in hierarchical controlled microgrids," *IEEE Transactions on Power Electronics*, vol. 32, no. 3, pp. 2427–2451, 2017.

[44] S. Hanwate, Y. V. Hote, and S. Saxena, "Adaptive policy for load frequency control," *IEEE Transactions on Power Systems*, vol. 33, no. 1, pp. 1142–1144, 2018.

[45] J. P. Hespanha, P. Naghshtabrizi, and Y. Xu, "A survey of recent results in networked control systems," *Proceedings of the IEEE*, vol. 95, no. 1, pp. 138–162, 2007.

[46] J. P. Hespanha, "Uniform stability of switched linear systems: Extensions of Lasalle's invariance principle," *IEEE Transactions on Automatic Control*, vol. 49, no. 4, pp. 470–482, 2004.

[47] J. P. Hespanha and A. S. Morse, "Stability of switched systems with average dwell-time," in *Proceedings of the 38th IEEE Conference on Decision and Control*, vol. 3. IEEE, 1999, pp. 2655–2660.

[48] S. A. Hosseini, M. Toulabi, A. S. Dobakhshari, A. Ashouri-Zadeh, and A. M. Ranjbar, "Delay compensation of demand response and adaptive disturbance rejection applied to power system frequency control," *IEEE Transactions on Power Systems*, vol. 35, no. 3, pp. 2037–2046, 2020.

[49] G. Hu, C. Makkar, and W. E. Dixon, "Energy-based nonlinear control of underactuated Euler–Lagrange systems subject to impacts," *IEEE Transactions on Automatic Control*, vol. 52, no. 9, pp. 1742–1748, 2007.

[50] J. Huang, S. Ri, T. Fukuda, and Y. Wang, "A disturbance observer based sliding mode control for a class of underactuated robotic system with mismatched uncertainties," *IEEE Transactions on Automatic Control*, vol. 64, no. 6, pp. 2480–2487, 2018.

[51] J. Huang, W. Wang, C. Wen, J. Zhou, and G. Li, "Distributed adaptive leader–follower and leaderless consensus control of a class of strict-feedback nonlinear systems: a unified approach," *Automatica*, vol. 118, p. 109021, 2020.

[52] P. A. Ioannou and J. Sun, *Robust Adaptive Control*. Courier Corporation, 2012.

[53] X. Jin, W. M. Haddad, and T. Yucelen, "An adaptive control architecture for mitigating sensor and actuator attacks in cyber-physical systems," *IEEE Transactions on Automatic Control*, vol. 62, no. 11, pp. 6058–6064, 2017.

[54] S. Kersting and M. Buss, "Direct and indirect model reference adaptive control for multivariable piecewise affine systems," *IEEE Transactions on Automatic Control*, vol. 62, no. 11, pp. 5634–5649, 2017.

[55] H. K. Khalil, *Nonlinear Systems, third edition*. Prentice Hall, 2002.

[56] H. Kimura, Y. Fukuoka, and A. H. Cohen, "Biologically inspired adaptive walking of a quadruped robot," *Philosophical Transactions of the Royal Society A: Mathematical, Physical and Engineering Sciences*, vol. 365, no. 1850, pp. 153–170, 2007.

[57] O. Kolesnichenko and A. S. Shiriaev, "Partial stabilization of underactuated Euler–Lagrange systems via a class of feedback transformations," *Systems & Control Letters*, vol. 45, no. 2, pp. 121–132, 2002.

[58] C. D. Korkas, S. Baldi, I. Michailidis, and E. B. Kosmatopoulos, "Occupancy-based demand response and thermal comfort optimization in microgrids with renewable energy sources and energy storage," *Applied Energy*, vol. 163, pp. 93 – 104, 2016.

[59] J. Lee, C. Lee, N. Tsagarakis, and S. Oh, "Residual-based external torque estimation in series elastic actuators over a wide stiffness range: Frequency domain approach," *IEEE Robotics and Automation Letters*, vol. 3, no. 3, pp. 1442–1449, 2018.

[60] F. L. Lewis, D. Dawson, and C. T. Abdallah, *Control of Robot Manipulators*. Prentice Hall PTR, 1993.

[61] C. Li, Y. Wu, Y. Sun, H. Zhang, Y. Liu, Y. Liu, and V. Terzija, "Continuous underfrequency load shedding scheme for power system adaptive frequency control," *IEEE Transactions on Power Systems*, vol. 35, no. 2, pp. 950–961, 2020.

[62] H. Li, A. Dimitrovski, J. B. Song, Z. Han, and L. Qian, "Communication infrastructure design in cyber physical systems with applications in smart grids: A hybrid system framework," *IEEE Communications Surveys Tutorials*, vol. 16, no. 3, pp. 1689–1708, 2014.

[63] P. Li, D. Liu, and S. Baldi, "Adaptive integral sliding mode control in the presence of state-dependent uncertainty," *IEEE/ASME Transactions on Mechatronics*, pp. 1–11, 2022.

[64] Z. Li, Z. Duan, and F. L. Lewis, "Distributed robust consensus control of multi-agent systems with heterogeneous matching uncertainties," *Automatica*, vol. 50, no. 3, pp. 883–889, 2014.

[65] D. Liberzon, *Switching in Systems and Control*. Springer Science & Business Media, 2003.

[66] H. Lin and P. J. Antsaklis, "Stability and stabilizability of switched linear systems: A short survey of recent results," in *Proceedings of the 2005 IEEE International Symposium on, Mediterrean Conference on Control and Automation Intelligent Control, 2005.* IEEE, 2005, pp. 24–29.

[67] D. Liu, S. Baldi, W. Yu, and G. Chen, "On distributed implementation of switch-based adaptive dynamic programming," *IEEE Transactions on Cybernetics*, pp. 1–7, 2020.

[68] T. Liu, D. J. Hill, and C. Zhang, "Non-disruptive load-side control for frequency regulation in power systems," *IEEE Transactions on Smart Grid*, vol. 7, no. 4, pp. 2142–2153, 2016.

[69] B. Lu and Y. Fang, "Gain-adapting coupling control for a class of underactuated mechanical systems," *Automatica*, vol. 125, p. 109461, 2021.

[70] B. Lu, Y. Fang, and N. Sun, "Continuous sliding mode control strategy for a class of nonlinear underactuated systems," *IEEE Transactions on Automatic Control*, vol. 63, no. 10, pp. 3471–3478, 2018.

[71] B. Lu, Y. Fang, N. Sun, and X. Wang, "Antiswing control of offshore boom cranes with ship roll disturbances," *IEEE Transactions on Control Systems Technology*, vol. 26, no. 2, pp. 740–747, 2017.

[72] M. Lu and L. Liu, "Leader–following consensus of multiple uncertain Euler-Lagrange systems with unknown dynamic leader," *IEEE Transactions on Automatic Control*, vol. 64, no. 10, pp. 4167–4173, 2019.

[73] M. Lu, L. Liu, and G. Feng, "Adaptive tracking control of uncertain Euler-Lagrange systems subject to external disturbances," *Automatica*, vol. 104, pp. 207–219, 2019.

[74] R. Ma and J. Zhao, "Backstepping design for global stabilization of switched nonlinear systems in lower triangular form under arbitrary switchings," *Automatica*, vol. 46, no. 11, pp. 1819–1823, 2010.

[75] M. S. Mahmoud, M. M. Hamdan, and U. A. Baroudi, "Modeling and control of cyber-physical systems subject to cyber attacks: A survey of recent advances and challenges," *Neurocomputing*, vol. 338, pp. 101 – 115, 2019.

[76] C. Makkar, G. Hu, W. G. Sawyer, and W. E. Dixon, "Lyapunov-based tracking control in the presence of uncertain nonlinear parameterizable friction," *IEEE Transactions on Automatic Control*, vol. 52, no. 10, pp. 1988–1994, 2007.

[77] E. Mallada, C. Zhao, and S. Low, "Optimal load-side control for frequency regulation in smart grids," *IEEE Transactions on Automatic Control*, vol. 62, no. 12, pp. 6294–6309, 2017.

[78] J. Mei, W. Ren, and G. Ma, "Distributed coordinated tracking with a dynamic leader for multiple Euler-Lagrange systems," *IEEE Transactions on Automatic Control*, vol. 56, no. 6, pp. 1415–1421, 2011.

[79] Z. Meng, W. Ren, and Z. You, "Distributed finite-time attitude containment control for multiple rigid bodies," *Automatica*, vol. 46, no. 12, pp. 2092–2099, 2010.

[80] H. Modares, F. L. Lewis, W. Kang, and A. Davoudi, "Optimal synchronization of heterogeneous nonlinear systems with unknown dynamics," *IEEE Transactions on Automatic Control*, vol. 63, no. 1, pp. 117–131, 2017.

[81] A. Moeini, I. Kamwa, P. Brunelle, and G. Sybille, "Open data IEEE test systems implemented in SimPowerSystems for education and research in power grid dynamics and control," in *2015 50th International Universities Power Engineering Conference (UPEC)*, 2015, pp. 1–6.

[82] J. M. Montenbruck, M. Bürger, and F. Allgöwer, "Practical synchronization with diffusive couplings," *Automatica*, vol. 53, pp. 235–243, 2015.

[83] N. T. Nguyen, "Optimal control modification for robust adaptive control with large adaptive gain," *Systems & Control Letters*, vol. 61, no. 4, pp. 485 – 494, 2012.

[84] B. Niu, P. Zhao, J.-D. Liu, H.-J. Ma, and Y.-J. Liu, "Global adaptive control of switched uncertain nonlinear systems: An improved MDADT method," *Automatica*, vol. 115, p. 108872, 2020.

[85] R. Olfati-Saber, "Normal forms for underactuated mechanical systems with symmetry," *IEEE Transactions on Automatic Control*, vol. 47, no. 2, pp. 305–308, 2002.

[86] R. Ortega, A. Loria, P. J. Nicklasson, and H. Sira-Ramirez, *Passivity-based Control of Euler-Lagrange Systems*. Springer, 2008.

[87] R. Ortega, J. A. L. Perez, P. J. Nicklasson, and H. J. Sira-Ramirez, *Passivity-based Control of Euler-Lagrange systems: Mechanical, Electrical and Electromechanical Applications*. Springer Science & Business Media, 2013.

[88] R. Ortega, M. W. Spong, F. Gómez-Estern, and G. Blankenstein, "Stabilization of a class of underactuated mechanical systems via interconnection and damping assignment," *IEEE Transactions on Automatic Control*, vol. 47, no. 8, pp. 1218–1233, 2002.

[89] R. Ortega, A. van der Schaft, B. Maschke, and G. Escobar, "Interconnection and damping assignment passivity-based control of port-controlled Hamiltonian systems," *Automatica*, vol. 38, no. 4, pp. 585–596, 2002.

[90] C. Pan and C. Liaw, "An adaptive controller for power system load-frequency control," *IEEE Transactions on Power Systems*, vol. 4, no. 1, pp. 122–128, 1989.

[91] B. S. Park, J.-W. Kwon, and H. Kim, "Neural network-based output feedback control for reference tracking of underactuated surface vessels," *Automatica*, vol. 77, pp. 353–359, 2017.

[92] C. Peng, J. Li, and M. Fei, "Resilient event-triggering H_∞ load frequency control for multi-area power systems with energy-limited DoS attacks," *IEEE Transactions on Power Systems*, vol. 32, no. 5, pp. 4110–4118, 2017.

[93] M. Pirani, S. Baldi, and K. H. Johansson, "Impact of network topology on the resilience of vehicle platoons," *IEEE Transactions on Intelligent Transportation Systems*, pp. 1–12, 2022.

[94] F. Plestan, Y. Shtessel, V. Bregeault, and A. Poznyak, "New methodologies for adaptive sliding mode control," *International Journal of Control*, vol. 83, no. 9, pp. 1907–1919, 2010.

[95] B. Polajžer, M. Petrun, and J. Ritonja, "Adaptation of load-frequency-control target values based on the covariances between area-control errors," *IEEE Transactions on Power Systems*, vol. 33, no. 6, pp. 5865–5874, 2018.

[96] V. Pradhan, A. M. Kulkarni, and S. A. Khaparde, "A model-free approach for emergency damping control using wide area measurements," *IEEE Transactions on Power Systems*, vol. 33, no. 5, pp. 4902–4912, 2018.

[97] A. M. Prostejovsky, M. Marinelli, M. Rezkalla, M. H. Syed, and E. Guillo-Sansano, "Tuningless load frequency control through active engagement of distributed resources," *IEEE Transactions on Power Systems*, vol. 33, no. 3, pp. 2929–2939, 2018.

[98] C. Rohrs, L. Valavani, M. Athans, and G. Stein, "Robustness of continuous-time adaptive control algorithms in the presence of unmodeled dynamics," *IEEE Transactions on Automatic Control*, vol. 30, no. 9, pp. 881–889, 1985.

[99] J. G. Romero, A. Donaire, R. Ortega, and P. Borja, "Global stabilisation of underactuated mechanical systems via PID passivity-based control," *Automatica*, vol. 96, pp. 178–185, 2018.

[100] S. Roy and S. Baldi, "A simultaneous adaptation law for a class of nonlinearly parametrized switched systems," *IEEE Control Systems Letters*, vol. 3, no. 3, pp. 487–492, 2019.

[101] S. B. Roy, S. Bhasin, and I. N. Kar, "Combined MRAC for unknown MIMO LTI systems with parameter convergence," *IEEE Transactions on Automatic Control*, vol. 63, no. 1, pp. 283–290, 2018.

[102] S. Roy and S. Baldi, "The role of uncertainty in adaptive control of switched Euler-Lagrange systems," in *2019 IEEE 58th Conference on Decision and Control (CDC)*. IEEE, 2019, pp. 72–77.

[103] S. Roy and S. Baldi, "Towards structure-independent stabilization for uncertain underactuated Euler-Lagrange systems," *Automatica*, vol. 113, p. 108775, 2020.

[104] S. Roy, S. Baldi, and L. M. Fridman, "On adaptive sliding mode control without a priori bounded uncertainty," *Automatica*, vol. 111, p. 108650, 2020.

[105] S. Roy, S. Baldi, and P. A. Ioannou, "An adaptive control framework for underactuated switched euler-lagrange systems," *IEEE Transactions on Automatic Control*, pp. 1–1, 2021.

[106] S. Roy, S. B. Roy, J. Lee, and S. Baldi, "Overcoming the underestimation and overestimation problems in adaptive sliding mode control," *IEEE/ASME Transactions on Mechatronics*, vol. 24, no. 5, pp. 2031–2039, 2019.

[107] S. Russ, "A translation of Bolzano's paper on the intermediate value theorem," *Historia Mathematica*, vol. 7, no. 2, pp. 156–185, 1980.

[108] Q. Sang and G. Tao, "Adaptive control of piecewise linear systems with applications to NASA GTM," in *Proceedings of the 2011 American Control Conference*, June 2011, pp. 1157–1162.

[109] Q. Sang and G. Tao, "Adaptive control of piecewise linear systems: the state tracking case," *IEEE Transactions on Automatic Control*, vol. 57, no. 2, pp. 522–528, Feb 2012.

[110] Q. Sang, G. Tao, and J. Guo, "Multivariable state feedback for output tracking MRAC for piecewise linear systems with relaxed design conditions," in *2014 American Control Conference*, June 2014, pp. 703–708.

[111] J. Sarangapani, *Neural Network Control of Nonlinear Discrete-time Systems*. CRC press, 2018.

[112] A. Sargolzaei, K. K. Yen, and M. N. Abdelghani, "Preventing time-delay switch attack on load frequency control in distributed power systems," *IEEE Transactions on Smart Grid*, vol. 7, no. 2, pp. 1176–1185, 2016.

[113] S. Saxena and Y. V. Hote, "Load frequency control in power systems via internal model control scheme and model-order reduction," *IEEE Transactions on Power Systems*, vol. 28, no. 3, pp. 2749–2757, 2013.

[114] J. Schiffer, F. Dorfler, and E. Fridman, "Robustness of distributed averaging control in power systems: Time delays & dynamic communication topology," *Automatica*, vol. 80, pp. 261 – 271, 2017.

[115] X. Shang-Guan, Y. He, C. Zhang, L. Jiang, J. W. Spencer, and M. Wu, "Sampled-data based discrete and fast load frequency control for power systems with wind power," *Applied Energy*, vol. 259, p. 114202, 2020.

[116] N. Sharma, S. Bhasin, Q. Wang, and W. E. Dixon, "Predictor-based control for an uncertain Euler-Lagrange system with input delay," *Automatica*, vol. 47, no. 11, pp. 2332–2342, 2011.

[117] A. Shkolnik and R. Tedrake, "High-dimensional underactuated motion planning via task space control," in *2008 IEEE/RSJ International Conference on Intelligent Robots and Systems*. IEEE, 2008, pp. 3762–3768.

[118] Y. Shtessel, M. Taleb, and F. Plestan, "A novel adaptive-gain supertwisting sliding mode controller: Methodology and application," *Automatica*, vol. 48, no. 5, pp. 759–769, 2012.

[119] J. W. Simpson-Porco, F. Dörfler, and F. Bullo, "Synchronization and power sharing for droop-controlled inverters in islanded microgrids," *Automatica*, vol. 49, no. 9, pp. 2603–2611, 2013.

[120] J. W. Simpson-Porco, F. Dorfler, and F. Bullo, "Synchronization and power sharing for droop-controlled inverters in islanded microgrids," *Automatica*, vol. 49, no. 9, pp. 2603 – 2611, 2013.

[121] B. Sonker, D. Kumar, and P. Samuel, "Dual loop IMC structure for load frequency control issue of multi-area multi-sources power systems," *International Journal of Electrical Power & Energy Systems*, vol. 112, pp. 476 – 494, 2019.

[122] S. Sönmez and S. Ayasun, "Stability region in the parameter space of pi controller for a single-area load frequency control system with time delay," *IEEE Transactions on Power Systems*, vol. 31, no. 1, pp. 829–830, 2015.

[123] M. W. Spong, "Partial feedback linearization of underactuated mechanical systems," in *Proceedings of IEEE/RSJ International Conference on Intelligent Robots and Systems (IROS'94)*. IEEE, 1994, pp. 314–321.

[124] M. W. Spong, "Underactuated Mechanical Systems," in *Control Problems in Robotics and Automation*. Springer, 1998, pp. 135–150.

[125] M. W. Spong, S. Hutchinson, and M. Vidyasagar, *Robot modeling and control*. John Wiley & Sons, 2020.

[126] N. Sun, Y. Fang, and X. Zhang, "Energy coupling output feedback control of 4-DOF underactuated cranes with saturated inputs," *Automatica*, vol. 49, no. 5, pp. 1318–1325, 2013.

[127] X.-M. Sun, J. Zhao, and D. J. Hill, "Stability and L2-gain analysis for switched delay systems: A delay-dependent method," *Automatica*, vol. 42, no. 10, pp. 1769–1774, 2006.

[128] Y. Sun, J. Zhao, and G. M. Dimirovski, "Adaptive control for a class of state-constrained high-order switched nonlinear systems with unstable subsystems," *Nonlinear Analysis: Hybrid Systems*, vol. 32, pp. 91 – 105, 2019.

[129] Y. Tang, M. Tomizuka, G. Guerrero, and G. Montemayor, "Decentralized robust control of mechanical systems," *IEEE Transactions on Automatic control*, vol. 45, no. 4, pp. 771–776, 2000.

[130] G. Tao, *Adaptive Control Design and Analysis*. John Wiley & Sons, 2003, vol. 37.

[131] G. Tao, "Multivariable adaptive control: A survey," *Automatica*, vol. 50, no. 11, pp. 2737–2764, 2014.

[132] T. Tao, S. Roy, and S. Baldi, "The issue of transients in leakage-based model reference adaptive control of switched linear systems," *Nonlinear Analysis: Hybrid Systems*, vol. 36, p. 100885, 2020.

[133] T. Tao, S. Roy, and S. Baldi, "Stable adaptation in multi-area load frequency control under dynamically-changing topologies," *IEEE Transactions on Power Systems*, vol. 36, no. 4, pp. 2946–2956, 2021.

[134] T. Tao, S. Roy, B. De Schutter, and S. Baldi, "Adaptive synchronization of uncertain underactuated euler-lagrange agents," manuscript submitted.

[135] T. Tao, S. Roy, B. De Schutter, and S. Baldi, "Distributed adaptive synchronization in euler lagrange networks with uncertain interconnections," *IEEE Transactions on Automatic Control*, contionally accepted.

[136] S. Tong and Y. Li, "Adaptive fuzzy output feedback control for switched nonlinear systems with unmodeled dynamics," *IEEE transactions on cybernetics*, vol. 47, no. 2, pp. 295–305, 2016.

[137] S. Trip and C. De Persis, "Distributed optimal load frequency control with non-passive dynamics," *IEEE Transactions on Control of Network Systems*, vol. 5, no. 3, pp. 1232–1244, 2018.

[138] V. Utkin, J. Guldner, and J. Shi, *Sliding Mode Control in Electromechanical Systems*. CRC Press, 2009.

[139] F. Valentinis, A. Donaire, and T. Perez, "Energy-based guidance of an underactuated unmanned underwater vehicle on a helical trajectory," *Control Engineering Practice*, vol. 44, pp. 138–156, 2015.

[140] K. Vrdoljak, N. Perić, and I. Petrović, "Sliding mode based load-frequency control in power systems," *Electric Power Systems Research*, vol. 80, no. 5, pp. 514 – 527, 2010.

[141] L. Vu and D. Liberzon, "Supervisory control of uncertain linear time-varying systems," *IEEE Transactions on Automatic Control*, vol. 56, no. 1, pp. 27–42, 2011.

[142] L. Vu, D. Chatterjee, and D. Liberzon, "Input-to-state stability of switched systems and switching adaptive control," *Automatica*, vol. 43, no. 4, pp. 639–646, 2007.

[143] B. Wang, Y. Lv, J. Jian, and X. Jiang, "New results on the trade-off performance of lti system with colored noise and encoder-decoder strategy," *Journal of the Franklin Institute*, vol. 356, no. 16, pp. 8971–8995, 2019.

[144] S. Wang, H. Zhang, S. Baldi, and R. Zhong, "Leaderless consensus of heterogeneous multiple euler-lagrange systems with unknown disturbance," *IEEE Transactions on Automatic Control*, pp. 1–1, 2022.

[145] X. Wang, Y. Wang, and Y. Liu, "Dynamic load frequency control for high-penetration wind power considering wind turbine fatigue load," *International Journal of Electrical Power & Energy Systems*, vol. 117, p. 105696, 2020.

[146] Y. Wang, L. Yang, J. Zhang, and G. Shen, "An observer based multivariable adaptive reconfigurable control method for the wing damaged aircraft," in *11th IEEE International Conference on Control Automation (ICCA)*, June 2014, pp. 95–100.

[147] Z. Wang, H. An, and X. Luo, "Switch detection and robust parameter estimation for slowly switched Hammerstein systems," *Nonlinear Analysis: Hybrid Systems*, vol. 32, pp. 202 – 213, 2019.

[148] J.-L. Wu, "Stabilizing controllers design for switched nonlinear systems in strict-feedback form," *Automatica*, vol. 45, no. 4, pp. 1092–1096, 2009.

[149] Y. Wu, Z. Wei, J. Weng, X. Li, and R. H. Deng, "Resonance attacks on load frequency control of smart grids," *IEEE Transactions on Smart Grid*, vol. 9, no. 5, pp. 4490–4502, 2018.

[150] W. Xiang, J. Lam, and J. Shen, "Stability analysis and l1-gain characterization for switched positive systems under dwell-time constraint," *Automatica*, vol. 85, pp. 1 – 8, 2017.

[151] R. Xu and Ü. Özgüner, "Sliding mode control of a class of underactuated systems," *Automatica*, vol. 44, no. 1, pp. 233–241, 2008.

[152] S. Xu and T. Chen, "H∞ output feedback control for uncertain stochastic systems with time-varying delays," *Automatica*, vol. 40, no. 12, pp. 2091–2098, 2004.

[153] H. A. Yousef, K. AL-Kharusi, M. H. Albadi, and N. Hosseinzadeh, "Load frequency control of a multi-area power system: An adaptive fuzzy logic approach," *IEEE Transactions on Power Systems*, vol. 29, no. 4, pp. 1822–1830, 2014.

[154] S. Yuan, B. De Schutter, and S. Baldi, "On robust adaptive control of switched linear systems," in *2017 13th IEEE International Conference on Control Automation (ICCA)*, July 2017, pp. 753–758.

[155] S. Yuan, L. Li, B. Cai, and L. Zhang, "Differential Riccati equation-based adaptive stabilization for switched linear systems," *International Journal of Robust and Nonlinear Control*, vol. 30, no. 1, pp. 51–64, 2020.

[156] S. Yuan, L. Zhang, O. Holub, and S. Baldi, "Switched adaptive control of air handling units with discrete and saturated actuators," *IEEE Control Systems Letters*, vol. 2, no. 3, pp. 417–422, July 2018.

[157] S. Yuan, B. De Schutter, and S. Baldi, "Adaptive asymptotic tracking control of uncertain time-driven switched linear systems," *IEEE Transactions on Automatic Control*, vol. 62, no. 11, pp. 5802–5807, 2016.

[158] S. Yuan, B. D. Schutter, and S. Baldi, "Robust adaptive tracking control of uncertain slowly switched linear systems," *Nonlinear Analysis: Hybrid Systems*, vol. 27, pp. 1–12, 2018.

[159] C. Zhang, T. Liu, and D. J. Hill, "Switched distributed load-side frequency control of power systems," *International Journal of Electrical Power & Energy Systems*, vol. 105, pp. 709 – 716, 2019.

[160] H. Zhang and F. L. Lewis, "Adaptive cooperative tracking control of higher-order nonlinear systems with unknown dynamics," *Automatica*, vol. 48, no. 7, pp. 1432–1439, 2012.

[161] J.-X. Zhang and G.-H. Yang, "Fault-tolerant output-constrained control of unknown Euler-Lagrange systems with prescribed tracking accuracy," *Automatica*, vol. 111, p. 108606, 2020.

[162] J. Zhang, X. Zhao, and J. Huang, "Synchronization control of neural networks with state-dependent coefficient matrices," *IEEE Transactions on Neural Networks and Learning Systems*, vol. 27, no. 11, pp. 2440–2447, 2016.

[163] L. Zhang, H. Gao, and O. Kaynak, "Network-induced constraints in networked control systems - a survey," *IEEE Transactions on Industrial Informatics*, vol. 9, no. 1, pp. 403–416, 2013.

[164] L. Zhang and W. Xiang, "Mode-identifying time estimation and switching-delay tolerant control for switched systems: An elementary time unit approach," *Automatica*, vol. 64, pp. 174 – 181, 2016.

[165] C. Zhao, U. Topcu, N. Li, and S. Low, "Design and stability of load-side primary frequency control in power systems," *IEEE Transactions on Automatic Control*, vol. 59, no. 5, pp. 1177–1189, 2014.

[166] J. Zhao, D. J. Hill, and T. Liu, "Synchronization of complex dynamical networks with switching topology: A switched system point of view," *Automatica*, vol. 45, no. 11, pp. 2502–2511, 2009.

[167] X. Zhao, L. Zhang, P. Shi, and M. Liu, "Stability and stabilization of switched linear systems with mode-dependent average dwell time," *IEEE Transactions on Automatic Control*, vol. 57, no. 7, pp. 1809–1815, July 2012.

[168] X. Zhao, P. Shi, X. Zheng, and L. Zhang, "Adaptive tracking control for switched stochastic nonlinear systems with unknown actuator dead-zone," *Automatica*, vol. 60, pp. 193–200, 2015.

[169] X. Zhao, S. Yin, H. Li, and B. Niu, "Switching stabilization for a class of slowly switched systems," *IEEE Transactions on Automatic Control*, vol. 60, no. 1, pp. 221–226, 2014.

[170] X. Zhao-xia, Z. Mingke, H. Yu, J. M. Guerrero, and J. C. Vasquez, "Coordinated primary and secondary frequency support between microgrid and weak grid," *IEEE Transactions on Sustainable Energy*, vol. 10, no. 4, pp. 1718–1730, 2019.

[171] L. Zhu, Z. Chen, and R. H. Middleton, "A general framework for robust output synchronization of heterogeneous nonlinear networked systems," *IEEE Transactions on Automatic Control*, vol. 61, no. 8, pp. 2092–2107, 2015.

[172] L. Zhu and D. J. Hill, "Synchronization of Kuramoto oscillators: A regional stability framework," *IEEE Transactions on Automatic Control*, vol. 65, no. 12, pp. 5070–5082, 2020.

SUMMARY

This thesis deals with adaptive control of interconnected systems and multi-agent systems, where adaptive control is used to deal with the presence of uncertainties. Generally, two types of uncertainties can occur. The first one is parametric uncertainty, which is most commonly addressed in the literature, and for which several design approaches for adaptive laws have been proposed. The second type of uncertainty is state-dependent uncertainty, which typically arises from the lack of structural knowledge about the dynamics of the system (a typical example being the presence of unmodelled dynamics). Guaranteeing stable adaptation in this scenario poses a big challenge since this type of uncertainty cannot be bounded a priori.

To start with, this thesis considers centralized control of linear uncertain interconnected dynamics with switching topologies. The literature has proven that leakage-based robust adaptive control is a valuable method to deal with this problem. However, attaining good transient behavior in leakage-based robust adaptive control is intrinsically challenging. In fact, because the gains of the inactive subsystems must exponentially vanish during inactive times as an effect of leakage actions, new learning transients will repeatedly arise at each switching instant. In order to mitigate these transients and to improve the performance of the system, a new leakage-based mechanism is proposed for robust adaptive control of uncertain switched systems: the key innovation of the proposed mechanism is that the adaptive gains of the inactive subsystems can be kept constant to their switched-off values, thus preventing vanishing gains.

Subsequently, a similar setting as above is considered, but for nonlinear Kuramoto-like dynamics. This scenario is motivated by a multi-area load frequency control (LFC) application in power grids. Multi-area LFC selects and controls a few generators in each area of the power system in an effort to dampen inter-area frequency oscillations. To effectively dampen such oscillations, it is required to enhance and lower the control activity dynamically during operation, so as to adapt to changing circumstances. Changing circumstances do not only include parametric uncertainties and unmodelled dynamics (e.g. aggregated area dynamics and bus dynamics), but also the topology reconfiguration mechanisms of modern power systems. As formal stability guarantees for the adaptive multi-area LFC concept are still lacking, we propose a framework in which adaptation and switching are combined in a provably stable way to handle parametric uncertainty, unmodeled dynamics, and dynamical interconnections of the power system.

Then, we turn our attention to distributed systems, while keeping the interest in nonlinear dynamics. We propose a new distributed synchronization protocol for multiple Euler-Lagrange systems without structural linear-in-the-parameters (LIP) knowledge of the uncertainty and where interconnection among neighboring agents is modelled by unknown state-dependent terms that intrinsically exist the dynamics, instead of just being a result of control protocol. This setting is meant to overcome two standard a priori

assumptions in the literature concerning uncertainty with a LIP structure and the absence of the interconnection terms intrinsically in the dynamics.

Finally, as the systems considered above are fully-actuated, we study distributed adaptive synchronization of uncertain underactuated Euler-Lagrange agents. We propose a distributed controller that can handle both state-dependent uncertain system dynamics terms and state-dependent uncertain interconnection terms among neighboring agents. By a suitable analysis of the non-actuated and actuated synchronization errors, respectively, stable non-actuated and actuated error dynamics perturbed by state-dependent uncertainty are obtained. In order to estimate and compensate for these synchronization errors, the leakage term of adaptive law is designed to be dependent on non-actuated and actuated errors, resulting in a more concise uniform ultimate boundedness condition compared with the standard leakage term.

In summary, this thesis has addressed the adaptive synchronization of multi-agent systems in the presence of uncertainties, such as switching topologies, unknown parameters, and state-dependent unmodeled dynamics.

SAMENVATTING

Dit proefschrift gaat over adaptieve besturing van onderling verbonden en multi-agent systemen, waarbij adaptieve besturing wordt gebruikt om met onzekerheden om te gaan. In het algemeen kunnen twee soorten onzekerheden optreden: *parametrische onzekerheid*, die in de literatuur het meest aan de orde komt en waarvoor verschillende adaptieve ontwerpen zijn voorgesteld; *toestandsafhankelijke onzekerheid*, die voortkomt uit het gebrek aan structurele kennis over de dynamiek van het systeem. Het garanderen van stabiele adaptatie in het laatste scenario vormt een grote uitdaging, aangezien dit soort onzekerheid niet a priori kan worden begrensd.

Om te beginnen beschouwt dit proefschrift gecentraliseerde controle van lineaire onzekere onderling verbonden dynamica met schakeltopologieën. De literatuur heeft bewezen dat op lekkage gebaseerde adaptieve controle een waardevolle methode is om dit probleem aan te pakken. Het bereiken van goed voorbijgaand gedrag in op lekkage gebaseerde adaptieve controle is echter intrinsiek een uitdaging. In feite, omdat de winsten van de inactieve controllers exponentieel verdwijnen tijdens inactieve tijden als een effect van lekkage, zodat nieuwe leertransiënten herhaaldelijk zullen optreden op elk schakelmoment. Om deze transiënten te verminderen en de prestaties te verbeteren, wordt een nieuw op lekkage gebaseerd mechanisme voorgesteld: de belangrijkste innovatie is dat de adaptieve winsten van de inactieve controllers constant kunnen worden gehouden tijdens hun inactieve intervallen, waardoor verdwijnende winsten worden voorkomen.

Vervolgens wordt een vergelijkbare instelling als hierboven overwogen voor niet-lineaire Kuramoto-achtige dynamiek. Dit scenario wordt gemotiveerd door een multi-area load frequency control (LFC) in elektriciteitsnetten. In multi-area LFC worden een paar generatoren in elk gebied van het voedingssysteem geselecteerd om frequentieoscillaties tussen gebieden te dempen. Om dergelijke oscillaties effectief te dempen, is het nodig om de regelactiviteit dynamisch te verbeteren en te verlagen om zich aan te passen aan parametrische onzekerheden, niet-gemodelleerde dynamiek (bijv. Geaggregeerde gebiedsdynamiek en busdynamiek) en de topologie-herconfiguratiemechanismen van moderne energiesystemen. We stellen een raamwerk voor waarin aanpassen en schakelen op een stabiele manier worden gecombineerd.

Vervolgens richten we onze aandacht op gedistribueerde systemen, terwijl we de interesse in niet-lineaire dynamiek behouden. We stellen een nieuw gedistribueerd synchronisatieprotocol voor voor meerdere Euler-Lagrange systemen zonder structurele lineaire-in-de-parameters (LIP) kennis van de onzekerheid met onbekende toestandsafhankelijke interconnectie tussen naburige agenten (niet alleen een resultaat van het controleprotocol). Deze instelling overwint twee standaardaannames in de literatuur met betrekking tot onzekerheid met de LIP-structuur en de intrinsieke afwezigheid van de interconnectietermen in de dynamiek.

Ten slotte bestuderen we, aangezien de hierboven beschouwde systemen volledig geactiveerd zijn, gedistribueerde synchronisatie van onzekere, onvoldoende geactiveerde Euler-Lagrange-agenten. We stellen een gedistribueerde controller voor die zowel toestandsafhankelijke onzekere systeemdynamiek als toestandsafhankelijke onzekere interconnectie tussen naburige agenten aankan. We bieden een geschikte analyse van de niet-aangedreven en geactiveerde synchronisatiefouten, verstoord door geparametriseerde toestandsafhankelijke onzekerheid. Om deze onzekerheid te compenseren, zijn nieuwe op lekkage gebaseerde adaptieve wetten ontworpen, die een beknoptere uniforme ultieme begrensdheidsvoorwaarde geven in vergelijking met standaard op lekkage gebaseerde wetten.

Samenvattend heeft dit proefschrift de adaptieve synchronisatie van multi-agent systemen behandeld in aanwezigheid van onzekerheden, zoals schakeltopologieën, onbekende parameters, toestandsafhankelijke ongemodelleerde dynamiek.

LIST OF PUBLICATIONS

Journals:

1. **T Tao**, S Roy, B. De Schutter, S. Baldi, "Adaptive synchronization of uncertain under-actuated Euler-Lagrange agents", submitted.
2. **T Tao**, S Roy, B. De Schutter, S. Baldi, "Distributed adaptive synchronization in Euler Lagrange networks with uncertain interconnections", *IEEE Transactions on Automatic Control*, conditionally accepted.
3. **T Tao**, S Roy, S. Baldi, "Stable adaptation in multi-area load frequency control under dynamically-changing topologies", *IEEE Transactions on Power Systems*, 2021, 36(4): 2946-2956.
4. **T Tao**, S Roy, S. Baldi, "The issue of transients in leakage-based model reference adaptive control of switched linear systems", *Nonlinear Analysis: Hybrid Systems*, 2020, 36: 100885.
5. S. Baldi, **T Tao**, Kosmatopoulos E B, "Adaptive hybrid synchronisation in uncertain Kuramoto networks with limited information", *IET Control Theory & Applications*, 2019, 13(9): 1229-1238.

Conferences:

1. **T Tao**, S Roy, S. Baldi, "Adaptive single-stage control for uncertain nonholonomic Euler-Lagrange systems", submitted.
2. **T Tao**, S Roy, S. Baldi, "Adaptive synchronization of uncertain complex networks under state-dependent a priori interconnections", *The 60th IEEE Conference on Decision and Control (CDC)*, 2021: 1777-1782.
3. **T Tao**, S Roy, S. Yuan, S. Baldi, "Robust adaptation in dynamically switching load frequency control", *The 21th World Congress of the International Federation of Automatic Control (IFAC World Congress)*, 2020, 53(2): 13460-13465.
4. **T Tao**, V. Jain, S. Baldi, "An adaptive approach to longitudinal platooning with heterogeneous vehicle saturations", *The 15th IFAC Symposium on Large Scale Complex Systems*, Delft, Netherland, 2019, 52(3): 7-12.

CURRICULUM VITAE

Tian TAO

Tian Tao received her B.S. degree in department of Electrical Engineering & Automation from Wuhan Polytechnic University, Wuhan, China in 2013. In 2018, She obtained her M.S. degree in Automation Engineering department from University of Electronic Science and Technology of China. In October 2018, she joined DCSC of Delft University of Technology, Netherlands as a PhD candidate under the supervision of Prof. dr. ir. Bart De Schutter and Prof. dr. Simone Baldi. Her research interests are adaptive switched control with applications in multi-agent and interconnected systems.